A microscopic image showing several hyphae of the fungus Paecilomyces variotii. The hyphae are composed of chains of oval-shaped spores. The spores are light yellowish-green with a distinct yellow outline. The hyphae are set against a dark blue background with some lighter blue and purple mottling. The overall appearance is that of a filamentous fungus with a high density of spores.

Heterogeneity in stress resistance of
Paecilomyces variotii and related food
spoilage fungi

Tom van den Brule

Heterogeneity in stress resistance of *Paecilomyces variotii* and related food spoilage fungi

Tom van den Brule

PhD thesis, Utrecht University, Utrecht, The Netherlands (2022)

The research described in this thesis was performed within the Food and Indoor Mycology research group at the Westerdijk Fungal Biodiversity Institute, Uppsalalaan 8, 3584 CT Utrecht, The Netherlands.

Copyright © T van den Brule. All rights reserved.

Cover photo: Jan Dijksterhuis

Cover design: Pleunet Snoek

Printed by: Ipskamp printing

ISBN: 978-94-6421-842-8

Heterogeneity in stress resistance of *Paecilomyces variotii* and related food spoilage fungi

Heterogeniteit in stress resistentie van *Paecilomyces variotii*
en gerelateerde voedselbederfschimmels
(met een samenvatting in het Nederlands)

Proefschrift

ter verkrijging van de graad van doctor aan de
Universiteit Utrecht
op gezag van de
rector magnificus, prof. dr. H.R.B.M. Kummeling,
ingevolge het besluit van het college voor promoties
in het openbaar te verdedigen op
woensdag 21 september 2022 des middags te 12.15 uur

door

Tom van den Brule

geboren op 28 juni 1987
te Breda

Promotor:

Prof. dr. H.A.B. Wösten

Copromotor:

Dr. J. Dijksterhuis

Beoordelingscommissie:

Prof. dr. J.H. de Winde

Prof. dr. E.E. Kuramae

Prof. dr. G.A. Kowalchuk

Prof. dr. P.W. Crous

Prof. dr. S. Avery

*“Life is like riding a bicycle. To keep your
balance you must keep moving”*

Albert Einstein

CONTENTS

Chapter 1	General introduction	9
Chapter 2	The most heat-resistant conidia observed to date are formed by distinct strains <i>Paecilomyces variotii</i>	21
Chapter 3	Conidial heat resistance of various strains of the food spoilage fungus <i>Paecilomyces variotii</i> correlates with mean spore size, spore shape and size distribution	43
Chapter 4	Intraspecific variability in heat resistance of fungal conidia	59
Chapter 5	Comparative genomic, transcriptomic and phenotypic analysis of <i>Paecilomyces variotii</i> strains reveal complexity in mechanisms involved in conidial heat stress resistance	97
Chapter 6	General discussion	141
Appendix	References	151
	Nederlandse samenvatting	165
	<i>Curriculum vitae</i>	169
	List of publications	170
	Acknowledgements	171

General introduction

1.1 MICROBIAL FOOD SPOILAGE

Food is the source of almost all essential molecules and energy we need to grow and maintain ourselves. As a chemoheterotrophic organism, we are not able to produce energy from abiotic factors like sunlight and carbon dioxide. We rely on carbohydrates, fatty acids and proteins that are produced by other organisms. Unfortunately, we have to compete with other chemoheterotrophic organisms for food. If we do not pay attention, if we blink with our eyes, or if we wait too long, there is a high chance that nutritious compounds in our food are being digested by one of the millions of bacteria, yeast or other fungal species we share this planet with.

How much food is lost and spoiled due to microbial activity is an educated guess. There are various papers citing that it is estimated 25% of the food produced worldwide is lost due to microbial spoilage (Bondi *et al.*, 2014; Geoghegan *et al.*, 2020; Gram *et al.*, 2002; Punt *et al.*, 2020; Snyder and Worobo, 2018). These references can be traced back to a 1985 report (National Research Council (US) Subcommittee on Microbiological Criteria, 1985). The committee stated that it is estimated that one-fourth of the world's food supply is lost through pre- and post-harvest microbial spoilage alone. Although it is unclear what the basis is of these estimations, it illustrates the magnitude of a problem with huge economic consequences. A major challenge of the coming decades is to limit food loss and spoilage to a minimum to keep feeding an increasing world population, in particular because there is hardly a possibility to enlarge the global area of arable land.

To prevent microbial spoilage, humanity has developed techniques for long time food preservation. Examples are pickling, salting, fermenting, heating, high pressure, ultra violet (UV) irradiation, modified atmosphere packaging, or adding preservative compounds such as sodium nitrate and weak acids such as sorbic and benzoic acid. Industrially processed food generally uses a mixture of preservation techniques, often referred to as preservation hurdles. In general, these hurdles create an unfavourable environment for microbial growth. Depending on the properties of the product, the hurdles are applied in such way that the product supposedly remains microbiologically stable, at least until the end of its shelf life.

The variability in microorganisms is enormous and some species are well adapted to survive in the diverse food environments. As spoilage organisms grow, the food is being degraded causing changes in structure and off-odour and -taste. In addition, food safety can be of concern when species grow unnoticeably that are pathogenic or that produce toxic compounds, causing potentially life threatening illness or food intoxication. The organisms causing these problems are mainly classified in the bacterial and fungal kingdoms.

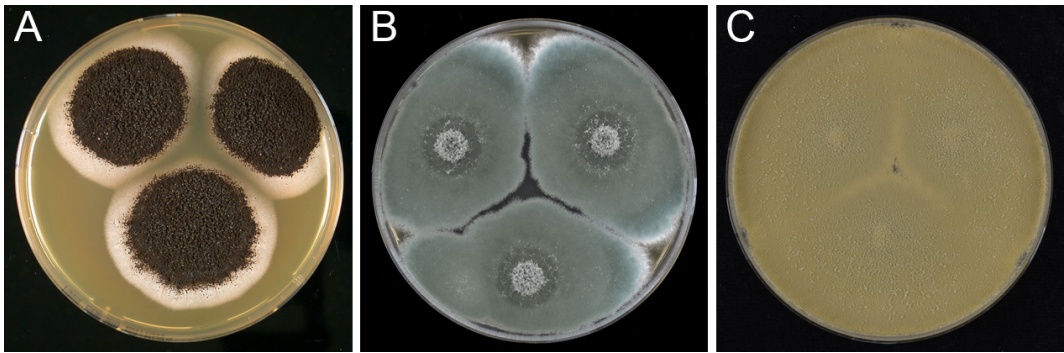


Figure 1.1. The fungal species used in this Thesis grown on malt extract agar. *Aspergillus niger* with its black conidia (A), *Penicillium roqueforti* producing green conidia (B) and *Paecilomyces variotii* with its olive brown conidia (C).

1.2 FILAMENTOUS FUNGI AND THEIR RELATIONSHIP WITH FOOD SPOILAGE

The huge variability in microorganisms is also manifested in fungi. Currently about 150.000 species have been described (<http://www.speciesfungorum.org/>, July 14,2021), which is only a slight percentage of the estimated total number of species. Estimates vary from 2.2 – 3.8 million (Hawksworth *et al.*, 2017) to 11.7 – 13.2 million species (Wu *et al.*, 2019). A large proportion of fungi has adopted a multicellular lifestyle (Hawksworth *et al.*, 2017) and are called filamentous fungi, often referred to as moulds. Filamentous fungi grow by means of branching hyphae that grow at their apices. As a result, an interconnected network of hyphae is formed that is called mycelium.

Fungi have diverse ecological roles. Many fungi have a saprotrophic lifestyle and are efficient degraders of plant material. Besides and in addition, fungi can have a mutualistic or parasitic relationship with other organisms. For instance, mycorrhizal fungi extend the root network of plants, providing better accessibility to nutrients and water. In exchange, the fungi receive carbohydrates from the plant. On the other hand, plant pathogenic fungi can have detrimental effects by killing the host or by lowering crop yield. In agriculture, this has huge economic consequences.

The filamentous fungi *Paecilomyces variotii*, *Aspergillus niger* and *Penicillium roqueforti* were used in this PhD project, of which the former was most intensely studied (Fig 1.1). All three fungal species are associated with food spoilage because of their stress resistance and their heterogeneous nature. They all belong to the order Eurotiales, but each has different properties in their ecology and spoilage specificity.

1.2.1 Eurotiales

The order Eurotiales of the Ascomycota harbours many fungal species that are associated with food spoilage, the indoor environment, and pathogenicity (Houbraken *et al.*, 2020).

Aspergillus, *Paecilomyces*, *Penicillium* and *Talaromyces* are just a few genera involved in this versatile and important fungal order. The order contains many of the filamentous fungi that are associated with spoilage of processed foods and some species are highly adapted to specific conditions of the food environment (Snyder *et al.*, 2019). The fact that they produce highly toxic secondary metabolites make them of high interest to maintain food safety.

Eurotiales are known for their ability to grow under extreme conditions. Psychrophilic species like *P. roqueforti* can grow at temperatures close to 0 °C. In fact, it was recently suggested that this fungus can even grow at temperatures below 0 °C, based on cardinal values of growth models (Nguyen Van Long *et al.*, 2021). On the other hand, halotolerant species such as *A. niger* have the ability to grow in highly acidified environments down to pH 1.4 (Schuster *et al.*, 2002), while other species can grow at high concentrations of weak acids that are widely used as preservatives, such as sorbic, benzoic and propionic acid (Garcia *et al.*, 2021). Xerophilic fungi are specialized in growing at low water activity ($a_w < 0.85$). *Xeromyces bisporus* and *Aspergillus penicillioides* can even germinate at an a_w as low as 0.64 (Stevenson *et al.*, 2017). Many Eurotiales are also well adapted to grow at hypoxic conditions. For instance, numerous *Aspergillus* species grow well at 0.2% oxygen (Hillmann *et al.*, 2015). Finally, heat resistant moulds (HRMs) can produce highly heat resistant spores. Filamentous fungi are regarded as HRM when their spores can survive more than 30 minutes at 75 °C (Pitt and Hocking, 2009; Samson *et al.*, 2019), but some species, such as *Talaromyces macrosporus* and *Aspergillus spinosus*, can even survive heat treatments above 90 °C for several minutes (Dijksterhuis, 2019).

Eurotiales reproduce both asexually and sexually (Fig. 1.2). In the asexual cycle, aerial hyphae differentiate into conidiophores on which conidia are formed. These asexual spores can be dispersed by wind, water and other vectors like insects. The genera *Aspergillus*, *Paecilomyces* and *Penicillium* produce conidia abundantly. Each conidiophore of *Aspergillus niger* can produce up to 10,000 conidia, resulting in the production of billions of spores from a single colony (Ijadpanahsaravi *et al.*, 2020). Many species of these genera are cosmopolitan and therefore, conidia can be found in virtually every cubic meter of air. Some species also produce asexual chlamydospores within their mycelium. These spores have thickened cell walls and are formed between hyphal cells. The primary functions of chlamydospores is to survive temporary unfavourable conditions.

Eurotiales reproduce sexually in different ways. In general, a compatible mating type is needed for sexual reproduction. Homothallic species are self-fertile and both mating types are present within their genome. Therefore, each individual colony can produce sexual spores, while it can also recombine with another strain. Heterothallic species, on the other hand, only contain one mating type in their genomes, meaning that they need to encounter another colony with the compatible mating type locus in order to reproduce sexually. During sexual reproduction, fruiting bodies like cleistothecia are formed, in which asci are produced that contain the sexually formed spores called ascospores.

Many heterothallic Eurotiales were assumed to be asexual because their sexual form of reproduction was never observed. For this reason, they were called anamorphic fungi,

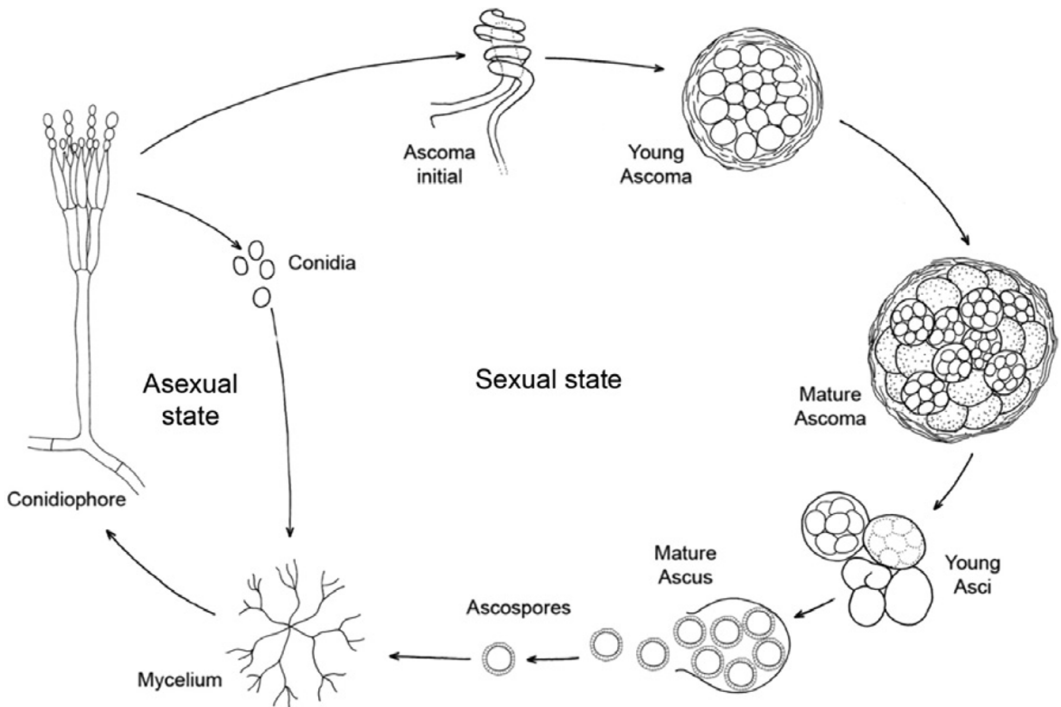


Figure 1.2. General life cycle of Eurotiales. conidia are formed in the asexual part of the life cycle, while in the sexual part ascospores are formed. Pictures are based on reproduction structures of *Talaromyces macrosporus*. Adapted from Wyatt *et al.* 2013.

Fungi Imperfecti or Deuteromycetes. However, sexual cycles have been revealed of such anamorphic species during the past two decades. The best example is the discovery of the sexual cycle of the human opportunistic pathogen *Aspergillus fumigatus* (O’Gorman *et al.*, 2009). The discovery of conditions promoting sexual reproduction together with genomic information has led to the conception that many of the anamorphic species have the potential to reproduce sexually (Dyer and O’Gorman, 2011; Ellena *et al.*, 2020).

Traditionally, fungi have been classified based on ecology, morphology and on the reproduction structures they produce. The asexual and sexual state have been described independently for many species, because morphologies can differ vastly between the two states. This resulted in a dual nomenclature with the anamorph describing the asexual state and the teleomorph describing the sexual state (Pitt and Hocking, 2009). Because this could lead to confusing situations, it was decided at the Amsterdam declaration on fungal nomenclature that one fungus should have one name (Hawksworth *et al.*, 2011). The state for the genus that was described first is the name that should be used.

1.2.2 *Paecilomyces variotii*

The common cosmopolitan filamentous fungus *P. variotii* can be found in soil, indoor environments, plants, animals, food and beverages, but it can also act as an opportunistic

human pathogen (Houbraken *et al.*, 2008, 2010; Pitt and Hocking, 2009; Samson *et al.*, 2019). It is a thermotolerant species and is able to grow at temperatures up to 50 °C (Samson *et al.*, 2019). In addition, it has the ability to grow at low oxygen concentrations and in the presence of preservatives. Therefore, this fungus is a spoilage organism of many food products. It is considered a heat resistant mould because of its heat resistant ascospores (Houbraken *et al.*, 2008). As a consequence, *P. variotii* can spoil heat treated products or resources, such as pectin, canned fruits, fruit juices and non-carbonated sodas. But it is also able to spoil a wide range of other products like margarine and bakery products, which are more likely to be contaminated through airborne conidia than by ascospores. The fungus is able to produce viriditoxin of which the biosynthetic gene cluster was recently described (Urquhart *et al.*, 2019), and which was shown to be toxic to mice (Lillehoj and Ciegler, 1972). Although it is unclear what the consequences are in terms of food safety, viriditoxin has antibacterial activity by inhibiting the cell division protein FtsZ (Wang *et al.*, 2003), while it also has cytotoxic activity against cancer cells (Kundu *et al.*, 2014; Park *et al.*, 2015).

Because of the dual nomenclature system, *P. variotii* can be found in literature under multiple synonym names. The fungus was first described in 1907 by Bainier, who dedicated the name to the French doctor and paediatrician Dr. Variot (Bainier, 1907). Few years later, the new genus *Byssochlamys* and an ascospore producing fungal species with the name *Byssochlamys nivea* were described (Westling, 1909). Six decades later, the relation between *Byssochlamys* and *P. variotii* was described (Stolk and Samson, 1971). The anamorphic species *Paecilomyces niveus*, *P. fulvus*, and *P. zollerniae* were linked to their teleomorphs *B. nivea*, *B. fulva* and *B. zollerniae*, respectively. More than two decades later, a new fungus, *Talaromyces spectabilis* with a *Paecilomyces* anamorph state was described (Udagawa and Suzuki, 1994). Later, morphologic observations showed that this fungus had a *Byssochlamys* teleomorph instead of *Talaromyces* teleomorph (Houbraken *et al.*, 2006). Molecular data and the discovery of its heterothallic sexual life cycle revealed that *P. variotii* is the anamorph of the teleomorph *Byssochlamys spectabilis* and is the same species as *T. spectabilis* (Houbraken *et al.*, 2008; Samson *et al.*, 2009). After the abolition of the dual nomenclature only the anamorph name, *P. variotii*, should be used (Hawksworth *et al.*, 2011).

Three different spore types can be formed by *P. variotii*. Asexually, it produces conidia abundantly and chlamydospores are usually present in colonies. Conidia are smooth and ellipsoid with usually flat apical edges. When two strains with a compatible mating type encounter each other, it is able to mate and reproduce sexually by means of ascospore formation (Fig. 1.3). Ascogonia coil around the swollen antheridia of the compatible strain, which forms the ascoma initial. At the tip, ascogenous cells are formed where karyogamy occurs between nuclei of the two different strains. This leads to meiosis followed by mitosis and results in an ascus containing eight ascospores. Although heat resistance of *P. variotii* ascospores has not been studied in large detail there are indications that they are able to survive heat treatments of 85 °C for more than an hour (Houbraken *et al.*, 2006). This makes them potentially more resistant than ascospores of the related heat resistant

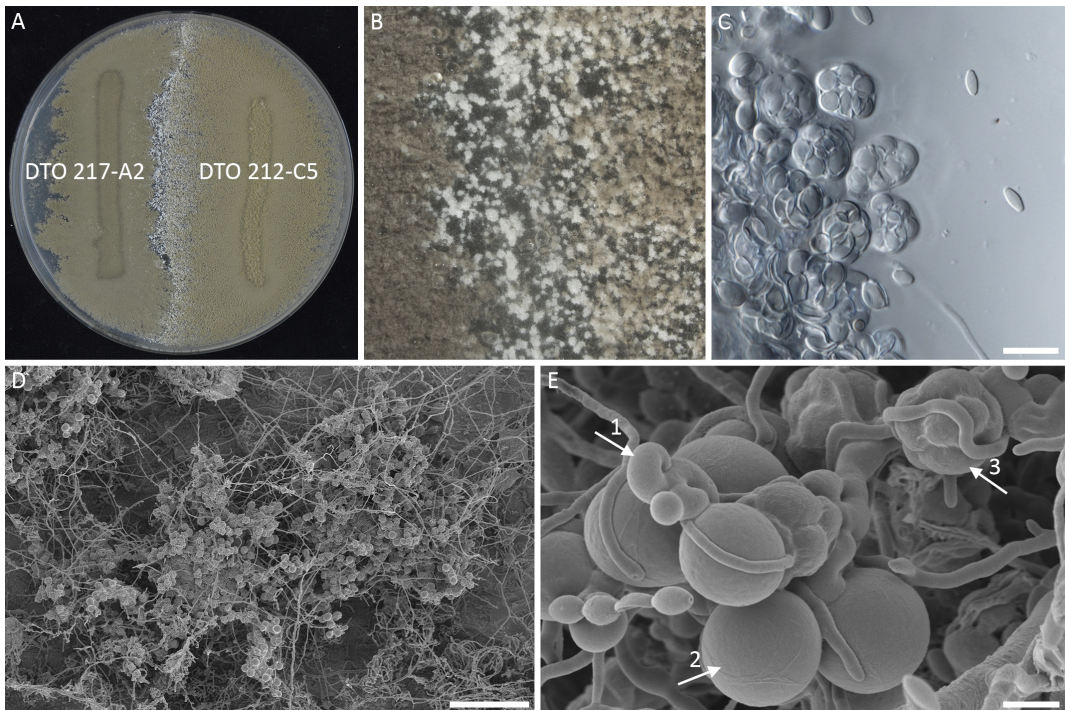


Figure 1.3. Sexual reproduction of *P. variotii*. (A) Two strains with compatible mating types, DTO 217-A2 and DTO 212-C5, grown for 6 weeks on potato dextrose agar at 30 °C. (B) Magnification of the area between the two strains by stereo microscopy. Asci are formed between the colonies resulting in typically white ascomata. (C) Light microscopy of asci, each containing 8 ascospores. (D) Cryo-SEM image of grouped asci. (E) Cryo-SEM image of ascogenous cell (1) forming young asci (2). The membrane of the asci shrinks when asci mature, revealing its individual ascospores (3). Scale bars indicate 10 μm (C), 100 μm (D) and 5 μm (E).

mould species *P. niveus* and *P. fulvus* (Beuchat and Rice, 1979). The ascospores of these species are produced in a homothallic manner and does not require crossing of strains, which makes them easier to work with. Chlamydospores and ascospores of *P. variotii* are considered more localized within the mycelium and less prone to distribution than its conidia.

The full genome sequences of *P. variotii* strains CBS 101075 and CBS 144490 are available at the Joint Genome Institute (JGI, jgi.doe.gov). Authors found evidence for an active repeat induced point mutation (RIP) system for the first time in an Eurotiales species (Urquhart *et al.*, 2018). It is thought that RIP is a fungal specific protection mechanism against the deleterious effects of transposons (Hane *et al.*, 2015). Recently, a large transposable element of approximately 85 kbp was identified in some, but not all, *P. variotii* strains, (Urquhart *et al.*, 2022). Genes located on this cluster are involved in stress resistance against the metals cadmium, lead, zinc, copper and arsenic. The genome of another strain was also sequenced under the name *P. variotii* No.5 (Oka *et al.*, 2014) but was reclassified as *Paecilomyces formosus* (Urquhart *et al.*, 2018).

1.2.3 *Aspergillus niger* and *Penicillium roqueforti*

The fungus *A. niger* is well known for its biotechnological applications and used for citric acid and enzyme production. Because of its industrial role, it has been widely used as a model organism to study fungal genetics (Pel *et al.*, 2007). In addition, it is a food spoilage fungus causing black rot in grapes, onions and other fruits and vegetables. The fungus grows well under acidic conditions and therefore, it is a common spoiler of yoghurt products (Gougouli and Koutsoumanis, 2017).

The fungus *P. roqueforti*, is known as the fermentation organism of blue vein cheeses (Coton *et al.*, 2020; Ropars *et al.*, 2012). It is well adapted to grow at low temperatures (Nguyen Van Long *et al.*, 2021) and is able to grow at high concentrations of weak acids (Samson *et al.*, 2019). Therefore, it is also an efficient spoiler of dairy products with a chilled chain storage. In addition, it is a common spoiler of bakery products and silage (Samson *et al.*, 2019).

Like *P. variotii*, both species are heterothallic and require mating with another strain with compatible mating type for sexual reproduction. Strains of *P. roqueforti* can recombine under specific conditions (Ropars *et al.*, 2014), while sexual reproduction of *A. niger* has not yet been observed. Nevertheless, there are conditions in which sexual structures called sclerotia are formed (Ellena *et al.*, 2021) and some strains can be recombined under lab conditions using the parasexual cycle (Arentshorst and Ram, 2018).

1.3 STRESS RESISTANCE IN EUROTIALES

The ability of a fungus to spoil food is largely determined by its stress resistance and, as a consequence, its ability to grow through hurdles applied within the food environments. Stress resistance of fungal spores, which are regarded dormant with minimal metabolic activity (Novodvorska *et al.*, 2016; Teertstra *et al.*, 2017) and growing vegetative mycelium is different. In general, spores are considered more stress resistant than vegetative cells (Wyatt *et al.*, 2013), but the resistance of mycelium to food preservative factors is equally important as it has to deal with low water activity and the presence of preservatives in order to grow.

Spores must be able to prevail prolonged periods in unfavourable and stressful conditions like drought, heat and ultra violet (UV) exposure in order to be successful. The protective mechanisms of these spores have been reviewed (Wyatt *et al.*, 2013). In general, spores have relatively thick cell walls that can contain high concentrations of melanin to protect against UV radiation (Belozerskaya *et al.*, 2017). In addition, they accumulate high concentrations of protective compounds in their cytosol, such as compatible solutes and heat shock proteins (HSPs). Compatible solutes are considered compounds that do not to interfere with cellular metabolism and are able to protect the cells to various stressors, such as heat stress, osmotic stress and oxidative stress. Typically, the compatible solutes trehalose, mannitol, glycerol, erythritol and arabitol can be found in fungal spores. These

solutes are kosmotropic in nature (Cray *et al.*, 2013), which means they have a larger affinity to form hydrogen bonds with water than water molecules with themselves. This stabilizes biomacromolecules like proteins (Collins, 1997; Washabaugh and Collins, 1986). Each compatible solute has different properties and the compatible solute composition differs per species, spore type and age, and environmental conditions (Hagiwara *et al.*, 2017; Nguyen Van Long *et al.*, 2017a) (Teertstra *et al.*, 2017; Wyatt *et al.*, 2015a). For instance, conidia of *A. niger* and *P. roqueforti* contain mannitol and arabitol, respectively, as their predominant compatible solute (Punt *et al.*, 2020; Teertstra *et al.*, 2017), whereas trehalose is the predominant compatible solute in *P. variotii* conidia (**Chapter 2, 4**).

The role of arabitol to protect fungi from stress conditions has not yet been systematically assessed. In contrast, trehalose has often been associated to heat stress resistance of fungal spores (Wyatt *et al.*, 2013), as well as to desiccation stress resistance and cryotolerance in *Saccharomyces cerevisiae* (Gadd *et al.*, 1987; Gélinas *et al.*, 1989; Kim *et al.*, 2018). In *Aspergillus oryzae*, a transcription factor *atfA* deficient strain produces conidia with reduced trehalose concentrations that are more sensitive to heat stress (Sakamoto *et al.*, 2008). Mannitol is associated with many types of stress protection, including heat, oxidative and osmotic stress (Ruijter *et al.*, 2003). The compatible solutes glycerol, erythritol, arabitol, and mannitol have a lower molecular weight than trehalose. Therefore, they can more easily accumulate to high concentrations in fungal cells, thereby providing protection against osmotic stress. All of these compatible solutes accumulate under salt stress conditions in *A. oryzae* mycelium (Ruijter *et al.*, 2004). Glycerol deficiency in *A. nidulans* results in reduced growth under salt stress conditions (De Vries *et al.*, 2003).

Weak acids, such as sorbic, benzoic and propionic acid, are widely used as preservatives in foods. Weak acids in water partially dissociate into an equilibrium depending on the dissociation constant K_a and the pH of the environment. At low pH, a larger proportion of the weak acids remain undissociated. This form can be internalized by cells where the compound dissociates into an anion and proton, causing a drop in pH of the cytoplasm (Plumridge *et al.*, 2004). The proton is actively removed through proton pumps under the expenditure of energy. As a result, germination and microbial growth can be significantly reduced in the presence of weak acids. Next to this “classical weak-acid theory”, sorbic acid also inhibits the plasma membrane H⁺-ATPase proton pump in *S. cerevisiae* (Stratford *et al.*, 2013a) and glucose uptake in *A. niger* (Novodvorska *et al.*, 2016). Fungal resistance to weak acids is associated with proteins that are able to catabolize these compounds. For instance, resistance of *A. niger* to benzoic acid is attributed to benzoate *para*-hydrolase (Boschloo *et al.*, 1991), while resistance to sorbic and cinnamic acid is mediated by decarboxylase CdcA and prenyltransferase PadA that are regulated by transcription factor SdrA (Lubbers *et al.*, 2019; Plumridge *et al.*, 2010). Recently, another transcription factor WarA was identified that is required for resistance to sorbic acid and other weak acids in *A. niger* and *A. fumigatus* (Geoghegan *et al.*, 2020). WarA regulates the transcription of the ABC-type transporter PdrA, which is thought to be involved in the efflux of weak acid anions from the cytoplasm.

Heat treatment is widely used as a preservation method in food manufacturing. By pasteurizing or sterilizing the product, microbial cells are inactivated. The microbial counts, usually expressed as colony forming units (CFUs), decreases over time during a heat treatment at a fixed temperature. Heat resistance of microbial cells is usually expressed as the *D*-value and *z*-value. The *D*-value indicates the time it takes to inactivate 1 log CFU at the given temperature. In other words, it is the negative reciprocal of the inactivation rate of a linear regression fitted to the inactivation data. In the case the inactivation is non-linear, a Weibull model can be used which is able to fit a convex or concave curve with a shape parameter (Dantigny, 2021; Metselaar *et al.*, 2013). The *z*-value describes the temperature increase of the heat treatment which is necessary to reduce the *D*-value by 1 log. Usually, *D*-values are determined at a lower temperature than the actual temperature of a heat treatment. With the *z*-value, it is possible to extrapolate the inactivation kinetics to higher temperatures. With these inactivation models, food manufacturers can predict the effect of a heat treatment on the microbial count in the product.

1.4 HETEROGENEITY WITHIN EUROTIALES

The success of a microorganism depends on how well it can adapt to environmental changes and how well it can survive stressful events. Variability between cells enables a population to respond more effectively to environmental stress and ultimately helps the species in persisting and pursuing its genes to next generations. Intra-species variability occurs at different levels. First, phenotypic characteristics can differ between strains of the same species such as in weak acid resistance in strains of the yeast *Zygosaccharomyces bailii* (Stratford *et al.*, 2013b). Phenotypic heterogeneity also occurs between colonies of genetically identical strains (de Bekker *et al.*, 2011) and even within colonies (Tegelaar *et al.*, 2020; Wösten *et al.*, 2013). Inter- and intra-strain variability is also found in fungal spores. It is thought that stochasticity and epigenetic modifications are important mechanisms to create phenotypic heterogeneity (Avery, 2006).

The history of a fungal spore can affect the degree of resistance. Growth conditions define the properties of fungal spores. Conidia of *A. fumigatus* originating from colonies grown at high temperature produce less pigment and accumulate more trehalose, making them more vulnerable for UV radiation but more resistant to heat (Hagiwara *et al.*, 2017). Similarly, *P. roqueforti* conidia show higher heat resistance when they have been produced at higher temperature (Punt *et al.*, 2020). It was recently shown that *A. nidulans* conidia are able to respond at transcriptional level to environmental changes as long as they remain attached to the colony, maximizing their survival into different environments (Wang *et al.*, 2021). This research has changed the traditional concept of conidia as static cells and makes them heterogeneous by definition. Spore properties are even variable within a colony of *A. niger*. A growing fungal colony contains spores of different ages (older in the centre and younger towards the colony periphery) and thus, a heterogeneous population of conidia is released during a dispersal event. These spores that differ in age have different degree of maturation and thereby different properties (Teertstra *et al.*, 2017).

This is illustrated by the fact that five-day-old conidia contain higher trehalose levels and show higher heat resistance than younger spores.

Heterogeneity is also reflected in germination characteristics of conidia. Environmental conditions can have a significant effect on germination time. It was shown that *P. roqueforti* conidia produced at 5 °C germinate significantly faster at 5 °C than spores produced above 20 °C (Nguyen Van Long *et al.*, 2017a). In addition, spores formed at low water activity germinate faster at such conditions than spores produced at high water activity (Dagnas *et al.*, 2017; Stevenson *et al.*, 2017). Furthermore, germination within a population of *A. niger* and *P. roqueforti* conidia occurs heterogeneously (Ijadpanahsaravi *et al.*, 2020; Punt *et al.*, 2022a). Germination of *A. niger* conidia is most effectively induced by the presence of the amino acids proline and alanine (Ijadpanahsaravi *et al.*, 2020), while *P. roqueforti* conidia are induced by arginine and alanine (Punt *et al.*, 2022a). Heterogeneity in germination is further illustrated by a longer germination time of an individual *Penicillium corylophilum* conidium compared to the germination time of a population of conidia (Dagnas *et al.*, 2015). In other words, the population lag time is determined by the fastest germinating conidium.

1.5 RESEARCH OUTLINE

Consumer trends put tension on the shelf life of industrially processed food (Leyva Salas *et al.*, 2017; Snyder and Worobo, 2018). Consumers request 'clean label', which means that the ingredient list is free of any chemical additives, such as the preservatives potassium sorbate or sodium nitrate. Second, they select products that are minimally processed to preserve organoleptic properties and healthy components such as vitamins. In addition, there is growing awareness that salt can lead to health issues and therefore, less salt is added to products. These developments make food products more prone to fungal spoilage. Therefore, there is an increased interest from food industry to understand spore heterogeneity. This knowledge is crucial to make risk assessments more realistic and helps redefining product shelf life. This has led to the TiFN¹ project "Heterogeneity in spores of food spoilage fungi", of which this dissertation is the result of one of four Ph.D. projects.

The aim of this thesis was to study inter- and intra-strain variability in stress resistance of *P. variotii* conidia. In particular, heat resistance was studied since this fungus is known to be highly resistant to this stress. Although its ascospores are more heat resistant than its conidia, the latter are assumed to have more impact on food spoilage because of the high number of these spores that are produced as well as their high dispersal. By studying their phenotypic variability and by comparing it to *A. niger* and *P. roqueforti*, we aimed for a better understanding in natural variability and limits of conidial resistance.

Heterogeneity of heat resistance of conidia between and within strains of *P. variotii* was determined in **Chapter 2**. Out of 108 strains, 31 isolates showed a conidial survival >10%

¹TiFN is a platform that connects industry with academia in food and nutrition related research.

after a 10-min-heat treatment at 59°C. Strains DTO 212-C5, DTO 032-I3 and DTO 217-A2 with different heat sensitivity were selected and showed a decimal reduction time at 60 °C (D_{60} -value) of 3.7, 5.5 and 22.9 minutes, respectively. Further in-depth analysis revealed that the most heat resistant strain formed larger conidia and contained higher trehalose levels. Together, conidia of DTO 217-A2 are the most heat-resistant conidia reported so far.

In **Chapter 3**, light microscopy, scanning electron microscopy, Coulter Counter and flow cytometry were used to measure spore size of five heat sensitive and five heat resistant strains. The various methods did not show significant differences in spore size and showed varying spore size between strains with a 2.4-fold volume difference between the extremes. In general, strains that produced large conidia were more heat resistant. Among the tested strains, DTO 195-F2 was found to have a D_{60} -value of 27.6 ± 3.12 min, which is even higher than that of DTO 217-A2 (see **Chapter 2**).

Chapter 4 quantified variability of heat resistance of 20 *P. variotii* strains, 21 *A. niger* strains and 20 *P. roqueforti* strains at strain level, biological level and experimental level. This was combined with a meta-analysis for *A. niger* and *P. roqueforti* showing that variability of all three species was in the same magnitude as heat resistance of bacterial spores and cells. In all cases, variability at strain level was the largest source of variability accounting for about 45% of the total variation.

The genomes of all strains studied in **Chapter 3** and **Chapter 4** were sequenced in **Chapter 5**. Correlation of heat resistance of conidia and mean size and trehalose levels of the spores as described in **Chapters 2** and **3** was confirmed in the dataset covering all strains. Comparative genomics and transcriptomics revealed a set of genes that are possibly involved in heat resistance of the conidia. In addition, a unique gene cluster of approximately 60 kbp was identified in most heat resistant strains. However, deletion of the cluster in DTO 217-A2 did not result in a more sensitive phenotype. Results are summarized and discussed in **Chapter 6**.

The most heat-resistant conidia observed
to date are formed by distinct strains
Paecilomyces variotii

Tom van den Brule, Maarten Punt, Wieke Teertstra, Jos Houbraken, Han
Wösten and Jan Dijksterhuis

ABSTRACT

Fungi colonize habitats by means of spores. These cells are stress-resistant compared to growing fungal cells. Fungal conidia, asexual spores, formed by cosmopolitan fungal genera like *Penicillium*, *Aspergillus* and *Paecilomyces* are dispersed by air. They are present in places where food products are stored and, as a result, they cause food spoilage. Here, we determined the heterogeneity of heat resistance of conidia between and within strains of *Paecilomyces variotii*, a spoiler of foods such as margarine, fruit juices, canned fruits and non-carbonized sodas. Out of 108 strains, 31 isolates showed a conidial survival >10% after a 10-minute-heat treatment at 59 °C. Three strains with different conidial heat resistance were selected for further phenotyping. Conidia of DTO 212-C5 and DTO 032-I3 showed 0.3% and 2.6% survival in the screening, respectively, while survival of DTO 217-A2 conidia was >10%. The decimal reduction times of these strains at 60 °C (D_{60} -value) were 3.7 ± 0.08 , 5.5 ± 0.35 , and 22.9 ± 2.00 minutes, respectively. Further in-depth analysis revealed that the three strains showed differences in morphology, spore size distributions, compatible solute composition and growth under salt stress. Conidia of DTO 217-A2 are the most heat-resistant reported so far. The ecological consequences of this heterogeneity of resistance, including food spoilage, are discussed.

2.1 INTRODUCTION

Fungi produce numerous spores that are distributed by water, air and other vectors (e.g. insects and soil movement). Airborne spores are present in every cubic meter of air and cause fungal colonization in all environments. As reviewed, conidia vary in several parameters (Dijksterhuis, 2017). For instance, 5-day-old *Aspergillus niger* conidia show higher trehalose content compared to spores of younger age (Teertstra *et al.*, 2017). Conidia of *Aspergillus fumigatus* show differences in pigmentation, compatible solute content and oxidative- and heat-resistance depending on the growth temperature of the conidia-forming colony (Hagiwara *et al.*, 2017). In general, spore parameters are influenced by conditions during spore formation and maturation. However, there is a scarcity of information on the extent of heterogeneity of spore populations, even if they originate from one colony. Stress resistance of spores and germination properties are both important for colonization but different in nature. Colonies from individual spores that enter a new ecosystem often have longer lag times compared to a population of spores (Dagnas *et al.*, 2015; Gougouli and Koutsoumanis, 2013). This is essentially caused because the spore that germinates fastest determines the lag time of a population. Further, germination of conidia is delayed markedly when conditions are suboptimal. In several studies, this has been tested in the case of water activity and temperature (Dagnas *et al.*, 2017; Nguyen Van Long *et al.*, 2017b; Stevenson *et al.*, 2017).

Heterogeneity encountered in conidia is relevant in the area of food spoilage; the strongest spore will define if spoilage occurs. In nature, the strongest spore enlarges the limits of growth of a species. Fungal spoilage of processed foods and drinks causes food

waste and economic losses (Gustavsson *et al.*, 2011). In general, industry prevents fungal food spoilage by using preservation hurdles like pasteurization, low water activity, low pH or low storage temperature. Consumer demands towards more natural- and preservative free food put a pressure on shelf life of food (Leyva Salas *et al.*, 2017). For instance, heat treatment at lower temperature could lead to more beneficial organoleptic characteristics of the product and better retainment of vitamins or other temperature sensitive healthy components. On the other hand, this procedure would introduce survival of heat-resistant cells and more risk for the product to be spoiled. In addition, consumers demand healthier alternatives, including products containing lower salt concentrations and less use of antimicrobial compounds. These trends towards milder processing methods make processed food products more prone to microbial spoilage and put a tension on the microbial safety limits of processed foods and drinks.

Paecilomyces variotii is a common thermo-tolerant fungus that occurs worldwide and has been isolated from food products, soil samples, clinical samples and indoor environments (Houbraken *et al.*, 2010). Recently, the genomes of *P. variotii* type strain CBS 101075 and CBS 144490 were sequenced (Urquhart *et al.*, 2018). *P. variotii* produces conidia abundantly and to a lesser extent chlamydoconidia. Besides these spore types, it is also known to produce highly heat resistant ascospores in a heterothallic manner (Houbraken *et al.*, 2008). Due to the resistant nature of these spores and its ability to grow at low oxygen concentrations, it is able to spoil pasteurized food products like fruit juices, canned fruits and non-carbonized sodas (Pitt and Hocking, 2009). Although *P. variotii* is a major spoilage fungus in a certain product niche, many aspects remain elusive in the resistance of its propagules.

Compatible solutes like trehalose, mannitol, glycerol, erythritol, and arabinose are accumulated in fungal spores (Wyatt *et al.*, 2013). Due to the kosmotropic nature of these compounds, they protect cells against various stressors (Cray *et al.*, 2013). Kosmotropic solutes have typically a larger affinity to form hydrogen bonds with water than water molecules with themselves, resulting in a stabilizing effect on biomacromolecules like proteins (Collins, 1997; Washabaugh and Collins, 1986). It is thought that trehalose plays an important role in the heat resistance of fungal spores (Wyatt *et al.*, 2013, 2015a). A decrease in trehalose concentration in *Aspergillus nidulans* and *Aspergillus oryzae* conidia results in a higher sensitivity to heat stress (Fillinger *et al.*, 2001; Sakamoto *et al.*, 2008).

Based on sequences of marker genes, *P. variotii* shows a higher genetic variability than related members of the Eurotiales (Houbraken *et al.*, 2008). In this research, we used the conidia of *P. variotii* as a model to explore the limits and variability of resistance to heat stress. We used 108 isolates from various substrates and locations to screen the conidia for heat resistance. Subsequently, we did an in-depth analysis of three strains of interest in their heat resistance, morphology and compatible solute composition. In addition, we explored the influence of salt stress on the growth rate. We used the results to reflect on the heterogeneity within and between *P. variotii* strains.

2.2 METHODS AND MATERIAL

2.2.1 Strain selection, sequencing and phylogenetic analysis

Strains were selected from the working collection of the Applied and Industrial Mycology (DTO) group at the Westerdijk Fungal Biodiversity Institute. All strains were stored in 30% glycerol at -80 °C. All isolates were identified by sequencing the β -tubulin gene (*benA*) as described (Houbraken *et al.*, 2008). In short, DNA from 3 to 4-day-old cultures grown on Malt Extract Agar (MEA, Oxoid, Hampshire, UK) was isolated using DNeasy UltraClean Microbial Kit (Qiagen, Venlo, the Netherlands) according to the manufacturer's protocol. Part of *benA* was amplified using primers Bt2a and Bt2b (Houbraken *et al.*, 2008), followed by a sequencing using the ABI Prism BigDye Terminator v.3.0 ready reaction cycle sequencing kit (Applied Biosystems, Foster City, CA). Samples were sequenced using a 3730XL DNA Analyzer (Applied Biosystems, Foster City, CA) and analyzed with SeqMan (DNASTar, Madison, WI, USA). Sequences were analysed using MEGA7 and aligned using ClustalW (Kumar *et al.*, 2016). Maximum Likelihood tree was computed with the Tamura 3-parameter model including gamma distribution and 1000 bootstrap replications.

2.2.2 Culture conditions and harvesting conidia

Conidia were harvested from 7-day-old colonies grown on MEA at 25 °C (Samson *et al.*, 2019). The conidia were rubbed into 10 mL ice cold ACES buffer [10 mM N-(2-acetamido)-2-aminoethanesulfonic acid, 0.02% Tween 80, pH 6.8] using a T-spatulum. After homogenizing, the conidia were filtered through sterile glass wool in a 30 mL syringe. Fifty mL Falcon tubes were filled up to 30 mL with ice-cold ACES buffer and centrifuged for 5 minutes at 1260 g at 4 °C. The pellet was washed with 40 mL ice-cold ACES buffer, centrifuged, and resuspended in 10 mL ice-cold ACES buffer. The conidia were counted using a counting chamber (haemocytometer, Bürker-Türk, VWR, Amsterdam, The Netherlands) or the Beckman Coulter Counter Multisizer3 (Beckman Coulter, Fichtenhain, Germany). Conidia were stored on ice until further treatment.

2.2.3 Screening and quantification heat resistance

Dilutions of 2×10^4 conidia mL⁻¹ were used for heat inactivation. A quantity of 150 μ L of such a suspension was transferred to a 1.5 mL Eppendorf tube and incubated in a water bath at 58 or 59 °C for 10 minutes. Of the heat treated samples, 50 μ L was used to inoculate on the surface of 9 cm MEA plates. All plates were inoculated in duplicate and incubated for 3 days at 25 °C. After incubation, pictures were made of the plates and colonies were counted.

To quantify conidial heat resistance, D_{60} -values were determined that express the time it takes to have 1 log reduction in colony forming units (CFUs) at 60 °C. For the determination of D -values, 19 mL ACES buffer was pre-heated in 100 mL Erlenmeyer

flasks in a water bath (120 rpm, 60 °C). At $t=0$, a volume of 1 mL of a 2×10^8 conidia mL^{-1} suspension was added to pre-heated buffer to reach a final concentration of 10^7 conidia mL^{-1} . After 2, 5, 10, 15, 20, 30 and 60 minutes incubation, 1 mL was removed from the flasks and immediately cooled on ice. These samples and untreated spore suspension were further diluted to 10^3 conidia mL^{-1} . Of each dilution, 100 μL of was used to inoculate MEA plates, resulting in inoculation of 10^6 , 10^5 , 10^4 , 10^3 and 10^2 conidia per plate. After 3 days incubation at 25 °C, colonies were counted and pictures of the plates were made. The inactivation curves were described by a linear regression ($R^2 > 0.98$). D -values were calculated by $\frac{-1}{\text{slope}}$.

2.2.4 Microscopy

Pictures of conidia suspensions were taken with a Zeiss AX10 microscope with 1000x magnification. Surfaces of 3-day-old colonies of *P. variotii* DTO 032-I3, DTO 212-C5 and DTO 217-A2 were studied by means of stereo microscopy with a Nikon SMZ25. Both microscopes were equipped with a Nikon DS-Ri2 camera.

For cryo-electron scanning microscopy (cryoSEM), small rectangular 5 x 5 mm blocks of agar were carefully excised at the rim of colonies with a scalpel and transferred into a copper cup for rapid freezing in nitrogen slush. The agar blocks were glued with frozen tissue medium (KP-Cryoblock; Klinipath, Duiven, The Netherlands) into the copper cup, which was placed on the transfer rod. The sample was coated 3 min (3 times 1 min) using a gold target. Electron microscopy was done with a JEOL 5600LV scanning electron microscope (JEOL, Tokyo, Japan) equipped with an Oxford CT1500 Cryostation. Electron micrographs were taken at an acceleration voltage of 2.5-5 kV.

2.2.5 Spore size distributions and measuring spore size

After harvesting the conidia, the spore suspensions were diluted 2 10^3 times in ISOTON II diluent (Beckman Coulter, Fichtenhain, Germany). A volume of 100 μL was used to determine spore size concentration and size distributions by a Beckman Coulter Counter Multisizer3 equipped with a 70 μm aperture tube. Approximately 10^3 data points were extracted and used for further analysis. Size of particles is expressed by the equivalent spherical diameter in μm . Conidia with a diameter < 2 and > 8 μm were excluded from the dataset. Particle volumes were calculated by $V = \frac{4}{3}\pi\left(\frac{\text{Diameter}}{2}\right)^3$.

A concentration of 2 10^7 conidia mL^{-1} was used to measure the spore size distribution by a fluorescence-activated cell sorter (FACS) machine (FACSVerse™; Becton Dickinson, Franklin Lakes, NJ, USA). The forward scatter (FSC) values of the particles were used as size parameter. A thousand data points were extracted from the dataset and used for further analysis.

Spore size distributions were analysed by the R package mixtools (Benaglia *et al.*, 2009). With the boot.comp function, we evaluated if we could describe the distributions by

a two-component mixture model by a parametric bootstrap. The data were bootstrapped 10^3 times. Subsequently, we computed the mixture model using expectation-maximization (EM) algorithm by the `normalmixEM` function. Next, a parametric bootstrap with 10^3 bootstrap samples was performed for standard error approximation of the parameters in the mixture model using the `boot.se` function.

2.2.6 Compatible solute concentrations

To extract the compatible solutes, 10^8 conidia were centrifuged 1 min at 21000 g at 4 °C. The supernatant was discarded and the pellet was flash-frozen in liquid nitrogen. After adding 2 stainless steel beads (diameter 3.2 mm), the tubes were transferred into pre-cooled adapters at -80 °C and the pellet was homogenized for 6 min at 30 Hz in a Qiagen Tissuelizer. Subsequently, 1 mL water was added to the broken conidia and samples were placed in a water bath at 95 °C for 30 min. Samples were centrifuged at 20,817 g for 30 min at 4 °C and the supernatant was filtered through an Acrodisc 0.2 µm nylon syringe filter (Pall Life Science, Mijdrecht, The Netherlands). Samples were stored at -20 °C, prior to HPLC analysis.

The HPLC equipment consisted of a Waters 515 HPLC pump (0.6 mL min^{-1}) with control module, a Waters 717 plus Autosampler and a Waters IR 2414 Refractive Index detector. To achieve a better separation between glycerol and mannitol, two Waters Sugar-Pak I columns, were placed in line and kept at 70 °C in a WAT380040 column heater module. A sample volume of 20 µL was injected on the mobile phase consisting of 0.1 mmol L^{-1} Ca EDTA in ultrapure water and samples were followed for 30 minutes. A mixture of trehalose, glucose, glycerol, erythritol, mannitol and arabitol (0.002 – 0.10% w/v) was used as reference. All calibration curves showed an $R^2 > 0.999$ with a limit of detection $< 0.0005\%$ (w/v) for each compatible solute. Empower software (Waters, Etten-Leur, the Netherlands) was used for peak integration and quantification. The mean volume of the conidia measured by the Coulter Counter was used to calculate the concentration.

2.2.7 Germination under salt stress

To study germination under salt stress conditions, 10^4 conidia were inoculated into a 96 wells plate in 100 µL complete medium (CM) (de Vries *et al.*, 2004) supplemented with an additional 0, 0.5, 1.0, 1.5 mol L^{-1} NaCl. Germination was followed in an oCelloScope (Philips BioCell A/S, Denmark) for 48 hours at 25 °C (Fredborg *et al.*, 2013). To allow the conidia to sediment, measurements started after 1 hour of incubation (Aunsbjerg *et al.*, 2015). Pictures were made each 30 minutes with a 4 times lens magnification factor and analysed with the UniExplorer software (version 8.1.0.7424, BioSense). The BCAnormalized algorithm was used to quantify the optical growth at each data point. BCAnormalized was further analysed using the R package `grofit` (Kahm *et al.*, 2010). Maximum growth rate μ ($\Delta\text{BCA hour}^{-1}$) was calculated by fitting a Gompertz curve to the BCAnormalized data.

2.3 RESULTS

2.3.1 Screening conidia for heat resistance

A total of 108 *P. variotii* isolates were used in this study. The strains were isolated from various substrates and locations, of which most originated from the USA or the Netherlands (Table 2.1). Of the 108 strains, 65 were isolated from food products or industry environment, 27 originated from indoor and outdoor environments and 16 were medical isolates from human patients or from a hospital environment. All strains were identified by DNA sequencing of the β -tubulin locus (Samson *et al.*, 2009). A Maximum Likelihood tree revealed that all *P. variotii* strains grouped together and were separated from *Paecilomyces brunneolus*, the closest related species, with a bootstrap value of 100% (Fig. 2.1). More intraspecific clades were identified than described before (Houbraken *et al.*, 2008). However, most of these clades showed bootstrap values below 70%. Within the *P. variotii* group, the overall mean distance was 0.013 ± 0.003 substitutions per site, indicating a low variation between the strains. Like recently described, the β -tubulin gene from the draft genome of the previously mis-identified *Paecilomyces formosus* No5. as *P. variotii*, groups with the type strain of *P. formosus* in the tree (Oka *et al.*, 2014; Urquhart *et al.*, 2018).

In order to study the variation of heat resistance of conidia among the different strains, conidia of each strain were heat-inactivated in a water bath at 58 or 59 °C for 10 minutes.

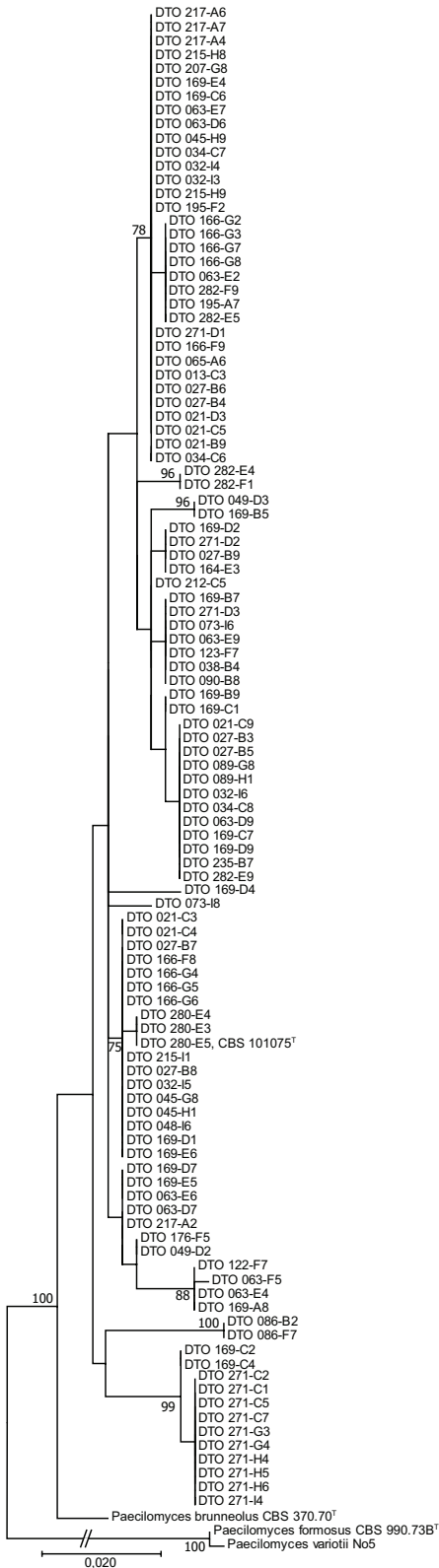


Figure 2.1. Maximum Likelihood tree of the partial β -tubulin gene of all the *P. variotii* strains used in this study. The type strain of *P. brunneolus* and *P. formosus* were used as outgroup. At the nodes, Bootstrap values > 70% are shown.

Subsequently, conidia survival was determined by inoculating 10^3 conidia on MEA. After three days incubation at 25 °C, the number of colonies was counted. For 31 isolates, more than 10% of the conidia survived the 59 °C heat treatment and showed more than 100 colonies on plates (Fig. S2.1). The remaining 77 strains showed a broad variety in the number of colonies, stretching from one to 94. After the 10-minute-heat treatment at 58 °C, 68 isolates showed more than 100 colonies after the treatment, while 40 strains showed between 13 and 95 colonies.

Table 2.1. Overview of the *P. variotii* isolates used in this chapter.

DTO no.	CBS no.	Substrate	Location	Genbank no. β -tubulin
DTO 013-C3		Indoor environment	The Netherlands	MN153213
DTO 021-B9		Spoiled sports drink	USA	MN153214
DTO 021-C3	CBS 145656	Spoiled sports drink	USA	MN153215
DTO 021-C4		Spoiled sports drink	USA	MN153216
DTO 021-C5		Spoiled sports drink	USA	MN153217
DTO 021-C9		Heat shocked sucrose	USA	MN153218
DTO 021-D3	CBS 145657	Heat shocked sucrose	USA	MN153219
DTO 027-B3	CBS 121577	Spoiled sports drink	USA	EU037084
DTO 027-B4	CBS 121578	Spoiled sports drink	USA	EU037083
DTO 027-B5	CBS 121579	Sucrose	USA	EU037082
DTO 027-B6	CBS 121580	Spoiled apple juice	The Netherlands	EU037081
DTO 027-B7	CBS 121581	Spoiled sweetened tea	USA	EU037080
DTO 027-B8	CBS 121582	Spoiled sweetened tea	USA	EU037079
DTO 027-B9	CBS 121583	Spoiled sports drink	USA	EU037078
DTO 032-I3	CBS 121585	High Fructose Corn Syrup after heat shock	USA	EU037077
DTO 032-I4	CBS 121586	Spoiled bottle of bottle of sweetened tea	USA	EU037076
DTO 032-I5	CBS 121587	Spoiled sports drink	USA	EU037075
DTO 032-I6	CBS 121588	Heat shocked sucrose	USA	EU037074
DTO 034-C6	CBS 729.96	Beach sand	Spain	MN153220
DTO 034-C7	CBS 108945	Pectin	The Netherlands	MN153221
DTO 034-C8	CBS 110036	Cerebrospinal fluid of 60-year-old female with diabetes and cancer	Turkey	MN153222
DTO 038-B4	CBS 115809	Horse stable, air sample	Germany	MN153223
DTO 045-G8	CBS 145658	Drink	USA	MN153224
DTO 045-H1		Drink	USA	MN153225
DTO 045-H9		Pseudo-outbreak	UK	GU968685
DTO 048-I6		Pseudo-outbreak	UK	MN153226
DTO 049-D2		Unknown (patient, or hospital environment)	UK	MN153227

Table 2.1. (Continued).

DTO no.	CBS no.	Substrate	Location	Genbank no. β-tubulin
DTO 049-D3		Unknown (patient, or hospital environment)	UK	MN153228
DTO 063-D6		Human; mouthwash	The Netherlands	GU968692
DTO 063-D7		Human; feces	The Netherlands	GU968693
DTO 063-D9		Human; mouthwash	The Netherlands	GU968695
DTO 063-E2		Unknown (patient, or hospital environment)	The Netherlands	GU968677
DTO 063-E4		Unknown (patient, or hospital environment)	The Netherlands	GU968679
DTO 063-E6		Unknown (patient, or hospital environment)	The Netherlands	GU968680
DTO 063-E7		Human; cerebral spinal fluid	The Netherlands	GU968681
DTO 063-E9		Human; mouthwash	The Netherlands	GU968682
DTO 063-F5		Human; abscess	The Netherlands	MN153229
DTO 065-A6		Indoor environment	Germany	MN153230
DTO 073-I6		Unknown (patient, or hospital environment)	The Netherlands	MN153231
DTO 073-I8		Unknown (patient, or hospital environment)	The Netherlands	MN153232
DTO 086-B2		Archive	The Netherlands	MN153233
DTO 086-F7		Filter flow cabinet Westerdijk institute	The Netherlands	MN153234
DTO 089-G8		Air in bedroom	The Netherlands	MN153235
DTO 089-H1		Air in bedroom	The Netherlands	MN153236
DTO 090-B8		Archive	The Netherlands	MN153237
DTO 122-F7		Bakery	Germany	MN153238
DTO 123-F7		Indoor environment	Germany	MN153239
DTO 164-E3	CBS 145659	Blueberry ingredients	The Netherlands	MN153240
DTO 166-F8		Ice pop, heat treated	The Netherlands	MN153241
DTO 166-F9		Ice pop, heat treated	The Netherlands	MN153242
DTO 166-G2		Pectin, heat treated	The Netherlands	MN153243
DTO 166-G3		Pectin, heat treated	The Netherlands	MN153244
DTO 166-G4	CBS 145660	Pectin, heat treated	The Netherlands	MN153245
DTO 166-G5		Pectin, heat treated	The Netherlands	MN153246
DTO 166-G6		Pectin, heat treated	The Netherlands	MN153247
DTO 166-G7		Pectin, heat treated	The Netherlands	MN153248
DTO 166-G8		Pectin, heat treated	The Netherlands	MN153249
DTO 169-A8		Indoor environment	USA	MN153250
DTO 169-B5		Indoor environment	USA	MN153251

Table 2.1. (Continued).

DTO no.	CBS no.	Substrate	Location	Genbank no. β-tubulin
DTO 169-B7		Indoor environment	USA	MN153252
DTO 169-B9		Indoor environment	USA	MN153253
DTO 169-C1		Indoor environment	USA	MN153254
DTO 169-C2		Indoor environment	USA	MN153255
DTO 169-C4		Indoor environment	USA	MN153256
DTO 169-C6	CBS 145661	Indoor environment	USA	MN153257
DTO 169-C7		Indoor environment	USA	MN153258
DTO 169-D1		Indoor environment	USA	MN153259
DTO 169-D2		Indoor environment	USA	MN153260
DTO 169-D4		Indoor environment	USA	MN153261
DTO 169-D7		Indoor environment	USA	MN153262
DTO 169-D9		Indoor environment	USA	MN153263
DTO 169-E4		Indoor environment	USA	MN153264
DTO 169-E5	CBS 145662	Indoor environment	USA	MN153265
DTO 169-E6		Indoor environment	USA	MN153266
DTO 176-F5		Seal of Tetra package	Germany	MN153267
DTO 195-A7		Margarine	Belgium	MN153268
DTO 195-F2	CBS 145663	Margarine	Belgium	MN153269
DTO 207-G8	CBS 145664	Fruit, ingredient	The Netherlands	MN153270
DTO 212-C5	CBS 145665	Vanilla	The Netherlands	MN153271
DTO 215-H8		Ice pop, heat treated	The Netherlands	MN153272
DTO 215-H9		Ice pop, heat treated	The Netherlands	MN153273
DTO 215-I1		Ice pop, heat treated	The Netherlands	MN153274
DTO 217-A2	CBS 145666	Ice pop, heat treated	The Netherlands	MN153275
DTO 217-A4		Pectin	The Netherlands	MN153276
DTO 217-A6		Pectin	The Netherlands	MN153277
DTO 217-A7		Pectin	The Netherlands	MN153278
DTO 235-B7		Apple mixture	The Netherlands	MN153279
DTO 271-C1		Ice tea	South Africa	MN153280
DTO 271-C2		Ice tea	South Africa	MN153281
DTO 271-C5		Ice tea	South Africa	MN153282
DTO 271-C7		Ice tea	South Africa	MN153283
DTO 271-D1		Industry environment	Unknown	MN153284
DTO 271-D2		Industry environment	Unknown	MN153285
DTO 271-D3	CBS 145667	Industry environment	Guatamala	MN153286
DTO 271-G3	CBS 145668	Ice tea	South Africa	MN153287

Table 2.1. (Continued).

DTO no.	CBS no.	Substrate	Location	Genbank no. β -tubulin
DTO 271-G4		Ice tea	South Africa	MN153288
DTO 271-H4		Ice tea	South Africa	MN153289
DTO 271-H5		Ice tea	South Africa	MN153290
DTO 271-H6		Ice tea	South Africa	MN153291
DTO 271-I4		Ice tea	South Africa	MN153292
DTO 280-E3	CBS 109072	Pectin	The Netherlands	EU037071
DTO 280-E4	CBS 109073	Pectin	The Netherlands	EU037070
DTO 280-E5	CBS 101075 [†]	Heat processed fruit beverage	Japan	EU037069
DTO 282-E4		Food product isolate	Unknown	MN153293
DTO 282-E5	CBS 145669	Margarine	Italy	MN153294
DTO 282-E9		Recycled paper packaging	Brazil	MN153295
DTO 282-F1		Recycled paper packaging	Brazil	MN153296
DTO 282-F9	CBS 145670	Wall covering, industry environment	UK	MN153297

[†] Type strain.

2.3.2 In-depth analysis of three strains

Strains DTO 032-I3, DTO 212-C5 and DTO 217-A2 were selected for an in-depth analysis in conidial heat resistance, morphology and compatible solute composition. Based on the screening, conidia from strain DTO 032-I3 were rather heat sensitive, showing 70 and 26 colonies after treatment at 58 and 59°C, respectively. Conidia from strain DTO 212-C5 were among the most heat sensitive, showing 58 and 3 colonies after heat treatment at 58 and 59°C, respectively. In contrast, conidia of strain DTO 217-A2 showed high heat resistance as judged by the outgrowth of more than 100 colonies after both heat treatments (Fig. 2.2A). D_{60} -values were determined to quantify the heat resistance of the conidia of the three strains. To this end, conidia were treated in a water bath at 60°C for different periods and plated. DTO 032-I3, DTO 212-C5 and DTO 217-A2 showed a D_{60} -value of 5.5 ± 0.35 , 3.7 ± 0.08 and 22.9 ± 2.00 minutes, respectively (Fig. 2.2B). In the case of DTO 032-I3 and DTO 212-C5, a log 6 reduction was achieved in 33 and 20 minutes, respectively. Strain DTO 217-A2 showed less than log 3 inactivation after 60 minutes of heat treatment. The inactivation kinetics of strain DTO 032-I3, DTO 212-C5 and DTO 217-A2 revealed a linear character and showed an $R^2 = 0.996$, 0.998 , and 0.989 , respectively. These results indicate that the D_{60} -value of conidia among the three strains varies 6.2 times.

The morphology of colonies and conidiophores (spore-forming structures) of the three strains was studied in detail. Stereo-microscopy and cryo electron microscopy of three-day old colonies showed variation in appearance. Heat resistant strain DTO 217-A2 showed colonies that formed spores at conidiophore heads that were present near

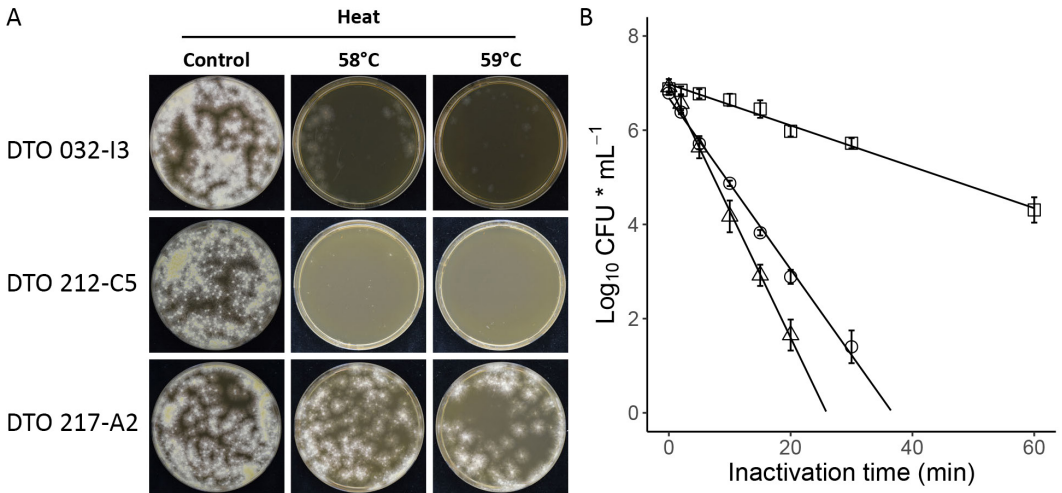


Figure 2.2. Strain variation in heat resistance of dormant *P. variotii* conidia. (A) The screening results of the strains used for the in-depth analysis. The numbers indicate the amount of colonies on plate. After heat treatments at 58 and 59 °C for 10 minutes, DTO 217-A2 showed least reduction in number of colonies and growth. The most sensitive conidia were formed by DTO 212-C5. (B) Inactivation curves of conidia at 60 °C. DTO 217-A2 (□) produced most heat resistant conidia with a D_{60} -value of 22.9 minutes. The most heat sensitive conidia were produced by DTO 212-C5 (Δ) with a D_{60} -value of 3.7 minutes and the conidia of DTO 032-I3 (○) showed a D_{60} -value of 5.5 minutes. Mean values of three biological replicates ± SD are shown.

the agar surface, designated as velvety (Fig. 2.3A, 2.3B). DTO 032-I3 produced more aerial structures, mostly elongated conidiophores, compared to DTO 217-A2 (Fig. 2.3B, 2.3E). On the other hand, heat sensitive strain DTO 212-C5 showed extensive formation of aerial hyphae with interspersed conidiophores (Fig. 2.3C, 2.3F). According to *Penicillium* morphology, the appearance of DTO 212-C5 could be designated as lanose (Samson *et al.*, 2019). These results showed that the colony morphology of *P. variotii* strains vary in branching patterns and formation of aerial structures.

In another strain (CBS 121579), a large variation in the size of conidia could be observed. Interestingly, conidia within a spore chain had the same size, but large variation was found between different chains of conidia (Fig. S2.2). Light microscopy (LM) pictures confirmed that colonies of strains DTO 032-I3, DTO 212-C5 and DTO 217-A2 produced conidia of various sizes (Fig. 2.4A). In addition, these pictures suggested that differences in size might occur between the strains. To study the spore size distribution in more detail, spore size of the three strains were measured by flow cytometry (FACS) and Coulter Counter (CC). We tested if we could describe the distributions by one component ($k=1$, normal distribution) or two components ($k=2$, bimodal distribution) by bootstrapping the data. In all cases, the three strains showed $P(k>1) < 0.001$ for the FACS data, as well for CC data. This suggests that the spore size distributions were heterogeneously distributed and that it is valid to describe spore size by means of two components. To this end, we computed a two-component mixture model using an expectation-maximization (EM) algorithm for each

distribution (Fig. 2.4B, 2.4C). In this model, component 1 and 2 represent subpopulations of small and large spores, respectively. The mean spore size (diameter in μm) of the total population and the two subpopulations, as well as the standard deviation (σ) and the weight (λ) of the two subpopulations are summarized in Table 2.2. The histograms of the spore size distributions measured by FACS and CC showed large similarity. Least variation in spore size was found for conidia produced by strain DTO 032-I3, while most

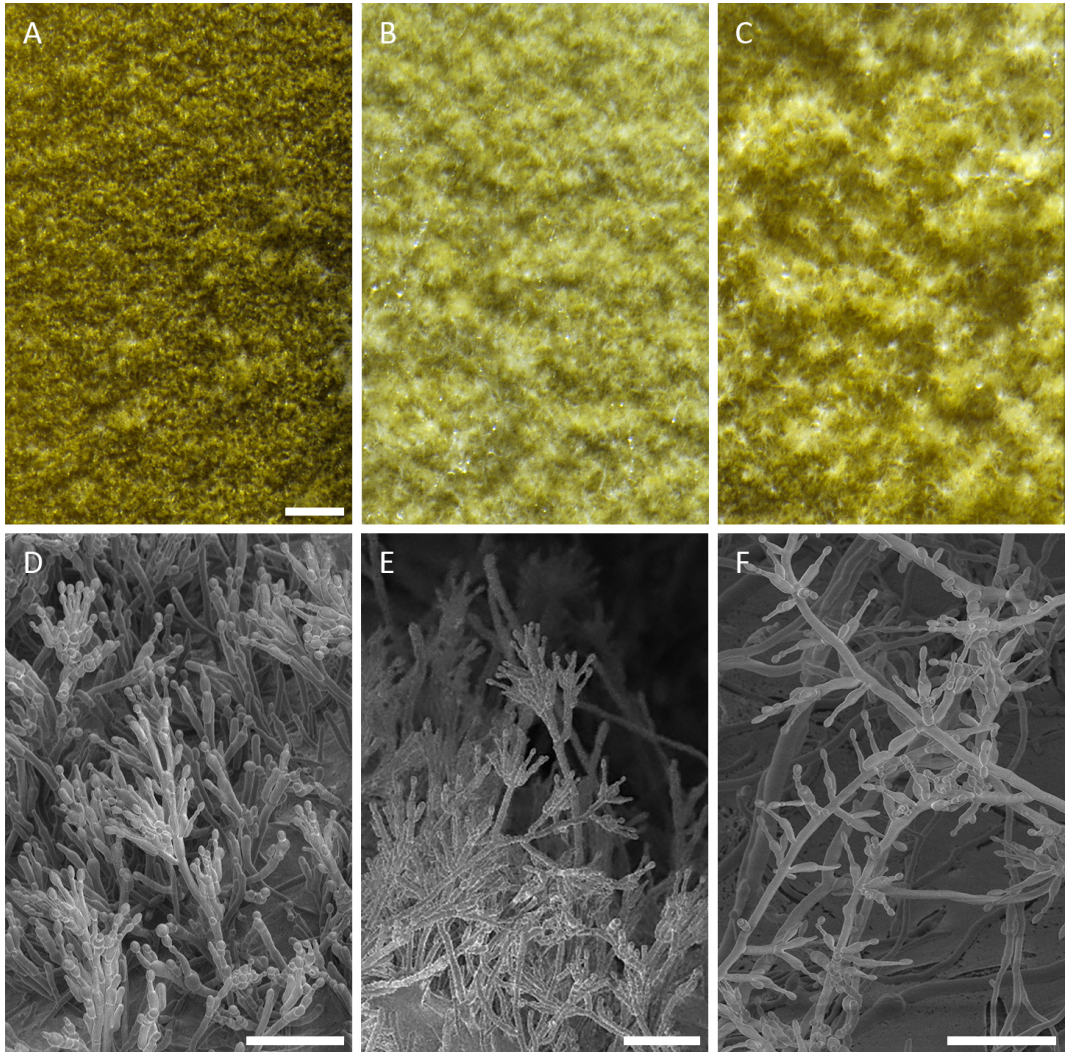


Figure 2.3. Colony morphology of DTO 217-A2 (A, D), DTO 032-I3 (B, E) and DTO 212-C5 (C, F). The stereo microscopy pictures show a detailed top view of a three-day-old colony (A-C). DTO 217-A2 produced short aerial hyphae with conidiophores and showed a velvety appearance. On the other hand, DTO 212-C5 produced aerial structures with conidiophores to a large extent and has a lanose appearance. DTO 032-I3 showed a morphology between the other two strains, it also produced larger aerial structures, but not as extensively as DTO 212-C5. CryoSEM pictures confirmed these findings (D-F). Scale bars indicate 500 μm (A-C) or 50 μm (D-F).

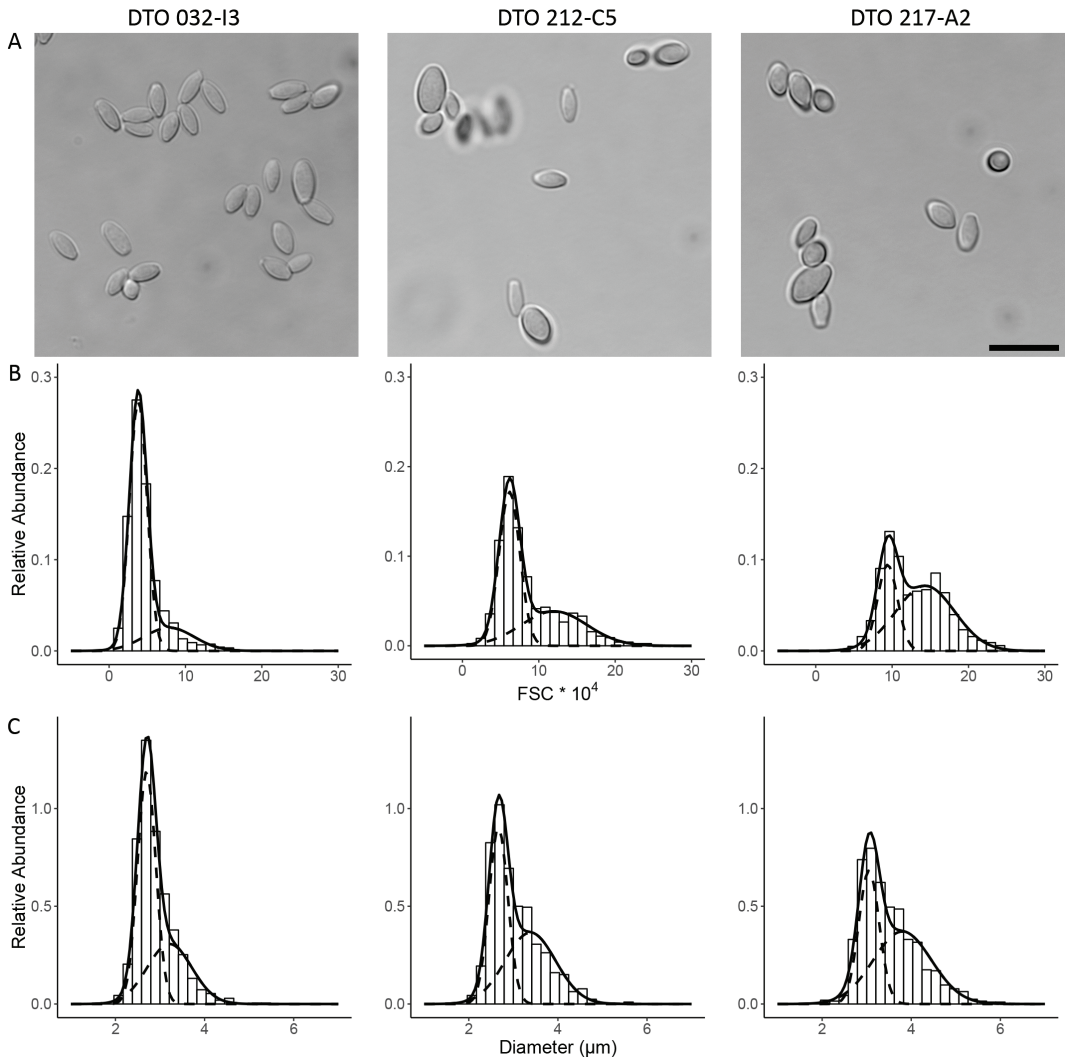


Figure 2.4. Conidia size distributions of DTO 032-I3, DTO 212-C5 and DTO 217-A2. (A) LM pictures of conidia of various sizes produced by a single colony. Histograms show spore size distributions as measured by flow cytometry (B) and Coulter Counter (C). Dashed lines indicate two computed subpopulations of small and large spores. The black line indicates the sum of the two subpopulations. The total surface area of each histogram equals 1.

variation was found for conidia of DTO 217-A2. For DTO 032-I3, the CC data showed that the weight of the subpopulation containing the small spores ($\lambda_1 = 0.61$) is larger than the subpopulation of large spores ($\lambda_2 = 0.39$). In contrast, DTO 217-A2 showed a larger weight for the subpopulation of large spores ($\lambda_1 = 0.39$, $\lambda_2 = 0.61$), while the weight of the subpopulations of DTO 212-C5 was almost equal ($\lambda_1 = 0.48$, $\lambda_2 = 0.52$). DTO 217-A2 produced the largest mean conidia size with a diameter of 3.51 μm , while DTO 032-I3 and DTO 212-C5 showed a mean conidia size of 2.90 and 3.04 μm , respectively. It is noteworthy that the subpopulation of small spores of DTO 217-A2 showed a larger mean

Table 2.2. Conidia size heterogeneity of colonies grown on MEA as measured by Coulter Counter (CC). Spore sizes are expressed by diameter (μm) of the spherical equivalent (Heywood diameter) for the CC data. The mean spore size is shown for the total population ($\text{size}_{\text{total}}$) and two subpopulations (size_1 and size_2) as used in the modelling. The standard deviation of the size distributions and the relative weight of each subpopulation is expressed by σ and λ , respectively. All values are shown \pm the bootstrapped SE.

Strain	Size _{total}	Size ₁	Size ₂	σ_1	σ_2	λ_1	λ_2
DTO 032-I3	2,90 \pm 0,01	2,70 \pm 0.01	3,21 \pm 0.11	0,21 \pm 0.01	0,50 \pm 0.04	0,61 \pm 0.07	0,39 \pm 0.07
DTO 212-C5	3,04 \pm 0,02	2,67 \pm 0.06	3,38 \pm 0.01	0,21 \pm 0.03	0,57 \pm 0.01	0,48 \pm 0.05	0,52 \pm 0.05
DTO 217-A2	3,51 \pm 0,02	3,05 \pm 0.01	3,80 \pm 0.07	0,23 \pm 0.01	0,65 \pm 0.06	0,39 \pm 0.05	0,61 \pm 0.05

spore size than the total population of the other two strains. Together, results show that heterogeneity in conidia size is not only found between strains, but also within strains.

Compatible solute composition of the three strains was assessed. Since we found differences in spore size between the strains, levels were corrected with the mean spore volumes measured by CC. This allowed us to estimate the internal conidia concentration of trehalose, glycerol, mannitol and arabitol (Fig. 2.5). Conidia contained predominantly trehalose. The heat resistant conidia of DTO 217-A2 contained a concentration of trehalose that was 40% higher compared to the other two strains. This might explain the differences in heat resistance. On the other hand, DTO 032-I3 conidia contained significantly more mannitol, while DTO 212-C5 conidia contained more arabitol. In all strains, minor amounts of glycerol were found, but without significant differences. Together, the three strains tested showed a different compatible solute composition. Results suggest that a lower trehalose concentration is compensated by other compatible solutes as mannitol or arabitol.

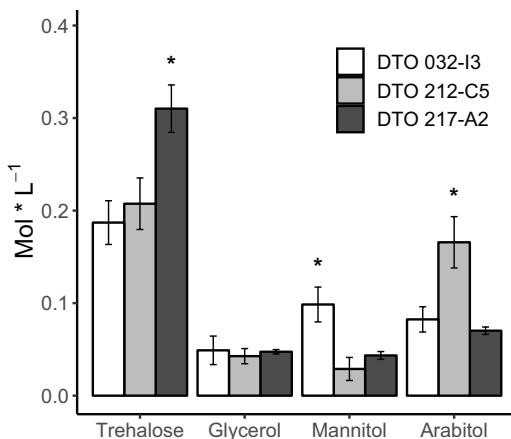


Figure 2.5. Compatible solute composition of three strains in mol L^{-1} . Mean values of three biological replicas are shown \pm SD. Asterisk indicates statistic significant differences of one strain compared to the other two strains (TukeyHSD $P < 0.01$).

The differences in compatible solute composition could point towards adaptation to different stress conditions. For this reason, we assessed if we could find a difference between strains in germination and early growth rates in NaCl enriched medium. Germination of conidia and early growth rates in complete medium (CM), supplemented with various concentrations of NaCl, was followed for 48 hours using the oCelloScope. Photos were taken every 30 minutes. After 24 hours, pictures of germinated conidia at 1 M NaCl showed differences between strains (Fig. 2.6A-C). DTO 032-I3 and DTO 212-C5 showed more growth than DTO 217-A2. In addition, we used the background

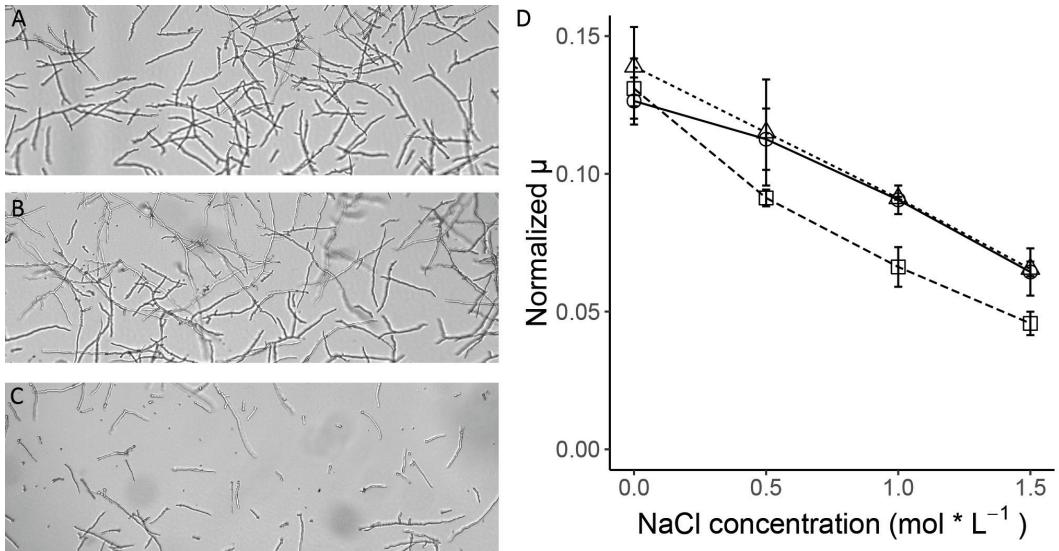


Figure 2.6. Growth of three *P. variotii* strains on NaCl supplemented media. Germination and growth was studied in a 96 wells plate in an oCelloScope for 48 hours. Pictures were taken of each well every 30 minutes. After 24 hours, DTO 032-I3 (A) and DTO 212-C5 (B) showed more growth than DTO 217-A2 (C) at 1.0 mol L⁻¹ NaCl. (D) The maximum growth rate (μ) of DTO 032-I3 (◻, solid line), DTO 212-C5 (Δ, dotted line) and DTO 217-A2 (◻, dashed line) was calculated by fitting a Gompertz curve to the background corrected absorption (BCA) at various NaCl concentrations. The mean of biological triplicates \pm SD are shown.

corrected absorption (BCA) algorithm provided by the oCelloScope software to model early growth rates. This algorithm measures object pixel intensities, which increases during germination and early growth. The maximum growth rate (μ) was calculated by fitting Gompertz curve to the BCA values. For all three strains, a lower μ was found when the medium was enriched with NaCl (Fig. 2.6D). Lowest μ was found at the highest NaCl concentrations. In all samples in medium with additional NaCl, μ was higher for DTO 032-I3 and DTO 212-C5 compared to DTO 217-A2. No difference was found in the control samples in medium without additional NaCl. This implies that DTO 032-I3 and DTO 212-C5 are better adapted to salt stress and germinate faster under salt stress compared to heat resistant strain DTO 217-A2.

2.4 DISCUSSION

In this study, we explored strain variability in conidial heat resistance of the food spoilage fungus *P. variotii*. Conidia of 108 isolates were screened, which resulted in a good overview of the variation in sensitivity to heat stress. Three strains were selected to characterize the heat resistance in more detail as well as morphology, spore size distribution, compatible solute composition and growth under salt stress conditions. In all aspects, we found differences between the three selected strains. To our knowledge, *P. variotii* DTO 217-

A2 conidia showed the highest D -value (i.e. 22.9 minutes) for this cell type at 60 °C ever measured. Compared to DTO 032-I3 and DTO 212-C5, DTO 217-A2 conidia were more heat resistant, produced less aerial structures, and larger conidia with higher trehalose concentration. On the other hand, DTO 217-A2 showed less growth and slower germination under salt stress conditions.

D_{60} -values of *P. variotii* conidia were in the same range as *Saccharomyces cerevisiae* ascospores, which showed D_{60} -values between 4.6 and 22.5 minutes (Milani *et al.*, 2015; Put and Jong, 1982). In general, conidial heat resistance is evaluated at temperatures lower than 60 °C, because conidia of most species do not survive heat treatments at this temperature for several minutes (Wyatt *et al.*, 2013). However, we showed that inactivation at 60 °C revealed large differences between the tested *P. variotii* strains. In a study with xerophilic fungi, the most heat resistant conidia of *Aspergillus ruber* showed 3% survival after a 10 minute heat treatment at 60 °C (Pitt and Christian, 1970). Conidia of *A. niger* showed a D_{60} -value of 2.2 minutes, about 10 times lower than *P. variotii* DTO 217-A2 (Baggerman, 1981). Although no D -values were determined, comparable heat resistance was found for *A. fumigatus* conidia (Hagiwara *et al.*, 2017). After a 15-minute heat treatment at 60 °C, approximately 7% of the conidia survived when cultures were grown at 25 °C. This would roughly correspond to a D_{60} -value of 13 minutes. Interestingly, increasing the culture incubation temperature to 37 and 45 °C dramatically increased the heat resistance of *A. fumigatus* conidia and hardly showed any reduction after identical heat treatments (Hagiwara *et al.*, 2017). These findings suggest that the limits of *P. variotii* conidial heat-resistance could possibly be stretched further by growing cultures at higher temperatures.

The heat resistance of *P. variotii* ascospores is much higher than observed for the conidia. Ascospores of closely related *Paecilomyces fulvus* and *Paecilomyces niveus* (both species have a byssochlamys-morph) survive heat treatments of 85 °C for several minutes (Beuchat and Rice, 1979; Dijksterhuis, 2019). The ascospores of *P. variotii* are possibly even more heat resistant, surviving 85 °C for more than an hour, although D -values are not accurately measured (Houbraken *et al.*, 2006). Ascospores are produced after mating of two compatible strains and formed within the mycelium and as such not distributed easily compared to airborne conidia. It has to be expected that ascospores can spoil food that is extensively (heat) processed, although being present at very low numbers (dos Santos *et al.*, 2018). On the other hand, ubiquitous air-borne conidia would contaminate mildly heat-treated processed food products. This is a subject that will need attention in future research, as well as the question if heat-resistant conidia forming strains also form more resistant ascospores.

Over the past decades, various HPLC methods and enzymatic assays have been developed to quantify internal compatible solute compositions (Al-Bader *et al.*, 2010; D'Enfert and Fontaine, 1997; Hagiwara *et al.*, 2014; Hallsworth and Magan, 1994a; van Leeuwen *et al.*, 2013a; Nguyen Van Long *et al.*, 2017a; Novodvorska *et al.*, 2013; Sakamoto *et al.*, 2009). These methods usually do not consider spore size and give values in pg spore⁻¹, or μmol (g dry weight)⁻¹. By obtaining accurate data about the cell volumes

by Coulter Counter, we were allowed for the first time to estimate the internal concentration of compatible solutes in fungal spores. *P. variotii* conidia showed a predominant concentration of trehalose, similar to *A. fumigatus* conidia (Hagiwara *et al.*, 2017). Despite the larger conidia size of heat resistant strain DTO 217-A2 compared to DTO 032-I3 and DTO 212-C5, the conidia of this strain contained a significant higher concentration of trehalose.

Interestingly, HPLC analysis showed that DTO 212-C5 conidia contained higher arabitol concentrations than DTO 032-I3 and DTO 217-A2. Arabitol is described to accumulate in fungal spores and vegetative cells under intermediate osmotic stress conditions (Hallsworth and Magan, 1994b; Rangel *et al.*, 2015; Ruijter *et al.*, 2004). Like glycerol, it has a lower molecular weight and higher solubility than trehalose and mannitol. Therefore, this compatible solute can accumulate at higher concentrations to protect cells better to osmotic stress conditions (de Lima Alves *et al.*, 2015). For this reason, we tested if we could find differences in germination and early growth under NaCl stress conditions between the three strains. DTO 217-A2 showed to have a lower maximum growth rate under the salt stress condition compared to the other two strains. Surprisingly, DTO 032-I3 was equally adapted to salt stress conditions as DTO 212-C5, while it showed a comparable arabitol concentration as DTO 217-A2. Although more mannitol was found in DTO 032-I3 conidia, mannitol can only be involved in osmoregulation to a limited extent due to its low solubility (de Lima Alves *et al.*, 2015). The ability to grow under NaCl stress is determined by the accumulation of compatible solutes in germinating spores and mycelium and not of dormant conidia. Possibly, measuring the mycelial compatible solutes would provide information in how these strains adapt to NaCl stress. Nevertheless, with this experiment we have shown that the three strains react differently to NaCl stress, implying that the three isolates are adapted to different stress environments.

The β -tubulin based phylogenetic analysis revealed that all isolates used in this study belong to *Paecilomyces variotii* (Samson *et al.*, 2009). Among the 108 strains sequence variation was found, resulting in formation of various clades. However, the bootstrap values <70% of most clades indicate that this variation is statistically irrelevant to the phylogeny (Hillis and Bull, 1993). Furthermore, low bootstrap values indicate that recombination events occur in the *P. variotii* isolates. We did not find indications that conidial-heat resistance is correlated with the position in the β -tubulin tree (data not shown). The strains that showed more than 100 colonies after the 10-minute heat treatment of conidia at 59 °C were positioned in various clades in the tree. In addition, we could not find a link between conidial heat resistance and the geographic origin and the substrate of isolation. Together, these results suggest that the variation found among the strains could be the same at every location and environment.

Notably, variation was found between the colony morphology of the three strains. Largest differences were found between DTO 217-A2 and DTO 212-C5 that produced conidia on short and long conidiophores, respectively. Conidia formed on these different aerial structures may develop differently. In addition, spore size distributions were different

between the three strains with respect to range, bimodal distribution and average size. The resistant strain produced relatively more conidia of large size than the two sensitive strains. These data show that heterogeneity occur between strains, but also within strains. This heterogeneity in size distribution was confirmed with two different counting techniques, namely flow cytometry and Coulter Counter. A bimodal spore size distribution has been observed earlier in the case of *Gloeosporium orbiculare* (Chapela, 1991). This, however, is certainly not common for other species. *Penicillium glabrum*, *Penicillium roqueforti* and *A. niger* showed narrow and symmetrical distributions (unpublished results).

Together, heterogeneity in conidia can be found within and between *P. variotii* strains. Physiological heterogeneity may be beneficial for *P. variotii* by enhancing its ability to adapt to different environments (Hewitt *et al.*, 2016). In fact, this might be one of the reasons why *P. variotii* can be isolated from a broad range of environments. With the recently sequenced genomes and the development of molecular tools, *P. variotii* conidia could potentially be a useful model to study fungal spore resistance and heterogeneity on a genetic and molecular level (Urquhart *et al.*, 2018).

2.5 SUPPLEMENTARY DATA

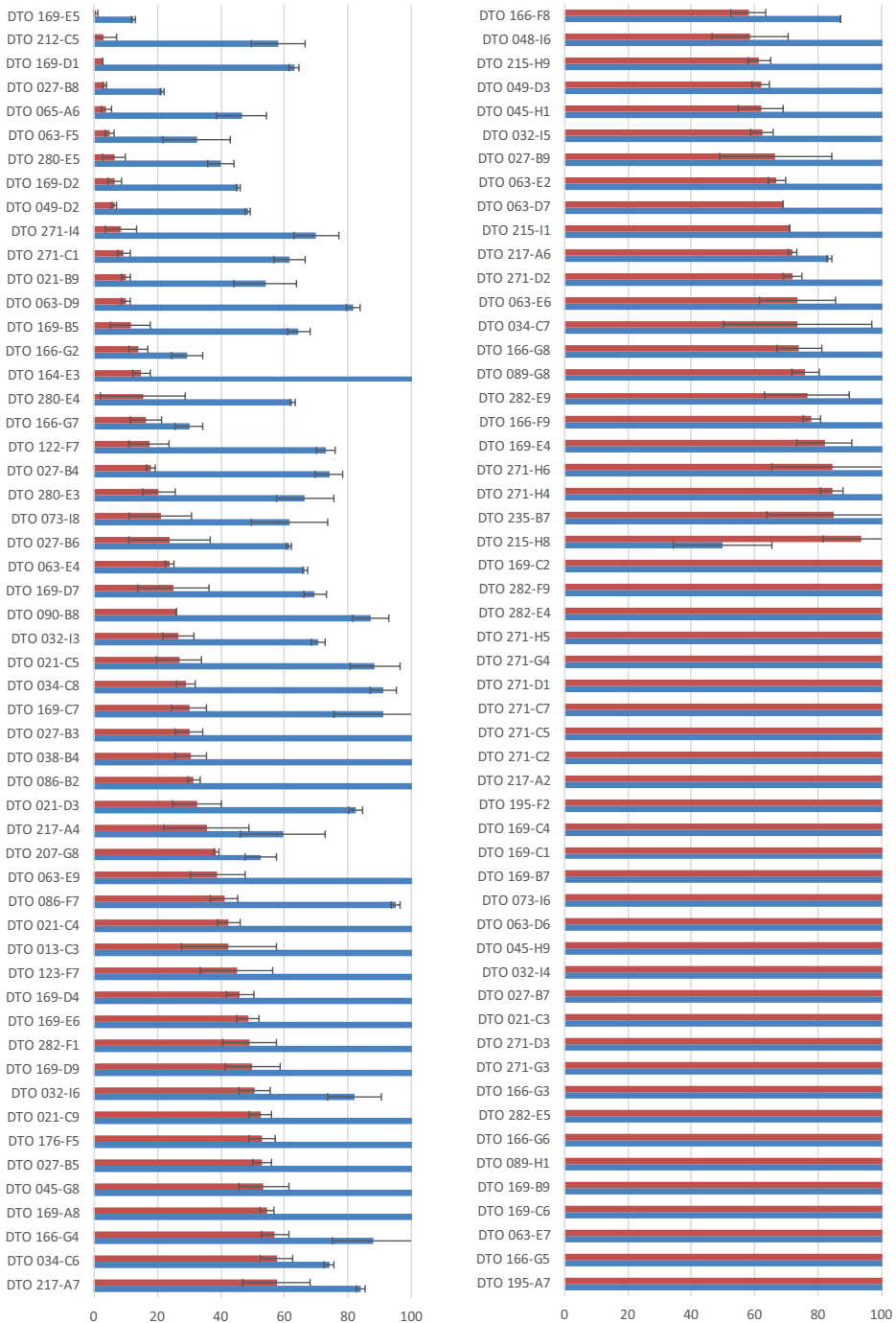
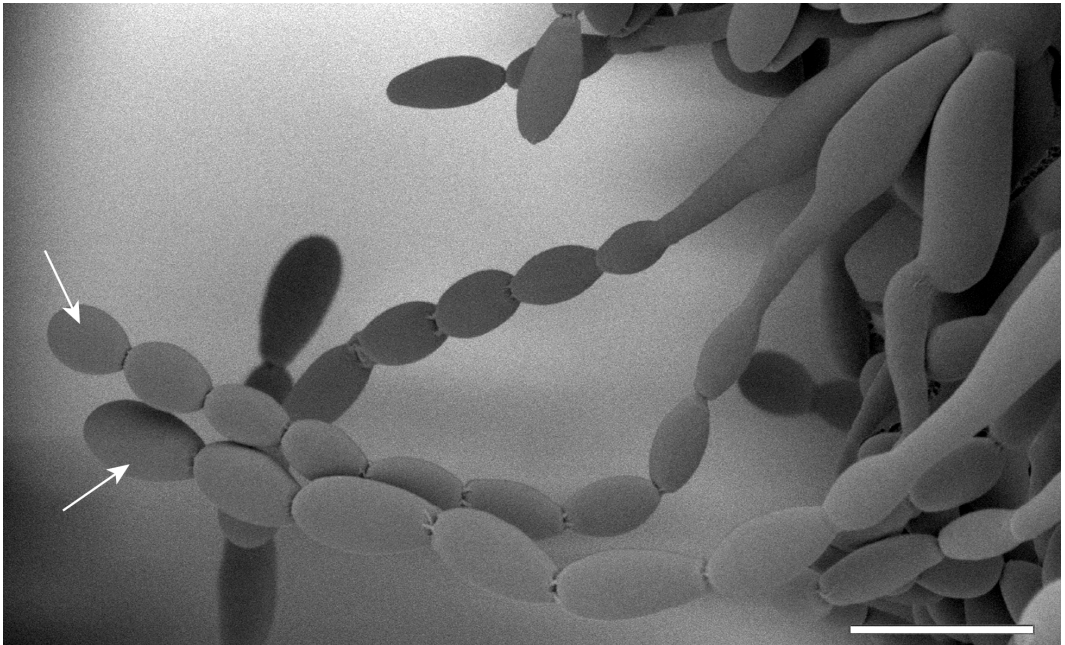


Figure S2.1. The results of screening 108 *P. variotii* strains for conidia heat resistance. The bars show number of colonies counted after heat treatment of the conidia at 58 °C (blue bars) and 59 °C (red bars). Average values of two plates \pm SD are shown.



2

Figure S2.2. Conidia of various sizes produced by one colony of *P. variotii* CBS 121579. Conidia were formed in chains and are produced by the phialides. Two chains of conidia depicted by the arrows clearly contained conidia of different sizes. Scale bar indicates 10 μm .

Conidial heat resistance of various strains of the food spoilage fungus *Paecilomyces variotii* correlates with mean spore size, spore shape and size distribution

Tom van den Brule, Cheuk Lam Sherlin Lee, Jos Houbraken, Pieter Jan Haas, Han Wösten and Jan Dijksterhuis

ABSTRACT

Contamination by spores is often the cause of fungal food spoilage. Some strains of the food spoilage fungus *Paecilomyces variotii* are able to produce highly heat resistant airborne conidia. Here, we compared four techniques to measure conidia size and distribution of five heat-sensitive and five heat-resistant *P. variotii* strains. Light microscopy (LM), scanning electron microscopy (SEM) and Coulter Counter (CC) were used to measure and compare the spherical equivalent diameter, while CC and flow cytometry were used to study spore size distributions. The flow cytometry data was useful to study spore size distributions, but only relative spore sizes were obtained. There was no statistical difference between the method used of spore size measurement between LM, SEM and CC, but spore size was significantly different between strains with a 2.4-fold volume difference between the extremes. Significant correlations were found between mean spore size, aspect ratio, roundness and skewness in relation to heat resistance. These data suggest that these parameters are indicative for the conidial heat resistance of a *P. variotii* strain.

3.1 INTRODUCTION

Fungal spores are main vehicles for distribution of filamentous ascomycetous fungi in space via water, air and other vectors (asexual conidia), or in time as dormant stress-resistant ascospores in sexual fruiting bodies (Wyatt *et al.*, 2013). Both types of spores can cause food spoilage; either by contamination of conidia by air or by ascospores through surviving heat treatments (dos Santos *et al.*, 2018). Reduction of fungal food spoilage has become an increasing priority with a growing world population. Besides, new trends in food industry put more pressure on the shelf life of processed food and drinks (Leyva Salas *et al.*, 2017). These include shorter heat inactivation treatments and a reduction in the concentration of compounds that counteract the development of microbes like salt, sugar and preservatives. For example, decrease of heat treatment leads to a better retainment of organoleptic characteristic of the product, as well as less damage of healthy components like vitamins. However, these developments make processed foods and drinks more prone to fungal spoilage.

Fungal spores are an important hallmark for identification of fungal species (Pitt and Hocking, 2009; Samson *et al.*, 2019). Even after the development of DNA sequencing, spore shape, size, and ornamentation are still significant morphological characteristics for polyphasic taxonomy. In many species descriptions, the spore size is described and differences occur between closely related species. For example, the black Aspergilli *A. niger* and *A. carbonarius* produce conidia with a diameter of 3.5–4.5 μm and 7–9 μm , respectively (Samson *et al.*, 2019). In addition, the shape of spores is variable between species, ranging from globose *Penicillium roqueforti* conidia to very complex topologies like the star shaped ascospores of *Aspergillus miraensis* (Chen *et al.*, 2016; Punt *et al.*, 2020).

Conidia of the genera *Aspergillus*, *Penicillium* and *Cladosporium* are predominant in air, as these fungi can form millions to billions of conidia per colony (Andersen *et al.*, 2011; Segers *et al.*, 2016; Ulevičius *et al.*, 2004). Conidia are moderately heat-tolerant, with D-values (log reduction time) of 5 minutes between roughly 55 °C and 64 °C (**Chapter 2**; van den Brule *et al.*, 2020b; Punt *et al.*, 2020; Wyatt *et al.*, 2013). For food industry, it is of importance to assess the contamination risk of these spores. Therefore, not only the average resistance of conidia to heat or other treatment is of importance, but also the variability of resistance within a colony or between strains. Yet, only recently has the topic of spore heterogeneity been addressed (**Chapter 2**; van den Brule *et al.*, 2020b; Geoghegan *et al.*, 2020; Punt *et al.*, 2020).

Historically, fungal spore size is measured using light microscopy (LM) (Samson *et al.*, 2019). Unless using Nomarski filters, a diffraction halo around the spores can lead to a bias in the measurements (Hitchins *et al.*, 1968). Cryo scanning electron microscopy (cryo-SEM) is a technique often used to study ornamentation of fungal spores and other structures (Staugaard *et al.*, 1990; van Veluw *et al.*, 2013). Since samples remain hydrated, spores remain their integrity, shrinkage of spores is prevented, and ornamentation is preserved (Aldrich and Todd, 1986). In addition, this technique does not cause a halo around the spores. Coulter Counter (CC) and flow cytometry (FC) are two other, non-microscopical methods to measure spore size. CC is an electrometric instrument, which uses the Coulter principle. The change in resistance when a particle is pulled through an aperture is proportional to the volume of the particle. This change is relatively independent of shape of the particle and therefore, it is a fast and reliable method to determine spore volume, including those of non-spherical conidia (**Chapter 2**; van den Brule *et al.*, 2020b; Valero-Jiménez *et al.*, 2014). The forward scatter pulse area (FSC) in flow cytometry (FC) can be used as a proxy for cell size and has been used to indicate the size of germinating conidia of *Aspergillus niger* (Hayer *et al.*, 2013, 2014). However, FSC intensities are not only influenced by the size of a cell or particle. The refraction index between the particle and the fluid, as well as the presence of pigment or other absorbing compounds can influence this parameter (Tzur *et al.*, 2011). In addition, FSC values can differ by the FSC measurement design, which can vary per flow cytometer. Therefore, FSC values are often used as a relative measure for size.

Paecilomyces variotii is a cosmopolitan food spoilage fungus that is capable of spoiling a broad range of products like canned fruits, non-carbonated sodas, margarine and rye bread (Pitt and Hocking, 2009). Previously, strain variation in *P. variotii* conidial heat resistance was studied by screening 108 isolates (**Chapter 2**; van den Brule *et al.*, 2020b). Three strains were used to quantify conidial heat resistance in terms of D-value and were further characterized by morphology, spore size distribution, compatible solute composition and their ability to grow in salt enriched medium. The conidia of strain DTO 217-A2 were more heat-resistant than any other fungal conidia. *P. variotii* conidia are ellipsoid of shape with flattened apical edges and they can vary in size within and between cultures of different strains. Notably, the *P. variotii* strain that produced the most heat-resistant conidia also produced conidia with the largest mean spore size as measured

by CC when compared to two other strains (**Chapter 2**; van den Brule *et al.*, 2020b). Moreover, the most heat-resistant strain also produced the widest spore size distribution with a bimodal character.

To investigate the influence of heterogeneity in spore size on stress resistance, it is important to measure spore size correctly. Therefore, our first objective in the present study was to compare spherical equivalent diameter obtained by LM, SEM and CC, while CC and flow cytometry were used to study spore size distributions. Secondly, the correlation between spore morphology as well as spore size distribution and heat resistance was assessed. To this end, conidial heat resistance was determined for five heat sensitive and five heat resistant strains.

3.2 METHODS AND MATERIALS

3.2.1 Strain selection and growth conditions

Based on a previous published screening for conidial heat resistance, five heat-sensitive and heat-resistant *P. variotii* strains were selected (**Chapter 2**; van den Brule *et al.*, 2020b; Table 2.1). Cultures were inoculated on malt extract agar (MEA, Oxoid, Hampshire, UK) from glycerol stocks stored at -80 °C and incubated for 7 days at 25 °C. To avoid glycerol contamination that could interfere with heat resistance, cultures were re-inoculated confluent on MEA. After another round of incubation for 7 days at 25 °C, spore suspensions were prepared as described (**Chapter 2**; van den Brule *et al.*, 2020b). Concentration of spore suspensions was determined by CC (see below) and set to a final concentration of $2 \cdot 10^8$ conidia mL^{-1} ACES buffer [10 mM N(2-acetamido)-2-aminoethanesulfonic acid, 0.02% Tween 80, pH 6.8]. Suspensions were stored on melting ice for maximum of 24 hours before further experiments.

3.2.2 Quantification of conidial heat-resistance

Conidial heat-resistance was quantified as described (**Chapter 2**; van den Brule *et al.*, 2020b). To inactivate 10^7 conidia mL^{-1} , 1 mL $2 \cdot 10^8$ conidia mL^{-1} was added to 19 mL pre-heated ACES buffer in 100 mL Erlenmeyer flasks at 60 °C and 120 rpm. After 2, 5, 15, 30 and 60 minutes, 1 mL samples were taken from the flasks and directly placed on ice to stop the inactivation process. All samples, including the untreated spore suspension, were further diluted to 10^3 conidia mL^{-1} . A volume of 100 μL of each dilution was plated on a 9 cm Petri dish. Plates that showed between 1 and 150 colonies after three days of incubation at 25 °C were used to determine the log colony forming units (CFU) mL^{-1} . Inactivation was described by a linear regression curve of the logCFU mL^{-1} against the inactivation time. The D_{60} -values that express the decimal reduction time were determined by $\frac{-1}{\text{slope}}$ of the inactivation curve. All experiments were performed using biological triplicates.

3.2.3 Microscopy

For LM, 10 μL of spore suspension was mixed with lactic acid which contained aniline blue (0.05% (w/v) methyl blue in 90% (S)-lactic acid) on glass slide. Images were captured by a Zeiss Axioskop 2 Plus Light microscope equipped with a Nikon DS-Fi1 with 63X oil objective to achieve a 630X magnification. The microscope was calibrated using a scale bar in the same magnification.

To prepare samples for cryo-SEM, a small piece of MEA of approximately 5 x 5 mm in size was glued in a copper cup by frozen tissue medium (KP-Cryoblock, Klinipath, Duiven, The Netherlands). Approximately 1 μL of conidia suspension was transferred to polycarbonate filter paper (GE Water & Process Technologies). The filter paper with conidia on top was then transferred to the surface of the agar block. The sample was snap-frozen in liquid nitrogen slush. Ice formed on sample surface was removed by sublimation at $-85\text{ }^\circ\text{C}$. The frozen specimen was sputter-coated using a gold target before imaging using a JEOL 5600LV microscope (Tokyo, Japan) with an Oxford CT1500 Cryostation, at acceleration voltage of 5 kV. The scan 4 mode was used for image acquisition.

Images of a hundred conidia per strain were selected randomly from both light- and electron microscopy micrographs for spore size measurement. The images were analyzed by ImageJ software (<https://imagej.nih.gov/ij/index.html>). An ellipse was fitted around the selected conidium and the major and minor axis, the area and perimeter were determined. Spore size is expressed by the diameter of the spherical equivalent and was calculated by $\phi = 2 * \sqrt[3]{\frac{major}{2} * (\frac{minor}{2})^2}$. The spore shape parameters aspect ratio (AR), circularity (C) and roundness (R) were calculated by $AR = \frac{major}{minor}$, $C = \frac{4\pi * area}{perimeter^2}$ and $R = \frac{4 * area}{\pi * major^2}$, respectively.

3.2.4 Coulter Counter and flow cytometry

Before the concentrations were set, spore suspensions were diluted $2 * 10^3$ times in ISOTON II diluent (Beckman Coulter, Fichtenhain, Germany) prior to CC analysis. A Beckman Coulter Counter Multisizer 3 equipped with a 70- μm aperture tube was used to determine the concentration of the original spore stocks. Pulse data of a thousand data points were randomly selected from the CC analysis to study spore size distribution. CC was calibrated using latex beads with a diameter of 5, 10 and 20 μm (Beckman Coulter, Brea, CA, USA). The following parameters were determined using the CC data. The P90/P10 ratio was calculated by dividing the ninth decile by the first decile. The span was calculated by $\frac{P90 - P10}{P50}$, where P50 represents the median. Skewness was determined by $b1 = \frac{m_3}{s^3} = \left(\frac{n-1}{n}\right)^{3/2} \frac{m_3}{m_2^{3/2}}$ where $m_r = \frac{1}{n} \sum (x_i - \mu)^r$ and $s^2 = \frac{1}{n-1} \sum (x_i - \mu)^2$ (Joanes and Gill, 1998).

For FC, $2 * 10^7$ conidia mL^{-1} was analyzed using a FACSVerse™ (Becton Dickinson, Franklin Lakes, NJ). Like the Coulter Counter data, a thousand data points of FSC pulse area were randomly selected to analyze spore size distributions.

3.2.5 Statistics

QQ-plots of LM, SEM and CC data revealed that not all data was normally distributed. Therefore, the Friedman's test ($\alpha < 0.05$) was used to describe differences in spore size between strains and methods. Boxplot elements indicate the median, the hinges representing the 25th and 75th percentiles, the upper whisker representing 1.5 times Inter Quartile Range (IQR) from the hinge and the lower whisker extends to the lowest value, at most 1.5 times IQR. Data beyond the range of the whiskers were considered outliers. Spore size distributions of CC and FC data were analyzed using the Mixtools package in R (Benaglia *et al.*, 2009). Data of both measurement methods were analyzed by means of a two-component mixture model. The boot.comp function with 1000 parametric bootstraps was used to test significance $P(k > 1) < 0.05$, where k is the number of components. In each distribution, two populations were computed using Expectation Maximization (EM) algorithm using the normalmixEM function. Standard errors of the mean (μ), standard deviation (σ) and weight related to the total population (λ) were determined by the boot.se function using 1000 parametric bootstraps.

Table 3.1. Strains used in this chapter (see **Chapter 2** and van den Brule *et al.*, 2020b).

DTO no.	CBS no.	Substrate	Location	Percentage survival after 10 minute heat treatment ¹		Conidial heat resistance
				58 °C	59 °C	
DTO 032-I3	CBS 121585	HFCS after heat shock	USA	7,05	2,65	Sensitive
DTO 032-I4	CBS 121586	Spoiled bottle of bottle of sweetened tea	USA	6,75	ND	Sensitive
DTO 063-F5		Human; abscess	The Netherlands	3,25	0,5	Sensitive
DTO 166-G5		Pectin, heat treated	The Netherlands	>10	>10	Resistant
DTO 169-C6	CBS 145661	Indoor environment	USA	>10	>10	Resistant
DTO 169-E5	CBS 145662	Indoor environment	USA	1,25	0,05	Sensitive
DTO 195-F2	CBS 145663	Margarine	Belgium	>10	>10	Resistant
DTO 212-C5	CBS 145665	Vanilla	The Netherlands	5,8	0,3	Sensitive
DTO 217-A2	CBS 145666	Ice pop, heat treated	The Netherlands	>10	>10	Resistant
DTO 282-E5	CBS 145669	Margarine	Italy	>10	>10	Resistant

3.3 RESULTS

3.3.1 Selection of *P. variotii* strains and quantification of conidial heat resistance

Ten strains of *P. variotii* were selected from the Westerdijk Fungal Biodiversity Institute collection (Table 3.1). Seven strains originated from food products, two from the indoor environment and one from a human patient. The strains were selected based on a screen for conidial heat resistance (**Chapter 2**; van den Brule *et al.*, 2020b). The conidial heat resistance of the 10 selected strains was quantified by studying inactivation kinetics at 60 °C (Table 3.2, Fig. 3.1). A total of 9 out of 10 strains the inactivation kinetics showed a highly linear character ($R^2 < 0.90$). Only DTO 169-E5 showed a lower value at $R^2 = 0.81$. From the inactivation curve, the decimal reduction time (D_{60} -value) was calculated, which represents the time to inactivate 1 log reduction at 60 °C. DTO 195-F2 produced the most heat-resistant conidia with a D_{60} -value of 27.6 ± 3.12 minutes, whereas the conidia of DTO 063-F5 were the most heat sensitive with a D_{60} -value of 3.5 ± 0.20 minutes. All heat-sensitive strains showed a D_{60} -value ≤ 6 min, while the five heat-resistant strains had a D_{60} -value > 9 min.

3.3.2 Comparison of light microscopy, scanning electron microscopy, and Coulter Counter to measure spore size

The size of the ellipsoid shaped conidia of *P. variotii* was expressed in one integer: the so-called Heywood diameter, which designates the spherical equivalent. In case of the two-dimensional microscopic pictures, this parameter was estimated by fitting an ellipse as accurately as possible around the spores (Fig. 3.2A-D). From this ellipse, the major and minor axis were determined and used to calculate the spherical equivalent diameter. The CC software converts the Heywood diameter based on calibration with latex beads of a defined size. Data of 100 randomly selected spores of the ten *P. variotii* strains were obtained using LM, SEM and CC (Fig. 3.2E). QQ-plots revealed that not all spore size distributions were normally distributed (data not shown). Therefore, we used non-parametric Friedman's test to test for significant differences between strains and methods. Significant differences in spore size were found ($\chi^2 = 19.873$, $df = 9$, $P = 0.019$) when spore size between strains was compared, while we did not find significant differences between the measuring methods ($\chi^2 = 0.6$, $df = 2$, $P = 0.741$).

Table 3.2. Conidial heat resistance expressed by D -value. Average value \pm SD is shown of three biological replicates.

Strain	D_{60} -value (min)	R^2
DTO 032-I3	6.0 ± 0.70	0,979
DTO 032-I4	4.9 ± 1.73	0,906
DTO 063-F5	3.5 ± 0.20	0,961
DTO 166-G5	11.9 ± 1.28	0,983
DTO 169-C6	9.4 ± 0.50	0,992
DTO 169-E5	5.0 ± 1.97	0,805
DTO 195-F2	27.6 ± 3.12	0,953
DTO 212-C5	3.6 ± 0.19	0,963
DTO 217-A2	20.1 ± 4.02	0,924
DTO 282-E5	14.2 ± 2.20	0,956

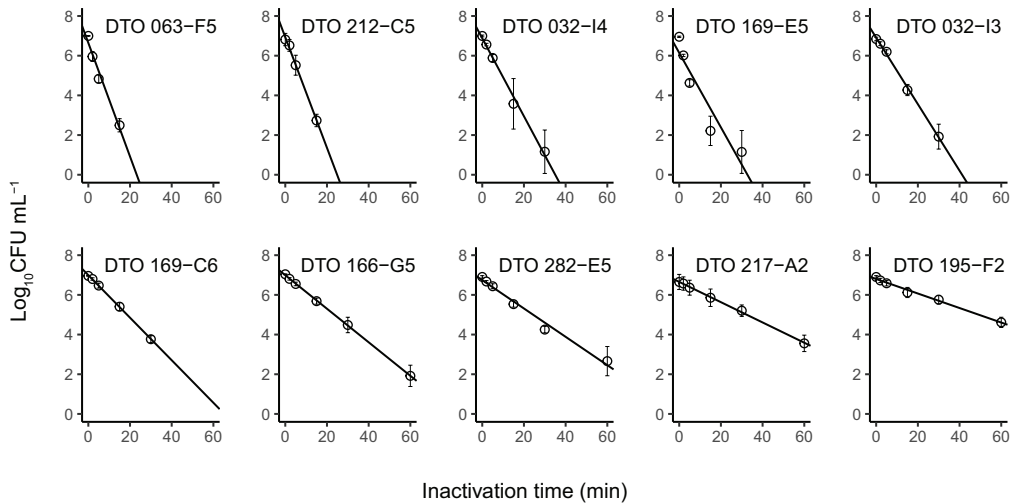


Figure 3.1. Heat inactivation curves of conidia originating from 10 *P. variotii* strains, ordered from most heat sensitive (DTO 063-F5) to most heat resistant (DTO 195-F2). A linear regression was fitted to the mean data points of three independent measurements. Error bars indicate standard deviations of biological triplicates.

3.3.3 Comparison of Coulter Counter and flow cytometry to study spore size distributions

A thousand data points of CC and FC were randomly selected to study spore size distributions. To test if the distributions could be described by more than one component, we tested $P(k > 1)$ using the `boot.comp` function with 1000 bootstraps of the `mixtools` package in R (Benaglia *et al.*, 2009). In all cases we found $P(k > 1) < 0.001$, meaning that the spore size distribution can be described by two or more normal distributions. Two normal distributions were computed for each spore size distribution using EM algorithm (Table 3.3). In this analysis, we modelled two populations of different spore size within one spore size distribution. The small size spore population contains a mean spore size of μ_1 with a standard deviation of σ_1 , whereas the large size spore population is expressed by μ_2 and σ_2 . The proportion of each population is expressed by weight parameter λ_1 and λ_2 for the population of small spore size and large spore size, respectively. To test if the means of the two populations were statistically different, a 99% confidence interval was calculated. All strains showed no overlap in the confidence interval of the two computed populations, indicating that μ_1 and μ_2 are significantly different in all cases.

Spore size distributions as measured with FC and CC showed similar patterns for 7 out of the 10 strains (Fig. 3.3, Table 3.3). The conidia population of strain DTO 217-A2 was predominated by λ_2 of 0.80 and 0.75 in the CC and FC results, respectively. In addition, clear predominance of λ_2 is observed in DTO 166-G5. DTO 032-I3 showed highest predominance of the small spore size population with λ_1 with 0.72 and 0.78 in the CC and FC results, respectively. Predominance of the λ_1 was seen in the case of strains

DTO 169-C6, DTO 063-F5 (only CC data) and DTO 169-E5 and 032-I4 (only FC data). Four strains showed about equal distribution of λ_1 (0.42–0.54) and λ_2 (0.46–0.58). Three strains showed difference of population predominance of large size conidia (λ_2 , strain DTO 063-F5) between CC ($\lambda_2 = 0.27$) and FC ($\lambda_2 = 0.44$). The opposite was found for DTO 032-I4 and DTO 169-E5, showing smaller weight for the population large spores when measured by FC ($\lambda_2 = 0.18$ and 0.28, respectively) than CC ($\lambda_2 = 0.45$ and 0.44, respectively). Together, these results revealed differences in spore size distribution among *P. variotii* strains.

3.3.4 Correlations of conidial heat resistance and mean spore size, spore shape, as well as size distributions

In a previous study, it was noted that heat-resistant strain DTO 217-A2 produced on average larger conidia than two heat-sensitive strains (**Chapter 2**; van den Brule *et al.*, 2020b). Furthermore, the λ_2 of this strain was larger compared to the other two strains. Pearson correlation analyses was used to test whether spore shape parameters correlate with heat resistance (Table 3.4, Fig. 3.4). The tested shape parameters included aspect ratio (AR), roundness (R) and circularity (C) and were based on the measurements of 100 conidia on

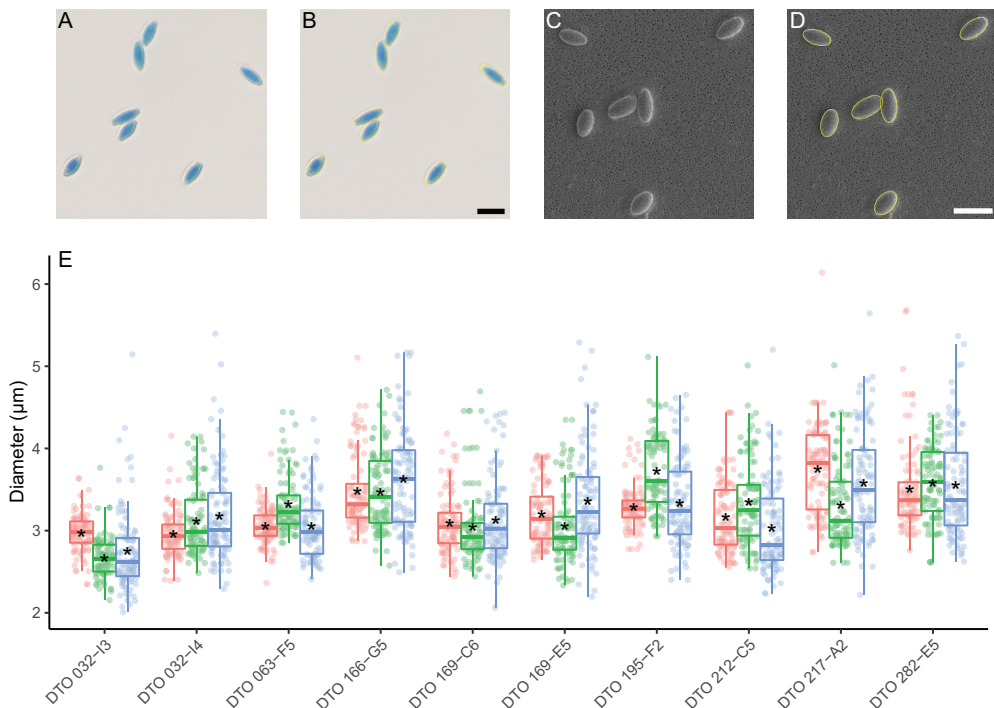


Figure 3.2. Conidia size measurements of *P. variotii* strains. Pictures of *P. variotii* DTO 032-I3 conidia made by light microscopy (A, B) or scanning electron microscopy (C, D). To measure spore size, a yellow ellipse was fitted around the particles (B, D). Scale bars indicate 10 µm. (E) Comparison of spore diameter distributions of 100 data points obtained by LM (red), SEM (green) and CC (blue) for 10 *P. variotii* strains. The asterisk indicates the mean spore size.

Table 3.3. Two populations of spore size as modelled by computation of the measurements by means of Coulter Counter (CC) and Flow Cytometry (FC). The mean and standard deviation are expressed by μ and σ , respectively. The weight each population compared to the total population is expressed by λ . Standard errors are included to each value of the mixture models.

Strain	Method	Population 1			Population 2		
		μ_1^a	σ_1^a	λ_1^b	μ_2^a	σ_2^a	λ_2^b
DTO 032-I3	CC	2.59 ± 0.011	0.23 ± 0.011	0.72 ± 0.036	3.33 ± 0.092	0.57 ± 0.045	0.28 ± 0.036
	FC	35601 ± 484	12228 ± 421	0.78 ± 0.019	100875 ± 5018	47650 ± 2915	0.22 ± 0.019
DTO 032-I4	CC	2.88 ± 0.015	0.24 ± 0.016	0.55 ± 0.045	3.5 ± 0.068	0.62 ± 0.029	0.45 ± 0.045
	FC	63844 ± 538	13046 ± 515	0.82 ± 0.028	103589 ± 6402	36007 ± 3259	0.18 ± 0.028
DTO 063-F5	CC	2.94 ± 0.011	0.24 ± 0.01	0.73 ± 0.029	3.59 ± 0.076	0.71 ± 0.036	0.27 ± 0.029
	FC	81358 ± 667	11525 ± 640	0.56 ± 0.031	92415 ± 2412	47697 ± 2008	0.44 ± 0.031
DTO 166-G5	CC	3.09 ± 0.015	0.17 ± 0.015	0.33 ± 0.031	3.71 ± 0.034	0.6 ± 0.018	0.67 ± 0.031
	FC	97702 ± 905	12158 ± 880	0.41 ± 0.032	136701 ± 2587	43699 ± 1327	0.59 ± 0.032
DTO 169-C6	CC	2.91 ± 0.019	0.29 ± 0.018	0.64 ± 0.062	3.6 ± 0.13	0.63 ± 0.055	0.36 ± 0.062
	FC	71419 ± 988	18005 ± 984	0.59 ± 0.036	136234 ± 5587	47599 ± 2904	0.41 ± 0.036
DTO 169-E5	CC	2.97 ± 0.017	0.27 ± 0.018	0.56 ± 0.05	3.73 ± 0.09	0.63 ± 0.04	0.44 ± 0.05
	FC	39821 ± 503	11781 ± 440	0.72 ± 0.021	99189 ± 4275	43807 ± 2393	0.28 ± 0.021
DTO 195-F2	CC	2.99 ± 0.019	0.24 ± 0.017	0.52 ± 0.058	3.68 ± 0.079	0.52 ± 0.037	0.48 ± 0.058
	FC	93725 ± 979	15692 ± 1038	0.58 ± 0.045	124187 ± 3668	40132 ± 1692	0.42 ± 0.045
DTO 212-C5	CC	2.69 ± 0.016	0.24 ± 0.017	0.52 ± 0.047	3.38 ± 0.072	0.59 ± 0.033	0.48 ± 0.047
	FC	59889 ± 618	12122 ± 600	0.56 ± 0.025	122312 ± 3414	45483 ± 1966	0.44 ± 0.025
DTO 217-A2	CC	2.95 ± 0.023	0.17 ± 0.025	0.2 ± 0.035	3.69 ± 0.035	0.56 ± 0.018	0.8 ± 0.035
	FC	91821 ± 1037	10064 ± 978	0.25 ± 0.026	143597 ± 2053	39486 ± 1198	0.75 ± 0.026
DTO 282-E5	CC	3.17 ± 0.019	0.27 ± 0.019	0.52 ± 0.053	3.92 ± 0.086	0.62 ± 0.039	0.48 ± 0.053
	FC	97258 ± 1479	18597 ± 1400	0.46 ± 0.049	159014 ± 5151	42850 ± 2640	0.54 ± 0.049

a. FC μ and σ values are expressed by Forward scatter (arbitrary units) and CC values expressed the spherical equivalent diameter (μm).

b. The sum of λ_1 and λ_2 equals 1.

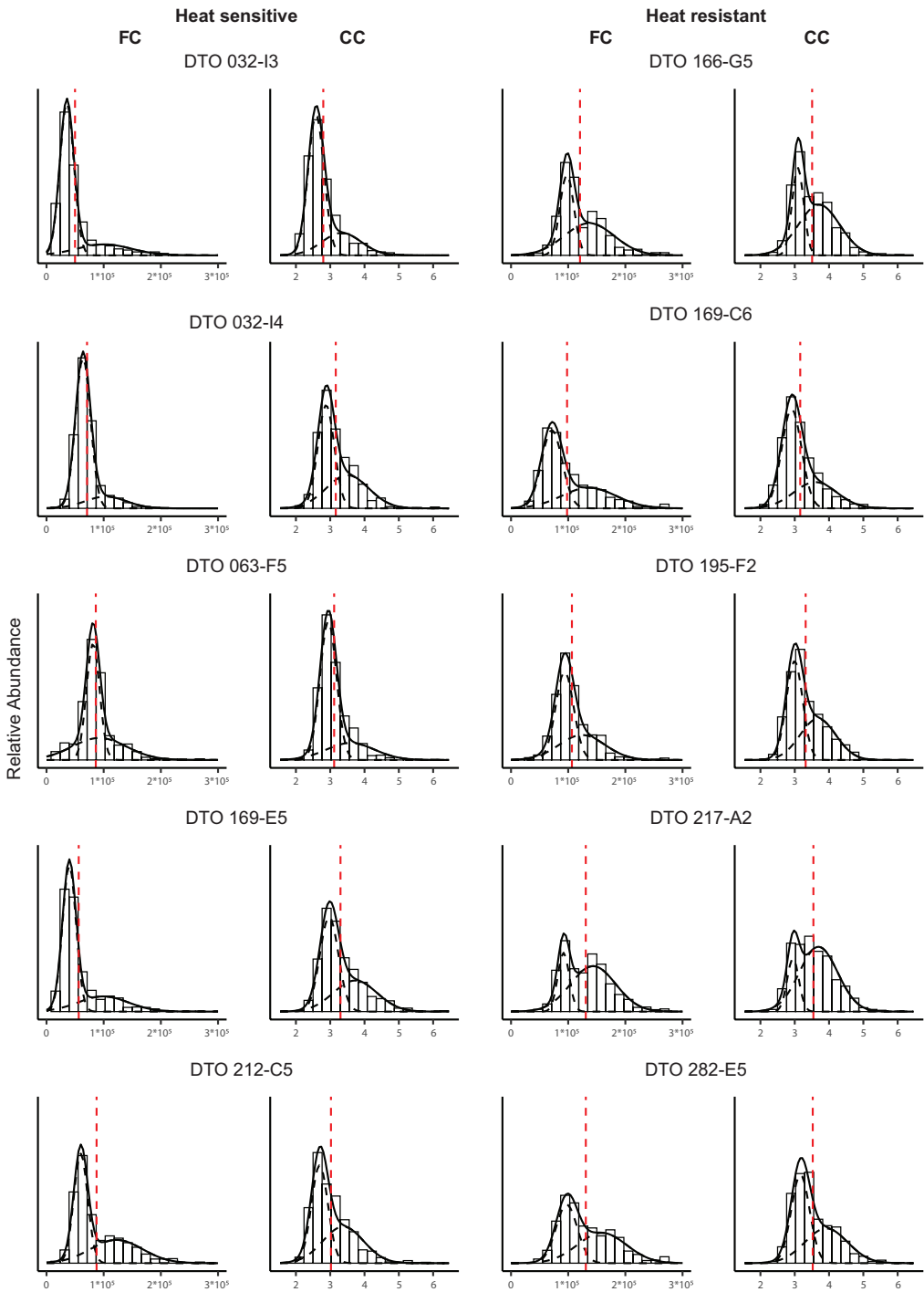


Figure 3.3. Spore size distributions of 10 *P. variotii* strains as measured by FC and CC. The total surface of the histogram bars equals 1. All distributions were described by two populations (black dashed lines) which were computed using EM algorithm. In addition, the sum of the two populations (black solid line) and the mean spore size values (red dashed line) is shown in the plots. FC values are expressed by FSC and CC values expressed the spherical equivalent diameter.

Table 3.4. Pearson correlations of conidial heat resistance ($\log_{10}D$ -value) with various spore size distribution and spore shape parameters.

Variable	Correlation coefficient (r)	P-value	Significance (p<0.05)
<i>Spore shape parameters</i>			
Mean spore size	0,65	0,044	*
AR*	-0,67	0,034	*
C*	0,67	0,033	*
R*	0,68	0,03	*
<i>Spore distribution parameters</i>			
λ_2	0,57	0,083	
p90p10	0,28	0,433	
sk*	-0,64	0,044	*
Span	0,2	0,583	

*Abbreviations: AR, Aspect Ratio; C, circularity; R, roundness; sk, skewness.

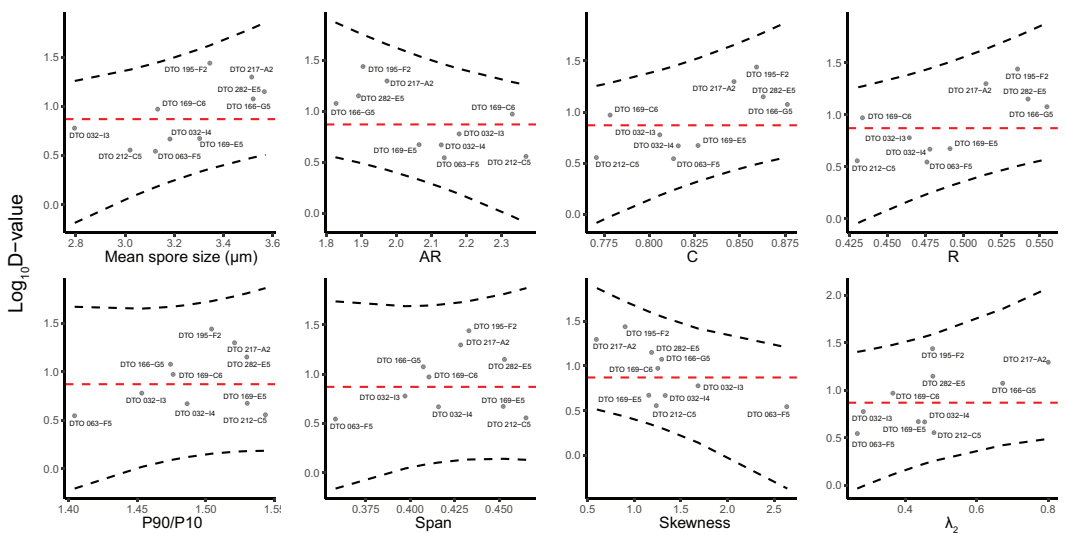


Figure 3.4. Pearson correlations of the $\log_{10} D$ -value and various spore size and spore shape parameters. The black dashed lines indicate the 95% prediction interval and the red dashed line indicates the boundary between heat resistant.

LM micrographs. In addition, as determined by a thousand data points obtained by CC, the mean spore size and the distribution parameters p90/p10 ratio, span, skewness and λ_2 were compared with the $\log D_{60}$ -value. The mean spore size was significantly positively correlated with heat resistance, suggesting that resistant strains produce larger spores than heat-sensitive strains. The shape parameters aspect ratio, circularity and roundness also correlated significantly with heat resistance. For all three parameters, a perfect circle has a value of 1. Since conidia of heat resistant strains tend to have values closer to 1 than

heat sensitive strains, these results suggest that the ellipsoidal spores of heat-resistant strains are more spherical in shape than those of sensitive strains that are more elongated. The values of the spore size distribution parameters p90/p10 and span, that both address the width of the spore size distribution, did not correlate with heat resistance. The weight of the population large conidia (λ_2) also did not correlate with heat resistance. Finally, the spore size distribution parameters skewness showed a significant negative correlation with heat resistance, implying that the sensitive strains produce relatively more outliers in respect to conidia size than resistant strains.

3.4 DISCUSSION

Heterogeneity in heat resistance, size and shape was determined of conidia of the food-spoiling fungus *P. variotii*. Five heat-sensitive and five heat-resistant strains were selected based on a previous screening (**Chapter 2**; van den Brule *et al.*, 2020b). Conidia of the five heat-sensitive strains showed a D_{60} -value of 3.5–6.0 min, while D_{60} -values of 9.4–27.6 min were observed for the resistant strains. Strain DTO 195-F2 produced most heat-resistant conidia and its spores are more resistant than those of *P. variotii* DTO 217-A2 that were so far the most heat-resistant conidia produced by fungi. Thus, DTO 195-F2 produces the most heat-resistant conidia ever reported. Also of interest, we here show a correlation between heat resistance and spore size and shape.

Conidia size was determined using LM, SEM, CC and FC. The latter did not show a linear correlation with cell size when forward scatter was used but can FC can be used to study the cell size distribution. Data obtained with LM, SEM and CC all confirmed differences in conidia size between the strains. For all three methods, we used the Heywood diameter as one integer to describe the ellipsoid conidia size. Spore size varies among the tested strains ranging from an average of 2.7 μm for DTO 032-I3 to 3.6 μm for DTO 166-G5. These differences in spore size imply a 2.4 fold difference in spore volume of the conidia of the strains producing the smallest and largest conidia.

Spore sizes measured with LM, SEM and CC were not statistically different. LM is based on transmitted light; SEM uses a scanning electron beam and CC measures the impedance of a particle in an aperture. These three methods each have their own sources of variation illustrated by the halo around objects in the case of LM and the drift of a sample during SEM. In another study, larger size was found when measuring *Penicillium* conidia by (environmental) SEM compared to LM, because the higher magnifications revealed the ornamentation of the spores better (Reponen *et al.*, 2001). In the case of the smooth walled *P. variotii* conidia this is not a problem, but it should be taken into account when measuring ornamented spores by microscopy. Of interest, CC showed a larger standard deviation in spore size than the microscopy techniques for all 10 strains. This may be caused by the fact that CC also occasionally measures hyphal fragments or phialides. In summary, our data show that as long as the machinery is calibrated well, it seems not to matter which technique is used to determine spore size. The advantages and disadvantages of each technique are summarized in Table 3.5.

Table 3.5. Advantages and disadvantages of each technique discussed in this study to measure spore size, spore shape and spore size distribution.

Technique	Advantages	Disadvantages
Light microscopy	<ul style="list-style-type: none"> • Available to every lab with a light microscope • Shape can be studied 	<ul style="list-style-type: none"> • Spore selection could lead to a bias in heterogeneity • Halo formation
Scanning electron microscopy	<ul style="list-style-type: none"> • No halo formation • Shape can be studied 	<ul style="list-style-type: none"> • Spore selection could lead to a bias in heterogeneity • Laborious
Coulter Counter	<ul style="list-style-type: none"> • Fast measurements • Measures particles regardless of shape 	<ul style="list-style-type: none"> • Spore complexes and other particles are not identified • Shape cannot be studied
Flow cytometry	<ul style="list-style-type: none"> • Fast measurements 	<ul style="list-style-type: none"> • FSC does not correlate with spherical equivalent diameter • Orientation of non-spherical spores may influence FSC values. • Shape cannot be studied

Spore size of *P. variotii* correlated with heat resistance thus suggesting a causal relation. This hypothesis is in agreement with results of ascospores of the closely related fungal species *Talaromyces flavus* and *Talaromyces macrospores* (Frisvad *et al.*, 1990). The size of the ellipsoidal ascospores is 4–5.5 × 3–3.5 μm for *T. flavus* and 5–6.5 × 4.5–5.5 μm for *T. macrosporus* and the ascospores of the latter are much more heat-resistant (Beuchat, 1988; Dijksterhuis, 2019; Yilmaz *et al.*, 2014). The spores of both species have a similar composition of compatible solutes and have a high concentration trehalose (Wyatt *et al.*, 2015b). Similarly, the large *Aspergillus spinosus* ascospores have a higher heat resistance than the smaller spores of *A. fischeri* (unpublished data). This could be even hold for other stresses; larger sporangiospores of *Mucor circinelloides* are more virulent and survive and germinate inside macrophages, while smaller spores do not (Li *et al.*, 2011).

An advantage in determining spore size using a microscope is that it gives extra spore shape parameters. The major and minor axis determined by the fitted ellipses around the spores were used to calculate the aspect ratio, circularity and roundness of the spores. Surprisingly, all these parameters correlated with heat resistance, indicating that conidia formed by heat-resistant strains have a higher sphericity than conidia formed by sensitive strains. Similar as small spore size, a low sphericity results in a larger surface-area-to-volume ratio and might therefore cause a higher susceptible to heat stress. We assume that the small spore sizes have a negligible effect on heat transfer into the spores with different size. Yet, the surface area of the plasma membrane would explain the differences

in heat resistance. Thus, future studies should assess whether the primary effect of conidial killing acts on the plasma membrane.

It has been described before that differences occur in spore size distributions among three *P. variotii* strains (**Chapter 2**; van den Brule *et al.*, 2020b). In this study, FC and CC analysis of seven additional strains confirmed that conidia spore size distribution are clearly different among strains. Interestingly, the skewness of the distribution was negatively correlated with heat resistance. This indicates that strains producing heat-sensitive spores are likely to produce more outliers in respect to conidia size than heat-resistant strains. Notably, all spore size distributions were slightly positively skewed. It should be noted that correlation coefficients are relatively low, indicating that exceptions might occur. This is illustrated by the heat-resistant conidia of DTO 169-C6 that show a low mean spore size and similar shape as characterized by the other heat-sensitive strains. Summarized, conidial size, shape and the skewness of the cell size distribution of *P. variotii* strains could be used as indicators for heat resistance.

With this study, we analysed spore size distributions of 10 *P. variotii* strains in detail. The diversity found in all parameters in this study contributes to a better understanding of spore heterogeneity of fungal species. Microbial heterogeneity is an important factor in predictive food mycology, since spoilage can occur if only one spore is able to germinate. In the end, the strongest spore determines if spoilage will occur.

Intraspecific variability in heat resistance of fungal conidia

Tom van den Brule, Maarten Punt, Sjoerd Seekles, Frank Segers, Jos Houbraeken, Wilma Hazeleger, Arthur Ram, Han Wösten, Marcel Zwietering, Jan Dijksterhuis and Heidy den Besten

ABSTRACT

Microbial species are inherently variable, which is reflected in intra-species genotypic and phenotypic differences. Strain-to-strain variation gives rise to variability in stress resistance and plays a crucial role in food safety and food quality. Here, strain variability in heat resistance of asexual spores (conidia) of the fungal species *Aspergillus niger*, *Penicillium roqueforti* and *Paecilomyces variotii* was quantified and compared to variability found in the literature. After heat treatment, a 5.4- to 8.6-fold difference in inactivation rate was found between individual strains within each species, while the strain variability of the three fungal species was not statistically different. We hypothesise that the degree of intra-species variability is uniform, not only within the fungal kingdom, but also between different microbial kingdoms. Comparison with three spore-forming bacteria and two non-spore-forming bacteria indeed revealed that the variability of the different species was in the same order of magnitude, which hints to a microbial signature of variation that exceeds kingdom boundaries.

4.1 INTRODUCTION

Diversity of microbial species is key to adapt to environmental changes and to thrive in different niches. Intra-species variability includes all variation within a species, including genotypic and phenotypic differences. Unravelling drivers and mechanisms for intra-species variability has been a broadly studied subject the past decade (Andersson, 2009; Choudoir *et al.*, 2017; Papke and Ward, 2004) including sources of phenotypic heterogeneity of genetic identical cell populations (Ackermann, 2015; Avery, 2006). Strain diversity can have huge consequences on diagnostics, virulence and antimicrobial treatments in clinical microbiology, or on the efficacy of food preservation methods (den Besten *et al.*, 2018a; Davies *et al.*, 2021; Lianou and Koutsoumanis, 2013a; Lianou *et al.*, 2020; Stratford *et al.*, 2013b).

As microbial species are inherently variable, strains of the same species may differ in their response to environmental and food preservation stresses. Indeed, large differences in stress robustness have been reported in bacterial species (den Besten *et al.*, 2018a). This suggests that microbial stress robustness is a relevant trait to quantify strain variability. Recently, strain variability in heat resistance has been quantified for bacterial vegetative cells of the pathogen *Listeria monocytogenes* (Aryani *et al.*, 2015) and the food-borne organism *Lactiplantibacillus plantarum* (Aryani *et al.*, 2016) [previously known as *Lactobacillus plantarum* (Zheng *et al.*, 2020)] and for bacterial spores of the pathogen *Bacillus cereus* (den Besten *et al.*, 2018a), and the food spoilers *Bacillus subtilis* (den Besten *et al.*, 2017) and *Geobacillus stearothermophilus* (Wells-Bennik *et al.*, 2019). Notably, strain variability was high for the tested organisms and inactivation rates of the most heat sensitive and most heat resistance strains of the same species could differ a factor ten. This means that when a similar temperature/time regime is applied, the most heat resistant strain will be reduced with a factor 10, while the most heat sensitive

strains will be reduced with a factor 10^{10} . This results in huge differences in heat treatment efficacies, depending on the heat stress robustness of the microbial contaminant (den Besten *et al.*, 2018a; Zwietering *et al.*, 2021).

Spores of bacteria and fungi are considered more stress resistant than vegetative cells (Wyatt *et al.*, 2013). The stress resistance of fungal spores varies strongly, ranging from spores that display stress resistance similar to that of vegetative cells to very high stress resistance that can be comparable to bacterial spores (Beuchat, 1986; Van Leeuwen *et al.*, 2010; Wyatt *et al.*, 2013). Filamentous Ascomycete fungi that belong to the order Eurotiales can produce asexual spores called conidia. Airborne conidia are resistant to various environmental stresses including ultra violet (UV) radiation, desiccation, cold and heat stress (Wyatt *et al.*, 2013). Conidia are an integral part of the fungal life cycle, and can be distributed in space by air, wind or other vectors and are abundantly present in the environment. For example, *Penicillium chrysogenum* conidia are so widespread that they are considered being cosmopolitan (Henk *et al.*, 2011). These airborne conidia are found in the air and soil in many different habitats (Amend *et al.*, 2010). Studies have shown that conidia can travel large distances. For instance, conidia of *Aspergillus sydowii* have been suggested to be transported over thousands of kilometres from the Sahara desert to the Caribbean reefs (Shinn *et al.*, 2000). Being airborne and widely present, conidia are often related to food spoilage, leading to considerable losses of food and feed (Dijksterhuis, 2017). In food industry, heat treatments are routinely used to inactivate or reduce the microbial count in a product, and quantitative data on the heat resistance of microorganisms is needed to predict treatment efficacy and product shelf life.

Recently, conidial heat resistance of various strains of the food spoilage fungus *Paecilomyces variotii* was reported to be highly variable. Decimal reduction times of thermal treatments at 60 °C (D_{60} -values) ranged from 3.5 to 27.6 minutes when different strains were used of the same species (**Chapter 3**; van den Brule *et al.*, 2020a). This prompted us to study a larger selection of isolates and to quantify variability in conidial heat resistance among strains of *P. variotii* in detail. Furthermore, we assessed strain variability in conidial heat resistance of the fermentative fungus *Penicillium roqueforti*, and for *Aspergillus niger*, which is commonly used as a model fungus. Both species are also known as food spoilers. The strain variabilities in heat resistance of the fungal species were compared to those of bacterial vegetative cells and spores to assess strain variability across kingdom borders.

4.2 MATERIAL AND METHODS

4.2.1 Strain selection and identification

Strains were selected from (originating from both food and non-food sources) and obtained from the CBS culture collection and the working collection of the Food and Indoor Mycology (DTO) group of the Westerdijk Fungal Biodiversity Institute (Table S4.1). Strains included the previously studied *A. niger* N402 (Bos *et al.*, 1988), *P. roqueforti* DTO 377-G3 (Punt

et al., 2020) and *P. variotii* DTO 032-I3, DTO 212-C5, DTO 217-A2 and DTO 280-E5 (CBS 101075) (**Chapter 2**; van den Brule *et al.*, 2020b; Urquhart *et al.*, 2018). Identity of strains was confirmed by sequencing the partial calmodulin (*caM*) gene for *A. niger* and the partial beta-tubulin (*benA*) gene for *P. roqueforti* and *P. variotii* that can be used as identification marker (Samson *et al.*, 2009; Varga *et al.*, 2011; Visagie *et al.*, 2014). After alignment using MUSCLE, a maximum likelihood tree of each species was computed with 1,000 bootstrap replications using MEGA7 (Kumar *et al.*, 2016). Reference sequences of closely related species and the type strain were included in the phylograms (Houbraken *et al.*, 2020). For each tree, the model with the lowest Bayesian Information Criterion (BIC) score was used. The Kimura 2-parameter model including gamma distribution (K2+G) was used for *A. niger*, and the Jukes-Cantor (JC) model and the Kimura 2-parameter model including invariant sites (K2+I) model were used for *P. roqueforti* and *P. variotii*, respectively.

4.2.2 Growth conditions and harvesting conidia

Culturing and harvesting of conidia were performed as described (**Chapter 2**; van den Brule *et al.*, 2020b). In short, fungal strains stored in 30% (w/v) glycerol at -80 °C were spot-inoculated on malt extract agar (MEA, Oxoid, Hampshire, UK) and incubated for 7 days at 25 °C. *A. niger* strains DTO 028-I3 and DTO 058-I1 were cultured at 30 °C because sporulation was not sufficient at 25 °C. Freshly harvested conidia were used to spread-inoculate a new MEA plate to anticipate on differences in age within the conidia population. Conidia were harvested after 7 days of incubation using ACES buffer [10 mM N(2-acetamido)-2-aminoethanesulfonic acid, 0.02% Tween 80, pH 6.8] and filtered using either sterile glass wool in a syringe or sterilized Amplitude EcoCloth wipes (Contec Europe, Vannes, France). Subsequently, conidia were washed two times in ACES buffer. The concentration of conidia in suspension was determined using a Coulter Counter Multisizer 3 (Beckman Coulter, Life Sciences, Indianapolis, USA) (**Chapter 3**; van den Brule *et al.*, 2020a), a Bio-Rad TC20 Automated Cell Counter (Bio-Rad Laboratories, Lunteren, The Netherlands), or a Bürker-Türk hemocytometer (VWR, Amsterdam, The Netherlands) and the conidia suspension was set at $2 \cdot 10^8$ conidia mL⁻¹.

4.2.3 Thermal treatments

A volume of 0.2 to 1 mL of conidia suspension was added to pre-heated ACES buffer to a total volume of 20 mL in Erlenmeyer flasks in a water bath. Conidia of *A. niger*, *P. roqueforti* and *P. variotii* were treated at 54, 56, and 60 °C, respectively. At various time points, 1 mL samples were taken, immediately chilled on ice, and decimally diluted. One hundred µL was surface-inoculated on MEA and plates were incubated at 25 °C. Non-heated conidia suspensions were also decimally diluted and plated to determine the initial viable concentration of conidia at $t=0$ minutes. Colonies of *P. variotii* were counted after three days of incubation, while *A. niger* and *P. roqueforti* colonies were counted after 7 days. The log₁₀ colony forming units (CFU) mL⁻¹ was calculated for each sampling time point.

4.2.4 Quantification of heat resistance

The reparameterised Weibull model (Eq. 1) (Metselaar *et al.*, 2013) was fitted to the \log_{10} CFU mL⁻¹ data of each inactivation experiment with the R package Growthrates using the Levenberg-Marquardt algorithm (Hall *et al.*, 2013). The Weibull model allows fitting linear, concave, and convex inactivation curves and was able to fit the different thermal inactivation curves of the strains.

$$\text{Log}_{10}(N_t) = \text{Log}_{10}(N_0) - \Delta \cdot \left(\frac{t}{t_{\Delta D}}\right)^\beta \quad (1)$$

where N_0 is the initial concentration of conidia (CFU mL⁻¹), N_t is the number of surviving conidia (CFU mL⁻¹) at time point t , Δ is the reference number of decimal reductions, $t_{\Delta D}$ represents the time needed to reduce the initial number of conidia with Δ decimals, while β represent the shape parameter where $\beta > 1$ gives a concave and $\beta < 1$ a convex behaviour. When β was significantly different from 1, the average D -value was estimated as $\frac{t_{\Delta D}}{\Delta}$. If not, the negative reciprocal of the linear regression slope, $\frac{-1}{\text{slope}}$, was used to estimate the D -value as described (**Chapter 2**; van den Brule *et al.*, 2020b).

4.2.5 Quantification of variability

Experimental, biological and strain variabilities were quantified using the method described by Aryani *et al.* (2015). For each strain, three biologically independent batches of conidial spores were prepared, and conidial heat resistance was tested in duplicate for each batch of conidial spores. Experimental variability (σ_e) was defined as the variability between parallel experimental replicates using the same batch of conidial spores, and expressed by the root mean square error ($\sqrt{MSE_e}$) of Eq. 2

$$MSE_e = \frac{RSS_e}{DF_e} = \frac{\sum_{S=1}^i \sum_{B=1}^3 \sum_{E=1}^2 (X_{EBS} - X_{BS})^2}{n-p} \quad (2)$$

where MSE_e is mean square error, RSS_e is Residual Sum of Squares, DF_e is Degrees of Freedom, X_{EBS} is the \log_{10} D -value of each experiment 'E' of biological replicate 'B' and strain 'S', X_{BS} is the average of the \log_{10} D -value of the experimental duplicates of each biological replicate 'B' of strain 'S', i is the number of strains used per species and DF_e is the number of data points ($n = 2 * 3 * i$) minus the number of parameters ($p = 3 * i$). Biological variability (σ_b) was expressed by $\sqrt{MSE_b}$ of Eq. 3

$$MSE_b = \frac{RSS_b}{DF_b} = \frac{\sum_{S=1}^i \sum_{B=1}^3 (X_{BS} - X_S)^2}{n-p} \quad (3)$$

where X_S is the average of X_{BS} from the biological triplicates of strain 'S' and DF_b is the number of data points ($n = 3 * i$) minus the number of parameters ($p = 1 * i$).

Strain variability (σ_s) was expressed by $\sqrt{MSE_s}$ of Eq. 4

$$MSE_s = \frac{RSS_s}{DF_s} = \frac{\sum_{S=1}^i (X_S - X)^2}{n-p} \quad (4)$$

where X is the average of X_S of all i strains and DF_s is the number of data points ($n = i$) minus the number of parameters ($p = 1$).

The 95% confidence intervals of σ_e , σ_b and σ_s were calculated according to Eq. 5

$$\sqrt{\frac{RSS}{\chi_{DF, \alpha/2}^2}} \leq \sigma \leq \sqrt{\frac{RSS}{\chi_{DF, 1-\alpha/2}^2}} \quad (5)$$

where χ^2 is the critical Chi-square value at $\alpha/2$ and $1 - \alpha/2$ with $\alpha = 0.05$, using the same RSS and DF definitions as in Eq. 2-4.

4.2.6 Meta-analysis

Data describing the inactivation kinetics of conidia of *A. niger* (Baggerman, 1981; Ballestra and Cuq, 1998; Belbahi *et al.*, 2017; Esbelin *et al.*, 2013; Fujikawa *et al.*, 2000; Rege and Pai, 1999; Reveron *et al.*, 2005; Shearer *et al.*, 2002) and *P. roqueforti* (Blank *et al.*, 1998; Bröker *et al.*, 1987a, 1987b; Kunz, 1981; Punt *et al.*, 2020; Shearer *et al.*, 2002) were collected from literature. The obtained D -values were \log_{10} transformed and the mean \log_{10} D -value of each strain tested in this study were added to the data set, resulting in 48 and 148 data points for *A. niger* and *P. roqueforti*, respectively. The \log_{10} D -values versus the temperature were used to calculate the z -value for each species, being negative reciprocal of the linear regression slope, $\frac{-1}{\text{slope}}$. Subsequently, the 95% prediction interval of the linear regression was calculated using Eq. 6

$$\text{Log}_{10} D_{ref} \pm t_{DF; 1-0.5\alpha} \sqrt{\frac{RSS}{DF}} \quad (6)$$

Where D_{ref} is the \log_{10} D -value at the reference temperature, t is the Student t -value with degrees of freedom (DF) $n - 2$ and $\alpha = 0.05$, RSS is the residual sum of squares calculated from the deviation of the data to the linear regression line. The overall variability (σ_t) was defined as the deviation of the data to the linear regression line, $\sqrt{\frac{RSS}{DF}}$ with RSS the residual sum of squares calculated from the deviation of the data to the linear regression line, and $n - 2$.

4.3 RESULTS

4.3.1 Verification of strain identity

In total, 21 *A. niger*, 20 *P. roqueforti* and 20 *P. variotii* strains were selected (Table S4.1) and their identity was verified by sequencing genetic marker genes according to the phylogenetic standards (Houbraken *et al.*, 2020). Based on the partial sequences of *caM*, all *A. niger* strains grouped together with type strain *A. niger* NRRL 326, with *Aspergillus welwitschiae*, the most closely related species, being the sister clade (Fig. 4.1A). Similarly, the partial *benA* sequences of the *P. roqueforti* strains grouped with type strain CBS 221.30 and segregated from the closely related *Penicillium mediterraneum* (Fig. 4.1B). In agreement with previous studies (Chapter 2; van den Brule *et al.*, 2020b; Houbraken *et al.*, 2008), we found more intra-species variation in the partial *benA* sequences of *P. variotii* compared to *A. niger* and *P. roqueforti*. However, all *P. variotii* strains clustered with type strain CBS 102.74, while *Paecilomyces brunneolus* was sister to this cluster (Fig. 4.1C).

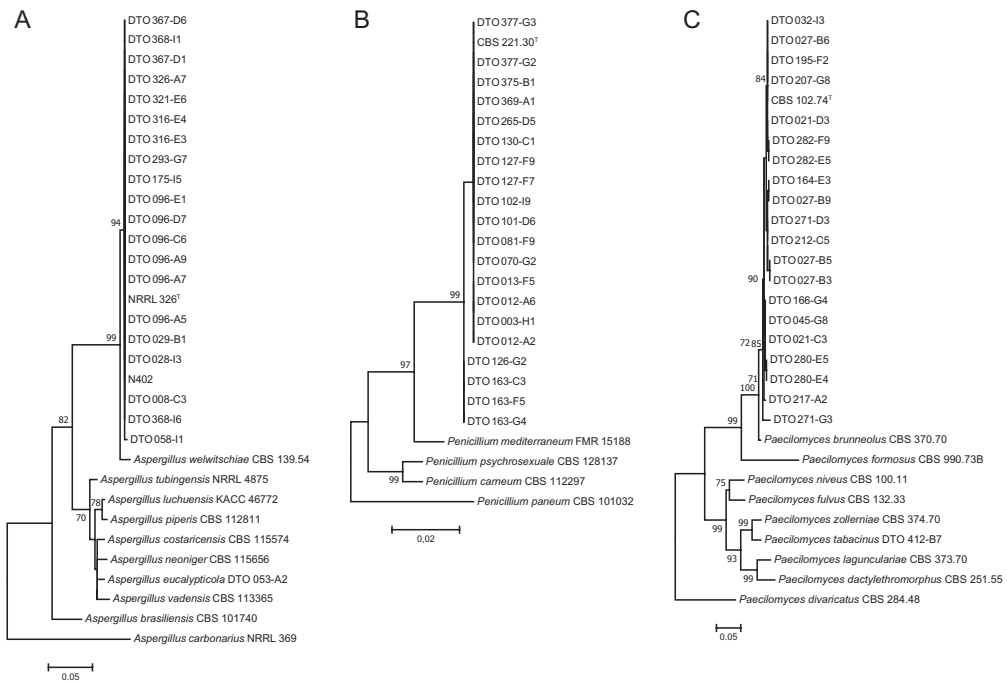


Figure 4.1. Maximum likelihood trees for strain identification. (A) Phylogram based on partial *caM* sequence of studied *A. niger* strains, including type strain NRRL 326 and other closely related *Aspergillus* species with *Aspergillus carbonarius* used as outgroup. (B) Phylogram based on partial *benA* sequences of *P. roqueforti* strains, including type strain CBS 221.30 and other closely related *Penicillium* species with *Penicillium paneum* as outgroup. (C) Phylogram based on partial *benA* gene sequences of *P. variotii* strains, including type strain CBS 102.74 and other closely related *Paecilomyces* species with *Paecilomyces divaricatus* as outgroup.

4.3.2 Quantification of heat resistance

Strains of *A. niger*, *P. roqueforti*, and *P. variotii* were heat-treated using biologically independent batches of conidia and technical duplicates. The differences between the technical replicates were rather small for all strains of the three species (Fig. 4.2A, D, G). The differences between the biological replicates were clearly higher than those of the experimental duplicates (Fig. 4.2B, E, H), but much higher differences were found between the individual strains per species (Fig. 4.2C, F, I). Most inactivation kinetics, *i.e.* 237 out of 366, did not show a significant tailing or a shoulder curvature, and a linear model was used to calculate the *D*-value. For the other data sets the reparameterized Weibull model (Eq. 1) was used to calculate the average *D*-value (Table S4.2).

The most heat-resistant *P. roqueforti* strain was DTO 013-F5, while the most heat-sensitive strain was DTO 130-C1 with D_{56} -values of 13.6 ± 3.0 and 1.6 ± 0.38 minutes, respectively. Similar to *P. roqueforti*, about an eight-fold difference was found between the

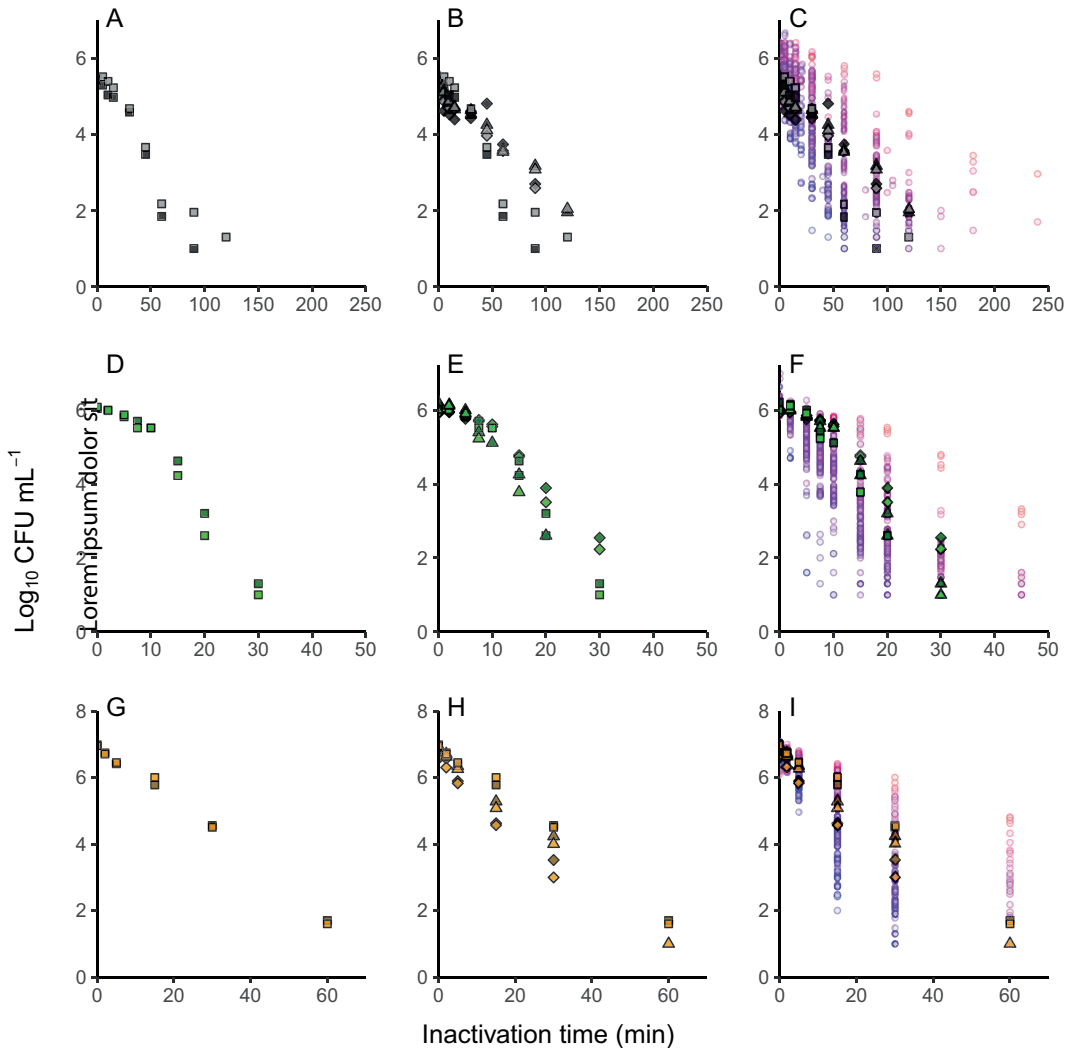


Figure 4.2. Variability in thermal inactivation of species. Thermal inactivation was performed at 54 °C for *A. niger* (A-C), 56 °C for *P. roqueforti* (D-F) and 60 °C for *P. variotii* (G-I). Experimental variability (A, D, G), biological variability (B, E, H) and strain variability (C, F, I) is depicted by the \log_{10} CFU mL^{-1} data of each experiment. The strains *A. niger* DTO 316-E3 (black; A-C), *P. roqueforti* DTO 163-C3 (green; D-F) and *P. variotii* DTO 166-G4 (orange; G-I) are highlighted, showing two experimental replicates (dark fill, light fill) of three biological replicates (\square , \diamond and \triangle). All other strains (\circ ; C, F, I) are coloured using a gradient from blue (heat-sensitive) to red (heat-resistant) based on the mean D -values presented in Table S4.2.

most heat-resistant *P. variotii* strain DTO 195-F2 and the most heat-sensitive strain DTO 212-C5, with corresponding D_{60} -values of 26.6 ± 3.4 and 3.5 ± 0.30 minutes, respectively. This indicates that for this specific heat treatment, one out of ten cells will survive for the most resistant strain, while only one out of 10^8 cells will survive for the most sensitive strain. Three out of 21 *A. niger* strains, DTO 028-I3, DTO 029-B1 and DTO 058-I1, did not

sporulate well after 7 days growth on MEA at 25 °C. A better sporulation was achieved when cultivating at 30 °C instead of 25 °C, and therefore this temperature was used to culture conidia. Interestingly, these three strains belonged to the most heat sensitive strains, with D_{54} -values of 12.6 ± 1.7 , 3.7 ± 0.60 and 9.9 ± 2.2 minutes, respectively. Impeded sporulation can be a sign of degeneration of a strain (Li *et al.*, 2014). Indeed, these three strains were deposited more than six decades ago into the CBS culture collection and it cannot be excluded that the strains degenerated over the years or arrived in a degenerated state when deposited. Because growing cultures at higher temperatures can significantly enhance heat resistance in the case of *Aspergillus fumigatus* (Hagiwara *et al.*, 2017) and *P. roqueforti* conidia (Punt *et al.*, 2020), it was decided to exclude DTO 028-I3, DTO 029-B1 and DTO 058-I1 for further analysis. This made DTO 367-D1 the most sensitive and DTO 326-A2 the most resistant *A. niger* strain with D_{54} -values of 9.4 ± 0.85 and 50.4 ± 11.9 minutes, respectively.

4.3.3 Quantification of variability

The experimental, biological and strain variability of the three species was quantitatively expressed in \sqrt{MSE} (i.e. the standard deviation, σ) of the $\log_{10} D$ -values, which is a measure of variability (Fig. 4.3). Indeed, as observed in Fig. 4.2, experimental variability was the lowest variability factor with σ_e values of 0.045, 0.044 and 0.033 for *A. niger*, *P. roqueforti* and *P. variotii*, respectively. Biological variability values were larger with a σ_b of 0.092, 0.096 and 0.084 for *A. niger*, *P. roqueforti* and *P. variotii*, respectively. Strain variability was clearly higher, with σ_s of 0.197, 0.179 and 0.230 for the three fungi, respectively. Interestingly, the 95% confidence intervals of the three species were overlapping for each of the variability factors. This indicates that there were no significant differences in the magnitude of the variability between the species. However, the variability factors were clearly different, with strain variability being higher than biological variability, and both being higher than experimental variability.

4.3.4 Meta-analysis

The conidial heat resistance of *A. niger* and *P. roqueforti* strains presented in this study was compared with available data from the literature (Table S4.3). Only recently, two studies described the heat resistance for *P. variotii* conidia (Chapter 2, 3; van den Brule *et*

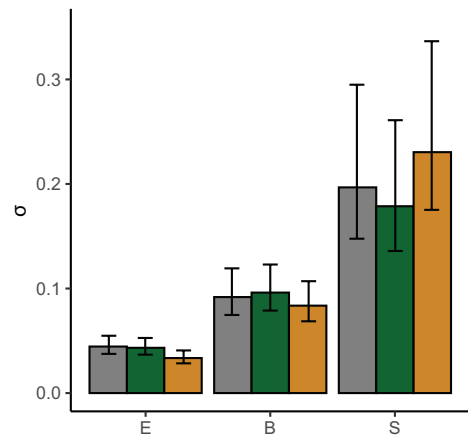


Figure 4.3. Quantification of variability. Experimental variability (E), biological variability (B) and strain variability (S) of *A. niger* (grey), *P. roqueforti* (green) and *P. variotii* (orange). For strain variability 18 *A. niger*, 20 *P. roqueforti* and 20 *P. variotii* strains were used to determine σ_s values. Error bars represent the 95% confidence interval of the σ values.

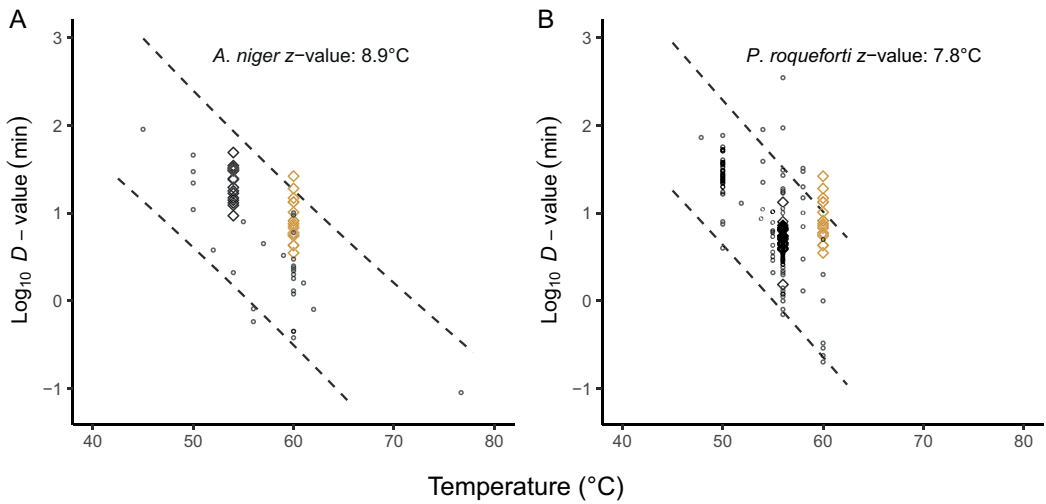


Figure 4.4. Meta-analysis of *A. niger* and *P. roqueforti* D -values. Log_{10} D -values from literature (○) and mean log_{10} D -values per strain presented in this study (◇) were combined to determine z -values and overall variability for *A. niger* (A) and *P. roqueforti* (B). Mean log_{10} D -values of *P. variotii* strains presented in this study are depicted as orange ◇ in both panels. The 95% prediction intervals of the linear regression analysis are depicted as dashed lines in both panels. All data from literature is summarized in Table S3.

al., 2020ab) and therefore this fungus was excluded for the meta-analysis. The D -values from literature for *A. niger* and *P. roqueforti* and the D -values collected in the current study are shown in Fig. 4.4A and 4.4B, respectively. The linear correlation between the log_{10} D -values and temperature allowed to calculate the z -value, indicating the temperature increase needed to decrease D -values 10-fold. The z -values were 8.9 °C for *A. niger* and 7.8 °C for *P. roqueforti*, respectively, which is comparable to z -values found for multiple bacterial species (van Asselt and Zwietering, 2006). The deviation of each data point to the linear regression between log_{10} D -value and temperature was used to quantify the overall variability σ_t , which was 0.432 for *A. niger* and 0.413 for *P. roqueforti*. With σ_s values 46% and 43% of the σ_t values for *A. niger* and *P. roqueforti*, respectively, these results indicate that strain variability is a substantial source of variability in the overall variability reported in literature.

4.3.5 Comparison with variability of bacterial species

It is well known that heat resistance of bacterial spores and vegetative cells differs enormously among species, and consequently the D -values are very different when determined at the same temperature. Interestingly, contrary to the magnitude, the intra-species variability of inactivation rates of bacterial species was in the same order of magnitude when five different bacterial species were compared (den Besten *et al.*, 2018a), including 3 spore-forming bacteria, *B. subtilis*, *B. cereus*, *G. stearothermophilus*, and 2

non-spore-forming bacteria, *L. monocytogenes* and *L. plantarum*. Because the current study used a similar experimental set up to determine heat resistance between fungal strains, taking into account the variability between biologically independent replicates and variability between technical duplicates, we could compare the σ_e , σ_b and σ_s values of the three fungal species to those of the five bacterial species (Fig. 4.5). Note that the *B. subtilis* strains were grouped in a high-level and low-level heat resistant group for quantification of strain variability. The *B. subtilis* strains that produced high-level heat resistant spores harbour a mobile genetic element, *spoVA*^{2mob}, that confers high-level heat resistance to spores (Berendsen *et al.*, 2016), giving genetic evidence for clustering the corresponding strains into two groups. Interestingly, for all microbial species, strain variability was larger than biological and experimental variabilities. Even though the difference was small, the experimental variability of the two *Bacillus* species was slightly higher than the rest of the species, although the variability of *B. cereus* was not significantly larger compared to *A. niger* and *P. roqueforti*. Both *Bacillus* species showed a significant higher biological variability than the other species, while the vegetative cells of *L. monocytogenes* and *L. plantarum* showed a significant lower biological variability compared to the bacterial and fungal spores. Less significant differences were found between strain variability of the different species. Together, these data suggest that the different levels of variability in heat resistance of fungal conidia are rather similar to those of bacterial spores and cells.

4.4 DISCUSSION

Intra-species variability is inherent in microbial species. We scrutinized conidial heat resistance of three fungal species and quantified variability at experimental, biological and strain levels. In total, 18 *A. niger*, 20 *P. roqueforti* and 20 *P. variotii* strains were used to quantify strain variability. Although some reference strains were included in the strain selection it is of importance to select the strains randomly in order to represent variability found in nature. In mycological research, it can be challenging to identify fungal isolates to species level as some are cryptic species. For instance, *A. niger* is difficult to distinguish from *Aspergillus luchuensis* and *Aspergillus welwitschiae* based on morphology (Samson *et al.*, 2019). Even identification by sequencing of genetic marker genes can be puzzling since databases can contain sequences of previously misidentified isolates (Hofstetter *et al.*, 2019; Lücking *et al.*, 2020). Identification of the strains used in this study by phylogenetic analysis of marker genes sequences of reference strains provided a robust identification of the current species. Therefore, the selection of fungal strains and the genetic locus used for comparison indicate that the observed variation in conidial heat resistance is truly intra-species.

Differences in heat resistance are not only caused by variation in genetic background. Heterogeneity in genetically uniform cells can contribute to survival against environmental stress in yeast species (Holland *et al.*, 2014; Tegelaar *et al.*, 2020). Some strains of *P. variotii* can produce conidia populations that are heterogeneous in size (**Chapter 3**; van den Brule *et al.*, 2020a). The same study stated that strains producing conidia with a larger

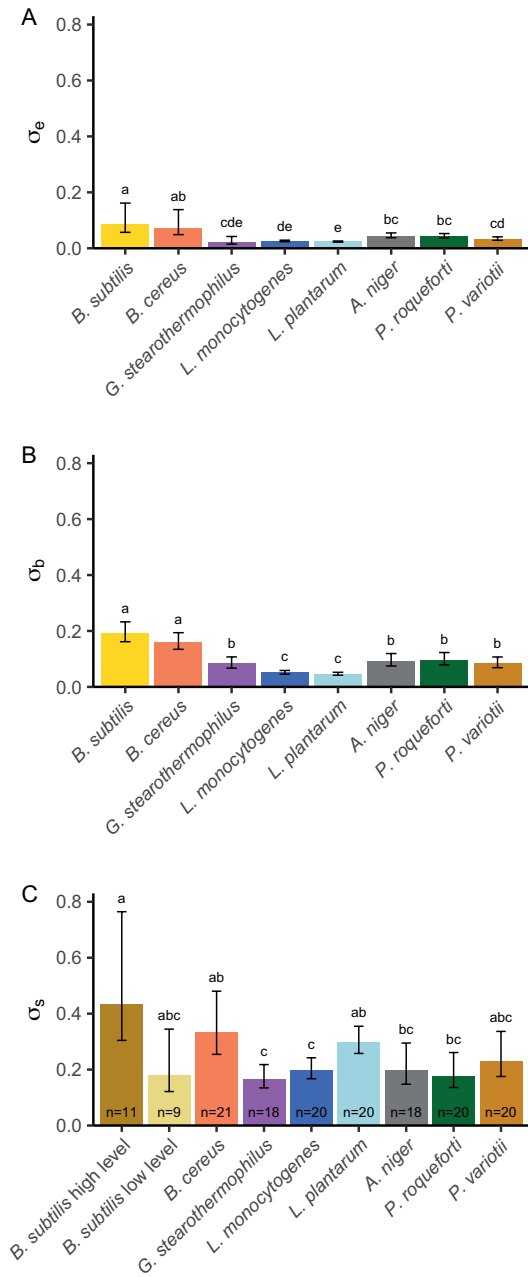


Figure 4.5. Comparison of variability in heat resistance between bacterial spores, vegetative cells and fungal conidia. Experimental (A), biological (B) and strain variability (C) in heat resistance of bacterial spores of *B. subtilis*, *B. cereus* and *G. stearothermophilus*, bacterial vegetative cells of *L. monocytogenes* and *L. plantarum* and fungal conidia of *A. niger*, *P. roqueforti* and *P. variotii*. For strain variability, n represents the number of strains used to determine σ_s values. Error bars represent the 95% confidence interval of the σ values. At each level of variability, significance groups are indicated above the error bars and are based on overlap between the 95% confidence intervals. Data of bacterial species was adapted from den Besten *et al.*, 2018.

mean size tend to be more heat resistant; hinting that the larger conidia within spore populations are more heat resistant compared to small size conidia. In addition to these examples of phenotypic heterogeneity, environmental growth conditions can have a significant effect on heat resistance. Besides cultivation temperature (Hagiwara *et al.*, 2017; Punt *et al.*, 2020), the maturation of conidia also plays a role in the development of heat resistance as conidia from older colonies of *A. niger* and *P. roqueforti* show higher robustness to heat treatment (Punt *et al.*, 2020; Teertstra *et al.*, 2017). On the other hand, environmental conditions during conidiation can also reduce heat resistance of fungal conidia. Growth of the insect-pathogenic fungus *Metarhizium robertsii* at pH 4.6 results in more sensitive conidia compared to the more optimal conditions at pH 8.0 (Rangel *et al.*, 2015). Intracellular compatible solutes and protective proteins are known to provide heat robustness to fungal species (van Leeuwen *et al.*, 2016; Wyatt *et al.*, 2013). Conidia of *A. niger* contain large amounts of Hsp70 transcripts (van Leeuwen *et al.*, 2013b) and mannitol (Teertstra *et al.*, 2017), while arabitol, the hydrophilins con-6 and con-10 and 17 predicted proteins with unknown function were implied to play a role in heat resistance of *P. roqueforti* conidia (Punt *et al.*, 2020). On the other

hand, *P. variotii* conidia contain predominantly trehalose as compatible solute (**Chapter 2**; van den Brule *et al.*, 2020b) and in higher amount than *A. niger* (Teertstra *et al.*, 2017) and *P. roqueforti* (Punt *et al.*, 2020), which might explain, at least in part, the higher heat resistance of this species.

Our experimental set up was aimed to reduce environmental variation as much as possible by spreading many conidia over one plate for inoculation. This way, we anticipated to differences due to colony age, which could be interpreted as environmental variation. In the meta-analysis, we compared our data with data available in literature, where different growth conditions and heating menstua were applied, to visualize this overall variability. This demonstrated that strain variability is a large, if not the largest source of the overall variability. This is consistent with bacterial species, where σ_s values are typically 40% to 75% of the overall variability found in literature (den Besten *et al.*, 2018a). For two other bacterial species, *Escherichia coli* O157:H7 (Whiting and Golden, 2002) and *Staphylococcus aureus* (Rodríguez-Calleja *et al.*, 2006), *D*-values have been determined for a large number of strains at one or two temperatures, allowing us also to quantify the strain variability for these two species using our approach (Eq. 4). This showed that the strain variability of *Escherichia coli* O157:H7 was 0.206 (n=17) as calculated by the \log_{10} *D*-value at 55 °C and 60 °C, whereas for *S. aureus* the strain variability was 0.360 (n=15) as calculated by the \log_{10} *D*-value at 58 °C. Interestingly, these values are in the same order of magnitude as presented in Fig. 4.4C. To the best of our knowledge, for one species, namely *Salmonella* spp., reported differences in heat resistance among strains isolated from various sources tend to be much smaller with σ_s values of 0.07 and 0.09 (den Besten *et al.*, 2018a; Gurtler *et al.*, 2015; Lianou and Koutsoumanis, 2013b), and this supports the relevance to quantify the strain variability of this species in more detail. Quantified microbial variability is crucial information to be included in risk assessments to realistically predict microbial behaviour.

In conclusion, strain variability in conidial heat resistance of the three fungal species was in the same order of magnitude as for several bacterial species, which hints to a natural diversity that stretches beyond kingdoms. In other fields of research, intra-species variability also occurs in virulence, growth and biofilm formation (Lianou *et al.*, 2020), and an intriguing question is whether strain variability is also comparable for other microbial traits.

4.5 SUPPLEMENTARY DATA

Table S4.1. Overview of the strains used in this study.

Strain No.	Other collections	Substrate	Location	Genbank accession number^a	Reference
DTO 008-C3	CBS 113.50	Leather	Germany	MW148182	1
DTO 028-I3	CBS 112.32	Unknown	Japan	MW148184	1
DTO 029-B1	CBS 124.48	Unknown	Ghana	MW148185	
DTO 058-I1	CBS 118.52	Unknown	Unknown	MW148186	
DTO 096-A5	CBS 147371; IBT 20381	Green coffee bean	India	GU195635	2
DTO 096-A7	CBS 147320; IBT 22937	Grape	Australia	MW148187	
DTO 096-A9	CBS 147321; IBT 23366	Artic soil	Svalbard, Norway	MW148188	
DTO 096-C6	CBS 147322; IBT 27294	Coffee	Brazil	MW148189	
DTO 096-D7	CBS 147323; IBT 29331	Raisin	Turkey	MW148190	
DTO 096-E1	CBS 147324; IBT 29884; NRRL 615			MW148191	3
DTO 175-I5	CBS 147482	Surface Water	Portugal	MW148192	
DTO 293-G7	CBS 147344	Coffee beans (Robusta)	Thailand	MW148193	
DTO 316-E3	CBS 133816; IBT 24631	Black pepper	Denmark	GU195636	2
DTO 316-E4	CBS 147345; IBT 26389; NRRL 599			MW148194	4
DTO 321-E6	CBS 147346	CF patient material	the Netherlands	MW148195	
DTO 326-A7	CBS 147347	Petridish from soft drink factory	the Netherlands	MW148196	
DTO 367-D1	CBS 769.97	Leather	Germany	MW148197	
DTO 367-D6	CBS 115989; NRRL 3122			MW148198	5
DTO 368-I1	CBS 147352	Air next to bottle blower	Mexico	MW148199	
DTO 368-I6	CBS 147353	Food factory	Italy	MW148200	
N402	ATCC 64974			MW148183	6

Aspergillus niger

Table S4.1. (Continued).

Strain No.	Other collections	Substrate	Location	Genbank accession number ^A	Reference
DTO 003-H1	CBS 147308	Environment dairy factory	the Netherlands	MW148162	
DTO 012-A2	CBS 147309	Tortilla (flour)	California, USA	MW148163	
DTO 012-A6	CBS 147310	Tortilla (corn)	California, USA	MW148164	
DTO 013-F5	CBS 147311	Margarine	the Netherlands	MW148165	
DTO 070-G2	CBS 147317	Wood	Unknown	MW148166	
DTO 081-F9	CBS 147318	Air in cheese warehouse	the Netherlands	MW148167	
DTO 101-D6	CBS 147325	Cheese surface	the Netherlands	MW148168	
DTO 102-I9	CBS 147326	Drink	The Netherlands	MW148169	
DTO 126-G2	CBS 147330	Air in bakery	USA	MW148170	
DTO 127-F7	CBS 147331	Chicory root extract	the Netherlands	MW148171	
DTO 127-F9	CBS 147332	Chicory root extract	the Netherlands	MW148172	
DTO 130-C1	CBS 147333	Air of cheese factory	the Netherlands	MW148173	
DTO 163-C3	CBS 147337	Single ascospore isolate of DTO 006-G1 and DTO 027-I6	the Netherlands	MW148174	
DTO 163-F5	CBS 147338	Cheese, Garstang Blue	UK	MW148175	
DTO 163-G4	CBS 147339	Barley	Denmark	MW148176	
DTO 265-D5	CBS 147372	Edge of brine bath	the Netherlands	MW148177	
DTO 369-A1	CBS 147354	From mayonnaise, containing K-sorbate	The Netherlands	MW148178	
DTO 375-B1	CBS 147355	Cheese	Mexico	MW148179	
DTO 377-G2	LCP 96.3914	Stewed fruit	France	MW148180	7
DTO 377-G3	LCP 97.4111	Wood	France	MW148181	7

Penicillium roqueforti

Table S4.1. (Continued).

Strain No.	Other collections	Substrate	Location	Genbank accession number ^A	Reference
DTO 021-C3	CBS 145656	Spoiled sports drink	USA	MN153215	8
DTO 021-D3	CBS 145657	Heat shocked sucrose	USA	MN153219	8
DTO 027-B3	CBS 121577	Spoiled sports drink	USA	EU037084	9
DTO 027-B5	CBS 121579	Sucrose	USA	EU037082	9
DTO 027-B6	CBS 121580	Spoiled apple juice	The Netherlands	EU037081	9
DTO 027-B9	CBS 121583	Spoiled sports drink	USA	EU037078	9
DTO 032-I3	CBS 121585	High Fructose Corn Syrup after heat shock	USA	EU037077	9
DTO 045-G8	CBS 145658	Drink	USA	MN153224	8
DTO 164-E3	CBS 145659	Blue berry ingredients	The Netherlands	MN153240	8
DTO 166-G4	CBS 145660	Pectin, heat treated	The Netherlands	MN153245	8
DTO 195-F2	CBS 145663	Margarine	Belgium	MN153269	8
DTO 207-G8	CBS 145664	Fruit, ingredient	The Netherlands	MN153270	8
DTO 212-C5	CBS 145665	Vanilla	The Netherlands	MN153271	8
DTO 217-A2	CBS 145666	Ice pop, heat treated	The Netherlands	MN153275	8
DTO 271-D3	CBS 145667	Industry environment	Guatemala	MN153286	8
DTO 271-G3	CBS 145668	Ice tea	South Africa	MN153287	8
DTO 280-E4	CBS 109073	Pectin	The Netherlands	EU037070	9
DTO 280-E5	CBS 101075	Heat processed fruit beverage	Japan	EU037069	9
DTO 282-E5	CBS 145669	Margarine	Italy	MN153294	8
DTO 282-F9	CBS 145670	Wall covering, industry environment	UK	MN153297	8

Paeclomyces variotii

^AGenbank accession numbers of partial *caM* gene sequences for the studied *A. niger* strains and partial *benA* gene sequences for the *P. roqueforti* and *P. variotii* strains.

Table S4.1. (Continued).**References**

- ¹Meijer M, Houbraeken J, Dalhuijsen S, Samson R, De Vries R. Growth and hydrolase profiles can be used as characteristics to distinguish *Aspergillus niger* and other black aspergilli. *Stud Mycol.* 2011;69:19-30.
- ²Mogensen JM, Nielsen KF, Samson RA, Frisvad JC, Thrane U. Effect of temperature and water activity on the production of fumonisins by *Aspergillus niger* and different *Fusarium* species. *BMC Microbiol.* 2009;9:281.
- ³Moyer AJ. Effect of alcohols on the mycological production of citric acid in surface and submerged culture. II. Fermentation of crude carbohydrates. *Appl Microbiol.* 1953;1(1):7-13.
- ⁴Ramachandran K, Walker TK. A biosynthesis of dimethylpyruvic acid. *Arch Biochem Biophys.* 1951;31(2):224-33.
- ⁵Van Lanen JM, Smith MB, inventors. Hiram Walker & Sons, Inc., assignee. *Process of producing glucamylase and an alcohol product.* United States Patent 3418211. 1968.
- ⁶Bos CJ, Debets AJM, Swart K, Huybers A, Kobus G, Slakhorst SM. Genetic analysis and the construction of master strains for assignment of genes to six linkage groups in *Aspergillus niger*. *Curr Genet.* 1988;14(5):437-43.
- ⁷Ropars J, Cruaud C, Lacoste S, Dupont J. A taxonomic and ecological overview of cheese fungi. *Int J Food Microbiol.* 2012;155(3):199-210.
- ⁸van den Brule T, Punt M, Teertstra W, Houbraeken J, Wösten H, Dijksterhuis J. The most heat-resistant conidia observed to date are formed by distinct strains of *Paecilomyces variotii*. *Environ Microbiol.* 2020;22(3):986-99.
- ⁹Houbraeken J, Varga J, Rico-Munoz E, Johnson S, Samson RA. Sexual reproduction as the cause of heat resistance in the food spoilage fungus *Byssoschlamys spectabilis* (anamorph *Paecilomyces variotii*). *Appl Environ Microbiol.* 2008;74(5):1613-9.

Table S4.2. *D*-values of experimental replicates (E) and biological replicates (B) of all strains used in this study. The temperature used to determine *D*-values was 54 °C for *A. niger*, 56 °C for *P. roqueforti* and 60 °C for *P. variotii* strains. Shaping parameter β including 95% confidence interval (CI) of the Weibull model was used to check significance of the model.

Species	Strain	B	E	<i>D</i> -value	β [95% CI]
<i>A. niger</i>	DTO 008-C3	1	1	12,6	1.3 [0.82 - 1.78]
			2	11,6	1.16 [0.8 - 1.52]
		2	1	16,3	1.61 [0.55 - 2.67]
			2	15,5	1.51 [0.44 - 2.59]
		3	1	11,8	1.33 [0.63 - 2.02]
			2	11,7	1.48 [1.21 - 1.75]
<i>A. niger</i>	DTO 028-I3	1	1	13,3	0.51 [0.32 - 0.7]
			2	13,1	0.47 [0.27 - 0.66]
		2	1	14,3	0.43 [0.23 - 0.63]
			2	13,9	0.42 [0.22 - 0.63]
		3	1	10,1	0.29 [0.15 - 0.44]
			2	11,0	0.3 [0.13 - 0.48]
<i>A. niger</i>	DTO 029-B1	1	1	3,7	0.58 [0.17 - 0.99]
			2	4,7	0.83 [-0.54 - 2.2]
		2	1	3,4	1.01 [0.27 - 1.75]
			2	3,0	1.08 [0.41 - 1.75]
		3	1	3,7	1.08 [0.32 - 1.84]
			2	3,9	1.23 [-0.18 - 2.65]
<i>A. niger</i>	DTO 058-I1	1	1	7,3	0.61 [0.32 - 0.9]
			2	6,8	0.6 [0.31 - 0.89]
		2	1	11,4	0.7 [0.5 - 0.9]
			2	11,5	0.7 [0.48 - 0.92]
		3	1	11,3	0.87 [0.53 - 1.21]
			2	11,2	1.11 [0.69 - 1.53]
<i>A. niger</i>	DTO 096-A5	1	1	13,3	1.05 [0.62 - 1.47]
			2	12,7	1.09 [0.43 - 1.75]
		2	1	13,6	0.94 [0.12 - 1.76]
			2	14,9	0.87 [0.05 - 1.69]
		3	1	15,0	1.05 [0.63 - 1.48]
			2	15,3	1.31 [0.67 - 1.96]
<i>A. niger</i>	DTO 096-A7	1	1	18,5	1.35 [1.14 - 1.57]
			2	17,4	1.2 [0.8 - 1.6]

Table S4.2. (Continued).

Species	Strain	B	E	D-value	β [95% CI]		
<i>A. niger</i>	DTO 096-A9	2	1	21,3	1.14 [0.77 - 1.5]		
			2	22,0	1.03 [0.48 - 1.58]		
		3	1	19,5	1.18 [0.97 - 1.39]		
			2	19,8	1.24 [0.9 - 1.57]		
		1	1	15,3	0.62 [-0.06 - 1.3]		
			2	14,1	0.68 [-0.03 - 1.39]		
		2	1	13,7	0.6 [0.16 - 1.04]		
			2	10,6	0.58 [0.17 - 0.99]		
		<i>A. niger</i>	DTO 096-C6	3	1	10,6	0.7 [0.2 - 1.2]
					2	10,6	0.7 [0.16 - 1.23]
1	1			43,4	0.66 [0.02 - 1.3]		
	2			46,4	1.78 [1.14 - 2.42]		
2	1			29,6	1.32 [0.74 - 1.89]		
	2			30,3	1.32 [0.69 - 1.95]		
3	1			31,9	1.31 [0.66 - 1.96]		
	2			31,1	1.54 [1.18 - 1.89]		
<i>A. niger</i>	DTO 096-D7			1	1	28,0	1.27 [0.73 - 1.81]
					2	31,2	1.43 [0.17 - 2.69]
		2	1	28,1	1.39 [1.32 - 1.46]		
			2	25,5	1.99 [1.28 - 2.7]		
		3	1	44,6	2.8 [-0.08 - 5.68]		
			2	39,0	2 [1.29 - 2.71]		
		1	1	26,2	1.19 [0.83 - 1.55]		
			2	19,6	1.07 [0.7 - 1.44]		
		<i>A. niger</i>	DTO 096-E1	2	1	32,5	0.66 [0.42 - 0.89]
					2	30,9	0.71 [0.55 - 0.88]
3	1			21,8	0.6 [0.34 - 0.86]		
	2			20,8	0.67 [0.4 - 0.93]		
1	1			14,2	1.57 [0.1 - 3.03]		
	2			15,3	1.4 [0.33 - 2.48]		
2	1			21,9	0.74 [0.32 - 1.15]		
	2			20,2	0.86 [0.45 - 1.26]		
3	1			19,5	0.67 [0.41 - 0.92]		
	2			18,0	0.92 [0.56 - 1.28]		

Table S4.2. (Continued).

Species	Strain	B	E	D-value	β [95% CI]		
<i>A. niger</i>	DTO 293-G7	1	1	30,5	0.62 [0.33 - 0.92]		
			2	33,9	0.57 [0.29 - 0.85]		
		2	1	16,1	0.96 [0.19 - 1.73]		
			2	16,3	0.96 [0.23 - 1.68]		
		3	1	28,6	0.79 [0.31 - 1.27]		
			2	26,1	0.81 [0.29 - 1.32]		
<i>A. niger</i>	DTO 316-E3	1	1	47,5	2.43 [0.19 - 4.67]		
			2	39,9	1.38 [1.01 - 1.74]		
		2	1	37,7	0.97 [0.57 - 1.37]		
			2	37,6	0.9 [0.6 - 1.21]		
		3	1	18,9	1.15 [0.53 - 1.77]		
			2	25,1	0.82 [0.33 - 1.32]		
		<i>A. niger</i>	DTO 316-E4	1	1	15,8	1.2 [0.77 - 1.63]
					2	26,3	1.05 [0.63 - 1.46]
2	1			18,0	0.96 [0.43 - 1.5]		
	2			17,5	0.98 [0.5 - 1.47]		
3	1			14,5	0.54 [0.29 - 0.78]		
	2			12,2	0.78 [0.58 - 0.97]		
<i>A. niger</i>	DTO 321-E6	1	1	47,1	0.41 [0.17 - 0.65]		
			2	37,8	0.68 [0.35 - 1]		
		2	1	28,3	0.74 [0.18 - 1.3]		
			2	26,5	0.77 [0.25 - 1.29]		
		3	1	23,8	0.71 [0.35 - 1.06]		
			2	24,9	0.63 [0.22 - 1.04]		
<i>A. niger</i>	DTO 326-A7	1	1	59,8	1.03 [0.31 - 1.74]		
			2	45,9	1.3 [1.04 - 1.56]		
		2	1	50,9	1.32 [0.95 - 1.69]		
			2	66,5	1.18 [0.79 - 1.56]		
		3	1	47,5	0.9 [0.53 - 1.27]		
			2	32,2	1.75 [0.8 - 2.7]		
<i>A. niger</i>	DTO 367-D1	1	1	10,8	1.06 [-0.3 - 2.43]		
			2	8,9	1.05 [0.4 - 1.7]		
		2	1	9,2	0.69 [0.52 - 0.86]		
			2	9,8	0.77 [0.57 - 0.97]		

Table S4.2. (Continued).

Species	Strain	B	E	D-value	β [95% CI]
<i>A. niger</i>	DTO 367-D6	3	1	9,5	0.91 [0.48 - 1.34]
			2	8,3	0.72 [0.34 - 1.09]
		1	1	15,9	1.01 [0.41 - 1.61]
			2	15,1	0.9 [0.46 - 1.35]
		2	1	15,3	1.06 [0.57 - 1.55]
			2	15,0	0.95 [0.58 - 1.31]
<i>A. niger</i>	DTO 368-I1	3	1	14,0	0.8 [0.48 - 1.12]
			2	14,6	0.71 [0.39 - 1.03]
		1	1	39,5	1.91 [1.36 - 2.45]
			2	40,1	1.92 [1.23 - 2.61]
		2	1	22,7	1.01 [0.57 - 1.46]
			2	20,5	1.29 [0.79 - 1.79]
<i>A. niger</i>	DTO 368-I6	3	1	33,3	0.69 [0.37 - 1.02]
			2	34,8	0.65 [0.26 - 1.04]
		1	1	34,4	0.9 [0.6 - 1.2]
			2	31,4	1.32 [0.89 - 1.76]
		2	1	31,3	1.3 [0.35 - 2.26]
			2	37,0	1.87 [1.28 - 2.47]
<i>A. niger</i>	N402	3	1	32,1	1.59 [1 - 2.18]
			2	31,2	1.27 [1.01 - 1.54]
		1	1	28,5	1.32 [0.54 - 2.09]
			2	26,7	1.24 [0.75 - 1.73]
		2	1	33,3	1.54 [0.92 - 2.16]
			2	32,2	1.6 [1.08 - 2.12]
<i>P. roqueforti</i>	DTO 003-H1	3	1	34,8	1.24 [0.88 - 1.59]
			2	33,4	1.15 [0.83 - 1.48]
		1	1	4,3	1.11 [0.65 - 1.58]
			2	4,4	1.06 [0.64 - 1.47]
		2	1	5,5	0.91 [0.53 - 1.3]
			2	5,7	0.82 [0.5 - 1.14]
<i>P. roqueforti</i>	DTO 012-A2	3	1	5,3	1.02 [0.28 - 1.77]
			2	7,7	0.7 [0.13 - 1.28]
		1	1	5,2	1.15 [0.81 - 1.5]
			2	5,0	1.26 [0.94 - 1.58]

Table S4.2. (Continued).

Species	Strain	B	E	D-value	β [95% CI]
<i>P. roqueforti</i>	DTO 012-A6	2	1	4,0	1.11 [0.82 - 1.39]
			2	3,9	1.11 [0.53 - 1.69]
		3	1	4,5	1.19 [0.53 - 1.86]
			2	4,6	1.28 [0.78 - 1.79]
		1	1	7,9	0.94 [0.2 - 1.67]
			2	8,0	0.88 [0.11 - 1.65]
		2	1	7,6	2.43 [1.96 - 2.9]
			2	9,2	1.27 [0.45 - 2.09]
		3	1	7,4	2.61 [2.06 - 3.16]
			2	7,7	2.51 [1.95 - 3.07]
<i>P. roqueforti</i>	DTO 013-F5	1	1	14,8	1.94 [1.6 - 2.28]
			2	15,6	1.6 [1.29 - 1.91]
		2	1	16,0	2 [1.88 - 2.13]
			2	15,8	2.26 [1.9 - 2.61]
		3	1	9,1	1.56 [1.1 - 2.02]
			2	10,5	1.86 [1.39 - 2.34]
		1	1	8,1	1.01 [0.4 - 1.62]
			2	7,5	1.7 [1.28 - 2.12]
		2	1	6,6	0.53 [0.18 - 0.89]
			2	4,5	1.02 [0.8 - 1.24]
3	1	7,8	1.18 [0.38 - 1.97]		
	2	7,2	1.97 [1.05 - 2.89]		
<i>P. roqueforti</i>	DTO 081-F9	1	1	7,3	2.14 [1.74 - 2.54]
			2	7,5	2.04 [1.79 - 2.29]
		2	1	6,0	1.75 [0.72 - 2.77]
			2	7,8	5 [-0.71 - 10.71]
		3	1	2,5	1.8 [1.38 - 2.23]
			2	2,5	1.63 [1.22 - 2.04]
		1	1	6,8	0.9 [0.54 - 1.25]
			2	8,1	0.77 [0.47 - 1.06]
		2	1	5,9	1.11 [0.89 - 1.33]
			2	6,1	1.26 [1.14 - 1.39]
3	1	6,5	0.95 [0.77 - 1.14]		
	2	6,3	0.95 [0.88 - 1.02]		

Table S4.2. (Continued).

Species	Strain	B	E	D-value	β [95% CI]		
<i>P. roqueforti</i>	DTO 102-I9	1	1	7,5	1.09 [0.62 - 1.55]		
			2	9,8	0.79 [0.51 - 1.07]		
		2	1	7,8	0.64 [0.38 - 0.9]		
			2	7,4	0.82 [0.37 - 1.27]		
		3	1	5,7	0.58 [0.17 - 0.98]		
			2	6,1	0.62 [0.26 - 0.98]		
<i>P. roqueforti</i>	DTO 126-G2	1	1	3,9	1.38 [0.85 - 1.92]		
			2	4,1	1.37 [1 - 1.74]		
		2	1	3,7	1.43 [0.91 - 1.95]		
			2	3,8	1.39 [0.91 - 1.87]		
		3	1	4,2	1.61 [1.3 - 1.93]		
			2	4,5	1.64 [-0.01 - 3.28]		
		<i>P. roqueforti</i>	DTO 127-F7	1	1	3,9	1.44 [1.14 - 1.75]
					2	3,9	1.82 [1.53 - 2.11]
2	1			4,3	1.51 [0.66 - 2.37]		
	2			5,2	0.83 [0.24 - 1.42]		
3	1			3,1	1.39 [1.08 - 1.71]		
	2			3,0	1.67 [1.28 - 2.06]		
<i>P. roqueforti</i>	DTO 127-F9	1	1	5,3	1.66 [1.2 - 2.12]		
			2	4,9	1.86 [1.14 - 2.57]		
		2	1	5,5	1.55 [0.76 - 2.35]		
			2	5,6	1.16 [0.77 - 1.54]		
		3	1	6,0	1.67 [1.28 - 2.06]		
			2	6,0	1.65 [1.22 - 2.08]		
		<i>P. roqueforti</i>	DTO 130-C1	1	1	1,9	0.99 [0.1 - 1.87]
					2	1,7	1.02 [0.59 - 1.46]
2	1			2,0	0.72 [0.14 - 1.31]		
	2			1,6	0.93 [-0.36 - 2.23]		
3	1			1,1	NA		
	2			1,1	NA		
<i>P. roqueforti</i>	DTO 163-C3	1	1	9,0	1.54 [1.12 - 1.97]		
			2	7,6	1.54 [0.89 - 2.19]		
		2	1	6,1	1.62 [1.17 - 2.07]		
			2	5,5	1.41 [0.83 - 2]		

Table S4.2. (Continued).

Species	Strain	B	E	D-value	β [95% CI]		
<i>P. roqueforti</i>	DTO 163-F5	3	1	5,4	1.79 [1.25 - 2.32]		
			2	6,2	1.7 [-0.07 - 3.46]		
		1	1	5,2	1.24 [1.03 - 1.44]		
			2	5,6	1 [0.74 - 1.26]		
		2	1	6,3	2.17 [1.15 - 3.2]		
			2	7,3	2.32 [0.91 - 3.72]		
<i>P. roqueforti</i>	DTO 163-G4	3	1	3,9	1.21 [0.87 - 1.55]		
			2	4,6	1.04 [0.67 - 1.41]		
		1	1	4,1	1.16 [0.92 - 1.39]		
			2	4,4	0.91 [0.5 - 1.32]		
		2	1	5,1	0.67 [0.29 - 1.05]		
			2	4,5	0.86 [0.63 - 1.09]		
		3	1	4,3	0.87 [0.68 - 1.06]		
			2	3,7	0.83 [0.34 - 1.32]		
		<i>P. roqueforti</i>	DTO 265-D5	1	1	5,8	1.13 [0.63 - 1.64]
					2	5,3	0.81 [0.43 - 1.19]
				2	1	4,2	1.1 [0.86 - 1.35]
					2	4,2	1.17 [0.85 - 1.49]
3	1			4,5	1.08 [0.5 - 1.66]		
	2			3,9	1.06 [0.03 - 2.1]		
<i>P. roqueforti</i>	DTO 369-A1	1	1	3,8	0.77 [0.25 - 1.3]		
			2	5,5	0.57 [0.06 - 1.08]		
		2	1	3,6	1 [0.53 - 1.47]		
			2	4,0	0.99 [0.7 - 1.28]		
		3	1	3,2	1.09 [0.46 - 1.73]		
			2	3,7	0.82 [0.42 - 1.23]		
		<i>P. roqueforti</i>	DTO 375-B1	1	1	5,2	1.32 [0.76 - 1.89]
					2	4,3	1.69 [0.45 - 2.94]
2	1			4,7	1.37 [0.63 - 2.11]		
	2			3,9	1.36 [0.68 - 2.04]		
<i>P. roqueforti</i>	DTO 377-G2	3	1	4,7	1.28 [0.91 - 1.66]		
			2	4,4	1.17 [0.7 - 1.63]		
		1	1	5,2	0.99 [0.77 - 1.22]		
			2	6,2	0.88 [0.7 - 1.07]		

Table S4.2. (Continued).

Species	Strain	B	E	D-value	β [95% CI]
<i>P. roqueforti</i>	DTO 377-G3	2	1	6,2	0.67 [0.3 - 1.03]
			2	5,9	0.63 [0.32 - 0.94]
		3	1	7,2	1.11 [0.86 - 1.36]
			2	7,5	0.99 [0.83 - 1.16]
		1	1	7,0	0.97 [0.35 - 1.59]
			2	7,5	0.99 [0.64 - 1.35]
		2	1	5,1	0.83 [0.63 - 1.02]
			2	3,9	1.19 [0.67 - 1.71]
		3	1	4,6	1.5 [1.09 - 1.92]
			2	4,1	1.69 [1.17 - 2.2]
<i>P. variotii</i>	DTO 021-C3	1	1	12,9	1.18 [1.04 - 1.31]
			2	13,5	1.05 [0.8 - 1.3]
		2	1	15,4	1.27 [0.68 - 1.85]
			2	15,5	1.37 [1.09 - 1.66]
		3	1	11,8	1.34 [0.86 - 1.83]
			2	12,1	1.17 [1.11 - 1.22]
		1	1	3,3	1.12 [0.47 - 1.77]
			2	3,5	1.27 [-0.98 - 3.51]
		2	1	4,6	1.2 [0.12 - 2.28]
			2	4,4	1.07 [-0.92 - 3.07]
<i>P. variotii</i>	DTO 027-B3	3	1	5,4	0.83 [0.28 - 1.39]
			2	5,2	0.83 [0.3 - 1.37]
		1	1	4,0	0.89 [0.76 - 1.02]
			2	4,0	1 [0.66 - 1.34]
		2	1	7,3	0.88 [0.49 - 1.28]
			2	7,4	0.94 [0.43 - 1.45]
		3	1	6,4	0.79 [0.39 - 1.19]
			2	6,0	0.8 [0.63 - 0.97]
		1	1	7,1	0.96 [0.36 - 1.56]
			2	6,7	1.45 [0.94 - 1.96]
<i>P. variotii</i>	DTO 027-B5	2	1	10,3	1.16 [0.54 - 1.77]
			2	11,1	0.99 [0.76 - 1.22]
		3	1	7,7	0.85 [0.47 - 1.22]
			2	7,1	0.98 [0.36 - 1.61]

Table S4.2. (Continued).

Species	Strain	B	E	D-value	β [95% CI]
<i>P. variotii</i>	DTO 027-B6	1	1	4,1	1.51 [0.57 - 2.44]
			2	4,0	1.19 [0.04 - 2.34]
		2	1	6,1	0.95 [0.46 - 1.43]
			2	6,1	1.05 [0.68 - 1.43]
		3	1	7,0	0.95 [0.44 - 1.45]
			2	6,8	0.99 [0.39 - 1.59]
<i>P. variotii</i>	DTO 027-B9	1	1	11,6	0.88 [0.62 - 1.14]
			2	9,4	1.05 [0.96 - 1.14]
		2	1	6,6	0.83 [0.57 - 1.08]
			2	6,2	0.82 [0.64 - 1]
		3	1	8,1	0.73 [0.39 - 1.06]
			2	8,4	0.74 [0.09 - 1.38]
<i>P. variotii</i>	DTO 032-I3	1	1	5,4	1.03 [0.64 - 1.42]
			2	4,8	0.8 [-0.02 - 1.63]
		2	1	6,8	0.94 [0.51 - 1.36]
			2	6,6	0.98 [0.5 - 1.45]
		3	1	5,9	1.03 [0.71 - 1.34]
			2	5,8	1.06 [0.91 - 1.2]
<i>P. variotii</i>	DTO 045-G8	1	1	7,3	1.21 [1.04 - 1.37]
			2	6,3	1.42 [1.2 - 1.65]
		2	1	6,4	0.92 [0.6 - 1.24]
			2	6,2	1.01 [0.82 - 1.2]
		3	1	10,0	0.75 [0.41 - 1.09]
			2	7,5	0.96 [0.67 - 1.25]
<i>P. variotii</i>	DTO 164-E3	1	1	5,1	0.81 [0.6 - 1.02]
			2	6,0	0.83 [0.4 - 1.26]
		2	1	4,5	0.89 [-0.07 - 1.84]
			2	5,1	0.88 [0.82 - 0.94]
		3	1	6,3	0.79 [0.28 - 1.3]
			2	6,7	0.8 [0.69 - 0.92]
<i>P. variotii</i>	DTO 166-G4	1	1	9,0	0.69 [0.23 - 1.16]
			2	8,4	0.86 [0.7 - 1.02]
		2	1	11,2	0.82 [0.41 - 1.23]
			2	10,4	0.92 [0.69 - 1.15]

Table S4.2. (Continued).

Species	Strain	B	E	D-value	β [95% CI]
<i>P. variotii</i>	DTO 195-F2	3	1	11,6	1.11 [0.9 - 1.32]
			2	11,4	1.2 [0.91 - 1.48]
		1	1	24,2	0.72 [0.32 - 1.12]
			2	21,3	0.71 [0.48 - 0.94]
		2	1	28,2	0.84 [0.67 - 1.02]
			2	26,4	1 [0.67 - 1.32]
<i>P. variotii</i>	DTO 207-G8	3	1	30,4	1.22 [0.42 - 2.02]
			2	29,2	0.79 [0.44 - 1.14]
		1	1	5,6	0.97 [0.27 - 1.67]
			2	5,8	1.07 [0.93 - 1.2]
		2	1	6,9	0.9 [0.26 - 1.53]
			2	6,9	0.96 [0.54 - 1.38]
<i>P. variotii</i>	DTO 212-C5	3	1	8,2	0.83 [0.61 - 1.06]
			2	7,8	0.89 [0.66 - 1.12]
		1	1	3,6	0.97 [-1.73 - 3.68]
			2	4,0	1.22 [-2.85 - 5.28]
		2	1	3,4	1.08 [-0.44 - 2.59]
			2	3,2	1.03 [-1.29 - 3.35]
<i>P. variotii</i>	DTO 217-A2	3	1	3,8	1.24 [0.48 - 2.01]
			2	3,2	1.24 [-2 - 4.49]
		1	1	24,5	0.79 [0.56 - 1.03]
			2	22,5	0.91 [0.54 - 1.29]
		2	1	19,2	1.02 [0.86 - 1.19]
			2	18,7	1.07 [0.98 - 1.16]
<i>P. variotii</i>	DTO 271-D3	3	1	16,3	1.28 [1.03 - 1.53]
			2	15,2	1.24 [0.95 - 1.53]
		1	1	7,2	0.83 [0.56 - 1.09]
			2	8,6	0.91 [0.61 - 1.21]
		2	1	8,4	1.03 [0.83 - 1.24]
			2	7,4	1.06 [0.94 - 1.18]
<i>P. variotii</i>	DTO 271-G3	3	1	7,8	1.26 [0.66 - 1.86]
			2	6,4	1.09 [0.88 - 1.3]
		1	1	5,9	0.85 [0.57 - 1.14]
	2	6,3	0.86 [0.29 - 1.43]		

Table S4.2. (Continued).

Species	Strain	B	E	D-value	β [95% CI]
<i>P. variotii</i>	DTO 280-E4	2	1	3,7	1.41 [0.42 - 2.39]
			2	2,9	1.25 [0.7 - 1.8]
		3	1	3,2	1.37 [0.78 - 1.96]
			2	4,7	0.83 [-0.51 - 2.16]
		1	1	6,3	0.7 [0.58 - 0.82]
			2	6,5	0.85 [0.6 - 1.1]
		2	1	4,5	0.78 [-0.43 - 1.98]
			2	3,8	0.86 [-0.6 - 2.32]
<i>P. variotii</i>	DTO 280-E5	3	1	6,2	0.85 [0.63 - 1.07]
			2	6,4	0.84 [0.67 - 1.02]
		1	1	5,1	0.81 [0.6 - 1.02]
			2	6,0	0.83 [0.4 - 1.26]
		2	1	6,8	0.74 [0.34 - 1.15]
			2	6,5	0.75 [0.39 - 1.11]
		3	1	6,0	0.9 [0.66 - 1.13]
			2	5,8	0.94 [0.67 - 1.21]
<i>P. variotii</i>	DTO 282-E5	1	1	16,1	0.73 [0.36 - 1.1]
			2	13,7	0.72 [0.48 - 0.96]
		2	1	11,7	0.87 [0.76 - 0.97]
			2	11,5	0.8 [0.51 - 1.09]
		3	1	14,2	0.72 [0.49 - 0.96]
			2	13,5	0.67 [0.44 - 0.89]
		1	1	17,0	1.12 [0.84 - 1.39]
			2	15,4	1.2 [1.07 - 1.33]
<i>P. variotii</i>	DTO 282-F9	2	1	13,8	1.17 [0.9 - 1.44]
			2	14,2	1.26 [1.1 - 1.43]
		3	1	14,5	1.01 [0.89 - 1.13]
			2	14,5	1 [0.9 - 1.09]

Table S4.3. (Continued).

Species	Ref	Strain	Log ₁₀ D-value			Environmental conditions			Heat inactivation			
			t (min)	°C	pH	aW	Media*	t (days)	T (°C)	Menstruum*	pH	aW
			Incubation									
	3	AB573988.1	0,380	60			PDA	10	25	PS + Tween 80		
	4	CM896	1,474	50			CA	15	25	Pilsen Beer	4,28	
	4	CM896	0,580	52			CA	15	25	Pilsen Beer	4,28	
	4	CM896	0,322	54			CA	15	25	Pilsen Beer	4,28	
	4	CM896	-0,237	56			CA	15	25	Pilsen Beer	4,28	
	5		-0,347	60			YMA	10	25	BBP + Tween-20 + Citrate buffer	3	
	5		-0,420	60			YMA	10	25	BBP + Tween-20 + Citrate buffer	3,5	
	5	ATCC	-0,347	60			YMA	10	25	BBP + Tween-20 + Citrate buffer	4	
	6	200930	0,362	60			PDA	7	25	BBP + Tween-20 + Citrate buffer	7	
	6	ATCC	0,255	60			PDA	7	25	Phosphate buffer + Tween	7	
	6	200930	0,301	60			PDA	7	25	Phosphate buffer + Tween	7	
	7	N402	-0,090	56			MEA	7	30	Water + Tween 80		
	8	NCIM 595	-1,046	76,7						Clarified pomegranate juice		

Aspergillus niger

Table S4.3. (Continued).

Species	Ref	Strain	Log ₁₀ D-value			Environmental conditions			Incubation			Heat inactivation		
			t (min)	°C	pH	aW	Media*	t (days)	T (°C)	Menstruum*	pH	aW		
<i>Penicillium roqueforti</i>	9	LCP 96.4111	0,048	56	56		MEA	7	15	ACES buffer	6,8			
	9	LCP 96.4111	0,299	56	56		MEA	3	25	ACES buffer	6,8			
	9	LCP 96.4111	0,539	56	56		MEA	5	25	ACES buffer	6,8			
	9	LCP 96.4111	0,534	56	56		MEA	7	25	ACES buffer	6,8			
	9	LCP 96.4111	0,725	56	56		MEA	10	25	ACES buffer	6,8			
	9	LCP 96.4111	0,623	56	56		MEA	7	30	ACES buffer	6,8			
	9	LCP 96.4111	0,600	56	56		MEA	10	30	ACES buffer	6,8			
	5		-0,697	60	60	6,2	YMA	10	25	Citrate buffer	3			
	5		-0,623	60	60	6,2	YMA	10	25	Citrate buffer	3,5			
	5		-0,538	60	60	6,2	YMA	10	25	Citrate buffer	4			
	10	309		1,380	50	5,4	MEA	21	25	2% Albumin from meat				
	10	309		1,447	50	5,4	MEA	21	25	4% Albumin from meat				
	10	309		1,756	50	5,4	MEA	21	25	6% Albumin from meat				
	10	309		1,380	50	5,4	MEA	21	25	2% Amino acid mixture				
	10	309		1,431	50	5,4	MEA	21	25	4% Amino acid mixture				
	10	309		1,716	50	5,4	MEA	21	25	6% Amino acid mixture				
	10	309		1,415	50	5,4	MEA	21	25	Borate-HCl buffer	8			
10	309		1,352	50	5,4	MEA	21	25	Borate-NaOH buffer	8				
10	309		1,477	50	5,4	MEA	21	25	2% CaCl2					
10	309		1,477	50	5,4	MEA	21	25	4% CaCl2					

Table S4.3. (Continued).

		Log ₁₀ D-value		Environmental conditions				Heat inactivation				
				Incubation								
Species	Ref	Strain	t (min)	°C	pH	aW	Media*	t (days)	T (°C)	Menstruum*	pH	aW
	10	309	1,477	50	5,4	0,99	MEA	21	25			
	10	309	1,398	50	5,4	0,99	MEA	21	25	Citrate-HCl buffer		3
	10	309	1,051	56	5,4	0,99	MEA	21	25	10% Fructose		
	10	309	1,237	56	5,4	0,99	MEA	21	25	20% Fructose		
	10	309	1,431	56	5,4	0,99	MEA	21	25	30% Fructose		
	10	309	1,973	56	5,4	0,99	MEA	21	25	40% Fructose		
	10	309	2,545	56	5,4	0,99	MEA	21	25	50% Fructose		
	10	309	-0,155	56	5,4	0,99	MEA	21	25	10% Glucose		
	10	309	-0,097	56	5,4	0,99	MEA	21	25	50% Glucose		
	10	309	0,079	56	5,4	0,99	MEA	21	25	20% Glucose		
	10	309	0,079	56	5,4	0,99	MEA	21	25	30% Glucose		
	10	309	0,114	56	5,4	0,99	MEA	21	25	40% Glucose		
	10	309	1,568	50	5,4	0,99	MEA	21	25	Glycine-HCl buffer		3
	10	309	1,574	50	5,4	0,99	MEA	21	25	2% KCl		
	10	309	1,574	50	5,4	0,99	MEA	21	25	4% KCl		
	10	309	1,574	50	5,4	0,99	MEA	21	25	6% KCl		
	10	309	1,491	50	5,4	0,99	MEA	21	25	Phosphate buffer		8
	10	309	0,875	50	5,4	0,99	MEA	21	25	KHP-HCl buffer		3
	10	309	0,556	56	5,4	0,99	MEA	21	25	Maize oil		

Penicillium roqueforti

Table S4.3. (Continued).

		Log ₁₀ D-value		Environmental conditions				Heat inactivation				
				Incubation								
Species	Ref	Strain	t (min)	°C	pH	aW	Media*	t (days)	T (°C)	Menstruum*	pH	aW
	10	309	1,568	50	5,4	0,99	MEA	21	25			
	10	309	1,568	50	5,4	0,99	MEA	21	25	2% MgCl2		
	10	309	1,568	50	5,4	0,99	MEA	21	25	4% MgCl2		
	10	309	1,568	50	5,4	0,99	MEA	21	25	6% MgCl2		
	10	309	1,380	50	5,4	0,99	MEA	21	25	Phosphate buffer	8	
	10	309	1,380	50	5,4	0,99	MEA	21	25	2% NaCl		
	10	309	1,380	50	5,4	0,99	MEA	21	25	4% NaCl		
	10	309	1,380	50	5,4	0,99	MEA	21	25	6% NaCl		
	10	309	0,778	56	5,4	0,99	MEA	21	25	Olive oil		
	10	309	1,491	56	5,4	0,99	MEA	21	25	Ölsäure		
	10	309	0,881	56	5,4	0,99	MEA	21	25	Paraffin		
	10	309	0,806	56	5,4	0,99	MEA	21	25	Peanut oil		
	10	309	1,301	50	5,4	0,99	MEA	21	25	2% MEA		
	10	309	1,371	50	5,4	0,99	MEA	21	25	4% MEA		
	10	309	1,580	50	5,4	0,99	MEA	21	25	6% MEA		
	10	309	1,217	50	5,4	0,99	MEA	21	25	2% MEA		
	10	309	1,301	50	5,4	0,99	MEA	21	25	4% MEA		
	10	309	1,556	50	5,4	0,99	MEA	21	25	6% MEA		
	10	309	1,243	50	5,4	0,99	MEA	21	25	2% MEA		
	10	309	1,342	50	5,4	0,99	MEA	21	25	4% MEA		

Penicillium roqueforti

Table S4.3. (Continued).

		Log ₁₀ D-value			Environmental conditions			Heat inactivation				
		Incubation										
Species	Ref	Strain	t (min)	°C	pH	aW	Media*	t (days)	T (°C)	Menstruum*	pH	aW
	10	309	1,431	50	5,4	0,99	MEA	21	25			
	10	309	0,000	56	5,4	0,99	MEA	21	25	6% MEA	PS	5,5
	10	309	0,079	56	5,4	0,99	MEA	21	25		PS	5,5
	10	309	0,342	56	5,4	0,99	MEA	21	25		PS	5,5
	10	309	0,415	56	5,4	0,99	MEA	21	25		PS	5,5
	10	309	0,477	56	5,4	0,99	MEA	21	25		PS	5,5
	10	309	0,860	56	5,4	0,99	MEA	21	25		PS	5,5
	10	309	1,380	50	5,4	0,99	MEA	21	25		PS	5,5
	10	309	1,380	50	5,4	0,99	MEA	21	25		PS	5,5
	10	309	0,531	56	5,4	0,99	MEA	21	25	10% Saccharose	PS	5,5
	10	309	0,602	56	5,4	0,99	MEA	21	25	20% Saccharose		
	10	309	0,716	56	5,4	0,99	MEA	21	25	30% Saccharose		
	10	309	0,833	56	5,4	0,99	MEA	21	25	40% Saccharose		
	10	309	1,255	56	5,4	0,99	MEA	21	25	50% Saccharose		
	10	309	0,380	56	5,4	0,99	MEA	21	25	10% Sorbitol solution		
	10	309	0,447	56	5,4	0,99	MEA	21	25	20% Sorbitol solution		
	10	309	0,462	56	5,4	0,99	MEA	21	25	30% Sorbitol solution		
	10	309	0,477	56	5,4	0,99	MEA	21	25	40% Sorbitol solution		
	10	309	0,505	56	5,4	0,99	MEA	21	25	50% Sorbitol solution		
	10	309	0,820	56	5,4	0,99	MEA	21	25	Soybean oil		

Penicillium roqueforti

Table S4.3. (Continued).

Species	Ref	Strain	Log ₁₀ D-value				Environmental conditions				Heat inactivation			
			t (min)	°C	pH	aW	Incubation				Menstruum*	pH	aW	
							Media*	t (days)	T (°C)	T (°C)				
	10	309	0,146	56	5,4	0,99	MEA	21	25	10% Xylitol solution				
	10	309	0,322	56	5,4	0,99	MEA	21	25	20% Xylitol solution				
	10	309	0,415	56	5,4	0,99	MEA	21	25	30% Xylitol solution				
	10	309	0,477	56	5,4	0,99	MEA	21	25	40% Xylitol solution				
	10	309	0,568	56	5,4	0,99	MEA	21	25	50% Xylitol solution				
	10	309	0,602	50	5,4	0,99	MEA	21	25	Unknown buffer	2			
	10	309	0,903	50	5,4	0,99	MEA	21	25	Unknown buffer	3			
	10	309	1,477	50	5,4	0,99	MEA	21	25	Unknown buffer	11			
	10	309	1,526	50	5,4	0,99	MEA	21	25	Unknown buffer	10			
	10	309	1,562	50	5,4	0,99	MEA	21	25	Unknown buffer	9			
	10	309	1,568	50	5,4	0,99	MEA	21	25	Unknown buffer	8			
	10	309	1,607	50	5,4	0,99	MEA	21	25	Unknown buffer	4			
	10	309	1,708	50	5,4	0,99	MEA	21	25	Unknown buffer	7			
	10	309	1,724	50	5,4	0,99	MEA	21	25	Unknown buffer	5			
	10	309	1,886	50	5,4	0,99	MEA	21	25	Unknown buffer	6			
	11	230	-0,481	60	5,4	0,99	MEA	21	25	PS	5,5			
	11	230	0,114	58	5,4	0,99	MEA	21	25	PS	5,5			
	11	230	0,724	56	5,4	0,99	MEA	21	25	PS	5,5			
	11	230	1,041	54	5,4	0,99	MEA	21	25	PS	5,5			
	11	287	0,301	60	5,4	0,99	MEA	21	25	PS	5,5			

Penicillium roqueforti

Table S4.3. (Continued).

		Log ₁₀ D-value		Environmental conditions				Heat inactivation				
				Incubation								
Species	Ref	Strain	t (min)	°C	pH	aW	Media*	t (days)	T (°C)	Menstruum*	pH	aW
<i>Penicillium roqueforti</i>	11	287	0,845	58	5,4	0,99	MEA	21	25		PS	5,5
	11	287	1,230	56	5,4	0,99	MEA	21	25		PS	5,5
	11	287	1,591	54	5,4	0,99	MEA	21	25		PS	5,5
	11	309	0,699	60	5,4	0,99	MEA	21	25		PS	5,5
	11	309	1,000	58	5,4	0,99	MEA	21	25		PS	5,5
	11	309	1,279	56	5,4	0,99	MEA	21	25		PS	5,5
	11	309	1,954	54	5,4	0,99	MEA	21	25		PS	5,5
	11	309	1,512	58	5,4	0,99	MEA	21	25		PS	5,5
	11	309	1,477	58	5,4	0,99	MEA	21	25		PS	5,5
	11	309	1,301	58	5,4	0,99	MEA	21	25		PS	5,5
	11	309	1,176	58	5,4	0,99	MEA	21	25		PS	5,5
	11	714	0,000	60	5,4	0,99	MEA	21	25		PS	5,5
	11	714	0,477	58	5,4	0,99	MEA	21	25		PS	5,5
11	714	1,000	56	5,4	0,99	MEA	21	25		PS	5,5	
11	714	1,352	54	5,4	0,99	MEA	21	25		PS	5,5	
12			0,934	53,85							PS	5,5
12			1,114	51,85							PS	5,5
12			1,863	47,85							PS	5,5
13	ATCC	10110	0,322	55	5,6	0,88	PDA	10	22	Water + Tween 80		

Table S4.3. (Continued).

		Log ₁₀ D-value	Environmental conditions			Heat inactivation						
Species	Ref	Strain	Incubation									
			t (min)	°C	pH	aW	Media* ¹	t (days)	T (°C)	Menstruum*	pH	aW
<i>Penicillium roqueforti</i>	13	ATCC 10110	0,462	55	5,6	0,88	PDA	10	22	Water + Tween 80		
	13	ATCC 10110	0,505	55	5,6	0,88	PDA	10	22	Water + Tween 80		
	13	ATCC 10110	0,556	55	5,6	0,9	PDA	10	22	Water + Tween 80		
	13	ATCC 10110	0,633	55	5,6	0,9	PDA	10	22	Water + Tween 80		
	13	ATCC 10110	0,732	55	5,6	0,97	PDA	10	22	Water + Tween 80		
	13	ATCC 10110	0,778	55	5,6	0,9	PDA	10	22	Water + Tween 80		
	13	ATCC 10110	0,799	55	5,6	0,97	PDA	10	22	Water + Tween 80		
	13	ATCC 10110	0,892	55	5,6	0,97	PDA	10	22	Water + Tween 80		
	13	ATCC 10110	1,013	55	5,6	0,99	PDA	10	22	Water + Tween 80		
	13	ATCC 10110	1,013	55	5,6	0,99	PDA	10	22	Water + Tween 80		
	13	ATCC 10110	1,013	55	5,6	0,99	PDA	10	22	Water + Tween 80		

*Abbreviations: MEA, malt extract agar; PDA, potato dextrose agar; YMA, yeast mould agar; CA, Czapek agar; RS, Ringer solution; PS, Physiologic salt; BBP, Butterfield's buffered phosphate.

References

- ¹Baggerman W. Heat resistance of yeast cells and fungal spores. In: Samson R, Hoekstra, ES and Van Oorschoot CAN, editor. Introduction to food-borne fungi Utrecht: Centraalbureau voor Schimmelcultures (CBS); 1981. p. 227-31.
- ²Ballestra P, Cug J-L. Influence of pressurized carbon dioxide on the thermal inactivation of bacterial and fungal spores. LWT-Food Sci Technol. 1998;31(1):84-8.

Table S4.3. (Continued).

- ³Belbahi A, Bohuon P, Leguérinel I, Meot J-M, Loiseau G, Madani K. Heat resistances of *Candida apicola* and *Aspergillus niger* spores isolated from date fruit surface. *J Food Process Eng.* 2017;40(1):e12272.
- ⁴Reveron IM, Barreiro JA, Sandoval AJ. Thermal death characteristics of *Lactobacillus paracasei* and *Aspergillus niger* in Pilsen beer. *J Food Eng.* 2005;66(2):239-43.
- ⁵Shearer AEH, Mazzotta AS, Chuyate R, Gombas DE. Heat resistance of juice spoilage microorganisms. *J Food Prot.* 2002;65(8):1271-5.
- ⁶Fujikawa H, Morozumi S, Smerage GH, Teixeira AA. Comparison of capillary and test tube procedures for analysis of thermal inactivation kinetics of mold spores. *J Food Prot.* 2000;63(10):1404-9.
- ⁷Esbelin J, Mallea S, J Ram AF, Carlin F. Role of pigmentation in protecting *Aspergillus niger* conidiospores against pulsed light radiation. *Photochem Photobiol.* 2013;89(3):758-61.
- ⁸Rege A, Pai JS. Development of thermal process for clarified pomegranate (*Punica granatum*) juice. *J Food Sci Technol.* 1999;36:261-3.
- ⁹Punt M, van den Brule T, Teertstra WR, Dijksterhuis J, den Besten HMW, Ohm RA, *et al.* Impact of maturation and growth temperature on cell-size distribution, heat-resistance, compatible solute composition and transcription profiles of *Penicillium roqueforti* conidia. *Food Res Int.* 2020;136:109287.
- ¹⁰Bröker U, Spicher, G., Ahrens, E. Zur Frage der Hitzeresistenz der Erreger der Schimmelbildung bei Backwaren. 2.Mitteilung: Einfluss endogener Faktoren auf die Hitzeresistenz von Schimmelsporen. *Getreide, Mehl und Brot.* 1987;41(9):278-84.
- ¹¹Bröker U, Spicher, G., Ahrens, E. Zur Frage der Hitzeresistenz der Erreger der Schimmelbildung bei Backwaren. 3.Mitteilung: Einfluss exogener Faktoren auf die Hitzeresistenz von Schimmelsporen. *Getreide, Mehl und Brot.* 1987;41(11):344-55.
- ¹²Kunz B. Untersuchungen über den Einfluß der Temperatur auf Konidien suspensionen ausgewählter Penicillien species. *Nahrung.* 1981;25(2):185-91.
- ¹³Blank G, Yang R, Scanlon MG. Influence of sporulation a_w on heat resistance and germination of *Penicillium roqueforti* spores. *Food Microbiol.* 1998;15(2):151-6.

Comparative genomic, transcriptomic and phenotypic analysis of *Paecilomyces variotii* strains reveal complexity in mechanisms involved in conidial heat stress resistance

Tom van den Brule, Maarten Punt, Sjoerd Seekles, Pepijn Teunissen, Véronique Ongenae, Eunice Then, Arthur Ram, Jos Houbraken, Han Wösten, Robin Ohm and Jan Dijksterhuis

ABSTRACT

The filamentous fungus *Paecilomyces variotii* produces high numbers of conidia. Previously, it was shown that \log_{10} inactivation times (D -values) of these asexual spores can vary up to 8-fold in a set of 20 strains. Here, we extended the heat resistance within this strain set by comparative genomics and transcriptomics and by analysis of conidia size, internal compatible solute composition and resistance towards sorbic and benzoic acid. Heat resistance significantly correlated with the size of the conidia and the amount of trehalose in these spores. Phylogenetic analysis with a principle component analysis showed clustering of heat resistant strains, which was confirmed by a phylogenetic analysis of 6331 unique conserved orthologous genes of the 20 strains and 5 additional *P. variotii* strains. Comparative genomics and transcriptomics revealed a set of 93 and 65 genes, respectively, that are possibly involved in conidial heat resistance. In addition, a genomic region of approximately 60 kbp was identified that was present in most heat resistant strains and absent in all heat sensitive strains. However, no phenotypic differences were found in a heat resistant strain in which the cluster was deleted, indicating that the cluster does not play a role in heat resistance. In conclusion, the large number of candidate genes that are potentially involved in heat resistance suggest that this type of stress resistance is caused by complex molecular mechanisms.

5.1 INTRODUCTION

Fungi belonging to the order Eurotiales are often associated with food spoilage (Dijksterhuis, 2017). These fungi produce asexual reproductive survival structures called conidia. Being airborne and produced in high numbers, conidia are ubiquitous in the environment and virtually present in every cubic meter of air (Dijksterhuis, 2017). This has consequences in terms of food spoilage, as conidia act as stress-resistant contaminants.

One of the most important preservation hurdles to inactivate conidia in industrially processed food is heat treatment. Heat stress affects many cellular components and processes (Mattoon *et al.*, 2021; Richter *et al.*, 2010). It can lead to protein denaturation and aggregation, lipid oxidation within cellular membranes, DNA and RNA damage and degeneration of cytoskeleton and organelles (Keyhani, 2018; Richter *et al.*, 2010). Upon exposure to heat, a stress response is induced which shows large similarities in all domains of life (Richter *et al.*, 2010). Methylated ribosomal RNAs (Bügl *et al.*, 2000), transcription factors and kinases initiate the heat stress response (Veri *et al.*, 2018). Enzymes involved in DNA- and RNA-modification are essential to repair heat induced DNA damage (Jantschitsch and Trautinger, 2003), while heat-shock proteins (HSPs) and proteins involved in the proteolytic system play a crucial role in protein homeostasis (Tereshina, 2005). In addition, proteins are involved in maintaining cellular structures like the cytoskeleton and the cell membrane (Welker *et al.*, 2010).

Being dormant with minimal metabolic activity (Novodvorska *et al.*, 2016; Teertstra *et al.*, 2017), conidia are not expected to be able to adapt to changing conditions after their release into the environment. Therefore, protective compounds (e.g. compatible solutes and protective proteins) accumulate in conidia during their formation to protect these spores against an array of harsh conditions (Wyatt *et al.*, 2013). The compatible solutes trehalose and mannitol have a protective function inside cells and are associated with heat and desiccation resistance (Wyatt *et al.*, 2013). Absence of either one of these compounds leads to more heat sensitive conidia in *Aspergillus niger* (Ruijter *et al.*, 2003; Seekles *et al.*, 2021a), *Aspergillus nidulans* (Fillinger *et al.*, 2001) and also in more sensitive vegetative *Saccharomyces cerevisiae* cells (De Virgilio *et al.*, 1994). Several proteins with a predicted protective function are found in conidia. In proteomic studies, heat shock proteins HSP70 and HSP90 have been found in *A. fumigatus* conidia (Schmidt *et al.*, 2018), while HSP90 and HSP30 were found in conidia of the entomopathogenic fungus *Metarhizium acridum* (Barros *et al.*, 2010). In addition, large amounts of transcripts of hydrophilin homologues of *con-6*, *con-10*, as well as *hsp12* are found in *A. niger* (van Leeuwen *et al.*, 2013b) and *A. fumigatus* conidia (Hagiwara *et al.*, 2017), as well as transcripts of the LEA-like protein LeamA in the case of *A. niger* (van Leeuwen *et al.*, 2016). *In vitro* analysis of heterologously expressed *Aspergillus fischeri* Hsp12A, Hsp12B and LeamA indicated a protective role against heat and desiccation stress and freeze-thaw cycles (van Leeuwen *et al.*, 2016). Conidiation specific genes *con-6* and *con-10* were discovered in *Neurospora crassa* (Berlin and Yanofsky, 1985) and are associated with development of conidia and with the heat stress response. Their precise role in stress resistance remains largely elusive because *con-6* and *con-10* deficient strains are not affected by heat stress (Springer *et al.*, 1992; White and Yanofsky, 1993). Knockout strains of the homologous genes *conF* and *conJ* in *A. nidulans* were also not affected by heat stress (Suzuki *et al.*, 2013). Instead, the absence of these genes result in higher accumulation of the low molecular weight compatible solutes glycerol and erythritol in conidia, which even leads to increased resistance against desiccation.

Conidia of the food spoilage fungus *Paecilomyces variotii* are the most heat resistant conidia reported in literature (**Chapter 2, 3**; van den Brule *et al.*, 2020ab). As a thermotolerant species, these spores accumulate trehalose as predominant compatible solute. Recently, variability in conidial heat resistance among 20 *P. variotii* strains was studied (**Chapter 4**). Their resistance varied widely with up to a 8-fold difference in \log_{10} inactivation times (*D*-values), thus leading to a ten-million-fold higher inactivation after a heat-treatment of 26 minutes at 60 °C.

Here, we related heat resistance of the 20 *P. variotii* strains with conidia size, compatible solute concentration and minimum inhibitory concentrations of sorbic and benzoic acid. In addition, we compared the genomes of the 20 strains, plus 5 additional *P. variotii* strains of which heat resistance had been quantified, and studied changes in transcriptome in response to different cultivation temperatures. A genome-wide association study (GWAS) resulted in 93 candidate genes, whereas the transcriptome analysis listed 45 up-regulated and 20 down-regulated when cultivation at 37 °C was compared with 25 °C. These genes

of interest have a vast variety in functions, such as HSPs and hydrophilins, and indicate that heat resistance results from multiple molecular mechanisms.

5.2 MATERIAL & METHODS

5.2.1 Strain selection and growth conditions

In total, 25 *P. variotii* strains were used in this study (Table 5.1). These strains had been isolated from different sources (**Chapter 2**; van den Brule *et al.*, 2020b) and their conidial heat resistance was previously quantified (van den Brule *et al.*, 2020a; **Chapter 3, 4**). The DTO collection numbers refer to the working collection of the Food and Indoor Mycology group at the Westerdijk Fungal Biodiversity Institute, except for CBS 101075, which was previously sequenced and published under its CBS collection number (Urquhart *et al.*, 2018). Conidia were stored in 30% (w/v) glycerol at -80 °C. Strains were grown for 3 to 5 days at 25 °C on Malt Extract Agar (MEA, Oxoid, Hampshire, UK). Conidia were harvested from these cultures (see below) and 10 µL of a spore suspension was spread on a MEA plate using an inoculation loop. The plate was incubated for 7 days at 25 °C, unless indicated differently. *Escherichia coli* was grown in Lysogeny Broth (LB, ThermoFisher, Waltham, MA, USA) at 37 °C and 200 rpm. The medium was supplemented with ampicillin (50 mg L⁻¹) in the case of plasmid-carrying strains.

5.2.2 Harvesting conidia and estimation of spore size

Harvesting of conidia was performed as described (**Chapter 2**; van den Brule *et al.*, 2020b). In short, 7-day-old conidia were taken up in 10 mL ice-cold ACES buffer (10 mM N-(2-acetamido)-2-aminoethanesulfonic acid, 0.02% Tween 80, pH 6.8) using a T-spatulum. The suspension was vortexed and filtered through glass wool. After centrifugation, the pellet was washed twice in ice-cold ACES buffer and stored on ice in 10 mL ACES buffer. The conidia concentration was measured using a Beckman Coulter Counter Multisizer3, equipped with a 70 µm aperture tube. To this end, conidial suspensions were diluted 2 · 10³ times in ISOTON II diluent (Beckman Coulter, Fichtenhain, Germany) of which 100 µL was sampled. About 10³ objects with a spherical equivalent diameter between 2 and 8 µm were used to determine conidia size. The mean spherical equivalent diameter was used to describe the conidia size. Due to legislation, conidia of genetically modified strains were first inactivated at 95 °C for 10 minutes prior to measuring. The number of particles measured during Coulter Counter analysis was used to set the undiluted suspension to 2 · 10⁹ conidia mL⁻¹ for further experiments.

5.2.3 Quantification of conidial heat resistance

ACES buffer (19 mL) was preheated in a water bath (120 rpm, 60 or 62 °C) in a 100 mL Erlenmeyer flask. At t=0, 1 mL conidia suspension was added to the pre-heated buffer

Table 5.1. *P. variotii* strains used in this study.

Strain	Other collection	Substrate	Origin	D_{60} -value (min)	Reference
DTO 021-C3	CBS 145656	Spoiled sports drink	USA	13.5 ± 1.8	Chapter 4
DTO 021-D3	CBS 145657	Heat shocked sucrose	USA	4.4 ± 1.0	Chapter 4
DTO 027-B3	CBS 121577	Spoiled sports drink	USA	5.8 ± 1.7	Chapter 4
DTO 027-B5	CBS 121579	Sucrose	USA	8.4 ± 2.1	Chapter 4
DTO 027-B6	CBS 121580	Spoiled apple juice	The Netherlands	5.7 ± 1.5	Chapter 4
DTO 027-B9	CBS 121583	Spoiled sports drink	USA	8.4 ± 2.1	Chapter 4
DTO 032-I3	CBS 121585	High fructose corn syrup after heat shock	USA	5.9 ± 0.8	Chapter 4
DTO 032-I4*	CBS 121586	Spoiled bottle of sweetened tea	USA	4.9 ± 1.7	Chapter 3
DTO 045-G8	CBS 145658	Drink	USA	7.3 ± 1.3	Chapter 4
DTO 063-F5*		Human; Abscess	The Netherlands	3.5 ± 0.2	Chapter 3
DTO 164-E3	CBS 145659	Blue berry ingredients	The Netherlands	5.6 ± 0.9	Chapter 4
DTO 166-G4	CBS 145660	Pectin, heat treated	The Netherlands	10.3 ± 1.4	Chapter 4
DTO 166-G5*		Pectin, heat treated	The Netherlands	11.9 ± 1.3	Chapter 3
DTO 169-C6*	CBS 145661	Indoor environment	USA	9.4 ± 0.5	Chapter 3
DTO 169-E5*	CBS 145662	Indoor environment	USA	5.0 ± 2.0	Chapter 3
DTO 195-F2	CBS 145663	Margarine	Belgium	26.6 ± 3.6	Chapter 4
DTO 207-G8	CBS 145664	Fruit, ingredient	The Netherlands	6.9 ± 1.1	Chapter 4
DTO 212-C5	CBS 145665	Vanilla	The Netherlands	3.5 ± 0.3	Chapter 4
DTO 217-A2	CBS 145666	Ice pop, heat treated	The Netherlands	19.4 ± 3.9	Chapter 4
DTO 271-D3	CBS 145667	Industry environment	Guatemala	7.6 ± 0.5	Chapter 4
DTO 271-G3	CBS 145668	Ice tea	South Africa	4.5 ± 1.5	Chapter 4
DTO 280-E4	CBS 109073	Pectin	The Netherlands	5.6 ± 1.3	Chapter 4
CBS 101075	DTO 280-E5	Heat processed fruit beverage	Japan	6.0 ± 0.6	Chapter 4
DTO 282-E5	CBS 145669	Margarine	Italy	13.4 ± 1.7	Chapter 4
DTO 282-F9	CBS 145670	Wall covering, industry environment	UK	14.9 ± 1.1	Chapter 4
CBS 144490 HYG1		Indoor environment	Australia	NA**	Urquhart <i>et al.</i> , 2018
DTO 217-A2 $\Delta ku70$	PT39.26			NA	Seekles <i>et al.</i> , 2021b
DTO 217-A2 $\Delta ku70 \Delta 60kb$					This study

*Strains not included in phenotypic characterization;

**Not Available.

resulting in a final concentration of 10^7 spores mL^{-1} . After 2, 5, 15, 30 and 60 min of heat treatment, samples of 1 mL were taken and immediately cooled on ice. Samples were 4 times 10-fold diluted to obtain a dilution series down to 10^3 conidia mL^{-1} and 100 μL of each dilution was inoculated per MEA plate. The untreated spore suspension was used as $t=0$ sample. The number of colony forming units (CFUs) was determined after 3 days of incubation at 25 °C. Inactivation curves were described by linear regression and D -values were determined by $\frac{-1}{\text{slope}}$ of the inactivation curve.

5.2.4 Quantification of compatible solutes in conidia

Compatible solute concentration in conidia was determined as described (**Chapter 2**; van den Brule *et al.*, 2020b). In short, 10^8 conidia were centrifuged 1 min at 21000 g (4 °C) and the resulting pellet was flash-frozen in liquid nitrogen. Two 3.2 mm stainless steel beads were added to the sample and the pellet was homogenized for 6 min at 30 Hz in a Qiagen TissueLyser in pre-cooled adaptors (-80 °C). Next, 1 mL ultrapure water was added and the samples were vortexed and transferred to a 95 °C water bath for 30 min to extract the compatible solutes and inactivate enzymes. Because strains DTO 217-A2 $\Delta ku70$ and DTO 217-A2 $\Delta ku70 \Delta 60 \text{ kbp}$ are classified as genetically modified organisms, another extraction procedure was followed; in this case conidia were not physically disrupted prior to extraction. To this end, 10^8 conidia in ACES buffer were incubated in a water bath for 3 hours at 95 °C to extract compatible solutes. No significant differences were found between the two extraction methods. All samples were centrifuged after extraction for 30 min at 21.000 g (4 °C) and the supernatant was filtered through an Acrodisc 0.2 μm nylon syringe filter (Pall Life Science, Mijdrecht, The Netherlands).

Compatible solutes were quantified by HPLC using equipment and a procedure as described (**Chapter 2**; van den Brule *et al.*, 2020b). A Waters 515 HPLC pump (0.6 mL min^{-1}) with control module, a Waters 717 plus Autosampler and two Waters Sugar-Pak I columns (placed in line and kept at 70 °C in a WAT380040 column heater module) were attached to a Waters IR 2414 Refractive Index detector. A sample volume of 20 μL was injected in the mobile phase (0.1 mM Ca EDTA in ultrapure water) using a 30 min run to separate the compatible solutes. A mixture of trehalose, glucose, glycerol, erythritol, mannitol and arabitol (0.002 – 0.10% w/v) was used as a reference. Peak integration and quantification were done using the apex algorithm with manual adjustments using Empower software (Waters, Etten-Leur, The Netherlands). To estimate the concentration, the mean volume of conidia was determined by $V = \frac{4}{3}\pi \left(\frac{\text{mean spore size}}{2}\right)^3$ using the mean conidia size as determined above.

5.2.5 Determination MIC K-sorbate and Na-benzoate

The minimum inhibitory concentration (MIC) of undissociated sorbic acid and benzoic acid was determined in Malt Extract Broth (MEB, Oxoid, Hampshire, UK) set at pH 4.0 using HCl and NaOH. MEB was supplemented with either 2400 ppm K-sorbate or 1368

ppm Na-benzoate, corresponding to a concentration of 13.5 mM undissociated sorbic acid and 6.5 mM undissociated benzoic acid. MEB with and without the supplemented salts were inoculated with 10^5 conidia mL⁻¹ and were used to make a 1.33-fold serial dilutions in 96-wells plates. The final concentrations of undissociated sorbic acid tested were 13.5, 10.1, 7.6, 5.7, 4.2, 3.2, 2.4, 1.8, 1.4, 1.0, and 0.76 mM, while this was 5.9, 4.4, 3.3, 2.5, 1.9, 1.4, 1.1, 0.8, 0.6, 0.4, and 0.3 mM in the case of undissociated benzoic acid using a final volume of 50 μ L. To prevent dehydration, plates were placed in a box containing compartments filled with water. Experiments were done in triplicate and mean and maximum MIC were determined per strain per condition after 28 days of incubation at 25 °C.

5.2.6 DNA isolation, genome sequencing, de novo assemblies and annotation

Conidia were harvested from a 7-day-old MEA culture as described above. The total amount of harvested spores was added in a 500 mL flask to 250 mL complete medium (CM; de Vries *et al.*, 2004) containing 1% glucose (w/v). Liquid cultures were incubated for 16 hours at 30 °C and 250 RPM. The cultures were filtered through a Miracloth filter in a funnel. The mycelium was rinsed with about 100 mL minimal medium (MM; de Vries *et al.*, 2004) without carbon source. The filter was folded and squeezed between two paper towels to remove excessive fluid, after which the mycelium was freeze-dried. The freeze-dried mycelium was homogenized in a Qiagen TissueLyser for 2 min at 25 Hz in 2 mL Eppendorf tubes containing two stainless steel beats. The mycelium powder was used to isolate genomic DNA with the DNeasy PowerPlant Pro Kit according to the protocol of the supplier (Qiagen, Venlo, the Netherlands).

The genomic DNA was sequenced using Illumina NextSeq500 150 bp paired-end technology (Utrecht Sequencing Facility, useq.nl), except DTO 032-I3, DTO 212-C5 and DTO 217-A2 that were sequenced using Illumina MiSeq 300 bp paired-end technology. Reads were trimmed for quality using BBDuk (<https://sourceforge.net/projects/bbmap/>). For each strain, a *de novo* assembly was made using SPAdes v 3.11.1. Scaffolds smaller than 1 kb were removed from the assemblies. Gene prediction was performed as described (Punt *et al.*, 2020). In short, BRAKER v 2.1.2 (Hoff *et al.*, 2016) was employed to train the *ab initio* gene predictor Augustus v 3.0.3 (Stanke *et al.*, 2006) using RNA-sequencing data of CBS 101075 (Urquhart *et al.*, 2018). With the generated parameter set and the RNA-sequencing reads individual gene predictions were performed for each isolate. Functional annotation of the predicted genes was performed essentially as described (de Bekker *et al.*, 2017), with the exception that PFAM v 32 was used (El-Gebali *et al.*, 2018).

5.2.7 Comparative genomics

The amino acid sequences of the predicted genes were used as input for Orthofinder v 2.5.2 (Emms and Kelly, 2019) to determine orthologous conserved genes between strains. *Paecilomyces formosus* No5 (Oka *et al.*, 2014) was included as outgroup in the

construction of a phylogenetic tree. All 6331 unique single-copy orthologous genes were aligned and subsequently concatenated. A maximum likelihood tree was generated using RAxML v 8.2.12 using the model GAMMA + JIT + F and 100 bootstrap replications. In addition, the genomes were aligned using NUCmer or PROmer of the MUMmer4 tool (Marçais *et al.*, 2018).

Single nucleotide polymorphisms (SNPs) of each strain were identified using the heat-resistant strain DTO 217-A2 as reference and a Genome Analysis Toolkit (GATK) best practices pipeline. To this end, the FastQ reads were mapped to the reference assembly using Bowtie2 v 2.2.9. Duplicates of the PCR were removed using Picard tools (MarkDuplicates, v 2.9.2). HaplotypeCaller (GATK, v 3.7) was used for variant calling with the following parameters: `-stand_call_conf 30`, `-ploidy 1` and `-ERC`. Single-sample variant files (GVCFs) were joined using CombineGVCF (GATK, v 3.7) prior to genotyping using GenotypeGVCFs (GATK, v 3.7) with `--sample-ploidy 1`. Because GATK is optimized for short read Illumina sequence data, CBS 101075 was excluded from this analysis since this strain was sequenced using PacBio technology (Urquhart *et al.*, 2018). SNPs were associated with heat-resistance using the log transformed *D*-values in PLINK v 1.90b6.18 (Purcell *et al.*, 2007), using the `--assoc --allow-extra-chr --allow-no-sex` flags. In addition, SnpEff v 4.3 (Cingolani *et al.*, 2012) was used to annotate the predicted biological effects of the SNPs.

5.2.8 RNA isolation and RNA sequencing

Conidia were harvested as described above, excluding the washing steps. After harvesting, the conidia suspension was centrifuged for 5 minutes at 1100 g and 4 °C. The pellet was resuspended in 100 µL RNA-later (ThermoFisher, Waltham, MA, USA) and immediately flash-frozen in liquid nitrogen. The frozen samples were transferred to a tungsten-steel grinding jar with a 20 mm bead (Qiagen, Hilden, Germany) that had been precooled in liquid nitrogen and grinded for 1 min at 30 Hz in a TissueLyser (Qiagen, Hilden, Germany). RNA was isolated with the RNeasy Plant Mini Kit (Qiagen, Hilden, Germany) including an on-column genomic DNA digestion with an RNase-Free DNase Set (Qiagen, Hilden, Germany). The RNA concentration was measured with Qubit (ThermoFisher, Waltham, MA, USA) and RNA integrity was checked using gel electrophoresis.

RNA sequencing was performed using Illumina NextSeq500, 75 bp single-end technology (Utrecht Sequencing Facility, useq.nl). For each strain, the transcripts were mapped against the genome assembly of DTO 217-A2 using HISAT v 2.1.0, using a minimum intron length of 20 and a maximum intron length of 1000. Subsequently, Cuffdiff v 2.2.1 (Trapnell *et al.*, 2013) was used to identify differentially expressed genes per condition and determined the reads per kilobase of transcript per million reads (RPKM).

5.2.9 Plasmid construction and generation knockout strain

A 60 kbp gene cluster was identified in strains producing heat resistant conidia. CRISPR/Cas9 technology was used to delete this cluster in DTO 217-A2. Two single-guide RNAs

(sgRNAs) were designed to perform a simultaneous double restriction in the 5' and 3' region of the 60 kbp cluster. Transformation procedures and plasmids were as described recently (van Leeuwe *et al.*, 2019; Seekles *et al.*, 2021b). In short, plasmid pFC332 (Nødvig *et al.*, 2015) was used as a vector to express the sgRNA, *cas9* and a hygromycin selection marker. The 5' and 3' flanking regions of sgRNA were amplified using plasmids PTLL108.1 and PTLL109.2 (Song *et al.*, 2018) as template (Table S5.1). The amplified products were fused by PCR (Table S5.1) and restricted using *PacI*. Subsequently, the product was ligated into *PacI* linearized pFC332 plasmid. The vector containing the sgRNA was then transformed into competent *E. coli* DH5 α cells for multiplication overnight. Plasmids were recovered from transformants using Quick Plasmid Miniprep Kit (ThermoFisher, Waltham, MA, USA) and digested using *SecII* to verify the presence of the sgRNA. Plasmids were sequenced by BaseClear (www.baseclear.com) to confirm the correct ligation of the sgRNA into the plasmid. To construct donor DNA, flanking regions of about 2000 bp upstream and downstream of the 60 kbp cluster were identified, amplified and subsequently fused using fusion PCR (Table S5.1). These regions flanked a unique 23 bp sequence GGAGTGGTACCAATATAAGCCGG with a protospacer adjacent motif (PAM) site for further genetic engineering.

Protoplasting was performed as described (Seekles *et al.*, 2021b). In short, *P. variotii* conidia were inoculated in 100 mL complete medium (Arentshorst *et al.*, 2012) and incubated overnight at 30 °C and 200 rpm. The mycelium was washed in SMC solution (1.33 M sorbitol, 50 mM CaCl₂, 20 mM MES buffer, pH 5.8) and incubated for 90 minutes at 37 °C in lysing enzymes from *Trichoderma harzianum* (Sigma-Aldrich, Zwijndrecht, the Netherlands) taken up in SMC. Protoplasts were resuspended in 1 mL STC (1.33 M sorbitol, 50 mM CaCl₂, 10 mM Tris/HCl, pH 7.5) and kept on ice after centrifugation for 5 min at 3000 g. Subsequent transformation was performed according to Seekles *et al.* (2021b). The deletion was confirmed with diagnostic PCR (Table S5.1).

5.3 RESULTS

5.3.1 Strain selection and phenotypic characterization of conidia

In our previous work, we characterized different phenotypic traits of various *P. variotii* strains (Table 5.1). Heat resistance was determined for 20 strains in order to quantify inter-strain variability (**Chapter 4**). These strains were selected randomly in order to have realistic estimations of strain diversity from food sources or industry environment. Some of these strains were further phenotypically characterized by determining the compatible solute composition of the conidia (**Chapter 2**; van den Brule *et al.*, 2020b) and studying spore size distributions parameters (**Chapter 3**; van den Brule *et al.*, 2020a). Here, we extended the phenotypic data set for all 20 strains used in **Chapter 4** (Table 5.2). The mean size of the conidia of these strains was determined, as well as the concentration of the compatible solutes trehalose, glycerol, mannitol and arabitol. In addition, the MIC of the undissociated form of sorbic acid and benzoic acid was determined. Notably, trehalose was the predominant compatible solute in all strains (Fig. S5.1).

Table 5.2. Phenotypic characterization of 20 *P. variotii* strains.

Strain	Heat resistance		Compatible Solutes					MIC	
	Log ₁₀ D-value (min)	Mean size (µm)	Trehalose (M)	Glycerol (M)	Mannitol (M)	Arabitol (M)	Sorbic acid (mM) [max]	Benzoic acid (mM) [max]	
DTO 021-C3	1.13 ± 0.057	3.11 ± 0.03	0.32 ± 0.018	0.06 ± 0.015	0.08 ± 0.007	0.11 ± 0.008	4.8 ± 0.82 [5.7]	4.1 ± 0.64 [4.4]	
DTO 021-D3	0.64 ± 0.096	2.87 ± 0.03	0.19 ± 0.005	0.06 ± 0.006	0.11 ± 0.017	0.08 ± 0.012	4.8 ± 0.82 [5.7]	4.1 ± 0.64 [4.4]	
DTO 027-B3	0.75 ± 0.137	2.98 ± 0.03	0.20 ± 0.023	0.02 ± 0.012	0.02 ± 0.003	0.17 ± 0.021	4.8 ± 0.82 [5.7]	3.7 ± 0.64 [4.4]	
DTO 027-B5	0.91 ± 0.103	3.02 ± 0.06	0.20 ± 0.028	0.04 ± 0.018	0.03 ± 0.006	0.17 ± 0.029	5.2 ± 0.82 [5.7]	4.1 ± 0.64 [4.4]	
DTO 027-B6	0.74 ± 0.122	2.88 ± 0.06	0.20 ± 0.017	0.04 ± 0.010	0.10 ± 0.018	0.11 ± 0.025	4.4 ± 1.25 [5.7]	3.4 ± 0.97 [4.4]	
DTO 027-B9	0.91 ± 0.106	3.09 ± 0.05	0.22 ± 0.020	0.03 ± 0.003	0.03 ± 0.005	0.11 ± 0.009	3.2 ± 0.00 [3.2]	3.3 ± 0.00 [3.3]	
DTO 032-I3	0.77 ± 0.059	2.87 ± 0.04	0.19 ± 0.024	0.05 ± 0.015	0.10 ± 0.019	0.08 ± 0.014	3.9 ± 0.62 [4.3]	3.3 ± 0.00 [3.3]	
DTO 045-G8	0.86 ± 0.072	3.04 ± 0.01	0.23 ± 0.037	0.02 ± 0.002	0.04 ± 0.020	0.07 ± 0.016	4.8 ± 0.82 [5.7]	4.4 ± 0.00 [4.4]	
DTO 164-E3	0.74 ± 0.068	2.89 ± 0.04	0.18 ± 0.013	0.04 ± 0.009	0.03 ± 0.007	0.09 ± 0.018	3.9 ± 0.62 [4.3]	3.3 ± 0.00 [3.3]	
DTO 166-G4	1.01 ± 0.062	3.48 ± 0.05	0.33 ± 0.033	0.06 ± 0.012	0.06 ± 0.003	0.04 ± 0.006	4.8 ± 0.82 [5.7]	4.4 ± 0.00 [4.4]	
DTO 195-F2	1.42 ± 0.060	3.31 ± 0.12	0.41 ± 0.092	0.05 ± 0.020	0.05 ± 0.019	0.01 ± 0.001	7.0 ± 1.10 [7.6]	4.9 ± 0.85 [5.9]	
DTO 207-G8	0.83 ± 0.074	2.93 ± 0.01	0.30 ± 0.046	0.07 ± 0.021	0.09 ± 0.017	0.09 ± 0.039	5.9 ± 1.67 [7.6]	5.4 ± 0.85 [5.9]	
DTO 212-C5	0.55 ± 0.030	3.02 ± 0.05	0.21 ± 0.028	0.04 ± 0.008	0.03 ± 0.012	0.17 ± 0.028	4.3 ± 0.00 [4.3]	4.4 ± 0.00 [4.4]	
DTO 217-A2	1.28 ± 0.087	3.58 ± 0.08	0.31 ± 0.026	0.05 ± 0.002	0.04 ± 0.004	0.07 ± 0.004	3.9 ± 0.62 [4.3]	4.4 ± 0.00 [4.4]	
DTO 271-D3	0.88 ± 0.027	3.35 ± 0.22	0.36 ± 0.144	0.08 ± 0.045	0.06 ± 0.026	0.09 ± 0.028	5.2 ± 0.82 [5.7]	4.4 ± 0.00 [4.4]	
DTO 271-G3	0.63 ± 0.137	2.81 ± 0.01	0.17 ± 0.019	0.03 ± 0.008	0.02 ± 0.001	0.02 ± 0.002	4.3 ± 0.00 [4.3]	4.1 ± 0.64 [4.4]	
DTO 280-E4	0.74 ± 0.108	3.31 ± 0.04	0.32 ± 0.091	0.06 ± 0.031	0.10 ± 0.034	0.08 ± 0.023	2.7 ± 0.46 [3.2]	3.7 ± 0.64 [4.4]	
CBS 101075	0.78 ± 0.041	3.36 ± 0.04	0.28 ± 0.046	0.05 ± 0.016	0.08 ± 0.020	0.06 ± 0.012	3.9 ± 0.62 [4.3]	4.1 ± 0.64 [4.4]	
DTO 282-E5	1.13 ± 0.056	3.53 ± 0.05	0.28 ± 0.036	0.05 ± 0.009	0.02 ± 0.002	0.02 ± 0.001	8.4 ± 1.46 [10.1]	4.4 ± 0.00 [4.4]	
DTO 282-F9	1.17 ± 0.033	3.05 ± 0.03	0.35 ± 0.060	0.05 ± 0.019	0.06 ± 0.021	0.10 ± 0.012	5.2 ± 0.82 [5.7]	4.9 ± 0.85 [5.9]	
Range [Min - Max]	[0.55 - 1.42]	[2.81 - 3.58]	[0.17 - 0.41]	[0.02 - 0.08]	[0.02 - 0.11]	[0.01 - 0.17]	[2.7 - 8.4]	[3.3 - 5.4]	

A principle component analysis (PCA) was performed using the log transformed D -values, mean conidia size, the concentrations of the four different compatible solutes and the MIC (maximum value of three replicate experiments) of sorbate and benzoate as variables of the 20 strains. Heat resistant strains with D -values > 9 minutes all clustered with respect to all variables (Fig. 5.1A). Notably, the log transformed D -values of the strains correlated with the mean spore size (Fig. 5.1B) and trehalose concentration (Fig. 5.1C), implying that heat resistant strains produce larger conidia that contain a higher trehalose concentration. The other variables used in the PCA did not show a significant correlation with heat resistance (Fig. S5.2).

5.3.2 The influence of cultivation temperature on heat resistance

The heat resistant strain DTO 217-A2, the heat sensitive strain DTO 212-C5 and the intermediate heat resistant and the previously sequenced strain CBS 101075 were cultivated at 25 °C, 37 °C and 45 °C to determine the influence of cultivation temperature

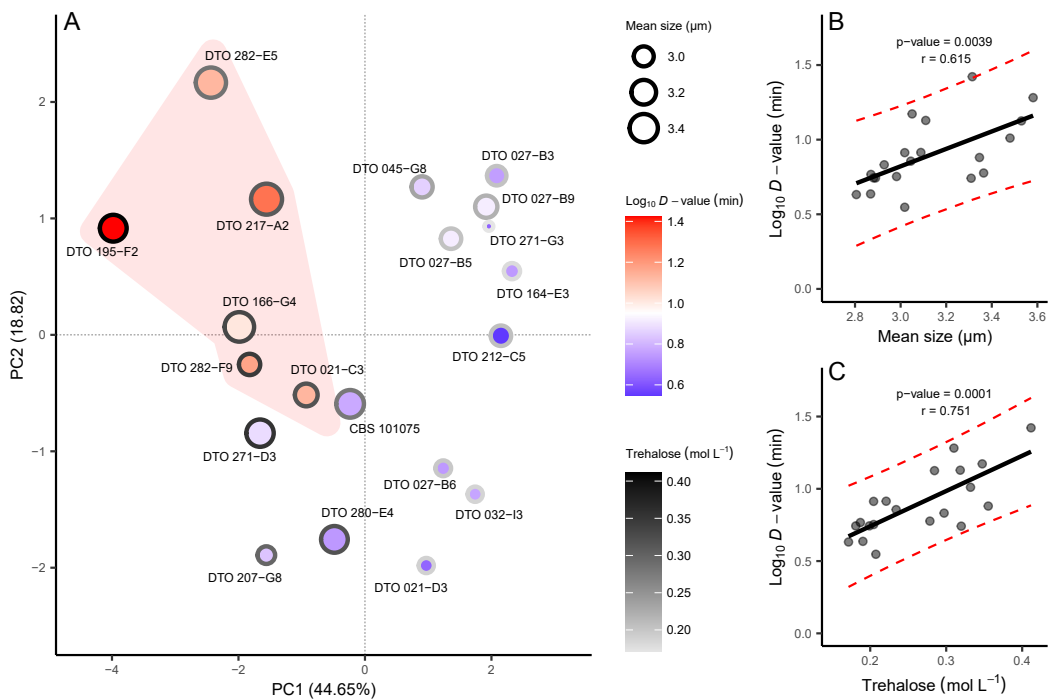


Figure 5.1. Phenotypic characterization of 20 *P. variotii* strains. A principle component analysis (PCA) of the phenotypic data presented in Table 5.2 (A), highlighting the mean spore size (represented by the diameter of the open circles), trehalose content (shading outer line of the circles) and the conidial heat resistance in terms of $\log_{10} D_{60}$ -value (colour fill of the open circles). The clustering of heat resistant strains in the PCA is indicated with the red polygon. Conidial heat resistance was correlated with mean conidia size (B) and trehalose concentration (C). The red dashed lines show the 95% prediction intervals of the solid linear regression line.

on heat resistance and other parameters of conidia (Fig. 5.2). Conidia suspensions were heat-treated at 62 °C instead of 60 °C to achieve sufficient inactivation to calculate D -values. Differences were highest for CBS 101075 with a 3.9-fold increase in D_{62} -values between conidia cultivated at 25 °C and 37 °C, whereas DTO 212-C5 and DTO 217-A2 showed a 2.3 and 3.6-fold increase at the same conditions, respectively. Interestingly, heat resistance did not increase any further when strains were cultivated at 45 °C. At this temperature, strains grew markedly slower than at 25 and 37 °C (results not shown), showing that at 45 °C the fungus experienced negative effects of the environmental condition. Although a clear difference in heat resistance was found, no significant differences were found in trehalose concentration for DTO 217-A2 (ANOVA, $p = 0.227$) and CBS 101075 (ANOVA,

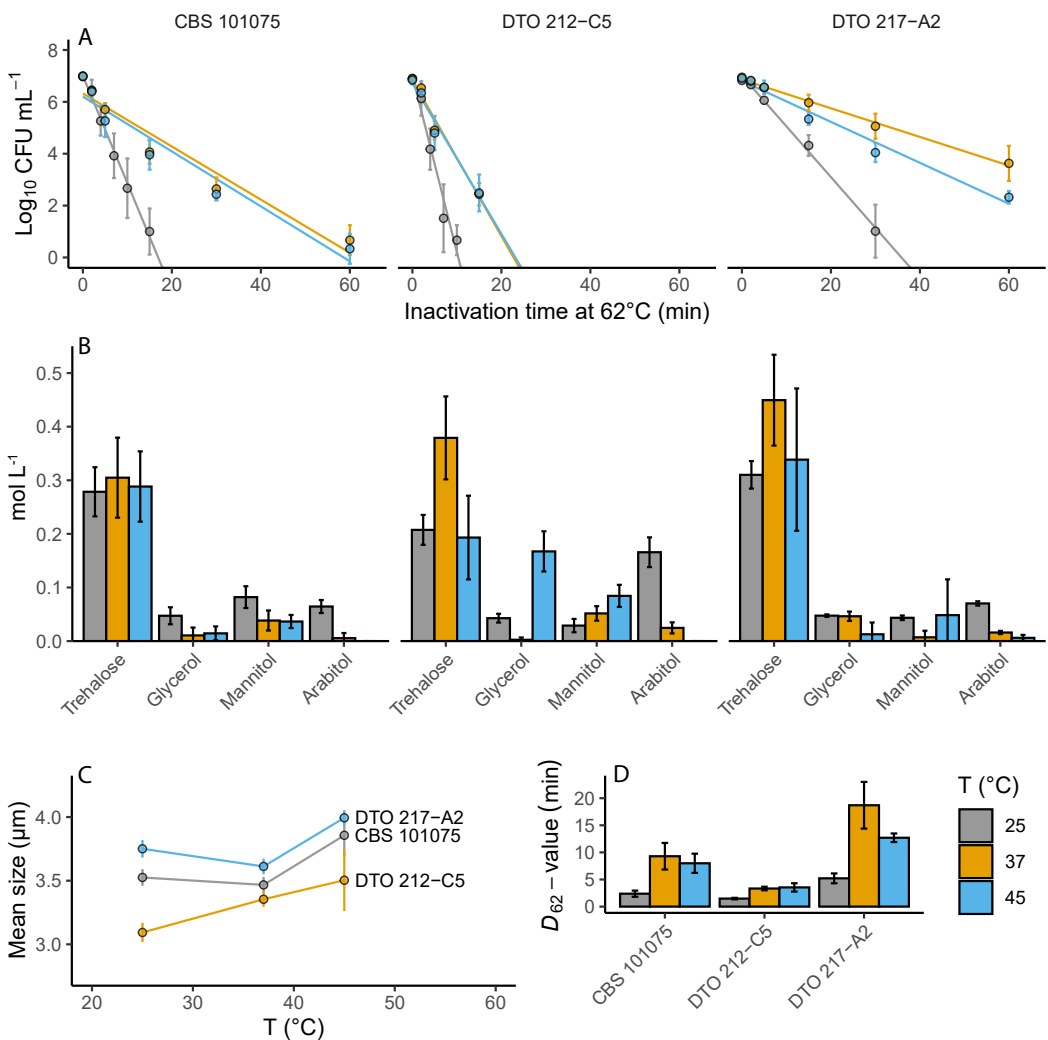


Figure 5.2. Effect of cultivation temperature on conidial heat resistance (A), compatible solute concentrations (B), mean conidia size (C) and D -value (D).

$p = 0.878$) when grown at the different temperatures. Only growth of DTO 212-C5 at 37 °C resulted in significant higher trehalose concentration when compared to growth at 25 °C (ANOVA, $p = 0.023$; Tukey HSD, $p = 0.042$) and 45 °C (ANOVA, $p = 0.023$; Tukey HSD, $p = 0.030$). Similar results were found for the mean spore size, where conidia size slightly decreased for DTO 217-A2 and CBS 101075 when grown at 37 °C compared to 25 °C, whereas conidia size of DTO 212-C5 increased consistently with the cultivation temperature.

5.3.3 Comparative genomics

5.3.3.1 Genome statistics and phylogenetic relationship

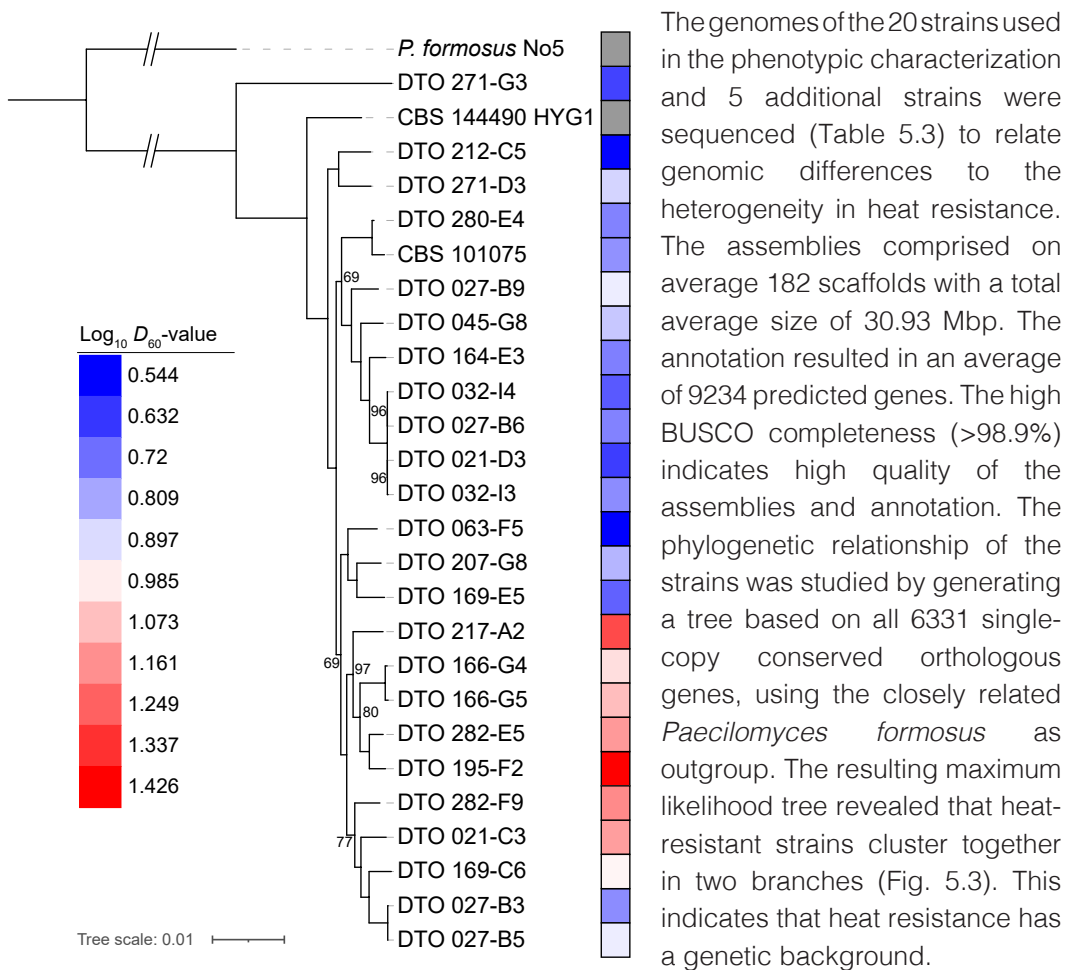


Figure 5.3. Maximum Likelihood tree of 6331 concatenated unique orthologous genes. The tree was generated using 100 bootstrap replications. Bootstrap values below 100 are shown. The heat resistance of each strain is expressed by the colour indicating the $\log_{10} D_{60}$ -value. Heat resistant strains with D_{60} -value > 9 min cluster in the bottom two branches. Heat resistance data was not available for strains showing a grey colour.

Table 5.3. Whole genome sequencing statistics of *P. variotii* strains.

Strain	Assembly			Annotation		
	No. Scaffolds	Total assembly length (Mbp)	Assembly GC content (%)	No. Genes	Genes with PFAM (total, %)	BUSCO2 completeness (fungi_odb9, %)
DTO 021-C3	215	30,99	45,89	9283	6961 (74.99%)	99,66
DTO 021-D3	156	31,02	45,62	9213	6942 (75.35%)	99,66
DTO 027-B3	189	30,9	46	9253	6961 (75.23%)	99,31
DTO 027-B5	206	30,9	46	9247	6964 (75.31%)	99,31
DTO 027-B6	160	31,03	45,61	9217	6940 (75.3%)	99,66
DTO 027-B9	166	30,81	45,79	9200	6919 (75.21%)	99,31
DTO 032-I3	177	31,03	45,63	9212	6942 (75.36%)	99,66
DTO 032-I4	135	31,03	45,61	9207	6941 (75.39%)	99,66
DTO 045-G8	151	30,66	45,88	9182	6915 (75.31%)	99,66
DTO 063-F5	176	30,74	45,95	9283	6963 (75.01%)	99,66
DTO 164-E3	437	30,85	45,87	9237	6951 (75.25%)	99,66
DTO 166-G4	194	31,29	45,62	9286	6974 (75.1%)	99,31
DTO 166-G5	185	31,39	45,54	9285	6978 (75.15%)	99,66
DTO 169-C6	201	31,17	45,76	9260	6954 (75.1%)	99,66
DTO 169-E5	153	30,9	45,77	9242	6961 (75.32%)	99,66
DTO 195-F2	193	31,41	45,51	9275	6947 (74.9%)	99,31
DTO 207-G8	170	30,41	46,18	9202	6927 (75.28%)	98,97
DTO 212-C5	172	31,67	45,21	9265	6983 (75.37%)	99,66
DTO 217-A2	226	31,27	45,67	9299	6992 (75.19%)	99,66
DTO 271-D3	126	30,58	45,81	9227	6934 (75.15%)	99,31
DTO 271-G3	58	28,7	47,37	8799	6812 (77.42%)	99,66
DTO 280-E4	152	31,29	45,58	9405	6971 (74.12%)	100
DTO 282-E5	200	31,04	45,78	9261	6934 (74.87%)	99,66
DTO 282-F9	178	31,16	45,87	9276	6996 (75.42%)	98,97

Table 5.3. (Continued).

Strain	Assembly			Annotation		
	No. Scaffolds	Total assembly length (Mbp)	Assembly GC content (%)	No. Genes	Genes with PFAM (total, %)	BUSCO2 completeness (fungi_odb9, %)
CBS 101075	86	30,11	46,71	9270	6931 (74.77%)	99,31
<i>P. formosus</i> No5	393	28,94	49,36	8877	7013 (79.0%)	97,59
Average	182	30,93	45,81	9234		
Min	58	28,7	45,21	8799		
Max	437	31,67	47,37	9405		

5.3.3.2 Transcriptome analysis of conidia grown at different cultivation temperatures

A genome-wide gene expression analysis was performed on conidia grown at 25 °C, 37 °C and 45 °C of the heat resistant strain DTO 217-A2, the heat sensitive strain DTO 212-C5 and the intermediate resistant strain CBS 101075 to compare the transcriptional landscapes of these conditions. Because the largest differences in heat resistance were found between conidia grown at 25 or 37 °C, genes were selected that were significantly higher expressed (by a four-fold difference) between these conditions (Table 5.4). Some genes of DTO 217-A2 that were highly expressed are predicted to be involved in a response against oxidative stress, such as an oxidoreductases (Protein ID 03107), thioredoxin (Protein ID 03166), a peroxisomal membrane protein (Protein ID 00866), or other putative enzymes with high redox potential like a multicopper oxidase (Protein ID 00546). In addition, conidiation-specific proteins and HSP20 are associated with a heat stress response, although their precise role remains elusive (Punt *et al.*, 2020). Two genes that were more than 7-fold higher expressed in conidia of DTO 217-A2 cultures grown at 37 °C compared to 25 °C were found to be homologous to con-6 (Protein ID 05853 and 07636). In contrast to DTO 217-A2, gene 07636 showed very low RPKM values for DTO 212-C5 and CBS 101075, while protein ID 05853 was only 3-fold higher expressed in DTO 212-C5 and 3-fold lower expressed in CBS 101075 when grown at 37 °C compared to 25 °C. Interestingly, HSP20-domain-containing-gene (Protein ID 07743), was abundantly present in conidia grown at 25 °C and highly downregulated at 37 °C and 45 °C (Table 5.5). This contrasted another HSP20-domain-containing-gene (Protein ID 04615), which was up-regulated at 37 °C compared to 25 °C.

Table 5.4 DTO 217-A2 genes that were significantly 4-fold up-regulated and of which the 37 °C condition showed RPKM > 1000. The RNA-sequencing reads of DTO 212-C5 and CBS 101075 were mapped against the assembly of DTO 217-A2 to determine their RPKM values. Genes in grey shadings were 4-fold upregulated in DTO 217-A2 but not in DTO 212-C5 and/or CBS 101075. The functional annotation was based on the predicted PFAM domains and homologous genes as determined by BLAST results. Values indicate RPKM.

Protein ID	RPKM										Predicted function
	DTO 217-A2			DTO 212-C5			CBS 101075				
	25°C	37°C	45°C	25°C	37°C	45°C	25°C	37°C	45°C		
00034	1293	5495	1360	2338	4926	2009	1139	3188	3143		Hypothetical protein
00544	355	1998	441	0	0	0	0	0	0	0	Copper fist DNA binding domain protein
00546	243	1426	620	0	0	0	0	0	0	0	Multicopper oxidase
00657	230	1435	223	581	3900	585	371	1245	496		Arginase-like protein
00760	403	1832	530	999	800	340	1627	1837	487		3-hydroxyanthranilate 3,4-dioxygenase Bna1, putative
00866	368	1551	391	603	1002	857	765	997	738		Peroxisomal membrane protein
00912	710	9769	1409	3571	8006	3885	6568	9602	1587		Gpr1 family protein
01234	19	1876	361	9974	10080	1525	7815	2593	695		BYS1 domain protein, putative
01490	167	1357	247	530	768	390	1743	944	221		Beta-lactamase-like protein
01912	104	1276	54	531	664	127	101	177	48		Hypothetical protein
02064	142	2230	170	122	218	140	105	283	218		Mediator complex-domain-containing protein
02322	279	1280	170	310	1461	711	321	946	598		Hypothetical protein
02513	470	1938	303	662	573	155	168	195	50		Urea hydro-lyase/cyanamide hydratase
02572	197	1045	208	202	459	390	190	372	521		Gamma-cysteine synthetase regulatory subunit, putative
02588	496	4548	2309	10463	10785	1901	11836	7208	1949		G-patch domain protein (Spp2), putative
02630	96	1338	155	299	1090	881	134	380	396		Hypothetical protein
02755	222	2200	1465	144	1727	3472	344	600	773		Hypothetical protein
03107	3	1341	471	224	785	161	1155	878	461		GMC oxidoreductase
03166	439	3073	405	2130	3170	1426	907	885	605		Thioredoxin

Table 5.4 (Continued).

Protein ID	RPKM										Predicted function
	DTO 217-A2		DTO 212-C5		CBS 101075						
	25°C	37°C	45°C	25°C	37°C	45°C	25°C	37°C	45°C		
03549	259	1801	454	239	624	401	557	648	648	648	Oleate delta-12 desaturase
03700	94	4079	285	95	1411	1215	100	1158	3431		Hypothetical protein
04174	329	1658	402	295	1126	561	246	957	534		Calcium ion transporter Vcx1
04296	179	14988	5691	13583	50454	9317	1496	5872	3747		Adhesin
04594	413	1757	404	1081	1698	829	1168	1106	495		MSF1 domain protein
04615	2389	11927	5621	462	1814	3637	3213	3458	2324		HSP20
05542	960	4110	1228	1380	3218	9152	1288	3041	3783		Translation initiation factor
05712	260	1415	242	562	969	444	349	809	468		Hypothetical protein
05852	624	5793	1492	442	1168	497	5790	2018	98		Hypothetical protein
05853	1394	10053	2464	633	1992	583	10379	3556	145		Conidiation protein 6-domain-containing protein
06134											Zinc knuckle transcription factor/splicing factor
	205	2947	298	1561	3622	2597	648	1394	1386		MSL5/ZFM1
06175	226	1091	48	73	55	20	162	176	16		C6 transcription factor
06872	395	1672	593	300	907	875	473	1244	871		Ubiquitin-conjugating enzyme type E2
07325	401	3936	515	349	872	948	490	1372	3050		Chitin synthesis regulation
07575	203	1447	708	417	1979	1852	960	1289	1223		PHD Zn-finger protein
07636	302	2454	394	1	8	2	9	38	1		Conidiation protein 6-domain-containing protein
07732	62	1011	190	48	279	188	70	541	285		Stress responsive A/B barrel domain protein
07760	89	3981	667	2083	6757	2864	1631	3315	1576		Galactose permease
07784	172	1014	206	98	136	13	1004	320	72		Glutathione S-transferase
07876	467	2246	316	544	993	894	1373	1817	1672		Methyltransferase
08326	389	1767	301	594	967	1199	1193	1891	988		Alpha/Beta hydrolase protein
08412	30	1083	126	304	361	632	162	369	223		Hypothetical protein

Table 5.4 (Continued).

Protein ID	RPKM								Predicted function	
	DTO 217-A2		DTO 212-C5		CBS 101075					
	25°C	37°C	45°C	25°C	37°C	45°C	25°C	37°C		45°C
08414	5	1582	296	213	502	971	410	744	628	4-hydroxyphenylpyruvate dioxygenase
08717	31	1171	66	115	508	132	550	973	198	Acetyltransferase, GNAT family
08860	397	1765	235	1685	1839	239	1082	793	392	Hypothetical protein
09265	261	1051	286	964	869	558	1070	623	442	Histone H4, partial

Table 5.5. DTO 217-A2 genes that were significantly 4-fold down-regulated and of which the 25 °C condition showed RPKM > 1000. The RNA-sequencing reads of DTO 212-C5 and CBS 101075 were mapped against the assembly of DTO 217-A2 to determine their RPKM values. Genes in grey shadings were 4-fold downregulated in DTO 217-A2 but not in DTO 212-C5 and/or CBS 101075. The functional annotation was based on the predicted PFAM domains and homologous genes as determined by BLAST results. Values indicate RPKM.

Protein ID	RPKM								Predicted function	
	DTO 217-A2		DTO 212-C5		CBS 101075					
	25°C	37°C	45°C	25°C	37°C	45°C	25°C	37°C		45°C
00276	1714	370	1087	1983	772	1048	1288	1354	1337	60S ribosomal protein L38
00729	1505	313	557	2196	644	188	2969	570	412	NACHT domain protein
00731	7053	1471	897	2183	693	124	11777	3238	423	Hypothetical protein
01967	1272	188	453	1322	130	109	0	0	0	Aryl-alcohol dehydrogenase
02695	1306	307	731	2205	827	842	1103	1048	930	60S ribosomal protein L9
03067	1323	270	875	2312	855	934	988	714	1009	60S acidic ribosomal protein P1
03218	13427	2864	1272	1631	325	136	22894	24665	1110	Hypothetical protein
03331	14878	3176	5694	9955	2717	1574	11483	2126	1422	Formate dehydrogenase
03580	1753	376	1032	2609	922	1187	1411	916	1241	60S ribosomal protein L35
03931	2170	243	318	1197	206	94	1092	614	199	Hypothetical protein
04162	1044	200	594	1696	519	622	727	466	688	40S ribosomal protein S8-A

Table 5.5. (Continued).

Protein ID	RPKM												Predicted function
	DTO 217-A2			DTO 212-C5			CBS 101075						
	25°C	37°C	45°C	25°C	37°C	45°C	25°C	37°C	45°C	25°C	37°C	45°C	
05031	1915	206	780	2900	547	591	1425	513	1023				60S acidic ribosomal protein P2
05296	1320	267	842	2155	766	1294	1009	776	1104				60S ribosomal protein L26
06375	3476	749	10596	3825	813	459	8064	572	6190				Hydrophobin
07367	4701	1130	2282	3614	856	291	3071	782	1323				ATP synthase subunit ATP9
07532	4228	336	143	2602	92	23	1059	246	53				Short-chain dehydrogenase
07743	17770	821	1105	619	343	157	3564	2109	618				HSP20-like chaperone
08219	1215	301	725	886	276	97	407	137	81				FKBP-domain protein
08376	1543	339	1163	2272	715	1185	1219	1113	1464				Ubiquitin-40S ribosomal protein S31 fusion protein
08654	1019	204	858	1594	603	959	813	882	1068				40S ribosomal protein S17

Remarkably, the two HSP20-domain-containing-proteins showed lower RPKM values and were not significantly differentially expressed in DTO 212-C5 and CBS 101075. Genes involved in protein synthesis (*i.e.* ribosomal proteins) were overrepresented in the set that was significantly down-regulated at 37 °C compared to 25 °C (Table 5.5), suggesting that protein synthesis is decreased in conidia when formed at higher temperatures.

Besides the conidiation-specific proteins con-6 and con-10, other hydrophilins like LEA-like proteins and proteins involved in compatible solute synthesis are associated with heat resistance of conidia and ascospores (Hagiwara *et al.*, 2017; van Leeuwen *et al.*, 2013b, 2016; Punt *et al.*, 2020). However, in a selection of the presumed homologous genes in DTO 217-A2 none were significantly differentially expressed, except the con-6 homologs (Protein ID 05853 and 07636; Table 5.6). Interestingly, hydrophilins con-10, HSP12 were the highest expressed genes in conidia at all three conditions.

5.3.3.3 Genome-wide Association Study

A Genome-wide Association Study (GWAS) was performed to identify SNPs that correlate with the heat resistance trait. The Illumina reads were aligned to the heat-resistant strain DTO 217-A2, which was used as the reference in this analysis. The GATK pipeline was used for SNP calling, resulting in 2,090,978 SNPs in the 23 strains (strain CBS 101075 was sequenced with PacBio

Table 5.6. RNA expression data of genes involved in compatible solute synthesis or hydrophilin homologues. Values indicate RPKM.

Protein ID	RPKM												Gene	NCBI homologue	
	DTO 217-A2				DTO 212-C5				CBS 101075						
	25°C	37°C	45°C		25°C	37°C	45°C		25°C	37°C	45°C				
05569	203	212	148	204	108	69		215	76	64			64	tppA	ANI_1_1432094
01371	293	281	189	276	156	97		310	126	144			144	tppB	ANI_1_48114
03731	53	53	47	27	25	36		39	50	33			33	tppC	ANI_1_2070064
00025	1605	2542	926	2015	1016	435		1442	742	432			432	tpsA	XP_001393155.1
03732	60	48	69	49	35	49		41	39	49			49	tpsB	ANI_1_1078064
05394	1038	404	176	392	112	79		707	227	36			36	tpsC	ANI_1_1216124
03343	2987	802	376	3647	791	272		2725	509	184			184	mtdA	ANI_1_736134
05304	801	421	688	683	320	166		977	369	334			334	mtdB	ANI_1_1156034
04056	1103	1145	467	1202	810	484		1686	636	270			270	mpdA	ANI_1_802024
06332	2604	1324	1055	2082	1073	599		2423	719	461			461	err1	ANI_1_172094
06763	40	43	32	12	46	13		76	41	19			19	lad1	ANI_1_1474014
05702	14	7	17	8	5	10		19	9	16			16	treA	AFUA_3G02280
02775	366	253	201	318	130	77		290	115	139			139	treB	AFUA_4G13530
05853	1394	10053	2464	633	1992	583		10379	3556	145			145	con-6	EAA26854
07636	302	2454	394	1	8	2		9	38	1			1	con-6	EAA26854
07245	82300	74665	20263	39206	14878	2498		215412	57756	6583			6583	con-10	NCU07325
00010	36714	31191	20996	86118	42423	40534		86560	23187	11404			11404	hsp12B	NFIA_058420
00650	8826	15306	3482	22556	12391	3853		16346	13254	4250			4250	lea	NFIA_065760

technology, precluding it from this analysis), of which 1049 were highly significantly linked to the phenotype ($P < 0.00001$, Fig. 5.4). Of these SNPs, 150 caused a non-synonymous substitution in a total of 93 predicted genes (Table 5.7). Four of these genes contained high impact SNPs, causing a frameshift variant, splice variant, premature stop-codon or a loss of start-codon. Gene 04648 has a predicted function in karyogamy and has homology with Kar5p, which is essential in nuclear fusion in *S. cerevisiae* (Rogers and Rose, 2015). Protein ID 07717 is a predicted dual-specific phosphatase 3, which has been reported to be involved in various signalling pathways, including a DNA damage response (Pavic *et al.*, 2015). Two hypothetical proteins with unknown function (Protein ID 02686 and 03281) contained SNPs causing a splice variant and a loss of the start codon, respectively.

Most of the genes with non-synonymous substitutions had low numbers of transcripts in the conidia, including the four genes containing a high impact SNP (Table S5.2). RPKM values did not exceed 100 for 74 out of the 93 genes with non-synonymous substitutions for all three strains and all conditions. Only three out of the 93 genes were significantly up-regulated (Protein ID 05194, 01938, 00334) in conidia from 37 °C cultures compared to 25 °C cultures, while gene with protein ID 06376 that encodes a hypothetical protein was the only down-regulated gene. The gene with protein ID 05194 putatively encodes the G1/S-specific cyclin Pcl5, which might be an important gene during germination and early development when nuclei are multiplied extensively (Wu *et al.*, 2004). The gene with protein ID 01938 has a predicted inositol 5-phosphatase domain and might have a role in actin regulation in the cytoskeleton (Funaki *et al.*, 2000), while the gene with protein ID 00334 is predicted to encode an aryl sulfotransferase.

5.3.3.4 Identification and analysis of a 60 kbp gene cluster

The genome assemblies of the sequenced strains were aligned to heat resistant strain DTO 217-A2 to identify genomic regions that are unique to heat resistant strains. A gene cluster of approximately 60 kbp (scaffold_003: 96635-156690) was identified as a gene cluster that was present in 6 out of 8 strains with D_{60} -values > 9 min, but absent in sensitive strains with D_{60} -values < 5 min (Fig. 5.5). The strains containing the cluster all belong to the two branches of heat resistant strains in the concatenated gene tree (Fig. 5.3) except for the highly related DTO 166-G4 and DTO 166-G5 strains. Heat resistant strain DTO 021-C3 showed a gap in the alignment of approximately 7 kb. On the gene cluster, 10 genes were identified and manually curated based on the mapped RNA-sequencing reads (Table 5.8). In fact, besides the 10 predicted genes, there were more regions in the cluster where RNA reads mapped. However, no suitable reading frame was detected in these locations and these may therefore represent pseudogenes. Transcripts of four out of the ten genes were significantly up-regulated in conidia of cultures grown at 37 °C compared to conidia produced at 25 °C. These genes encode for a copper fist DNA-binding domain protein (Protein ID 00544), a multicopper oxidase (Protein ID 00546), a heavy metal stress associated P-type ATPase (Protein ID 00548) and an aegerolysin-like protein (Protein ID 00549).

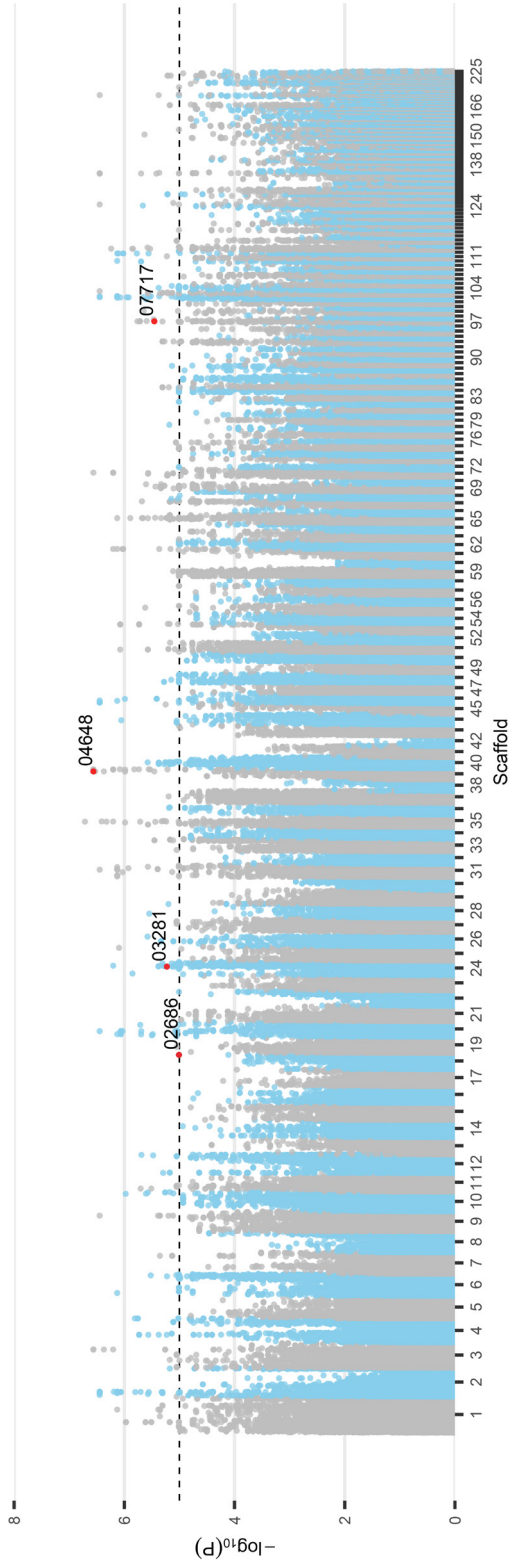


Figure 5.4. Manhattan plot of SNPs associated to heat resistance. SNPs were called against the assembly of heat resistant strain DTO 217-A2 as reference. The dashed line indicates the significance level at $P < 0.00001$ and SNPs above this line can be considered to be associated with conidial heat resistance as a phenotype. Significant SNPs that are expected to have high impact (*i.e.* causing frameshift variant or premature stop-codon) in the predicted genes indicated with their gene ID are shown as red dots.

Table 5.7. Genes containing a SNP resulting in an alternative protein, associated with conidial heat resistance.

Gene ID	SNP annotation	Coding sequence	AA sequence	Putative function
1	00046	missense variant	538C>G Arg180Gly	FAD binding monooxygenase
2	00184	missense variant	38T>C Leu13Ser	Hypothetical protein
3	00321	missense variant	1106A>C Gln369Pro	NIF domain protein
4	00332	missense variant	287A>G His96Arg	short-chain dehydrogenase
5	00334	missense variant	1606A>G Thr536Ala	Arylsulfotransferase
		missense variant	1138C>G Gln380Glu	
		missense variant	733A>G Thr245Ala	
6	00335	missense variant	590T>C Ile197Thr	Hypothetical protein
		missense variant	178A>G Arg60Gly	
		missense variant	103T>C Ser35Pro	
		missense variant	1649C>T Thr550Met	
7	00336	missense variant	1241T>C Val14Ala	Hypothetical protein
		missense variant	1098A>C Leu366Phe	
8	00509	missense variant	1228A>G Lys410Glu	vacuolar membrane-associated protein iml1
		missense variant	1145C>A Thr382Asn	
		missense variant	1150G>A Val384Ile	
9	00792	missense variant	1425A>C Lys475Asn	beta-N-acetylglucosaminidase
		missense variant	1570T>C Tyr524His	
		missense variant	1215T>G Asn405Lys	
10	01005	missense variant	1070G>A Arg357His	beta-glucosidase M
		missense variant	1016T>C Val339Ala	
		missense variant	859A>G Ile287Val	cyclin
11	01034	missense variant	1078G>A Val360Met	Hypothetical protein
12	01111	missense variant	602G>A Arg201Lys	
13	01125	missense variant	536G>A Arg179Lys	Putative DNA helicase

Table 5.7. (Continued).

Gene ID	SNP annotation	Coding sequence	AA sequence	Putative function	
14	01128	missense variant	1582A>G	Ile528Val	Hypothetical protein
15	01129	missense variant	1245T>G	Asp415Glu	DNA repair protein
16	01135	missense variant	1276A>G	Ser426Gly	1,3-beta-glucanosyltransferase Gel1
17	01140	missense variant	313T>G	Tyr105Asp	cytochrome P450
18	01477	missense variant	445A>G	Ile149Val	flavin-containing amine oxidase
19	01695	missense variant	2096G>A	Arg699His	cohesin loading factor-domain-containing protein
20	01697	missense variant	1225T>G	Ser409Ala	
21	01938	missense variant	106A>G	Met36Val	Alpha/Beta hydrolase protein
22	02686	splice acceptor variant & intron variant	976-3_976-2insC	Ala73Thr	inositol 5-phosphatase
23	03271	missense variant	257T>C	Ile86Thr	Hypothetical protein
24	03281	frameshift variant & start lost	1dupA	Met1fs	ubiquitin-like activating enzyme
25	03284	missense variant	418G>C	Ala140Pro	Hypothetical protein
26	03286	missense variant	920T>G	Val307Gly	WD40-repeat-containing domain protein
27	03287	missense variant	544G>A	Ala182Thr	WD repeat-containing protein
28	03310	missense variant	265T>C	Tyr89His	HAD superfamily hydrolase
29	03311	missense variant	1244C>T	Ala415Val	oleate delta-12 desaturase
30	03887	missense variant	206C>G	Thr69Ser	alpha/beta fold family hydrolase
31	03965	missense variant	593T>C	Val198Ala	
32	03968	missense variant	938G>A	Arg313His	Putative oxidoreductase
33	04081	missense variant	290A>G	Gln97Arg	ADP-ribose 1-phosphate phosphatase
34	04303	missense variant	654_656dupCGC	Ala219dup	Cupredoxin
		missense variant	1940T>C	Val647Ala	ubiquitin-specific protease
		missense variant	179G>T	Arg60Met	Hypothetical protein

Table 5.7. (Continued).

Gene ID	SNP annotation	Coding sequence	AA sequence	Putative function	
35	04648	missense variant missense variant stop gained missense variant	1036G>A 1207C>A 1595G>A 1602A>C	Ala346Thr Leu403Ile Trp532* Leu534Phe	nuclear membrane fusion protein Kai5
36	04649	missense variant	197T>C	Leu66Pro	Hypothetical protein
37	04666	missense variant missense variant	404G>A 407G>A	Arg135Lys Arg136Lys	Hypothetical protein
38	04669	missense variant missense variant	190A>G 407A>G	Thr64Ala His136Arg	salicylate hydroxylase
39	04698	missense variant	279A>C	Arg93Ser	Ankyrin repeat protein
40	04707	missense variant	1829C>G	Thr610Ser	Hypothetical protein
41	05066	missense variant	220A>G	Thr74Ala	forkhead transcription factor Fkh1/2
42	05194	missense variant	1600T>G	Ser534Ala	G1/S-specific cyclin Pcl5
43	05235	missense variant missense variant missense variant	407G>A 535C>G 667A>G	Arg136His Leu179Val Thr223Ala	Hypothetical protein
44	05242	missense variant	1610T>C	Met537Thr	glycoside hydrolase superfamily
45	05620	missense variant	761C>A	Pro254His	steroid dehydrogenase
46	05763	missense variant missense variant	479G>A 493A>G	Arg160Lys Asn165Asp	Hypothetical protein
47	05905	missense variant	1082C>G	Ala361Gly	NRPS-like enzyme
48	05974	missense variant	745A>G	Thr249Ala	aspartate transaminase
49	05979	missense variant missense variant	540T>G 521T>C	Asp180Glu Leu174Pro	Hypothetical protein
50	05985	missense variant	353T>G	Val118Gly	Hypothetical protein

Table 5.7. (Continued).

Gene ID	SNP annotation	Coding sequence	AA sequence	Putative function	
51	05993	missense variant	1621A>C	Ile541Leu	ribonuclease P complex subunit Pop1
		missense variant	2717T>C	Val906Ala	
		missense variant	409A>G	Thr137Ala	
52	05994	missense variant	592A>G	Met198Val	DUF1690-domain-containing protein
		missense variant	574A>G	Asn192Asp	
		missense variant	427G>A	Glu143Lys	
		missense variant	397G>A	Glu133Lys	
		missense variant	352G>A	Val118Ile	
		missense variant	157A>G	Lys53Glu	
53	05996	missense variant	118C>T	His40Tyr	Hypothetical protein
		missense variant	4A>T	Thr2Ser	
		missense variant	37C>T	Arg13Cys	
		missense variant	67G>A	Asp23Asn	
		missense variant	307G>A	Val103Ile	
		missense variant	553C>G	Gln185Glu	
		missense variant	622G>A	Glu208Lys	
		missense variant	74A>C	Gln25Pro	
		missense variant	32G>A	Arg11His	
		missense variant	1258G>A	Ala420Thr	
54	05997	missense variant	2634A>G	Ile878Met	nuclear pore complex subunit Nup159
		missense variant	2084T>G	Phe695Cys	
55	06177	missense variant	154T>C	Ser52Pro	Transcription factor?
		missense variant	453C>G	His151Gln	
56	06189	missense variant	693T>G	Ile231Met	prolyl aminopeptidase
		missense variant			
57	06193	missense variant			RecQ family helicase MusN
		missense variant			
58	06195	missense variant			alcohol dehydrogenase
		missense variant			
59	06199	missense variant			
		missense variant			
60	06202	missense variant			
		missense variant			
61	06363	missense variant			
		missense variant			

Table 5.7. (Continued).

Gene ID	SNP annotation	Coding sequence	AA sequence	Putative function
62	06366	missense variant	457T>G Ser153Ala	Hypothetical protein
63	06367	missense variant	14G>A Gly5Glu	Hypothetical protein
64	06370	missense variant	380A>G Lys127Arg	Hypothetical protein
		missense variant	392G>C Ser131Thr	
65	06372	missense variant	1253T>G Phe418Cys	ceramide glucosyltransferase
		missense variant	1300G>A Gly434Ser	
66	06376	missense variant	452G>A Gly151Asp	Hypothetical protein
67	06395	missense variant	770G>C Cys257Ser	methyltransferase domain-containing protein
		missense variant	1220A>C Asn407Thr	
68	06492	missense variant	1219A>T Asn407Tyr	RNA-directed RNA polymerase
		missense variant	1211C>T Ala404Val	
69	06566	missense variant	322G>A Ala108Thr	transcription factor and DNA repair complex, core
		missense variant	1286C>T Ser429Leu	
70	06573	missense variant	1054T>G Cys352Gly	Hypothetical protein
71	06841	missense variant	3234C>A Asp1078Glu	sister chromatid cohesion and DNA repair protein
72	06891	missense variant	687A>T Glu229Asp	Hypothetical protein
		missense variant	685G>A Glu229Lys	
73	07158	missense variant	217C>G Leu73Val	Aldehyde/histidinol dehydrogenase
74	07219	missense variant	547G>A Gly183Arg	short-chain dehydrogenase/reductase family protein
		missense variant	380A>G Glu127Gly	
75	07220	missense variant	222G>T Gln74His	Hypothetical protein
		missense variant	266A>G Lys89Arg	
76	07241	missense variant	1158C>G Phe386Leu	Hypothetical protein
		missense variant	1102A>G Lys368Glu	

Table 5.7. (Continued).

Gene ID	SNP annotation	Coding sequence	AA sequence	Putative function
77	07259	missense variant	1621G>T Ala541Ser	permease of the major facilitator superfamily
78	07261	missense variant	752A>G Glu251Gly	ubiquitin-conjugating enzyme E2-binding protein
79	07715	missense variant	168A>T Glu56Asp	SNF2 family helicase/ATPase PasG
		missense variant	1969A>C Lys657Gln	
		missense variant	1934G>C Arg645Pro	
		missense variant	1249T>C Tyr417His	
80	07716	missense variant	1039G>C Ala347Pro	Hypothetical protein
		missense variant	748T>G Ser250Ala	
		missense variant	417A>T Gln139His	
		conservative inframe deletion	939_941delCTG Cys314del	
		stop gained	942C>A Cys314*	
81	07717	missense variant	842G>A Arg281Gln	dual specificity protein phosphatase 3
		missense variant	798A>G Ile266Met	
82	07718	conservative inframe deletion	244_246delATT Ile82del	Hypothetical protein
83	07898	missense variant	16A>C Ile6Leu	Hypothetical protein
84	07906	missense variant	1066C>T His356Tyr	Hypothetical protein
85	07907	missense variant	4T>C Tyr2His	flavin-containing monooxygenase
86	07968	missense variant	1926A>C Arg642Ser	phosphatase regulatory subunit-domain-containing protein
		missense variant	2128A>G Ser710Gly	
		missense variant	22A>G Ile8Val	
87	07970	missense variant	24A>G Ile8Met	mitochondrial carrier protein
		missense variant	1166A>T Asp389Val	
88	07972	missense variant	1057A>C Lys353Gln	Hypothetical protein

Table 5.7. (Continued).

Gene ID	SNP annotation	Coding sequence	AA sequence	Putative function
89	07977	missense variant	1108T>G Ser370Ala	gluconolactone oxidase
90	08180	missense variant	1294A>G Thr432Ala	Hypothetical protein
91	08248	missense variant	724A>G Ile242Val	actin interacting protein 2
92	08283	missense variant	1126A>G Thr376Ala	nuclear division Rft1 protein
93	09276	conservative inframe insertion	190_192dupGCG Ala64dup	Hypothetical protein

The 60 kbp cluster was blasted against the whole-genome shotgun contigs (wgs) database at NCBI using blastn. The cluster showed homology with regions in various *Penicillium* species and partial homology with *Aspergillus* species. The well annotated genome of *Penicillium rubens* Wisconsin 54-1255 (van den Berg *et al.*, 2008) was one of the genomes that showed homology. Genomes of strains that showed at least 25% coverage of the cluster in DTO 217-A2 were aligned against DTO 217-A2 and *P. rubens* Wisconsin 54-1255 (Fig. 5.7). All *P. variotii* strains showed high identity in the alignment with DTO 217-A2, including the flanking regions of the cluster. Almost the entire cluster was also present in all *Penicillium* strains, while the cluster showed partial homology with all *Aspergillus* strains. In most *Aspergillus* strains, the region containing genes with ID 00544 to 00550 seemed best conserved. The flanking regions of the DTO 217-A2 60 kbp cluster were largely absent in the penicillia and aspergilli. On the other hand, the flanking regions of the *P. rubens* Wisconsin 54-1255 60 kbp cluster were absent in the *P. variotii* strains, but present in all *Penicillium* strains, except for *Penicillium roqueforti* DTO 369-A1. Larger regions in the *Aspergillus* genomes aligned with the *P. rubens* 60 kbp cluster, indicating a higher homology to the cluster of this species compared to the *P. variotii* 60 kbp cluster.

Gene density of the *P. rubens* 60 kbp cluster is higher with 25 predicted genes compared to the 10 predicted genes of *P. variotii*. Since this may be an artefact of the differences in gene predictions, we used the standard gene model parameters for *A. nidulans* and *Fusarium graminearum* of the program Augustus to repredict genes on the DTO 217-A2 and *P. rubens* Wisconsin 54-1255 assemblies. Using this consistent approach to gene prediction, we identified 7 and 6 out of 10 genes, respectively, on the DTO 217-A2 60 kbp cluster, while 14 and 13 out of 25 genes, respectively, were identified on the *P. rubens* Wisconsin 54-1255 60 kbp cluster. Although we did not identify all genes using these alternative gene models, still twice as many genes were predicted on the *P. rubens* Wisconsin 54-1255 cluster. Together, data suggest that the cluster indeed encodes more genes in *Penicillium* species than in *P. variotii*.

To study whether the 60 kbp cluster is involved in heat resistance, a strain was constructed in which the 60 kbp cluster was deleted using CRISPR/Cas9 technology. To facilitate DNA repair through heterologous recombination, the knockout strain was constructed in DTO 217-A2 $\Delta ku70$ (Seekles *et al.*, 2021b). The knockout strain DTO 217-A2 $\Delta ku70 \Delta 60 kbp$ was

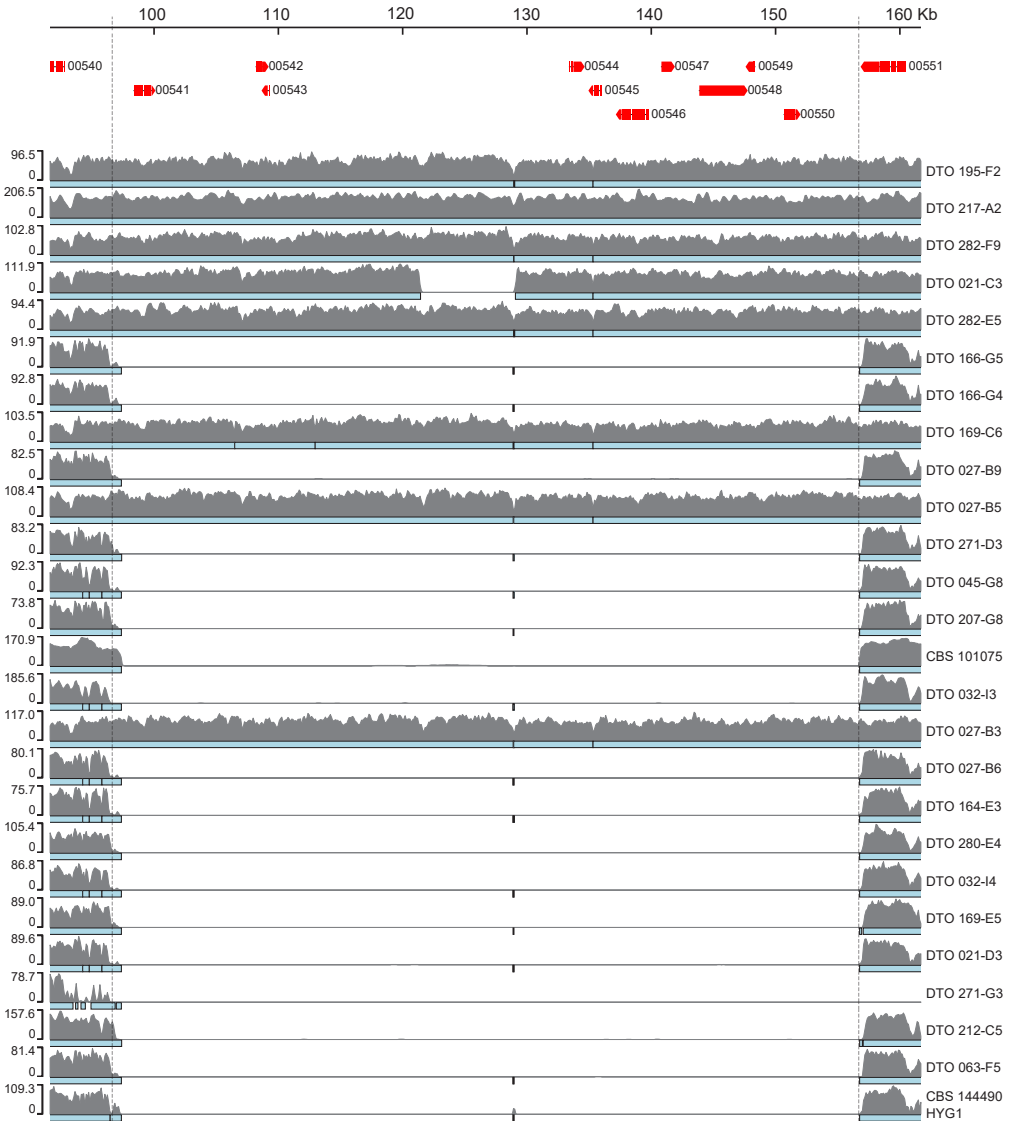


Figure 5.5. Alignment of *P. variotii* genomes to the assembly of heat resistant strain DTO 217-A2. The x-axis on top indicates the location of scaffold_003 of the assembly of DTO 217-A2. Strains are organized based on their conidial heat resistance with the most resistant strain DTO 195-F2 on top (except CBS 144490 of which the heat resistant data was not available). Each strain shows the coverage of mapped reads against the reference genome DTO 217-A2. The skyblue bars indicate the alignment using Nucmer. The vertical lines indicate the boundaries of an approximately 60 kbp gene cluster that is present in most heat resistant strains, but absent in all sensitive strains. The genes located on the cluster are shown in red.

verified through diagnostic PCR (Fig. S5.3). Strains DTO 217-A2 $\Delta ku70$ and DTO 217-A2 $\Delta ku70 \Delta 60 kbp$ did not show differences in heat resistance when compared to the wild-type, nor in compatible solute concentration and mean size of the conidia (Fig. 5.6). This indicates that the 60 kbp cluster is not involved in conidial heat resistance.

5.4 DISCUSSION

In this study, strains of the food spoilage fungus *P. variotii* were phenotyped and sequenced to find genetic clues for the high variation in heat resistance of their conidia. The phenotypic analysis showed a correlation between conidial heat resistance and mean spore size and between conidial heat resistance and trehalose concentration among 20 strains. Thus, conidia of strains that were heat resistant were larger and contained a higher concentration trehalose than strains that were heat sensitive. In a previous study, it was proposed that small spores are more heat sensitive due to a larger surface-area-to-volume ratio (**Chapter 3**; van den Brule *et al.*, 2020a), but the precise mechanisms remain elusive. On the other hand, the role of trehalose in heat resistance, has been established in literature. The maximal trehalose concentration of 0.41 ± 0.092 M corresponds to 2.66 ± 0.358 pg conidium⁻¹ in the most heat-resistant strain DTO 195-F2. This is about two times higher than *A. fumigatus* conidia grown at 25 °C (Hagiwara *et al.*, 2017). In our study, between a 2.3- and 3.9-fold difference in *D*-value of the conidia was observed for three strains when cultivated at 25 °C and 37 °C. Notably, no correlation was found between trehalose concentration and the increased conidial heat resistance when the fungus was grown at higher temperatures. Indeed, genes involved in trehalose, and also mannitol synthesis, did not have increased expression in conidia formed at higher temperatures. In contrast, increased heat resistance of conidia of *A. fumigatus* (Hagiwara *et al.*, 2017) and *P. roqueforti* (Punt *et al.*, 2020) that had been formed at higher temperature does correlate with higher trehalose concentration.

Table 5.8. Genes located on 60kb cluster and the transcription data of DTO 217-A2. The functional annotation is based on BLAST results and predicted PFAM domains. Genes in grey shadings are significantly four-fold upregulated at 37 °C compared to 25 °C. Values indicate RPKM.

Protein ID	RPKM			Predicted function
	25°C	37°C	45°C	
00541	1	1	2	Phosphotransferase enzyme family
00542	108	227	326	Hypothetical protein
00543	2368	2819	2518	Hypothetical protein
00544	355	1998	441	Copper fist DNA binding domain protein
00545	1345	1127	2587	Multicopper oxidase
00546	243	1426	620	Multicopper oxidase
00547	839	2545	651	Zn-transporter
00548	41	171	64	Heavy metal associated ATPase
00549	26	563	229	Aegerolysin-like protein
00550	56	72	68	Hypothetical protein

Recently, however, it was shown that trehalose deficient and highly heat sensitive *A. niger* strains still enhance conidial heat resistance when grown at higher temperatures (Seekles *et al.*, 2021a). This shows that also other mechanisms can contribute to increased heat resistance. Together, trehalose is likely to play an important role in the high conidial heat resistance of the most resistant strains, but other factors are involved in increased heat stress resistance due to environmental changes.

The adaptation of the colony to higher temperatures is reflected in the transcriptional landscape of the conidia. Similar as in *A. niger* (van Leeuwen *et al.*, 2013b), *A. fumigatus* (Hagiwara *et al.*, 2017) and *P. roqueforti* (Punt *et al.*, 2020) conidia, large amounts of transcripts of hydrophilins con-6, con-10 and Hsp12 and leamA were found in *P. variotii* conidia. In fact, con-10 and HSP12 were the highest expressed genes at all three conditions. Of the hydrophilins, only the two homologous genes of con-6 were differentially expressed in DTO 217-A2 cultures grown at 37 °C compared to 25 °C. Interestingly, only one con-6 homologue was expressed in the heat sensitive strain DTO 212-C5 and the intermediate resistant strain CBS 101075, which was not significantly differentially expressed in both strains at 37 °C or 45 °C compared to 25 °C (Table 5.6). The high number of transcripts of hydrophilins in conidia illustrate their importance in asexual development and stress resistance. However, our RNA-sequencing experiments do not indicate a direct relation with elevated heat stress resistance in *P. variotii* caused by an increase in cultivation temperature. Together, our data indicate that apart from trehalose also hydrophilins play a role in the heat resistance of *P. variotii* conidia. Yet, also in this case hydrophilins do not seem to play a role in increased heat resistance caused by environmental growth conditions such as the growth temperature.

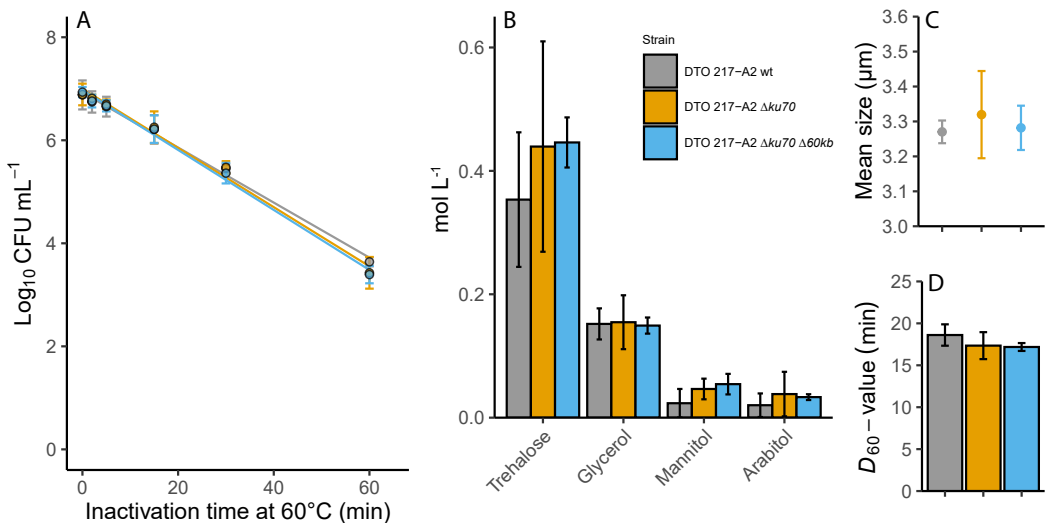


Figure 5.6. Phenotypic characterization of 60 kbp cluster knockout mutant. Heat resistance (A), compatible solute concentration (B), mean size (C) and D-value (D) of the conidia was quantified of DTO 217-A2 wild type strain (grey), DTO 217-A2 $\Delta ku70$ (yellow) and DTO 217-A2 $\Delta ku70 \Delta 60 kbp$ (blue).

Trehalose and hydrophilins can play a major role in protection against drought. As conidia of *P. variotii* are dispersed through air, it is essential that they are able to withstand prolonged drought periods. During drying, the trehalose molecule works as a kosmotrope, influencing and maintaining the water structure directly around proteins and membranes by a mechanism called preferential exclusion (Wyatt *et al.*, 2013). Trehalose and other compatible solutes have many hydroxyl groups, which can form hydrogen bonds with proteins upon drying (Mensink *et al.*, 2017). This phenomenon is the foundation of the water replacement theory, which describes protein stabilization from a thermodynamic point of view (Chang and Pikal, 2009) and helping to maintain the native conformation of proteins during drought or heat stress (Wyatt *et al.*, 2013). Although the molecular mechanisms of hydrophilins are largely unknown, it shares functions in desiccation stress with trehalose. Due to glycine-rich regions and high hydrophilicity, these proteins interact with other proteins and cellular components. For instance, in *S. cerevisiae* hydrophilin Hsp12 interacts with the cell membrane where it has a protective function (Welker *et al.*, 2010) and is shown to have a role in desiccation-rehydration stress resistance in synergy with trehalose (Kim *et al.*, 2018).

In addition to conidia size and compatible solute concentration, the ability of conidia to germinate in medium supplemented with sorbic acid and benzoic acid was studied. These weak acids are generally used in food industry for preservation purposes. Although heat resistance did not correlate significantly with weak acid resistance, the two strains that are most resistant to sorbic acid were heat resistant strain DTO 282-E5 and DTO 195-F2. In addition, the most heat-resistant conidia of DTO 195-F2 are fairly resistant to benzoic acid as well with an average MIC of 4.9 mM. Another heat-resistant strain, DTO 282-F9, is equally resistant to benzoic acid as DTO 195-F2. These three strains, DTO 195-F2, DTO 282-E5 and DTO 282-F9, can thus be considered as most problematic strains in terms of food spoilage. Weak acid resistance is associated with the presence of specific genes to catabolize these compounds (Geoghegan *et al.*, 2020; Lubbers *et al.*, 2019). The comparative genomics and transcriptomics in this study focussed on conidial heat resistance, and thus the presence of homologous weak acid resistance genes was not studied. Recently, the same GWAS methods were used to identify weak acid resistance gene cluster SORBUS in *P. roqueforti* (Punt *et al.*, 2022b). For every *P. variotii* strain used in this study, a higher MIC for sorbic acid was found than previously reported for a *P. variotii* strain isolated from a South American soft drink production facility (Stratford *et al.*, 2009). In another study, a *P. variotii* strain isolated from bakery products was able to grow at extremely high concentrations of potassium sorbate up until 128 mM in Yeast Extract Sucrose broth at pH 5.0 (Garcia *et al.*, 2021). This concentration corresponds to 45 mM undissociated sorbic acid, which is more than 4 times higher than the highest MIC found in this study. The range of heterogeneity of the MICs of sorbic acid and benzoic acid of the *P. variotii* strains can be used to improve predictive food mycology models.

The phylogenetic analysis covering all unique conserved orthologues genes of the 25 sequenced strains revealed a clustering of heat resistant strains in two related subclades. Notably, heat-sensitive strain DTO 271-G3 showed a markedly large distance to

the other *P. variotii* strains in the phylogenetic tree. This is in agreement with a phylogenetic analysis that was based on partial beta-tubulin sequences (**Chapter 2**; van den Brule *et al.*, 2020b). Here, we also showed that DTO 271-G3 contains a smaller genome of 28.7 Mbp with a slightly higher GC content and lower amount of predicted genes compared to the other *P. variotii* strains. In addition, DTO 271-G3 showed smaller spores containing a lower concentration of each compatible solute compared to the other *P. variotii* strains. Together, DTO 271-G3 could arguably be described as a novel species that is closely related to *P. variotii*.

More than two million SNPs were identified among 24 *P. variotii* genomes using DTO 217-A2 as a reference. We focussed on SNPs causing an effect in the predicted protein sequences of DTO 217-A2 to identify genes that may be related to heat resistance. These SNPs were located throughout the entire genome and many genes with such polymorphisms have a predicted function in metal transport or metal binding, such as cupredoxin (Protein ID 03968). The 60 kbp cluster that was found in 6 out of 8 heat resistant strains but not in heat sensitive strains contained genes encoding a copper fist binding DNA domain protein, two multicopper oxidases, a zinc transporter and a heavy metal associated P-type ATPase. Genes with similar function were recently found on a 85 kbp *HEPHAESTUS* (*H ϕ*) transposable element in *P. variotii* CBS 144490 and three other *P. variotii* strains isolated in Australia (Urquhart *et al.*, 2022). This element contains a P-type ATPase which confers cadmium and lead resistance, a zinc transporter involved in zinc resistance and a multicopper oxidase conferring copper resistance. In addition, *H ϕ* contains a subregion conferring resistance to arsenic compounds. We identified *H ϕ* partially in *P. variotii* strains DTO 021-C3, DTO 027-B3, DTO 027-B5 and DTO 169-C6. Interestingly, these strains also contain the 60 kbp cluster and all miss the subregion in *H ϕ* conferring resistance to arsenic compounds.

Although some of the genes on the 60 kbp cluster were differentially expressed in conditions resulting in conidia with higher heat resistance, we did not find any evidence that this cluster is involved in conidial heat resistance. Through CRISPR/Cas9 technology we were able to delete the 60 kbp cluster in the heat resistant strain DTO 217-A2. However, no phenotypic differences in heat resistance, compatible solute concentration, spore size or morphology were observed. Because of the similarity in function of genes located in *H ϕ* , the 60 kbp cluster could have a function in metal resistance.

Besides the eight *P. variotii* strains containing the 60 kbp cluster, the cluster was identified in nine of the 21 *P. chrysogenum* assemblies currently available on NCBI (<https://www.ncbi.nlm.nih.gov/assembly/?term=penicillium+chrysogenum>, June 21, 2021) and in one out of 34 newly sequenced *P. roqueforti* genomes (Punt *et al.*, 2022b). In addition, various *Aspergillus* species contain fragments of the 60 kbp cluster. We hypothesize that the 60 kbp was introduced in *P. variotii* through horizontal transfer. However, in contrast to *H ϕ* , there are no indications that the 60 kbp cluster can act a transposon since a transposase gene and flanking palindromic regions are absent. There are more examples of horizontal transfer of large DNA fragments in *Penicillium* species involved in cheese fermentation (Cheeseman

et al., 2014; Coton *et al.*, 2020) and in even entire chromosomes in plant pathogenic *Fusarium* species (Ma *et al.*, 2010). Germinating conidia are able to form anastomosis tubes, which may introduce an open connection and nucleus transfer between different strains of a fungal species or even different fungal species (Gabriela Roca *et al.*, 2005). For instance, intergeneric fusion has been observed between *Aspergillus oryzae* and various *Penicillium* species (Ishitani and Sakaguchi, 1956). These mechanisms might pave the way for exchange of DNA fragments via recombinatory mechanisms. Similar mechanisms are involved in horizontal chromosome transfer in *Fusarium oxisporum* (Shahi *et al.*, 2016).

In conclusion, the results presented in this paper highlight the complexity of the molecular mechanisms underlying conidial heat resistance. Many genes with a variety of functions were associated with heat resistance through comparative genomics and through comparative transcriptomics of conditions affecting conidial heat resistance. Growing cultures at higher temperatures resulted in conidia that have higher resistance towards heat stress. This might have implications for food industry in geographically warmer regions. As conidia, and potentially other spores such as sexual ascospores, are more resistant due to climate conditions, heat treated food products can be more prone to microbial spoilage in warmer regions than in temperate regions. How these mechanisms work, remains elusive. Nevertheless, our research indicated the importance of trehalose and hydrophilins in *P. variotii* conidia and provided leads for further investigation.

5.5 ACKNOWLEDGEMENTS

We thank Utrecht Sequencing Facility for providing sequencing service and data. Utrecht Sequencing Facility is subsidized by the University Medical Center Utrecht, Hubrecht Institute, Utrecht University and The Netherlands X-omics Initiative (NWO project 184.034.019).

5.6 DATA AVAILABILITY

The genome assemblies and the predicted genes have been deposited at NCBI GenBank [will be released upon publication in a peer reviewed journal]. Moreover, the genomes, genes and functional annotations can be analysed interactively on <https://fungalgenomics.science.uu.nl/>.

5.7 SUPPLEMENTARY DATA

Table S5.1. Primers used for plasmid and donor DNA construction and diagnostic PCR. The target sequences of the guide RNA, as well as the unique sequence in the donor DNA are shown in red.

Amplification	Template DNA	Primer name	Primer sequence	Polymerase	Remarks
		pTE1_for	CCTTAATTAAGCTCCGCCGAAACGT ACTG		Amplification of the 5' flank containing PacI restriction site and promoter region of sgRNA, the reverse primer contains target sequence in 5' region of 60 kbp cluster (in red).
5' flank sgRNA 5' target	pTLL108.1	gRNA_ROI1_Rv	AGGTGATGGCTCATTCCGA GACGAGCTTACTCGTTTCG	Phusion	
		gRNA_ROI1_Fw	TCGGAAATGAGCCATCACCT GTTTTAGAGCTAGAAATAGCAAG		Amplification of the 3' flank containing sgRNA and terminator sequence and PacI restriction site, the forward primer contains complementary target sequence in 5' region of 60 kbp cluster (in red).
3' flank sgRNA 5' target	pTLL109.2	pTE1_rev	CCTTAATTAAGCTCCGCCGAAACGT AAGGTACAAAAAAGC	Phusion	
		pTE1_for	CCTTAATTAAGCTCCGCCGAAACGT ACTG		Amplification of the 5' flank containing PacI restriction site and promoter region of sgRNA, the reverse primer contains target sequence in 3' region of 60 kbp cluster.
5' flank sgRNA 3' target	pTLL108.1	gRNA_ROI4_Rv	CCGTTGGTATATTGAATACG GACGAGCTTACTCGTTTCG	Phusion	

Table S5.1. (Continued).

Amplification	Template DNA	Primer name	Primer sequence	Polymerase	Remarks
3' flank sgRNA 3' target	pTLL109.2	gRNA_ROI4_Fw pTE1_rev	CGTATTCAATATACCAACGG GTTTAGAGCTAGAAATAGCAAG CCTTAATTAATAAGCAAAAAAGG AAGGTACAAAAAAGC	Phusion	Amplification of the 3' flank containing sgRNA and terminator sequence and PacI restriction site, the forward primer contains complimentary target sequence in 3' region of 60 kbp cluster.
sgRNA 5' region flank fusion	5' flank sgRNA 5' region 3' flank sgRNA 5' region	pTE1_for pTE1_rev	CCTTAATTAATAACTCCGCCGAACGT ACTG CCTTAATTAATAAGCAAAAAAGG AAGGTACAAAAAAGC	Phusion	Fusion of the 5' and 3' flank of the 5' target sequence.
sgRNA 3' region flank fusion	5' flank sgRNA 3' region 3' flank sgRNA 3' region	pTE1_for pTE1_rev	CCTTAATTAATAACTCCGCCGAACGT ACTG CCTTAATTAATAAGCAAAAAAGG AAGGTACAAAAAAGC	Phusion	Fusion of the 5' and 3' flank of the 3' target sequence.
2 kbp 5' flank 60 kbp	Genomic DNA DTO 217-A2	60kb_up_fw 60kb_up_rev	AAGTTGTCCTGGAGTTGCG GGAGTGGTACCAATATAAGCCGG ACGACTGCTGGCATGAAACG	Phusion	Amplification of the upstream 2 kbp flank of the 60 kbp cluster, the reverse primer contains a unique 23 bp sequence (in red).
2 kbp 3' flank 60 kbp	Genomic DNA DTO 217-A2	60kb_down_fw 60kb_down_rev	CCGGCTTATATTGGTACCACTCC AGCCACATCTGTCTGCATGG AGCGAATGTCAAGGCACTCG	Phusion	Amplification of the downstream 2 kbp flank of the 60 kbp cluster, the forward primer contains a unique 23 bp complementary sequence (in red).

Table S5.1. (Continued).

Amplification	Template DNA	Primer name	Primer sequence	Polymerase	Remarks
Fusion donor DNA	2 kbp 5' flank 60 kbp 2 kbp 3' flank 60 kbp	60kb_up_fw 60kb_down_rv	AAGTTGTCCCTGGAGTTGCG AGCGAATGTCAAGGCACTCG	Phire	Fusion of the donor DNA with two 2 kbp flanks of the 60 kbp cluster, containing a unique 23 bp sequence in the center.
Diagnostic positive control	Genomic DNA	ddna_fw ddna_rv	TCCTGATCATCCACGTTGCC ATCGAACTAGGCTCTGACGC	Phire	Amplification of the flanking regions of the donor DNA. No band is expected in wild type strains containing the 60 kbp cluster, since 64 kbp is to large to amplify. A band around 5 kbp is expected in wild type strains without the cluster and a band around 4 kbp is expected in successful transformants.
Diagnostic negative control	Genomic DNA	217A2_3F 217A2_3R	TCACCGACTCTTCTGGGTGC TAGGTGGGTAGGTATTGCGC	Phusion	Amplification of gene 00547, located on the 60 kpb cluster. A band around 1 kbp is expected in strains containing the cluster.

Table S5.2. RNA expression data of genes containing a SNP resulting in an alternative protein, associated with conidial heat resistance. Genes in grey shadings are significantly 4-fold differentially expressed between the 25 °C and 37 °C condition of DTO 217-A2. Values indicate RPKM.

Gene ID	RPKM								
	DTO 217-A2			DTO 212-C5			CBS 101075		
	25°C	37°C	45°C	25°C	37°C	45°C	25°C	37°C	45°C
00046	0	0	1	0	0	0	1	2	1
00184	9	10	55	35	43	40	43	45	70
00321	62	59	44	70	73	76	78	65	58
00332	116	82	63	77	57	44	41	52	27
00334	6	50	18	12	37	21	8	17	11
00335	10	12	27	26	20	11	6	19	17
00336	89	170	92	151	165	169	141	122	165
00509	24	23	26	18	21	16	20	20	20
00792	5	20	21	5	20	17	22	37	14
01005	19	15	3	2	1	1	2	2	1
01034	27	37	30	28	39	58	23	45	50
01111	2	7	5	12	19	7	20	16	5
01125	21	21	17	14	19	6	15	15	12
01128	4	5	7	4	3	11	4	7	14
01129	2	3	6	2	2	8	1	4	12
01135	17	14	30	127	14	38	10	38	30
01140	11	14	10	13	30	33	11	20	10
01477	45	48	46	42	68	33	25	44	34
01695	37	70	44	22	44	69	25	43	53
01697	12	16	18	13	11	4	12	15	13
01938	100	507	73	246	225	138	347	301	457
02686	0	0	0	0	0	0	0	1	0
03271	159	130	70	154	135	97	193	138	82
03281	0	0	1	0	0	0	0	1	0
03284	22	9	16	7	7	12	8	6	9
03286	8	2	1	8	4	3	15	8	3
03287	55	41	43	50	45	54	55	42	40
03310	0	0	1	0	0	0	11	45	11
03311	0	0	4	0	0	0	11	84	23
03887	7	3	7	14	10	8	10	3	2
03965	7	7	8	3	6	3	4	21	8
03968	7	10	7	9	56	55	7	12	4
04081	73	55	60	51	46	59	42	33	70
04303	9	38	5	20	84	5	33	75	9

Table S5.2. (Continued).

Gene ID	RPKM								
	DTO 217-A2			DTO 212-C5			CBS 101075		
	25°C	37°C	45°C	25°C	37°C	45°C	25°C	37°C	45°C
04648	6	0	3	8	3	2	3	3	2
04649	38	35	47	33	59	90	55	69	95
04666	0	0	1	0	0	0	1	3	2
04669	6	4	12	10	4	5	3	7	8
04698	1	0	4	0	0	0	1	3	0
04707	80	78	57	70	63	65	51	86	69
05066	113	312	203	178	224	198	175	128	319
05194	84	361	130	156	458	479	105	186	486
05235	0	1	2	3	2	2	9	12	8
05242	15	11	21	7	6	6	5	7	10
05620	0	0	1	1	0	1	1	1	6
05763	19	11	28	20	17	25	12	39	24
05905	3	3	1	6	9	2	5	4	1
05974	81	56	120	75	51	46	55	45	112
05979	3	1	1	1	0	0	1	1	1
05985	5	9	3	4	12	6	2	4	2
05993	12	10	10	16	17	28	18	9	53
05994	256	222	245	225	197	143	187	213	233
05996	0	0	1	0	0	1	0	2	0
05997	0	2	7	0	3	2	1	8	3
06177	18	24	17	13	23	22	29	45	20
06189	0	0	0	0	1	1	0	2	1
06193	33	24	39	27	28	44	35	24	42
06195	11	12	11	18	15	6	39	27	12
06199	19	6	25	24	19	13	10	13	15
06202	12	9	17	11	15	23	5	11	15
06363	2845	1197	646	2326	571	173	2407	366	139
06366	35	20	47	40	52	78	46	71	70
06367	52	60	44	83	116	127	74	79	70
06370	495	543	227	426	107	46	1242	987	126
06372	29	33	30	43	91	76	45	50	30
06376	223	35	1130	702	734	1001	182	362	1225
06395	4	9	18	4	5	8	3	6	12
06492	177	113	19	165	82	13	78	45	8
06566	87	100	54	78	84	58	89	64	46
06573	10	4	8	8	11	7	11	8	5
06841	15	9	15	4	2	3	7	9	12

Table S5.2. (Continued).

Gene ID	RPKM								
	DTO 217-A2			DTO 212-C5			CBS 101075		
	25°C	37°C	45°C	25°C	37°C	45°C	25°C	37°C	45°C
06891	5	4	7	1	12	2	2	8	3
07158	88	111	278	93	80	122	65	59	157
07219	21	13	18	23	10	5	29	12	5
07220	0	4	0	1	1	0	1	0	0
07241	11	8	21	14	12	28	22	20	30
07259	4	2	8	8	9	12	7	10	7
07261	27	43	28	27	50	40	31	55	29
07715	20	18	37	12	9	11	5	15	27
07716	3	3	3	5	4	2	7	6	2
07717	7	4	22	10	9	9	5	16	17
07718	2	0	8	4	1	6	2	2	15
07898	26	36	47	31	50	152	29	79	66
07906	0	0	0	0	0	0	0	0	0
07907	0	0	0	1	5	6	5	48	7
07968	204	366	198	436	259	158	415	221	408
07970	261	328	177	210	167	111	390	241	124
07972	2	9	8	3	6	11	2	9	9
07977	1	1	3	4	2	2	1	1	3
08180	14	12	26	12	17	17	9	14	23
08248	67	34	36	42	19	11	86	25	20
08283	30	63	23	50	98	46	38	76	53
09276	95	73	86	157	81	81	190	112	138

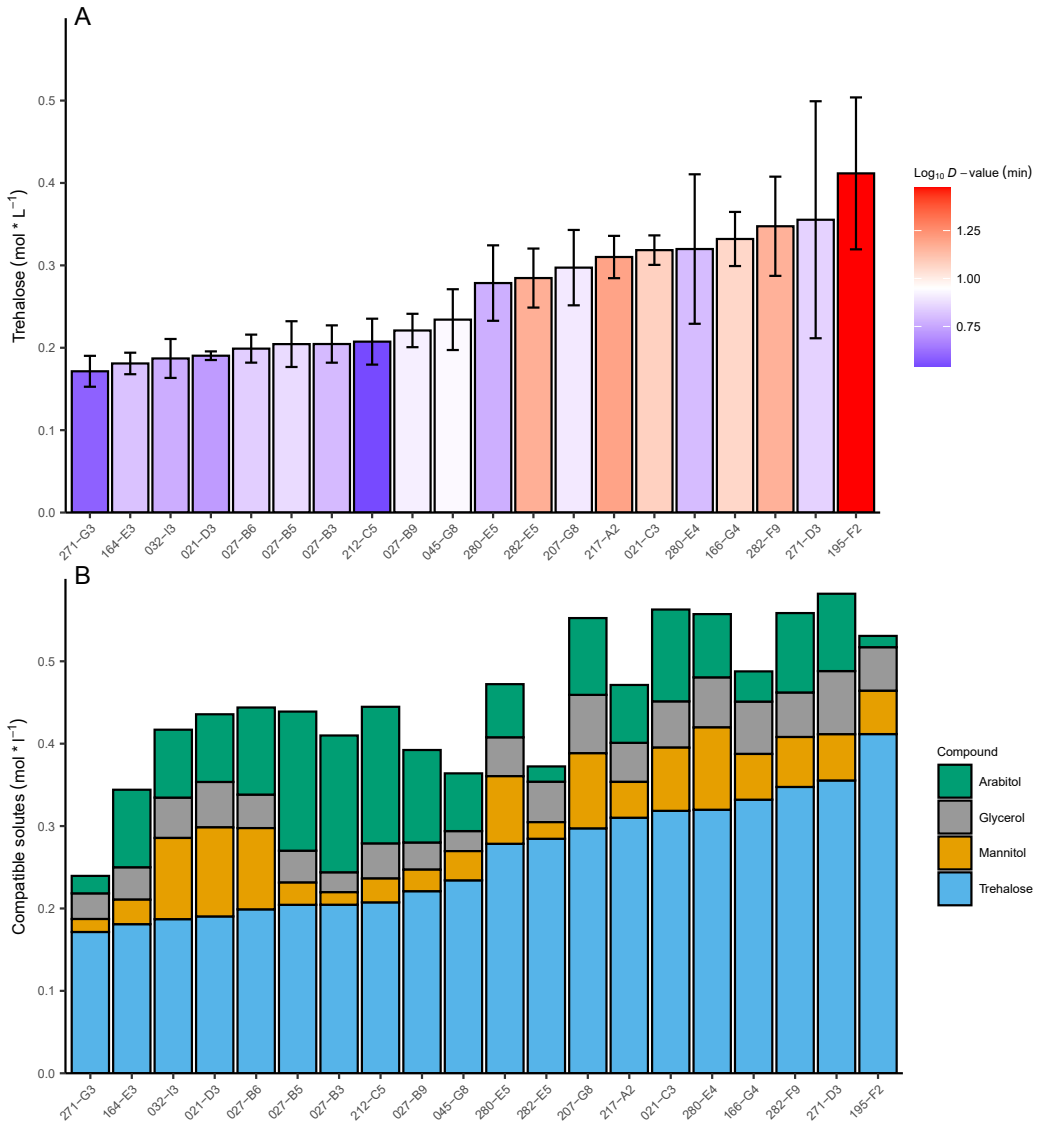


Figure S5.1. Compatible solute concentrations per strain. Strains are ordered on trehalose concentration and colors indicate heat resistance in a gradient (A), while (B) represents the concentration of the different compatible solutes in each of the strains. Mean values of three biological replicates are shown and error bars indicate standard deviation.

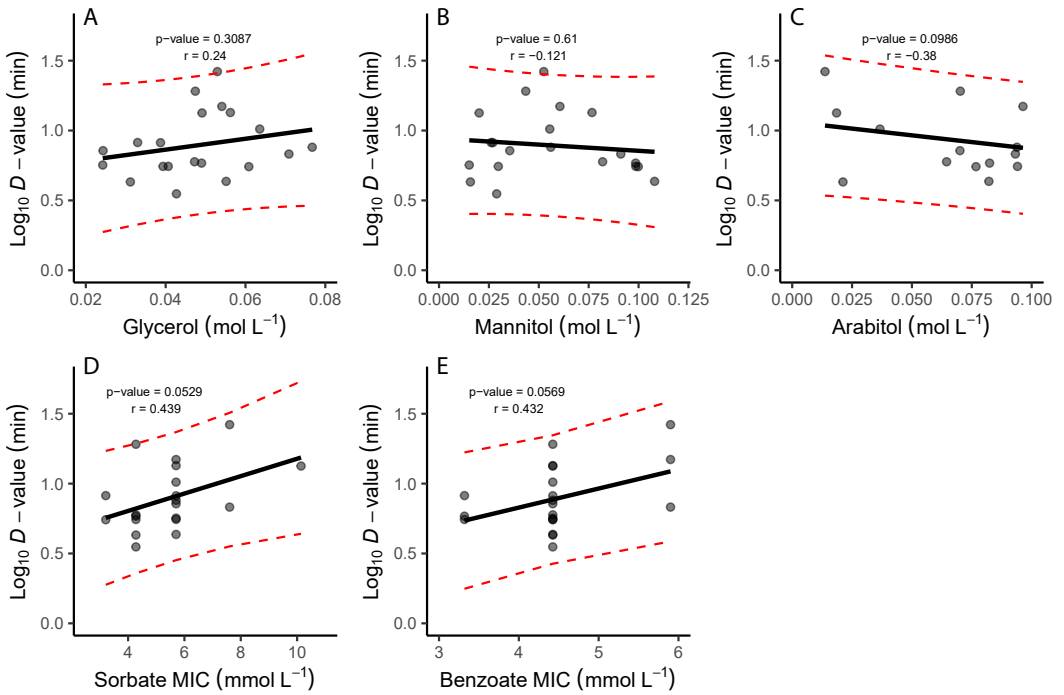


Figure S5.2. Correlation plots of conidial heat resistance in terms of \log_{10} D -value with internal glycerol (A), mannitol (B), arabitol (C) concentrations and sorbate (D) and benzoate (E) MIC.

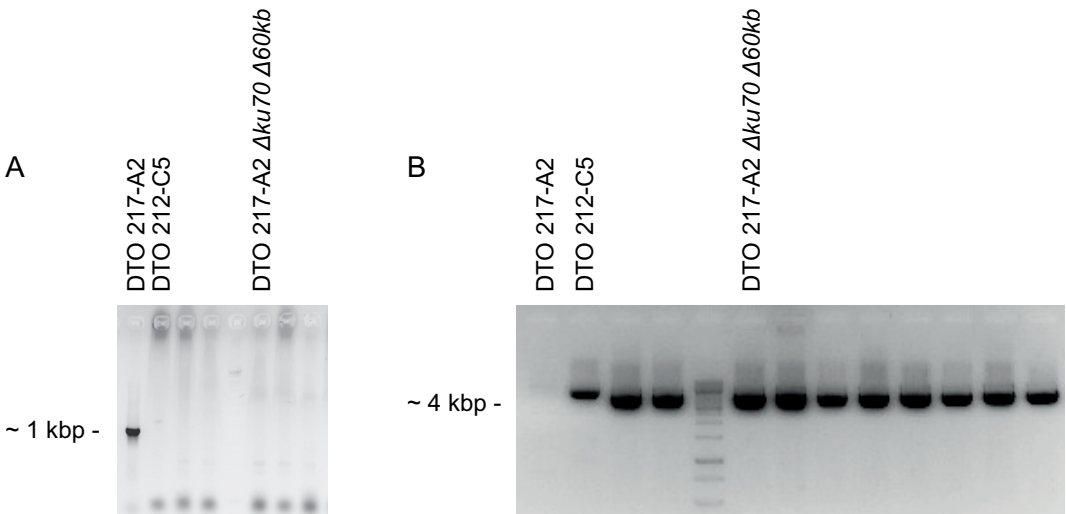


Figure S5.3. Results of diagnostic PCR to verify the absence of the 60 kbp cluster (A) and the correct integration of the donor DNA (B) in DTO 217-A2 $\Delta ku70 \Delta 60$ kbp. Details of the diagnostic PCR are provided in Table S5.1.

General discussion

A quarter of all food that is produced has been estimated to be spoiled by microbes (National Research Council (US) Subcommittee on Microbiological Criteria, 1985). Reducing this number will help in the challenge to keep feeding an increasing world population. Food industry aims to develop products that are safe by design to prevent spoilage and growth of pathogens before the end of the shelf life. However, spoilage and safety incidents do occur, leading to recalls, food waste and economic losses. To limit these losses, industrially processed food products are designed with preservation hurdles. This is a concept of applying a mixture of processing tools and adapting levels of key product parameters, such as pH, water activity or weak acids, in order to inactivate or inhibit growth of target microorganisms. As a result of current consumer trends, products are redesigned by using milder processing methods, less salt and without the use of preservatives (Leyva Salas *et al.*, 2017; Snyder and Worobo, 2018). These developments put a tension on shelf-lives, because they favour microbial growth. To estimate the potential growth of microorganisms in food, industry uses microbiological risk assessments. These cover all scientific information, including processing parameters, chemical analysis of key product parameters, microbiological modelling and challenge test results. Microbiological modelling is essential to make these assessments quantitative. The degree of uncertainty and variability should be explicitly considered in these analyses to make them more realistic (Codex Alimentarius Commission, 1999).

The fungus *Paecilomyces variotii* is a common spoiler of heat treated products, such as canned fruits and non-carbonated sodas, which is assumed to be due to the high heat resistance of its ascospores (Houbraken *et al.*, 2008). Indeed, heat processed food products can be spoiled by ascospores (dos Santos *et al.*, 2018). However, ascospores are formed within the mycelium and, as a consequence, they are not distributed as easily compared to airborne conidia that are formed on spore-forming structures, dubbed conidiophores. These spores are ubiquitous in the environment and are thought to cause spoilage of mildly heat treated food products or by contamination after processing. Spoilage of products as margarine and products containing preservatives are commonly associated with contamination of *P. variotii* conidia. Similarly, conidia of *A. niger* spoil dairy products and cause rot in onions, grapes and other fruits and vegetables, while *P. roqueforti* conidia spoil dairy products, bakery products and silage (Samson *et al.*, 2019).

The ability to grow in processed food, is largely determined by the capability of spores to overcome the preservation hurdles during germination, but also the growing hyphae have to negotiate stressors during further outgrowth of the mycelium. In addition, the conidia have to address transient inactivation treatments such as a heat treatment. Heat resistance of fungal spores is associated with the accumulation of protective compounds in the cytosol such as the compatible solutes trehalose and mannitol or heat shock proteins (Wyatt *et al.*, 2013), whereas osmotic stress resistance of growing hyphae is largely determined by accumulation of the compatible solutes glycerol and erythritol (Stevenson *et al.*, 2017). On the other hand, resistance to ultra violet (UV) radiation is associated with melanin in the cell wall (Seekles *et al.*, 2021b), while weak acid resistance is associated with proteins that catabolize or transport these compounds (Geoghegan *et al.*, 2020).

Phenotypic heterogeneity occurs between and even within strains of filamentous fungi. Genetic differences result in phenotypic variation between strains, whereas stochasticity and epigenetic modifications are important mechanisms to create heterogeneity within genetic uniform colonies (**Chapter 1**). In addition, environmental conditions and maturation impact stress resistance and germination of fungal spores (**Chapter 1**). Heterogeneity of stress resistance of conidia and the ability of hyphae to address preservation hurdles should be taken into account to accurately predict shelf life of products. Therefore, it is important to study stress resistance of multiple strains as well as the variation within a strain due to stochasticity, epigenetic modifications, environmental conditions and spore maturation. Notably, phenotypic heterogeneity in stress resistance has hardly been studied in filamentous fungi.

In this thesis, inter- and intra-strain variability of *P. variotii*, *A. niger* and *P. roqueforti* was studied with a focus on the former fungus. To this end, 108 *P. variotii* strains, 21 *A. niger* strains and 20 *P. roqueforti* strains were studied, which were isolated from various locations and substrates. Identity of the strains was verified according to the current taxonomic standards, which assures that the variability described in this study is truly intra-species. Results show that the heterogeneity in stress resistant conidia is considerable within the three different species, which is of high relevance for the food industry.

6.1 PHENOTYPIC VARIABILITY BETWEEN AND WITHIN *PAECILOMYCES VARIOTII* STRAINS SUGGEST A NEW *PAECILOMYCES* SPECIES

The identity of all 108 *P. variotii* strains was confirmed according to the taxonomy standards (Samson *et al.*, 2009) using a partial *benA* sequence (**Chapter 2**). A phylogenetic tree of these sequences revealed multiple clades, one of them having a *benA* sequence with higher difference compared to the other strains. This strain, DTO 271-G3, was genome sequenced and included in a phylogenetic analysis based on sequences of all unique orthologous genes, using 24 other *P. variotii* strains (**Chapter 4**). Indeed, DTO 271-G3 showed a relatively large distance to the other *P. variotii* strains and was located next to *P. formosus*, which was used as outgroup. Notably, strain DTO 271-G3 also contained a smaller genome size with higher GC content compared to the other *P. variotii* strains. In addition, this strain that was isolated from ice tea in South Africa, produced the smallest conidia that were heat sensitive and that contained a lower concentration of compatible solutes. Further genetic and phenotypic testing of DTO 271-G3 and the other strains belonging to this clade is required to confirm that a new *Paecilomyces* species has been identified.

6.1.2 Heat resistance of *Paecilomyces variotii*

Paecilomyces variotii is recognized as thermos-tolerant by being able to grow at temperatures up to 50 °C (Pitt and Hocking, 2009; Samson *et al.*, 2019) and as a heat-resistant mould (HRM) due to its heat resistant ascospores. Ascospores of HRMs

typically survive heat treatments at 75 °C for more than 30 minutes (Samson *et al.*, 2019). The two homothallic species *Paecilomyces fulvus* and *Paecilomyces niveus* that are closely related to *P. variotii* produce ascospores that survive heat treatments at 85 °C for several minutes (Beuchat and Rice, 1979). Because *P. variotii* is an heterothallic species, it is harder and more laborious to quantify its ascospore heat resistance. First of all, it takes six weeks to produce ascospores by crossing two strains with compatible mating types (Houbraken *et al.*, 2008). Second, physical force is necessary to separate the grouped ascospores in tough asci. Using the methods described in literature (Houbraken *et al.*, 2008), we always ended up with unbroken asci in suspension. Third, it is challenging to enumerate the separated ascospore concentrations in suspensions by microscopy or cell counting, since ascospores are usually outnumbered by conidia while having a similar size and shape. And finally, it turns out that it is challenging to produce reliable inactivation curves to describe the kinetics illustrated by the two log inactivation after heat treatments at 85 °C for two hours (Houbraken *et al.*, 2006). During this project, a single attempt was made to quantify ascospore heat resistance by crossing DTO 217-A2, a strain producing heat resistant conidia, with heat sensitive strain DTO 212-C5, producing sensitive conidia, which resulted in a D_{90} -value of 61 minutes. This number relates to the D_{90} -values of 19 – 91 minutes of *Thermoascus crustaceus* ascospores, which is arguably the most heat resistant fungus in nature (Dijksterhuis, 2019; Scaramuzza and Berni, 2014). However, a poor fit of a linear model ($R^2=0.79$) and a total reduction of only one log raised questions about the reliability of these results. Nonetheless, it demonstrates the highly heat resistant nature of *P. variotii* ascospores and suggests that it is probably superior in heat resistance when compared to *P. fulvus* and *P. niveus*. It would be interesting to see whether even more resistant ascospores could be obtained by crossing two strains that both produce heat resistant conidia, rather than by crossing a heat sensitive and heat resistant strain.

The fact that the high abundance of conidia probably give rise to more food spoilage than ascospores made us focus on these asexual spores in the remaining part of the project. Conidia of the 108 strains were heat treated for 10 minutes at 58 °C and 59 °C (**Chapter 2**). In most cases, these treatments resulted in a one to three log reduction in colony forming units (CFU). However, 31 strains showed less than one log reduction after the 59 °C heat treatment, and were therefore classified as heat resistant strains. In **Chapter 2-4**, heat resistance of in total 25 strains was further quantified by determination of D -values. This showed that strain DTO 195-F2 produced the most heat resistant fungal conidia measured to date with a D_{60} -value of 27.6 ± 3.1 minutes, while strain DTO 212-C5 produced the most sensitive conidia of the *P. variotii* strains with a D_{60} -value of 3.5 ± 0.3 minutes. This difference in D -value indicates that a heat treatment of 27.6 minutes at 60 °C will result in almost 7 log scales more inactivation of the heat sensitive strain. Therefore, this variation is relevant for microbial modelling in food products. Together, it was concluded that heat sensitive *P. variotii* strains have a D_{60} -value ≤ 6 minutes, while heat resistant strains have a D_{60} -values ≥ 9 minutes. Even the most heat-sensitive *P. variotii* conidia are more stress resistant than conidia of *A. niger* and *P. roqueforti* conidia that had to be

assessed at 54 and 56 °C, respectively, to ensure that part of the conidia survived during the heat treatments when using ACES buffer as a menstruum (**Chapter 4**). Previously, a D_{60} -values of 2.2 minutes (Baggerman, 1981) was determined for *A. niger* but in this case the menstruum was not clear. A study that quantified heat resistance of moulds in fruit juices reported D_{60} -values between 0.38 and 0.45 minutes for *A. niger* and between 0.20 and 0.29 minutes for *P. roqueforti* (Shearer *et al.*, 2002). Together, *P. variotii* forms highly heat resistant conidia. Their heat resistance is in the same range of *Saccharomyces cerevisiae* ascospores, which have D_{60} -values between 4.6 and 22.5 minutes (Milani *et al.*, 2015; Put and Jong, 1982) and as such, are also known to contaminate for instance beer products (Suiker *et al.*, 2021).

The human pathogen *Aspergillus fumigatus* is also a thermotolerant species. It can grow at temperatures up to 50 °C (Samson *et al.*, 2019) and about 7 % of its conidia survive after a heat treatment of 15 minutes at 60 °C (Hagiwara *et al.*, 2017). This would translate to an estimated D_{60} -value of 13 minutes. Interestingly, preculturing *A. fumigatus* at 37 or 45 °C instead of 25 °C drastically increased heat resistance of its conidia (Hagiwara *et al.*, 2017). Conidia produced at these temperatures hardly show any reduction in survival after the heat treatment. Similar effects were found when *P. roqueforti* conidia were grown at different temperatures (Punt *et al.*, 2020). This prompted us to evaluate the heat resistance of *P. variotii* conidia at similar environmental conditions as used in Hagiwara *et al.*, 2017 (**Chapter 5**). Like *A. fumigatus* and *P. roqueforti*, heat resistance of *P. variotii* conidia was higher when formed at elevated growth temperatures. In fact, inactivation at 60 °C was too low to make reliable inactivation curves. Therefore, heat resistance was evaluated using heat treatments of 62 °C. The D_{62} -values increased between 2.3 and 3.9-fold when cultures were cultivated at 37 °C compared to 25 °C. The highest D_{62} -value of 18.7 ± 4.30 was obtained for heat resistant strain DTO 217-A2 when cultivated at 37 °C. Heat resistance did not further increase by growing cultures at 45 °C. These results have consequences for processing of food in (sub-)tropical regions. Results imply that predictive models should be adapted to geographic location, as conidia from (sub-)tropical regions would be more resistant than conidia from temperate regions.

Maturation of conidia is another factor that impacts stress resistance of conidia. Heat resistance increases with conidia age in the case of *A. niger* (Teertstra *et al.*, 2017) and *P. roqueforti* (Punt *et al.*, 2020). This has also been found for *Aspergillus fischeri* ascospores (Wyatt *et al.*, 2015a). As indicated above, also the composition of the heating menstruum is important to assess heat resistance. High sugar concentrations, as in fruit juices, can create a protective environment for the conidia during heat treatment, resulting in higher D -values (Bröker *et al.*, 1987a). On the other hand, low pH of the menstruum results in lower D -values of *P. roqueforti* conidia (Bröker *et al.*, 1987a; Shearer *et al.*, 2002), whereas a decrease in water activity by added glycerol increases D -values of *A. niger* conidia (Baggerman, 1981). It is not only important to take these endogenous and exogenous factors into account when comparing D -values of different experiments and species but also when one designs heat processing of a food product.

Finally, experimental, biological and strain variability in heat resistance of *A. niger*, *P. roqueforti*, and *P. variotii* conidia was quantified (expressed as the root mean square error (RMSE) or σ). These data were complemented with literature data to include additional growth media and conditions and heating menstua for the former two fungi (**Chapter 4**). Experimental variability was lowest for each species, followed by biological variability and strain variability, while there was no significant difference between the three species. In fact, the RMSE values showed remarkable similarities with heat resistance of spores and cells of bacterial spoilers (den Besten *et al.*, 2018a). Together, our results indicate that strain variability is the largest source of the overall variability and thus that modelling approaches used for bacterial spoilers may also be applied for filamentous fungi.

6.1.2 Compatible solutes in *Paecilomyces variotii* conidia and their association with stress resistance

Heat resistance of fungal spores is generally associated with accumulation of the compatible solutes trehalose and mannitol (Wyatt *et al.*, 2013). Various enzymatic assays and HPLC methods have been developed to measure the internal compatible solute composition of conidia (Al-Bader *et al.*, 2010; D'Enfert and Fontaine, 1997; Hagiwara *et al.*, 2014; Hallsworth and Magan, 1994a; van Leeuwen *et al.*, 2013b; Nguyen Van Long *et al.*, 2017a; Novodvorska *et al.*, 2013; Sakamoto *et al.*, 2009). However, none of these methods take spore size into account and usually give absolute values in pg conidium⁻¹ or $\mu\text{mol (g dry weight)}^{-1}$. In an early stage of the research project, it was shown that spore size varies between *P. variotii* strains. To be able to compare compatible solute concentrations in conidia of different strains, it was essential to reliably measure the size of the ellipsoid shaped conidia of *P. variotii*. Light microscopy (LM), scanning electron microscopy (SEM), Coulter Counter (CC) and flow cytometry (FC) were used to determine size of *P. variotii* conidia (**Chapter 3**). The forward scatter of FC did not show a linear relationship with spore size but can be used to study heterogeneity in spore size. No statistical differences were found between spore size measured by LM, SEM and CC. Since the microscopical methods required manual measurements of each spore, CC is the most reliable and most efficient method to measure *P. variotii* conidia size. Using CC, differences were found in the mean conidia size of 20 strains ranging between 2.81 and 3.68 μm (**Chapter 5**). This difference in diameter results in a 2.4-fold volume difference between the smallest and largest conidia and shows the importance to include the mean spore size into the compatible solute analysis. The internal compatible solute concentrations were estimated by translating the absolute values in pg conidium⁻¹ to mol L⁻¹ by using the volume that was calculated with the mean conidia size. To our knowledge, this is the first study that used concentrations instead of absolute values for measurements of compatible solutes in conidia.

The *P. variotii* strains contained trehalose as predominant compatible solute. This might explain, at least in part, the high heat resistance compared to *A. niger*, which has mannitol as predominant compatible solute (Teertstra *et al.*, 2017), and *P. roqueforti*, which has

arabitol as predominant compatible solute in their conidia (Punt *et al.*, 2020). *A. fumigatus* also has trehalose as predominant compatible solute in its conidia (Hagiwara *et al.*, 2017) but the absolute amount was two-fold lower when compared to conidia of *P. variotii* strain DTO 195-F2 when grown under similar conditions (**Chapter 5**). The finding that *P. variotii* strains with heat resistant conidia contain more trehalose also show the importance of this compatible solute in heat resistance (**Chapter 2, 5**). Also, increased heat resistance resulting from conidia formation at higher growth temperature is accompanied with an increase in trehalose concentration both in *A. fumigatus* (Hagiwara *et al.*, 2017) and in *P. roqueforti* conidia (Punt *et al.*, 2020). However, we did not find such a correlation in *P. variotii*. Indeed, transcriptome analysis revealed that trehalose and mannitol synthesis genes of *P. variotii* were not significantly higher expressed at higher cultivation temperatures (**Chapter 5**). Recently, trehalose deficient strains of *A. niger* still showed enhanced heat resistance when grown at higher temperatures (Seekles *et al.*, 2021a). Together, results indicate that other factors or mechanisms can also be involved in enhanced heat stress resistance due to environmental conditions.

Under osmotic stress, arabitol accumulates in fungal spores and vegetative cells (Hallsworth and Magan, 1994b; Rangel *et al.*, 2015; Ruijter *et al.*, 2004). Interestingly, conidia of the heat resistant *P. variotii* strain DTO 212-C5 contained higher arabitol concentrations than heat resistant strain DTO 217-A2 and the moderate resistant strain DTO 032-I3 (**Chapter 2**). DTO 032-I3, however, was equally well adapted to NaCl stress conditions as DTO 212-C5. This paradox may be explained, at least in part, by the finding that DTO 032-I3 contained more mannitol in its conidia than the other two strains. Mannitol can also be involved in osmoregulation but its low solubility limits its effect in osmotic stress resistance (de Lima Alves *et al.*, 2015). Measuring compatible solutes in mycelium instead of conidia might provide more information in how these strains are adapted to osmotic stress. Nevertheless, these results show that strains of the same species could be adapted to different stress environments.

6.1.3 Conidia size, shape and distribution parameters are linked with heat resistance

In addition to trehalose, a significant correlation was found between conidial heat resistance and mean conidia size (**Chapter 3, 5**). These results indicate that strains with heat resistant conidia produce larger conidia than heat sensitive strains. Although it is unclear if this is a causal relationship, this phenomenon has also been found in other species, such as *Talaromyces flavus* and *Talaromyces macrosporus* (Frisvad *et al.*, 1990). The ascospores of *T. macrosporus* are larger and much more heat resistant than those of *T. flavus* (Beuchat, 1988; Dijksterhuis, 2019; Yilmaz *et al.*, 2014). The compatible solute composition of both *Talaromyces* species is similar with predominantly trehalose (Wyatt *et al.*, 2015b). In addition, the ascospores of *Aspergillus spinosus* are larger and more heat resistant than those of the close relative *A. fischeri* (unpublished data). Spore size can also be important to provide robustness against other stressors, as larger sporangiospores of the fungal pathogen *Mucor circinelloides* are more virulent and survive and germinate

better in macrophages than smaller spores (Li *et al.*, 2011). Spore shape parameters as determined by microscopical analyses revealed that conidia of heat resistant strains were more circular than those of sensitive strains (**Chapter 3**). Both, size and circularity, influence the surface-area-to-volume ratio of the conidia. The effect on heat transfer into spores might be neglectable for spores with such small size, but the relative larger surface area of the heat sensitive strains might be one of the reasons that these conidia are more sensitive. To elucidate this, the effect of heat stress on the plasma membrane should be assessed in future studies.

The size of conidia did not only differ between strains, but also within strains. Size of conidia populations were non-homogeneously distributed for all strains measured in **Chapter 2** and **3**. The skewness of the distribution was negatively correlated with heat resistance, indicating that heat sensitive strains contained relatively more large sized outliers than heat resistant strains. In some cases, like in the heat resistant strain DTO 217-A2, a bimodal size distribution was found, suggesting the presence of a small sized conidia population and a large sized conidia population. Differences in conidia size might be caused by variability in the width of the phialidal neck. In **Chapter 2**, it was found that wide phialides produced chains of large sized conidia, compared to phialides with a narrow neck. A bimodal spore size distribution is not common as *P. roqueforti* (Punt *et al.*, 2020) and *A. niger* (unpublished data) conidia showed a symmetrical size distribution, although it has been observed for *Gloeosporium orbiculare* (Chapela, 1991). With spore size being correlated with heat resistance, the bimodal distributions suggest the existence of a large sized sub-population that is heat resistant and a small sized sup-population that is heat sensitive. To verify this hypothesis, attempts have been made to separate these populations using a FC equipped with a cell sorter. Unfortunately, only low numbers of conidia were obtained per fraction and contaminations were found after heat treatments.

6.1.4 Most problematic *Paecilomyces variotii* strains for food industry

Apart from heat treatments, weak acids are generally used as preservation hurdle in industry. Therefore, the ability for conidia to germinate and grow in potassium sorbate or sodium benzoate enriched medium was assessed (**Chapter 5**). Minimum inhibitory concentrations (MICs) for sorbic acid were 1.4 – 4.4-fold higher when compared to that of a *P. variotii* strain isolated from a South American soft drink facility (Stratford *et al.*, 2009). On the other hand, up to four time higher MIC values were found for a *P. variotii* strain isolated from bakery products, albeit in a different experimental setup (Garcia *et al.*, 2021). Although heat resistance was not significantly correlated with sorbic or benzoic acid resistance, the two most sorbic acid resistant strains, DTO 195-F2 and DTO 282-E5, were also heat resistant. Similarly, heat resistant strains DTO 195-F2 and DTO 282-F9 were fairly resistant to benzoic acid. Together, strains DTO 195-F2, DTO 282-E5 and DTO 282-F9 could be described as most problematic in terms of food spoilage and are of interest in test panels to assess novel preservation techniques.

6.2 GENETIC AND TRANSCRIPTOMIC CLUES FOR MECHANISMS UNDERLYING CONIDIAL HEAT RESISTANCE

Inter-strain phenotypic variation in conidial heat resistance hint to genetic differences. The genomes of all 25 strains used in **Chapter 3** and **4** were sequenced, except for the previously sequenced strain CBS 101075 (Urquhart *et al.*, 2018). No relationship was found between conidial heat resistance, the geographic origin, the substrate from which strains were isolated from and the position in the *benA* tree in **Chapter 2**. This indicates that these features are not related to *P. variotii* phylogeny. Notably, the phylogenetic tree based on 6331 unique orthologous genes showed two clades in which the heat resistant strains clustered (**Chapter 5**). This indicates that heat resistance has evolved in two separate branches of *P. variotii*.

A genome wide association study using heat resistant strain DTO 217-A2 as reference revealed a list of 93 candidate genes that are possibly involved in conidial heat resistance. However, the majority of these genes showed low numbers of transcripts in conidia. Four of these genes were predicted to have a high-impact single nucleotide polymorphism in the heat sensitive strains but their role still need to be assessed. Transcriptome analysis was also performed on conidia grown at 25, 37 or 45°C (**Chapter 5**). Some of the genes that were significantly higher expressed at 37 °C showed a predicted function as hydrophilin or are predicted to function in oxidative stress resistance. Heat resistance has a link with oxidative stress resistance, as heat stress increases the presence of reactive oxygen species (Davidson *et al.*, 1996). In addition, hydrophilins, such as small heat shock proteins and conidiation-specific proteins con-6 and con-10, have been associated with heat stress resistance, although its precise mechanisms remain elusive (van Leeuwen *et al.*, 2016; Punt *et al.*, 2020). For all tested conditions, large amounts of transcripts were found in conidia of the hydrophilins con-6, con-10, Hsp12 and LeamA. Hydrophilins share function with trehalose in desiccation stress resistance (Kim *et al.*, 2018). Hsp12 has a protective function of the cell membrane in *S. cerevisiae* (Welker *et al.*, 2010) and acts synergistically with trehalose in desiccation-rehydration stress (Kim *et al.*, 2018). Together, these genes are suggested to play an important role in stress resistance of *P. variotii* conidia.

A gene cluster of approximately 60 kbp was identified in 6 out of 8 heat resistant strains, but absent in all heat sensitive strains. The cluster showed homology with a gene cluster that is present in nine out of 21 *Penicillium chrysogenum* genomes and one out of 34 *P. roqueforti* genomes (**Chapter 5**). Moreover, various *Aspergillus* species contain parts of the cluster. Data suggest that the 60 kb cluster originates from *P. chrysogenum* and was introduced to *P. variotii* through horizontal gene transfer. Absence of a transposase gene and palindrome regions indicate that it has not been a transposon mediated transfer. Four out of 10 predicted genes on the cluster showed similarities in function with genes of a recently described 85 kbp transposon in *P. variotii*, which is involved in metal resistance (Urquhart *et al.*, 2022). Although the 60 kbp cluster was present in most heat resistant

strains, no evidence was found that it is involved in conidial heat resistance. A 60 kbp knock-out mutant of heat resistant strain DTO 217-A2 showed similar heat resistance, compatible solute composition, spore size and growth behaviour of the germ tube when compared to the parental strain.

6.3 IMPLICATIONS AND FUTURE RESEARCH

Reduction in food loss and waste will contribute to global food security for the decades to come. This Thesis contributes to a better understanding of inter- and intra-strain heterogeneity of *P. variotii* and, more general, the Eurotiales. This data can be used as input to improve predictive models in food industry that describe spoilage due to contamination by airborne conidia and more specifically, by *P. variotii* conidia. In the end, the most resistant spore defines if spoilage by a fungus can occur. Therefore, implementation of variability in microbiological modelling could lead to microbiological risk assessments with higher precision (den Besten *et al.*, 2018b), which results in less recalls, less economic losses, and most importantly: less food waste.

In **Chapter 5**, genomic data of 24 strains and transcriptomic data of three strains was presented. The results of our comparative genomics and transcriptomic study indicate that mechanisms involved in conidial heat resistance are complex, since many genes with a variety of functions can be linked to thermal stress resistance. With an efficient CRISPR/Cas9 method to genetically modify *P. variotii* strains, the way is paved for functional analysis of these genes (Seekles *et al.*, 2021b; **Chapter 5**). Genome Wide Association Studies (GWAS) can also be used to identify genes involved in heat and weak acid resistance. The gene cluster SORBUS in *P. roqueforti* involved in sorbate resistance was identified using GWAS, which is homologous to the *A. niger* cluster that mediates weak acid resistance (Punt *et al.*, 2022b). Hence, this example indicates that many more mechanisms of stress resistance could be studied by using the datasets presented in this research project. Identified genes involved in stress resistance may be targets for novel food processing strategies.

APPENDIX

REFERENCES

NEDERLANDSE SAMENVATTING

CURRICULUM VITAE

LIST OF PUBLICATIONS

ACKNOWLEDGEMENTS

REFERENCES

- Ackermann, M. (2015). A functional perspective on phenotypic heterogeneity in microorganisms. *Nat. Rev. Microbiol.* *13*, 497–508.
- Al-Bader, N., Vanier, G., Liu, H., Gravelat, F.N., Urb, M., Hoareau, C.M.-Q., Campoli, P., Chabot, J., Filler, S.G., and Sheppard, D.C. (2010). Role of trehalose biosynthesis in *Aspergillus fumigatus* development, stress response, and virulence. *Infect. Immun.* *78*, 3007–3018.
- Aldrich, H.C., and Todd, W.J. (1986). *Ultrastructure techniques for microorganisms* (Plenum Press, New York).
- Amend, A.S., Seifert, K.A., Samson, R., and Bruns, T.D. (2010). Indoor fungal composition is geographically patterned and more diverse in temperate zones than in the tropics. *Proc. Natl. Acad. Sci. U. S. A.* *107*, 13748–13753.
- Andersen, B., Frisvad, J.C., Søndergaard, I., Rasmussen, I.S., and Larsen, L.S. (2011). Associations between fungal species and water-damaged building materials. *Appl. Env. Microbiol.* *77*, 4180–4188.
- Andersson, J.O. (2009). Gene transfer and diversification of microbial eukaryotes. *Annu. Rev. Microbiol.* *63*, 177–193.
- Arentshorst, M., and Ram, A.F.J. (2018). Parasexual crossings for bulk segregant analysis in *Aspergillus niger* to facilitate mutant identification via whole genome sequencing. In: *Fungal Genomics: Methods in Molecular Biology*, vol 1775. R.P. de Vries, A. Tsang, and I. V Grigoriev, eds. (Humana Press, New York, NY), pp. 277–287.
- Arentshorst, M., Ram, A.F.J., and Meyer, V. (2012). Using non-homologous end-joining-deficient strains for functional gene analyses in filamentous fungi. In: *Plant Fungal Pathogens. Methods in Molecular Biology (Methods and Protocols)*, vol 835. M. Bolton, and B. Thomma, eds. (Humana Press), pp. 133–150.
- Aryani, D.C., den Besten, H.M., Hazeleger, W.C., and Zwietering, M.H. (2015). Quantifying variability on thermal resistance of *Listeria monocytogenes*. *Int. J. Food Microbiol.* *193*, 130–138.
- Aryani, D.C., den Besten, H.M.W., and Zwietering, M.H. (2016). Quantifying variability in growth and thermal inactivation kinetics of *Lactobacillus plantarum*. *Appl. Environ. Microbiol.* *82*, 4896–4908.
- van Asselt, E.D., and Zwietering, M.H. (2006). A systematic approach to determine global thermal inactivation parameters for various food pathogens. *Int. J. Food Microbiol.* *107*, 73–82.
- Aunbjerg, S.D., Andersen, K.R., and Knochel, S. (2015). Real-time monitoring of fungal inhibition and morphological changes. *J. Microbiol. Methods* *119*, 196–202.
- Avery, S. V (2006). Microbial cell individuality and the underlying sources of heterogeneity. *Nat. Rev. Microbiol.* *4*, 577–587.
- Baggerman, W.I. (1981). Heat resistance of yeast cells and fungal spores. In *Introduction to Food-Borne Fungi*, R.A. Samson, Hoekstra, E.S. and van Oorschot, C.A.N., ed. (Utrecht: Centraalbureau voor Schimmelcultures), pp. 227–231.
- Bainier, G. (1907). *Paecilomyces*, genre nouveau de Mucedinées. *Bull. Soc. Mycol. Fr.* *23*, 26–27.
- Ballestra, P., and Cuq, J.-L. (1998). Influence of pressurized carbon dioxide on the thermal inactivation of bacterial and fungal Spores. *LWT-Food Sci. Technol.* *31*, 84–88.
- Barros, B.H.R., da Silva, S.H., dos Reis Marques, E., Rosa, J.C., Yatsuda, A.P., Roberts, D.W., and Braga, G.U.L. (2010). A proteomic approach to identifying proteins differentially expressed in conidia and mycelium of the entomopathogenic fungus *Metarhizium acridum*. *Fungal Biol.* *114*, 572–579.
- de Bekker, C., van Veluw, G.J., Vinck, A., Wiebenga, L.A., and Wösten, H.A.B. (2011). Heterogeneity of *Aspergillus niger* microcolonies in liquid shaken cultures. *Appl. Env. Microbiol.* *77*, 1263–1267.
- de Bekker, C., Ohm, R.A., Evans, H.C., Brachmann, A., and Hughes, D.P. (2017). Ant-infecting *Ophiocordyceps* genomes reveal a high diversity of potential behavioral manipulation genes

- and a possible major role for enterotoxins. *Sci. Rep.* 7, 12508.
- Belbahji, A., Bohuon, P., Leguérinel, I., Meot, J.-M., Loiseau, G., and Madani, K. (2017). Heat resistances of *Candida apicola* and *Aspergillus niger* spores isolated from date fruit surface. *J. Food Process. Eng.* 40, e12272.
- Belozerskaya, T.A., Gessler, N.N., and Aver'yanov, A.A. (2017). Melanin Pigments of Fungi. In *Fungal Metabolites*, J.-M. Mérillon, and K.G. Ramawat, eds. (Cham: Springer International Publishing), pp. 263–291.
- Benaglia, T., Chauveau, D., Hunter, D., and Young, D. (2009). mixtools: An R package for analyzing finite mixture models. *J. Stat. Softw.* 32, 1–29.
- Berendsen, E.M., Boekhorst, J., Kuipers, O.P., and Wells-Bennik, M.H.J. (2016). A mobile genetic element profoundly increases heat resistance of bacterial spores. *ISME J.* 10, 2633–2642.
- van den Berg, M.A., Albang, R., Albermann, K., Badger, J.H., Daran, J.M., Driessen, A.J., Garcia-Estrada, C., Fedorova, N.D., Harris, D.M., Heijne, W.H., *et al.* (2008). Genome sequencing and analysis of the filamentous fungus *Penicillium chrysogenum*. *Nat. Biotechnol.* 26, 1161–1168.
- Berlin, V., and Yanofsky, C. (1985). Isolation and characterization of genes differentially expressed during conidiation of *Neurospora crassa*. *Mol. Cell. Biol.* 5, 849–855.
- den Besten, H.M.W., Berendsen, E.M., Wells-Bennik, M.H.J., Straatsma, H., and Zwietering, M.H. (2017). Two complementary approaches to quantify variability in heat resistance of spores of *Bacillus subtilis*. *Int. J. Food Microbiol.* 253, 48–53.
- den Besten, H.M.W., Wells-Bennik, M.H.J., and Zwietering, M.H. (2018a). Natural diversity in heat resistance of bacteria and bacterial spores: Impact on food safety and quality. *Annu. Rev. Food Sci. Technol.* 9, 383–410.
- den Besten, H.M.W., Amézquita, A., Bover-Cid, S., Dagnas, S., Ellouze, M., Guillou, S., Nychas, G., O'Mahony, C., Pérez-Rodríguez, F., and Membré, J.-M. (2018b). Next generation of microbiological risk assessment: Potential of omics data for exposure assessment. *Int. J. Food Microbiol.* 287, 18–27.
- Beuchat, L.R. (1986). Extraordinary heat resistance of *Talaromyces flavus* and *Neosartorya fischeri* ascospores in fruit products. *J. Food Sci.* 51, 1506–1510.
- Beuchat, L.R. (1988). Influence of organic acids on heat resistance characteristics of *Talaromyces flavus* ascospores. *Int. J. Food Microbiol.* 6, 97–105.
- Beuchat, L.R., and Rice, S.L. (1979). *Byssochlamys* spp. and their importance in processed fruits. *Adv. Food Res.* 25, 237–288.
- Blank, G., Yang, R., and Scanlon, M.G. (1998). Influence of sporulation aw on heat resistance and germination of *Penicillium roqueforti* spores. *Food Microbiol.* 15, 151–156.
- Bleichrodt, R., Vinck, A., Krijghsheld, P., van Leeuwen, M.R., Dijksterhuis, J., and Wösten, H.A.B. (2013). Cytosolic streaming in vegetative mycelium and aerial structures of *Aspergillus niger*. *Stud. Mycol.* 74, 31–46.
- Bondi, M., Messi, P., Halami, P.M., Papadopoulou, C., and de Niederhausen, S. (2014). Emerging microbial concerns in food safety and new control measures. *Biomed. Res. Int.* 2014, 251512.
- Bos, C.J., Debets, A.J.M., Swart, K., Huybers, A., Kobus, G., and Slakhorst, S.M. (1988). Genetic analysis and the construction of master strains for assignment of genes to six linkage groups in *Aspergillus niger*. *Curr. Genet.* 14, 437–443.
- Boschloo, J.G., Moonen, E., van Gorcom, R.F.M., Hermes, H.F.M., and Bos, C.J. (1991). Genetic analysis of *Aspergillus niger* mutants defective in benzoate-4-hydroxylase function. *Curr. Genet.* 19, 261–264.
- Bröker, U., Spicher, G., and Ahrens, E. (1987a). Zur Frage der Hitzeresistenz der Erreger der Schimmelbildung bei Backwaren. 2. Mitteilung: Einfluss endogener Faktoren auf die Hitzeresistenz von Schimmelsporen. *Getreide, Mehl Und Brot* 41, 278–284.
- Bröker, U., Spicher, G., and Ahrens, E. (1987b). Zur Frage der Hitzeresistenz der Erreger der Schimmelbildung bei Backwaren. 3. Mitteilung: Einfluss exogener Faktoren auf die Hitzeresistenz

- von Schimmelsporen. Getreide, Mehl Und Brot 41, 344–355.
- van den Brule, T., Lee, C.L.S., Houbraken, J., Haas, P.-J., Wösten, H.A.B., and Dijksterhuis, J. (2020a). Conidial heat resistance of various strains of the food spoilage fungus *Paecilomyces variotii* correlates with mean spore size, spore shape and size distribution. *Food Res. Int.* 137, 109514.
- van den Brule, T., Punt, M., Teertstra, W., Houbraken, J., Wösten, H.A.B., and Dijksterhuis, J. (2020b). The most heat-resistant conidia observed to date are formed by distinct strains of *Paecilomyces variotii*. *Environ. Microbiol.* 22, 986–999.
- Bügl, H., Fauman, E.B., Staker, B.L., Zheng, F., Kushner, S.R., Saper, M.A., Bardwell, J.C.A., and Jakob, U. (2000). RNA methylation under heat shock control. *Mol. Cell* 6, 349–360.
- Chang, L., and Pikal, M.J. (2009). Mechanisms of protein stabilization in the solid state. *J. Pharm. Sci.* 98, 2886–2908.
- Chapela, I.H. (1991). Spore size revisited: analysis of spore populations using automated particle size. *Sydowia* 43, 1–14.
- Cheeseman, K., Ropars, J., Renault, P., Dupont, J., Gouzy, J., Branca, A., Abraham, A.-L., Ceppi, M., Conseiller, E., Debuchy, R., *et al.* (2014). Multiple recent horizontal transfers of a large genomic region in cheese making fungi. *Nat. Commun.* 5, 2876.
- Chen, A.J., Frisvad, J.C., Sun, B.D., Varga, J., Kocsubé, S., Dijksterhuis, J., Kim, D.H., Hong, S.B., Houbraken, J., and Samson, R.A. (2016). *Aspergillus* section *Nidulantes* (formerly *Emericella*): Polyphasic taxonomy, chemistry and biology. *Stud. Mycol.* 84, 1–118.
- Choudoir, M.J., Panke-Buisse, K., Andam, C.P., and Buckley, D.H. (2017). Genome surfing as driver of microbial genomic diversity. *Trends Microbiol.* 25, 624–636.
- Cingolani, P., Platts, A., Wang, L.L., Coon, M., Nguyen, T., Wang, L., Land, S.J., Lu, X., and Ruden, D.M. (2012). A program for annotating and predicting the effects of single nucleotide polymorphisms, SnpEff. *Fly (Austin)*. 6, 80–92.
- Codex Alimentarius Commission (1999). Principles and guidelines for the conduct of microbiological risk assessment. CAC/GL 30-1999 (Rome: World Health Organization: Food and Agriculture Organization of the United Nations).
- Collins, K.D. (1997). Charge density-dependent strength of hydration and biological structure. *Biophys. J.* 72, 65–76.
- Coton, E., Coton, M., Hymery, N., Mounier, J., and Jany, J.-L. (2020). *Penicillium roqueforti*: an overview of its genetics, physiology, metabolism and biotechnological applications. *Fungal Biol. Rev.* 34, 59–73.
- Cray, J.A., Russell, J.T., Timson, D.J., Singhal, R.S., and Hallsworth, J.E. (2013). A universal measure of chaotropicity and kosmotropicity. *Env. Microbiol.* 15, 287–296.
- D'Enfert, C., and Fontaine, T. (1997). Molecular characterization of the *Aspergillus nidulans* *treA* gene encoding an acid trehalase required for growth on trehalose. *Mol. Microbiol.* 24, 203–216.
- Dagnas, S., Gougouli, M., Onno, B., Koutsoumanis, K.P., and Membre, J.M. (2015). Modeling red cabbage seed extract effect on *Penicillium corylophilum*: Relationship between germination time, individual and population lag time. *Int. J. Food Microbiol.* 211, 86–94.
- Dagnas, S., Gougouli, M., Onno, B., Koutsoumanis, K.P., and Membré, J.-M. (2017). Quantifying the effect of water activity and storage temperature on single spore lag times of three moulds isolated from spoiled bakery products. *Int. J. Food. Microbiol.* 240, 75–84.
- Dantigny, P. (2021). Applications of predictive modeling techniques to fungal growth in foods. *Curr. Opin. Food Sci.* 38, 86–90.
- Davidson, J.F., Whyte, B., Bissinger, P.H., and Schiestl, R.H. (1996). Oxidative stress is involved in heat-induced cell death in *Saccharomyces cerevisiae*. *Proc. Natl. Acad. Sci. U. S. A.* 93, 5116–5121.
- Davies, C.R., Wohlgemuth, F., Young, T., Violet, J., Dickinson, M., Sanders, J.-W., Vallieres, C., and Avery, S.V. (2021). Evolving challenges and strategies for fungal control in the food supply

- chain. *Fungal Biol. Rev.* *36*, 15–26.
- Dijksterhuis, J. (2017). The fungal spore and food spoilage. *Curr. Opin. Food Sci.* *17*, 68–74.
- Dijksterhuis, J. (2019). Fungal spores: Highly variable and stress-resistant vehicles for distribution and spoilage. *Food Microbiol.* *81*, 2–11.
- Dyer, P.S., and O’Gorman, C.M. (2011). A fungal sexual revolution: *Aspergillus* and *Penicillium* show the way. *Curr. Opin. Microbiol.* *14*, 649–654.
- El-Gebali, S., Mistry, J., Bateman, A., Eddy, S.R., Luciani, A., Potter, S.C., Qureshi, M., Richardson, L.J., Salazar, G.A., Smart, A., *et al.* (2018). The Pfam protein families database in 2019. *Nucleic Acids Res.* *47*, D427–D432.
- Ellena, V., Sauer, M., and Steiger, M.G. (2020). The fungal sexual revolution continues: discovery of sexual development in members of the genus *Aspergillus* and its consequences. *Fungal Biol. Biotechnol.* *7*, 17.
- Ellena, V., Bucchieri, D., Arcalis, E., Sauer, M., and Steiger, M.G. (2021). Sclerotia formed by citric acid producing strains of *Aspergillus niger*: Induction and morphological analysis. *Fungal Biol.* *125*, 485–494.
- Emms, D.M., and Kelly, S. (2019). OrthoFinder: phylogenetic orthology inference for comparative genomics. *Genome Biol.* *20*, 238.
- Esbelin, J., Mallea, S., J Ram, A.F., and Carlin, F. (2013). Role of pigmentation in protecting *Aspergillus niger* conidiospores against pulsed light radiation. *Photochem. Photobiol.* *89*, 758–761.
- Fillinger, S., Chaverocche, M.K., van Dijck, P., de Vries, R., Ruijter, G., Thevelein, J., and d’Enfert, C. (2001). Trehalose is required for the acquisition of tolerance to a variety of stresses in the filamentous fungus *Aspergillus nidulans*. *Microbiology* *147*, 1851–1862.
- Fredborg, M., Andersen, K.R., Jørgensen, E., Droce, A., Olesen, T., Jensen, B.B., Rosenvinge, F.S., and Sondergaard, T.E. (2013). Real-time optical antimicrobial susceptibility testing. *J. Clin. Microbiol.* *51*, 2047–2053.
- Frisvad, J.C., Filtenborg, O., Samson, R.A., and Stolk, A.C. (1990). Chemotaxonomy of the genus *Talaromyces*. *Antonie van Leeuwenhoek* *57*, 179–189.
- Fujikawa, H., Morozumi, S., Smerage, G.H., and Teixeira, A.A. (2000). Comparison of capillary and test tube procedures for analysis of thermal inactivation kinetics of mold spores. *J. Food Prot.* *63*, 1404–1409.
- Funaki, M., Asano, T., Ijuin, T., Mochizuki, Y., Fukami, K., and Takenawa, T. (2000). Identification and characterization of a novel inositol polyphosphate 5-phosphatase. *J. Biol. Chem.* *275*, 10870–10875.
- Gabriela Roca, M., Read, N.D., and Wheals, A.E. (2005). Conidial anastomosis tubes in filamentous fungi. *FEMS Microbiol. Lett.* *249*, 191–198.
- Gadd, G.M., Chalmers, K., and Reed, R.H. (1987). The role of trehalose in dehydration resistance of *Saccharomyces cerevisiae*. *FEMS Microbiol. Lett.* *48*, 249–254.
- Garcia, M.V., Garcia-Cela, E., Magan, N., Copetti, M.V., and Medina, A. (2021). Comparative growth inhibition of bread spoilage fungi by different preservative concentrations using a rapid turbidimetric assay system. *Front. Microbiol.* *12*, 678406
- Gélinas, P., Fiset, G., Leduy, A., and Goulet, J. (1989). Effect of growth conditions and trehalose content on cryotolerance of bakers’ yeast in frozen doughs. *Appl. Environ. Microbiol.* *55*, 2453–2459.
- Geoghegan, I.A., Stratford, M., Bromley, M., Archer, D.B., and Avery, S.V. (2020). Weak Acid Resistance A (WarA), a novel transcription factor required for regulation of weak-acid resistance and spore-spore heterogeneity in *Aspergillus niger*. *MSphere* *5*, e00685-19.
- Gougouli, M., and Koutsoumanis, K.P. (2013). Relation between germination and mycelium growth of individual fungal spores. *Int. J. Food Microbiol.* *161*, 231–239.
- Gougouli, M., and Koutsoumanis, K.P. (2017). Risk assessment of fungal spoilage: A case study of

- Aspergillus niger* on yogurt. *Food Microbiol.* *65*, 264–273.
- Gram, L., Ravn, L., Rasch, M., Bruhn, J.B., Christensen, A.B., and Givskov, M. (2002). Food spoilage—interactions between food spoilage bacteria. *Int. J. Food Microbiol.* *78*, 79–97.
- Gurtler, J.B., Hinton, A., Bailey, R.B., Cray, W.C., Meinersmann, R.J., Ball, T.A., and Jin, T.Z. (2015). *Salmonella* isolated from ready-to-eat pasteurized liquid egg products: Thermal resistance, biochemical profile, and fatty acid analysis. *Int. J. Food Microbiol.* *206*, 109–117.
- Gustavsson, J., Cederberg, C., Sonesson, U., van Otterdijk, R., and Meybeck, A. (2011). Global food losses and food waste: extent, causes and prevention. (Rome, Italy: Food and Agriculture Organization of the United Nations).
- Hagiwara, D., Suzuki, S., Kamei, K., Gonoï, T., and Kawamoto, S. (2014). The role of AtfA and HOG MAPK pathway in stress tolerance in conidia of *Aspergillus fumigatus*. *Fungal Genet. Biol.* *73*, 138–149.
- Hagiwara, D., Sakai, K., Suzuki, S., Umemura, M., Nogawa, T., Kato, N., Osada, H., Watanabe, A., Kawamoto, S., Gonoï, T., *et al.* (2017). Temperature during conidiation affects stress tolerance, pigmentation, and tryptacin accumulation in the conidia of the airborne pathogen *Aspergillus fumigatus*. *PLoS One* *12*, e0177050.
- Hall, B.G., Acar, H., Nandipati, A., and Barlow, M. (2013). Growth rates made easy. *Mol. Biol. Evol.* *31*, 232–238.
- Hallsworth, J.E., and Magan, N. (1994a). Effect of carbohydrate type and concentration on polyhydroxy alcohol and trehalose content of conidia of three entomopathogenic fungi. *Microbiology* *140*, 2705–2713.
- Hallsworth, J.E., and Magan, N. (1994b). Effects of KCl concentration on accumulation of acyclic sugar alcohols and trehalose in conidia of three entomopathogenic fungi. *Lett. Appl. Microbiol.* *18*, 8–11.
- Hane, J.K., Williams, A.H., Taranto, A.P., Solomon, P.S., and Oliver, R.P. (2015). Repeat-Induced Point Mutation: A fungal-specific, endogenous mutagenesis process. In *Genetic Transformation Systems in Fungi*, Volume 2, M.A. van den Berg, and K. Maruthachalam, eds. (Cham: Springer International Publishing), pp. 55–68.
- Hawksworth, D.L., Crous, P.W., Redhead, S.A., Reynolds, D.R., Samson, R.A., Seifert, K.A., Taylor, J.W., Wingfield, M.J., Abaci, O., Aime, C., *et al.* (2011). The Amsterdam declaration on fungal nomenclature. *IMA Fungus* *2*, 105–112.
- Hawksworth, D.L., Lücking, R., Heitman, J., and James, T.Y. (2017). Fungal diversity revisited: 2.2 to 3.8 million species. *Microbiol. Spectr.* *5*, 5.4.10.
- Hayer, K., Stratford, M., and Archer, D.B. (2013). Structural features of sugars that trigger or support conidial germination in the filamentous fungus *Aspergillus niger*. *Appl. Env. Microbiol.* *79*, 6924–6931.
- Hayer, K., Stratford, M., and Archer, D.B. (2014). Germination of *Aspergillus niger* conidia is triggered by nitrogen compounds related to L-amino acids. *Appl. Env. Microbiol.* *80*, 6046–6053.
- Henk, D.A., Eagle, C.E., Brown, K., Van Den Berg, M.A., Dyer, P.S., Peterson, S.W., and Fisher, M.C. (2011). Speciation despite globally overlapping distributions in *Penicillium chrysogenum*: the population genetics of Alexander Fleming’s lucky fungus. *Mol. Ecol.* *20*, 4288–4301.
- Hewitt, S.K., Foster, D.S., Dyer, P.S., and Avery, S.V. (2016). Phenotypic heterogeneity in fungi: Importance and methodology. *Fungal Biol. Rev.* *30*, 176–184.
- Hillis, D.M., and Bull, J.J. (1993). An empirical test of bootstrapping as a method for assessing confidence in phylogenetic analysis. *Syst. Biol.* *42*, 182–192.
- Hillmann, F., Shekhova, E., and Kniemeyer, O. (2015). Insights into the cellular responses to hypoxia in filamentous fungi. *Curr. Genet.* *61*, 441–455.
- Hitchins, A.D., Kahn, A.J., and Slepecky, R.A. (1968). Interference contrast and phase contrast microscopy of sporulation and germination of *Bacillus megaterium*. *J. Bacteriol.* *96*, 1811–1817.
- Hoff, K.J., Lange, S., Lomsadze, A., Borodovsky, M., and Stanke, M. (2016). BRAKER1: Unsupervised

- RNA-seq-based genome annotation with GeneMark-ET and AUGUSTUS. *Bioinformatics* 32, 767–769.
- Hofstetter, V., Buyck, B., Eyssartier, G., Schnee, S., and Gindro, K. (2019). The unbearable lightness of sequenced-based identification. *Fungal Divers.* 96, 243–284.
- Holland, S.L., Reader, T., Dyer, P.S., and Avery, S. V (2014). Phenotypic heterogeneity is a selected trait in natural yeast populations subject to environmental stress. *Environ. Microbiol.* 16, 1729–1740.
- Houbraken, J., Samson, R.A., and Frisvad, J.C. (2006). *Byssoschlamys*: significance of heat resistance and mycotoxin production. *Adv. Exp. Med. Biol.* 571, 211–224.
- Houbraken, J., Varga, J., Rico-Munoz, E., Johnson, S., and Samson, R.A. (2008). Sexual reproduction as the cause of heat resistance in the food spoilage fungus *Byssoschlamys spectabilis* (anamorph *Paecilomyces variotii*). *Appl. Environ. Microbiol.* 74, 1613–1619.
- Houbraken, J., Verweij, P.E., Rijs, A.J.M.M., Borman, A.M., and Samson, R.A. (2010). Identification of *Paecilomyces variotii* in clinical samples and settings. *J. Clin. Microbiol.* 48, 2754–2761.
- Houbraken, J., Kocsubé, S., Visagie, C.M., Yilmaz, N., Wang, X.C., Meijer, M., Kraak, B., Hubka, V., Samson, R.A., and Frisvad, J.C. (2020). Classification of *Aspergillus*, *Penicillium*, *Talaromyces* and related genera (Eurotiales): An overview of families, genera, subgenera, sections, series and species. *Stud. Mycol.* 95, 5–169.
- Ijadpanahsaravi, M., Punt, M., Wösten, H.A.B., and Teertstra, W.R. (2021). Minimal nutrient requirements for induction of germination of *Aspergillus niger* conidia. *Fungal Biol.* 115, 231–238.
- Ishitani, C., and Sakaguchi, K.-I. (1956). Hereditary variation and recombination in Koji-moulds (*Aspergillus oryzae* and *Asp. Sojae*). *J. Gen. Appl. Microbiol.* 2, 345–400.
- Jantschitsch, C., and Trautinger, F. (2003). Heat shock and UV-B-induced DNA damage and mutagenesis in skin. *Photochem. Photobiol. Sci.* 2, 899–903.
- Joanes, D.N., and Gill, C.A. (1998). Comparing measures of sample skewness and kurtosis. *J. R. Stat. Soc., Ser. D Stat.* 47, 183–189.
- Kahm, M., Hasenbrink, G., Lichtenberg-Fraté, H., Ludwig, J., and Kschischo, M. (2010). grofit: Fitting biological growth curves with R. *J. Stat. Softw.* 33, 21.
- Keyhani, N.O. (2018). Lipid biology in fungal stress and virulence: Entomopathogenic fungi. *Fungal Biol.* 122, 420–429.
- Kim, S.X., Çamdere, G., Hu, X., Koshland, D., and Tapia, H. (2018). Synergy between the small intrinsically disordered protein Hsp12 and trehalose sustain viability after severe desiccation. *Elife* 7, e38337.
- Kumar, S., Stecher, G., and Tamura, K. (2016). MEGA7: Molecular evolutionary genetics analysis version 7.0 for bigger datasets. *Mol. Biol. Evol.* 33, 1870–1874.
- Kundu, S., Kim Hyung, T., Yoon Hyun, J., Shin, H.-S., Lee, J., Jung H., J., and Kim Sik, H. (2014). Viriditoxin regulates apoptosis and autophagy via mitotic catastrophe and microtubule formation in human prostate cancer cells. *Int. J. Oncol.* 45, 2331–2340.
- Kunz, B. (1981). Untersuchungen über den Einfluß der Temperatur auf Konidien suspensionen ausgewählter Penicillien Species. *Nahrung* 25, 185–191.
- van Leeuwe, T.M., Arentshorst, M., Ernst, T., Alazi, E., Punt, P.J., and Ram, A.F.J. (2019). Efficient marker free CRISPR/Cas9 genome editing for functional analysis of gene families in filamentous fungi. *Fungal Biol. Biotechnol.* 6, 13.
- van Leeuwen, M.R., Krijghsheld, P., Wyatt, T.T., Golovina, E.A., Menke, H., Dekker, A., Stark, J., Stam, H., Bleichrodt, R., Wosten, H.A.B., *et al.* (2013a). The effect of natamycin on the transcriptome of conidia of *Aspergillus niger*. *Stud. Mycol.* 74, 71–85.
- van Leeuwen, M.R., Krijghsheld, P., Bleichrodt, R., Menke, H., Stam, H., Stark, J., Wösten, H.A.B., and Dijksterhuis, J. (2013b). Germination of conidia of *Aspergillus niger* is accompanied by major changes in RNA profiles. *Stud. Mycol.* 74, 59–70.
- van Leeuwen, M.R., Wyatt, T.T., van Doorn, T.M., Lugones, L.G., Wösten, H.A.B., and Dijksterhuis,

- J. (2016). Hydrophilins in the filamentous fungus *Neosartorya fischeri* (*Aspergillus fischeri*) have protective activity against several types of microbial water stress. *Environ. Microbiol. Rep.* *8*, 45–52.
- Van Leeuwen, M.R., Van Doorn, T.M., Golovina, E.A., Stark, J., and Dijksterhuis, J. (2010). Water- and air-distributed conidia differ in sterol content and cytoplasmic microviscosity. *Appl. Environ. Microbiol.* *76*, 366–369.
- Leyva Salas, M., Mounier, J., Valence, F., Coton, M., Thierry, A., and Coton, E. (2017). Antifungal microbial agents for food biopreservation—A Review. *Microorganisms* *5*, 37.
- Li, C.H., Cervantes, M., Springer, D.J., Boekhout, T., Ruiz-Vazquez, R.M., Torres-Martinez, S.R., Heitman, J., and Lee, S.C. (2011). Sporangiospore size dimorphism is linked to virulence of *Mucor circinelloides*. *PLoS Pathog.* *7*, e1002086.
- Li, L., Hu, X., Xia, Y., Xiao, G., Zheng, P., and Wang, C. (2014). Linkage of oxidative stress and mitochondrial dysfunctions to spontaneous culture degeneration in *Aspergillus nidulans*. *Mol. Cell. Proteom.* *13*, 449–461.
- Lianou, A., and Koutsoumanis, K.P. (2013a). Strain variability of the behavior of foodborne bacterial pathogens: A review. *Int. J. Food Microbiol.* *167*, 310–321.
- Lianou, A., and Koutsoumanis, K.P. (2013b). Evaluation of the strain variability of *Salmonella enterica* acid and heat resistance. *Food Microbiol.* *34*, 259–267.
- Lianou, A., Nychas, G.-J.E., and Koutsoumanis, K.P. (2020). Strain variability in biofilm formation: A food safety and quality perspective. *Food Res. Int.* *137*, 109424.
- Lillehoj, E.B., and Ciegler, A. (1972). A toxic substance from *Aspergillus viridi-nutans*. *Can. J. Microbiol.* *18*, 193–197.
- de Lima Alves, F., Stevenson, A., Baxter, E., Gillion, J.L.M., Hejazi, F., Hayes, S., Morrison, I.E.G., Prior, B.A., McGenity, T.J., Rangel, D.E.N., *et al.* (2015). Concomitant osmotic and chaotropicity-induced stresses in *Aspergillus wentii*: compatible solutes determine the biotic window. *Curr. Genet.* *61*, 457–477.
- Lubbers, R.J.M., Dilokpimol, A., Navarro, J., Peng, M., Wang, M., Lipzen, A., Ng, V., Grigoriev, I.V., Visser, J., Hildén, K.S., *et al.* (2019). Cinnamic acid and sorbic acid conversion are mediated by the same transcriptional regulator in *Aspergillus niger*. *Front. Bioeng. Biotechnol.* *7*, 249.
- Lücking, R., Aime, M.C., Robbertse, B., Miller, A.N., Ariyawansa, H.A., Aoki, T., Cardinali, G., Crous, P.W., Druzhinina, I.S., Geiser, D.M., *et al.* (2020). Unambiguous identification of fungi: where do we stand and how accurate and precise is fungal DNA barcoding? *IMA Fungus* *11*, 14.
- Ma, L.-J., van der Does, H.C., Borkovich, K.A., Coleman, J.J., Daboussi, M.-J., Di Pietro, A., Dufresne, M., Freitag, M., Grabherr, M., Henrissat, B., *et al.* (2010). Comparative genomics reveals mobile pathogenicity chromosomes in *Fusarium*. *Nature* *464*, 367–373.
- Marçais, G., Delcher, A.L., Phillippy, A.M., Coston, R., Salzberg, S.L., and Zimin, A. (2018). MUMmer4: A fast and versatile genome alignment system. *PLOS Comput. Biol.* *14*, e1005944.
- Mattoon, E.R., Casadevall, A., and Cordero, R.J.B. (2021). Beat the heat: correlates, compounds, and mechanisms involved in fungal thermotolerance. *Fungal Biol. Rev.* *36*, 60–75.
- Mensink, M.A., Frijlink, H.W., van der Voort Maarschalk, K., and Hinrichs, W.L.J. (2017). How sugars protect proteins in the solid state and during drying (review): Mechanisms of stabilization in relation to stress conditions. *Eur. J. Pharm. Biopharm.* *114*, 288–295.
- Metselaar, K.I., den Besten, H.M.W., Abee, T., Moezelaar, R., and Zwietering, M.H. (2013). Isolation and quantification of highly acid resistant variants of *Listeria monocytogenes*. *Int. J. Food Microbiol.* *166*, 508–514.
- Milani, E.A., Gardner, R.C., and Silva, F.V.M. (2015). Thermal resistance of *Saccharomyces* yeast ascospores in beers. *Int. J. Food Microbiol.* *206*, 75–80.
- National Research Council (US) Subcommittee on Microbiological Criteria (1985). An evaluation of the role of microbiological criteria for foods and food ingredients (Washington (DC): The National Academies Press (US)).

- Nguyen Van Long, N., Vasseur, V., Coroller, L., Dantigny, P., Le Panse, S., Weill, A., Mounier, J., and Rigalma, K. (2017a). Temperature, water activity and pH during conidia production affect the physiological state and germination time of *Penicillium* species. *Int. J. Food Microbiol.* *241*, 151–160.
- Nguyen Van Long, N., Rigalma, K., Coroller, L., Dadure, R., Debaets, S., Mounier, J., and Vasseur, V. (2017b). Modelling the effect of water activity reduction by sodium chloride or glycerol on conidial germination and radial growth of filamentous fungi encountered in dairy foods. *Food Microbiol.* *68*, 7–15.
- Nguyen Van Long, N., Rigalma, K., Jany, J.-L., Mounier, J., and Vasseur, V. (2021). Intraspecific variability in cardinal growth temperatures and water activities within a large diversity of *Penicillium roqueforti* strains. *Food Res. Int.* *148*, 110610.
- Nødvig, C.S., Nielsen, J.B., Kogle, M.E., and Mortensen, U.H. (2015). A CRISPR-Cas9 system for genetic engineering of filamentous fungi. *PLoS One* *10*, e0133085.
- Novodvorska, M., Hayer, K., Pullan, S.T., Wilson, R., Blythe, M.J., Stam, H., Stratford, M., and Archer, D.B. (2013). Transcriptional landscape of *Aspergillus niger* at breaking of conidial dormancy revealed by RNA-sequencing. *BMC Genomics* *14*, 246.
- Novodvorska, M., Stratford, M., Blythe, M.J., Wilson, R., Beniston, R.G., and Archer, D.B. (2016). Metabolic activity in dormant conidia of *Aspergillus niger* and developmental changes during conidial outgrowth. *Fungal Genet. Biol.* *94*, 23–31.
- O’Gorman, C.M., Fuller, H.T., and Dyer, P.S. (2009). Discovery of a sexual cycle in the opportunistic fungal pathogen *Aspergillus fumigatus*. *Nature* *457*, 471–474.
- Oka, T., Ekino, K., Fukuda, K., and Nomura, Y. (2014). Draft genome sequence of the formaldehyde-resistant fungus *Byssoschlamys spectabilis* No. 5 (Anamorph *Paecilomyces variotii* No. 5) (NBRC109023). *Genome Announc.* *2*, e01162-13.
- Papke, R.T., and Ward, D.M. (2004). The importance of physical isolation to microbial diversification. *FEMS Microbiol. Ecol.* *48*, 293–303.
- Park, J.H., Noh, T.H., Wang, H., Kim, N.D., and Jung, J.H. (2015). Viriditoxin induces G2/M cell cycle arrest and apoptosis in A549 human lung cancer cells. *Nat. Prod. Sci.* *21*, 282–288.
- Pavic, K., Duan, G., and Köhn, M. (2015). VHR/DUSP3 phosphatase: structure, function and regulation. *FEBS J.* *282*, 1871–1890.
- Pel, H.J., de Winde, J.H., Archer, D.B., Dyer, P.S., Hofmann, G., Schaap, P.J., Turner, G., de Vries, R.P., Albang, R., Albermann, K., *et al.* (2007). Genome sequencing and analysis of the versatile cell factory *Aspergillus niger* CBS 513.88. *Nat. Biotechnol.* *25*, 221–231.
- Pitt, J.I., and Christian, J.H.B. (1970). Heat resistance of xerophilic fungi based on microscopical assessment of spore survival. *Appl. Microbiol.* *20*, 682–686.
- Pitt, J.I., and Hocking, A.D. (2009). *Fungi and food spoilage* (New York: Springer).
- Plumridge, A., Hesse, S.J.A., Watson, A.J., Lowe, K.C., Stratford, M., and Archer, D.B. (2004). The weak acid preservative sorbic acid inhibits conidial germination and mycelial growth of *Aspergillus niger* through intracellular acidification. *Appl. Environ. Microbiol.* *70*, 3506–3511.
- Plumridge, A., Melin, P., Stratford, M., Novodvorska, M., Shunburne, L., Dyer, P.S., Roubos, J.A., Menke, H., Stark, J., Stam, H., *et al.* (2010). The decarboxylation of the weak-acid preservative, sorbic acid, is encoded by linked genes in *Aspergillus* spp. *Fungal Genet. Biol.* *47*, 683–692.
- Punt, M., van den Brule, T., Teertstra, W.R., Dijksterhuis, J., den Besten, H.M.W., Ohm, R.A., and Wösten, H.A.B. (2020). Impact of maturation and growth temperature on cell-size distribution, heat-resistance, compatible solute composition and transcription profiles of *Penicillium roqueforti* conidia. *Food Res. Int.* *136*, 109287.
- Punt, M., Teertstra, W.R., and Wösten, H.A.B. (2022a). *Penicillium roqueforti* conidia induced by L-amino acids can germinate without detectable swelling. *Antonie van Leeuwenhoek* *115*, 103–110.
- Punt, M., Seekles, S.J., van Dam, J.L., de Adelhart Toorop, C., Martina, R.R., Houbraken, J., Ram,

- A.F.J., Wösten, H.A.B., and Ohm, R.A. (2022b). High sorbic acid resistance of *Penicillium roqueforti* is mediated by the SORBUS gene cluster. *BioRxiv* 2022.02.10.479849.
- Purcell, S., Neale, B., Todd-Brown, K., Thomas, L., Ferreira, M.A.R., Bender, D., Maller, J., Sklar, P., de Bakker, P.I.W., Daly, M.J., *et al.* (2007). PLINK: A tool set for whole-genome association and population-based linkage analyses. *Am. J. Hum. Genet.* *81*, 559–575.
- Put, H.M.C., and Jong, J. De (1982). The heat resistance of ascospores of four *Saccharomyces* spp. isolated from spoiled heat-processed soft drinks and fruit products. *J. Appl. Bacteriol.* *52*, 235–243.
- Rangel, D.E.N., Braga, G.U.L., Fernandes, É.K.K., Keyser, C.A., Hallsworth, J.E., and Roberts, D.W. (2015). Stress tolerance and virulence of insect-pathogenic fungi are determined by environmental conditions during conidial formation. *Curr. Genet.* *61*, 383–404.
- Rege, A., and Pai, J.S. (1999). Development of thermal process for clarified pomegranate (*Punica granatum*) juice. *J. Food Sci. Technol.* *36*, 261–263.
- Reponen, T., Grinshpun, S.A., Conwell, K.L., Wiest, J., and Anderson, M. (2001). Aerodynamic versus physical size of spores: Measurement and implication for respiratory deposition. *Grana* *40*, 119–125.
- Reveron, I.M., Barreiro, J.A., and Sandoval, A.J. (2005). Thermal death characteristics of *Lactobacillus paracasei* and *Aspergillus niger* in Pilsen beer. *J. Food Eng.* *66*, 239–243.
- Richter, K., Haslbeck, M., and Buchner, J. (2010). The heat shock response: life on the verge of death. *Mol. Cell* *40*, 253–266.
- Rodríguez-Calleja, J.M., Cebrián, G., Condón, S., and Mañas, P. (2006). Variation in resistance of natural isolates of *Staphylococcus aureus* to heat, pulsed electric field and ultrasound under pressure. *J. Appl. Microbiol.* *100*, 1054–1062.
- Rogers, J. V., and Rose, M.D. (2015). Kar5p is required for multiple functions in both inner and outer nuclear envelope fusion in *Saccharomyces cerevisiae*. *G3-Genes Genom. Genet.* *5*, 111–121.
- Ropars, J., Cruaud, C., Lacoste, S., and Dupont, J. (2012). A taxonomic and ecological overview of cheese fungi. *Int. J. Food Microbiol.* *155*, 199–210.
- Ropars, J., López-Villavicencio, M., Dupont, J., Snirc, A., Gillot, G., Coton, M., Jany, J.-L., Coton, E., and Giraud, T. (2014). Induction of sexual reproduction and genetic diversity in the cheese fungus *Penicillium roqueforti*. *Evol. Appl.* *7*, 433–441.
- Ruijter, G.J., Bax, M., Patel, H., Flitter, S.J., van de Vondervoort, P.J., de Vries, R.P., vanKuyk, P.A., and Visser, J. (2003). Mannitol is required for stress tolerance in *Aspergillus niger* conidiospores. *Eukaryot. Cell* *2*, 690–698.
- Ruijter, G.J.G., Visser, J., and Rinzema, A. (2004). Polyol accumulation by *Aspergillus oryzae* at low water activity in solid-state fermentation. *Microbiology* *150*, 1095–1101.
- Sakamoto, K., Arima, T., Iwashita, K., Yamada, O., Gomi, K., and Akita, O. (2008). *Aspergillus oryzae atfB* encodes a transcription factor required for stress tolerance in conidia. *Fungal Genet. Biol.* *45*, 922–932.
- Sakamoto, K., Iwashita, K., Yamada, O., Kobayashi, K., Mizuno, A., Akita, O., Mikami, S., Shimoj, H., and Gomi, K. (2009). *Aspergillus oryzae atfA* controls conidial germination and stress tolerance. *Fungal Genet. Biol.* *46*, 887–897.
- Samson, R.A., Houbraeken, J., Varga, J., and Frisvad, J.C. (2009). Polyphasic taxonomy of the heat resistant ascomycete genus *Byssoschlamys* and its *Paecilomyces* anamorphs. *Persoonia* *22*, 14–27.
- Samson, R.A., Houbraeken, J., Thrane, U., Frisvad, J.C., and Andersen, B. (2019). Food and indoor fungi. *Westerdijk Laboratory Manual Series No. 2* (Utrecht: Westerdijk Fungal Biodiversity Institute).
- dos Santos, J.L.P., Samapundo, S., Biyikli, A., Van Impe, J., Akkermans, S., Höfte, M., Abatih, E.N., Sant’Ana, A.S., and Devlieghere, F. (2018). Occurrence, distribution and contamination levels of heat-resistant moulds throughout the processing of pasteurized high-acid fruit products. *Int. J.*

- Food Microbiol. *281*, 72–81.
- Scaramuzza, N., and Berni, E. (2014). Heat-resistance of *Hamigera avellanea* and *Thermoascus crustaceus* isolated from pasteurized acid products. *Int. J. Food Microbiol.* *168–169*, 63–68.
- Schmidt, H., Vlais, S., Krüger, T., Schmidt, F., Balkenhol, J., Dandekar, T., Guthke, R., Kniemeyer, O., Heinekamp, T., and Brakhage, A.A. (2018). Proteomics of *Aspergillus fumigatus* conidia-containing phagolysosomes identifies processes governing immune evasion. *Mol. Cell. Proteomics* *17*, 1084–1096.
- Schuster, E., Dunn-Coleman, N., Frisvad, J., and van Dijck, P. (2002). On the safety of *Aspergillus niger* – a review. *Appl. Microbiol. Biotechnol.* *59*, 426–435.
- Seekles, S.J., Punt, M., Brule, T. van den, Ijadpanahsaravi, M., Meuken, G., Ongenae, V., Arentshorst, M., Dijksterhuis, J., de Winde, J.H., Wösten, H.A.B., *et al.* (2021a). Dissecting the pivotal role of mannitol and trehalose as compatible solutes in heat resistance of conidia, germination, and population heterogeneity in the filamentous fungus *Aspergillus niger*. In *Genetic and Environmental Factors Determining Heterogeneity in Preservation Stress Resistance of Aspergillus niger Conidia*, S.J. Seekles, ed. pp. 205–256.
- Seekles, S.J., Teunisse, P.P.P., Punt, M., van den Brule, T., Dijksterhuis, J., Houbraken, J., Wösten, H.A.B., and Ram, A.F.J. (2021b). Preservation stress resistance of melanin deficient conidia from *Paecilomyces variotii* and *Penicillium roqueforti* mutants generated via CRISPR/Cas9 genome editing. *Fungal Biol. Biotechnol.* *8*, 4.
- Segers, F.J.J., van Laarhoven, K.A., Huinink, H.P., Adan, O.C.G., Wösten, H.A.B., and Dijksterhuis, J. (2016). The indoor fungus *Cladosporium halotolerans* Survives humidity dynamics markedly better than *Aspergillus niger* and *Penicillium rubens* despite less growth at lowered steady-state water activity. *Appl. Env. Microbiol.* *82*, 5089.
- Shahi, S., Beerens, B., Bosch, M., Linmans, J., and Rep, M. (2016). Nuclear dynamics and genetic rearrangement in heterokaryotic colonies of *Fusarium oxysporum*. *Fungal Genet. Biol.* *91*, 20–31.
- Shearer, A.E.H., Mazzotta, A.S., Chuyate, R., and Gombas, D.E. (2002). Heat resistance of juice spoilage microorganisms. *J. Food Prot.* *65*, 1271–1275.
- Shinn, E.A., Smith, G.W., Prospero, J.M., Betzer, P., Hayes, M.L., Garrison, V., and Barber, R.T. (2000). African dust and the demise of Caribbean coral reefs. *Geophys. Res. Lett.* *27*, 3029–3032.
- Snyder, A.B., and Worobo, R.W. (2018). Fungal spoilage in food processing. *J. Food Prot.* *81*, 1035–1040.
- Snyder, A.B., Churey, J.J., and Worobo, R.W. (2019). Association of fungal genera from spoiled processed foods with physicochemical food properties and processing conditions. *Food Microbiol.* *83*, 211–218.
- Song, L., Ouedraogo, J.-P., Kolbusz, M., Nguyen, T.T.M., and Tsang, A. (2018). Efficient genome editing using tRNA promoter-driven CRISPR/Cas9 gRNA in *Aspergillus niger*. *PLoS One* *13*, e0202868.
- Springer, M.L., Hager, K.M., Garrett-Engle, C., and Yanofsky, C. (1992). Timing of synthesis and cellular localization of two conidiation-specific proteins of *Neurospora crassa*. *Dev. Biol.* *152*, 255–262.
- Stanke, M., Keller, O., Gunduz, I., Hayes, A., Waack, S., and Morgenstern, B. (2006). AUGUSTUS: ab initio prediction of alternative transcripts. *Nucleic Acids Res.* *34*, W435–W439.
- Staugaard, P., Samson, R.A., and Van der Horst, M.I. (1990). Variation in *Penicillium* and *Aspergillus* conidia in relation to preparatory techniques for scanning electron and light microscopy. In *Modern Concepts in Penicillium and Aspergillus Classification*, R.A. Samson, and J.I. Pitt, eds. (Boston, MA: Springer), pp. 39–48.
- Stevenson, A., Hamill, P.G., Medina, Á., Kminek, G., Rummel, J.D., Dijksterhuis, J., Timson, D.J., Magan, N., Leong, S.-L.L., and Hallsworth, J.E. (2017). Glycerol enhances fungal germination at the water-activity limit for life. *Env. Microbiol.* *19*, 947–967.

- Stolk, A.C., and Samson, R.A. (1971). Studies on *Talaromyces* and related genera I. *Hamigera* gen. nov. and *Byssochlamys*. Persoonia - Mol. Phylogeny Evol. Fungi 6, 341–357.
- Stratford, M., Plumridge, A., Nebe-von-Caron, G., and Archer, D.B. (2009). Inhibition of spoilage mould conidia by acetic acid and sorbic acid involves different modes of action, requiring modification of the classical weak-acid theory. Int. J. Food Microbiol. 136, 37–43.
- Stratford, M., Nebe-von-Caron, G., Steels, H., Novodvorska, M., Ueckert, J., and Archer, D.B. (2013a). Weak-acid preservatives: pH and proton movements in the yeast *Saccharomyces cerevisiae*. Int. J. Food Microbiol. 161, 164–171.
- Stratford, M., Steels, H., Nebe-von-Caron, G., Novodvorska, M., Hayer, K., and Archer, D.B. (2013b). Extreme resistance to weak-acid preservatives in the spoilage yeast *Zygosaccharomyces bailii*. Int. J. Food Microbiol. 166, 126–134.
- Suiker, I.M., Arkesteijn, G.J.A., Zeegers, P.J., and Wösten, H.A.B. (2021). Presence of *Saccharomyces cerevisiae* subsp. *diastaticus* in industry and nature and spoilage capacity of its vegetative cells and ascospores. Int. J. Food Microbiol. 347, 109173.
- Suzuki, S., Sarikaya Bayram, O., Bayram, O., and Braus, G.H. (2013). conF and conJ contribute to conidia germination and stress response in the filamentous fungus *Aspergillus nidulans*. Fungal Genet. Biol. 56, 42–53.
- Teertstra, W.R., Tegelaar, M., Dijksterhuis, J., Golovina, E.A., Ohm, R.A., and Wösten, H.A.B. (2017). Maturation of conidia on conidiophores of *Aspergillus niger*. Fungal Genet. Biol. 98, 61–70.
- Tegelaar, M., Bleichrodt, R.-J., Nitsche, B., Ram, A.F.J., and Wösten, H.A.B. (2020). Subpopulations of hyphae secrete proteins or resist heat stress in *Aspergillus oryzae* colonies. Environ. Microbiol. 22, 447–455.
- Tereshina, V.M. (2005). Thermotolerance in fungi: The role of heat shock proteins and trehalose. Microbiology 74, 247–257.
- Trapnell, C., Hendrickson, D.G., Sauvageau, M., Goff, L., Rinn, J.L., and Pachter, L. (2013). Differential analysis of gene regulation at transcript resolution with RNA-seq. Nat. Biotechnol. 31, 46–53.
- Tzur, A., Moore, J.K., Jorgensen, P., Shapiro, H.M., and Kirschner, M.W. (2011). Optimizing optical flow cytometry for cell volume-based sorting and analysis. PLoS One 6, e16053.
- Udagawa, S., and Suzuki, S. (1994). *Talaromyces spectabilis*, a new species of food-borne ascomycetes. Mycotaxon 50, 81–88.
- Ulevičius, V., Pečiulytė, D., Lugauskas, A., and Andriejauskienė, J. (2004). Field study on changes in viability of airborne fungal propagules exposed to UV radiation. Environ. Toxicol. 19, 437–441.
- Urquhart, A.S., Mondo, S.J., Mäkelä, M.R., Hane, J.K., Wiebenga, A., He, G., Mihaltcheva, S., Pangilinan, J., Lipzen, A., Barry, K., et al. (2018). Genomic and genetic insights into a cosmopolitan fungus, *Paecilomyces variotii* (Eurotiales). Front. Microbiol. 9.
- Urquhart, A.S., Hu, J., Chooi, Y.H., and Idnurm, A. (2019). The fungal gene cluster for biosynthesis of the antibacterial agent viriditoxin. Fungal Biol. Biotechnol. 6, 2.
- Urquhart, A.S., Chong, N.F., Yang, Y., and Idnurm, A. (2022). A large transposable element mediates metal resistance in the fungus *Paecilomyces variotii*. Curr. Biol. 32, 937–950.e5.
- Valero-Jiménez, C.A., Debets, A.J.M., van Kan, J.A.L., Schoustra, S.E., Takken, W., Zwaan, B.J., and Koenraadt, C.J.M. (2014). Natural variation in virulence of the entomopathogenic fungus *Beauveria bassiana* against malaria mosquitoes. Malar. J. 13, 479.
- Varga, J., Frisvad, J.C., Kocsubé, S., Brankovics, B., Tóth, B., Sziget, G., and Samson, R.A. (2011). New and revisited species in *Aspergillus* section Nigri. Stud. Mycol. 69, 1–17.
- van Veluw, G.J., Teertstra, W.R., de Bekker, C., Vinck, A., van Beek, N., Muller, W.H., Arentshorst, M., van der Mei, H.C., Ram, A.F.J., Dijksterhuis, J., et al. (2013). Heterogeneity in liquid shaken cultures of *Aspergillus niger* inoculated with melanised conidia or conidia of pigmentation mutants. Stud. Mycol. 74, 47–57.
- Veri, A.O., Robbins, N., and Cowen, L.E. (2018). Regulation of the heat shock transcription factor

- Hsf1 in fungi: implications for temperature-dependent virulence traits. *FEMS Yeast Res.* *18*, foy041.
- De Virgilio, C., Hottiger, T., Dominguez, J., Boller, T., and Wiemken, A. (1994). The role of trehalose synthesis for the acquisition of thermotolerance in yeast. *Eur. J. Biochem.* *219*, 179–186.
- Visagie, C.M., Houbraeken, J., Frisvad, J.C., Hong, S.B., Klaassen, C.H.W., Perrone, G., Seifert, K.A., Varga, J., Yaguchi, T., and Samson, R.A. (2014). Identification and nomenclature of the genus *Penicillium*. *Stud. Mycol.* *78*, 343–371.
- de Vries, R.P., Burgers, K., van de Vondervoort, P.J.I., Frisvad, J.C., Samson, R.A., and Visser, J. (2004). A new black *Aspergillus* species, *A. vadensis*, is a promising host for homologous and heterologous protein production. *Appl. Env. Microbiol* *70*, 3954–3959.
- De Vries, R.P., Flitter, S.J., Van De Vondervoort, P.J.I., Chaverroche, M.-K., Fontaine, T., Fillinger, S., Ruijter, G.J.G., D'Enfert, C., and Visser, J. (2003). Glycerol dehydrogenase, encoded by *gldB* is essential for osmotolerance in *Aspergillus nidulans*. *Mol. Microbiol.* *49*, 131–141.
- Wang, F., Sethiya, P., Hu, X., Guo, S., Chen, Y., Li, A., Tan, K., and Wong, K.H. (2021). Transcription in fungal conidia before dormancy produces phenotypically variable conidia that maximize survival in different environments. *Nat. Microbiol.* *6*, 1066–1081.
- Wang, J., Galgoci, A., Kodali, S., Herath, K.B., Jayasuriya, H., Dorso, K., Vicente, F., González, A., Cully, D., Bramhill, D., *et al.* (2003). Discovery of a small molecule that inhibits cell division by blocking FtsZ, a novel therapeutic target of antibiotics. *J. Biol. Chem.* *278*, 44424–44428.
- Washabaugh, M.W., and Collins, K.D. (1986). The systematic characterization by aqueous column chromatography of solutes which affect protein stability. *J. Biol. Chem.* *261*, 12477–12485.
- Welker, S., Rudolph, B., Frenzel, E., Hagn, F., Liebisch, G., Schmitz, G., Scheuring, J., Kerth, A., Blume, A., Weinkauff, S., *et al.* (2010). Hsp12 is an intrinsically unstructured stress protein that folds upon membrane association and modulates membrane function. *Mol. Cell* *39*, 507–520.
- Wells-Bennik, M.H.J., Janssen, P.W.M., Klaus, V., Yang, C., Zwietering, M.H., and Den Besten, H.M.W. (2019). Heat resistance of spores of 18 strains of *Geobacillus stearothermophilus* and impact of culturing conditions. *Int. J. Food Microbiol.* *291*, 161–172.
- Westling (1909). *Byssosclamyces nivea*, en föreningslänk mellan familjerna Gymnoascaceae och Endomycetaceae. *Sven. Bot. Tidskr.* *3*, 125–137.
- White, B.T., and Yanofsky, C. (1993). Structural characterization and expression analysis of the *Neurospora* conidiation gene *con-6*. *Dev. Biol.* *160*, 254–264.
- Whiting, R.C., and Golden, M.H. (2002). Variation among *Escherichia coli* O157:H7 strains relative to their growth, survival, thermal inactivation, and toxin production in broth. *Int. J. Food Microbiol.* *75*, 127–133.
- Wösten, H.A.B., van Veluw, G.J., de Bekker, C., and Krijghsheld, P. (2013). Heterogeneity in the mycelium: implications for the use of fungi as cell factories. *Biotechnol. Lett.* *35*, 1155–1164.
- Wu, B., Hussain, M., Zhang, W., Stadler, M., Liu, X., and Xiang, M. (2019). Current insights into fungal species diversity and perspective on naming the environmental DNA sequences of fungi. *Mycology* *10*, 127–140.
- Wu, D., Dou, X., Hashmi, S.B., and Osmani, S.A. (2004). The Pho80-like cyclin of *Aspergillus nidulans* regulates development independently of its role in phosphate acquisition. *J. Biol. Chem.* *279*, 37693–37703.
- Wyatt, T.T., Wosten, H.A.B., and Dijksterhuis, J. (2013). Fungal spores for dispersion in space and time. In *Advances in Applied Microbiology*, pp. 43–91.
- Wyatt, T.T., Golovina, E.A., van Leeuwen, R., Hallsworth, J.E., Wosten, H.A., and Dijksterhuis, J. (2015a). A decrease in bulk water and mannitol and accumulation of trehalose and trehalose-based oligosaccharides define a two-stage maturation process towards extreme stress resistance in ascospores of *Neosartorya fischeri* (*Aspergillus fischeri*). *Env. Microbiol.* *17*, 383–394.
- Wyatt, T.T., van Leeuwen, M.R., Golovina, E.A., Hoekstra, F.A., Kuenstner, E.J., Palumbo, E.A.,

- Snyder, N.L., Visagie, C., Verkennis, A., Hallsworth, J.E., *et al.* (2015b). Functionality and prevalence of trehalose-based oligosaccharides as novel compatible solutes in ascospores of *Neosartorya fischeri* (*Aspergillus fischeri*) and other fungi. *Env. Microbiol.* *17*, 395–411.
- Yilmaz, N., Visagie, C.M., Houbraeken, J., Frisvad, J.C., and Samson, R.A. (2014). Polyphasic taxonomy of the genus *Talaromyces*. *Stud. Mycol.* *78*, 175–341.
- Zheng, J., Wittouck, S., Salvetti, E., Franz, C.M.A.P., Harris, H.M.B., Mattarelli, P., O'Toole, P.W., Pot, B., Vandamme, P., Walter, J., *et al.* (2020). A taxonomic note on the genus *Lactobacillus*: Description of 23 novel genera, emended description of the genus *Lactobacillus* Beijerinck 1901, and union of Lactobacillaceae and Leuconostocaceae. *Int. J. Syst. Evol.* *70*, 2782–2858.
- Zwietering, M.H., Garre, A., and den Besten, H.M.W. (2021). Incorporating strain variability in the design of heat treatments: A stochastic approach and a kinetic approach. *Food Res. Int.* *139*, 109973.

NEDERLANDSE SAMENVATTING

Van de wereldwijde voedselproductie gaat naar schatting een kwart verloren door microbiel bederf. Het tegengaan van dit bederf draagt bij aan de uitdaging om een groeiende wereldpopulatie te kunnen blijven voeden. In de voedselindustrie ontwikkelt men producten die microbiologisch stabiel zijn om te voorkomen dat er bederforganismen, waaronder pathogenen, in kunnen groeien, voor het einde van de houdbaarheidsdatum. Echter, incidenten komen voor die kunnen leiden tot terugvorderingen, meer voedselafval en economische verliezen.

Om deze verliezen te beperken worden industrieel bewerkte producten ontworpen met zogenaemde hordes. Volgens dit concept maakt men gebruik van een mix van productieprocessen, producteigenschappen en ingrediënten om micro-organismen te remmen in hun groei of zelfs te doden. Voorbeelden hiervan zijn pasteurisatie, een lage pH, een lage wateractiviteit en het toevoegen van conserveermiddelen, zoals zout en / of zwakke zuren. Consumenten wensen dat producten steeds minder bewerkt worden en dat er geen of minder conserveermiddelen worden gebruikt. Deze ontwikkelingen zullen zorgen voor een beperktere houdbaarheid van producten, omdat ze groei van micro-organismen minder goed zullen tegenhouden. Om de groei van micro-organismen te kunnen inschatten gebruikt men in de industrie microbiologische risicoanalyses. Om deze zo realistisch mogelijk te maken, moet de mate van onzekerheid en variabiliteit zo nauwkeurig mogelijk in kaart worden gebracht.

De algemeen voorkomende schimmel *Paecilomyces variotii* staat bekend als veroorzaker van bederf in hittebehandelde producten, zoals ingeblikt fruit en frisdranken zonder koolzuur. Dit komt doordat deze schimmel seksuele sporen maakt die extreem hitteresistent zijn. Echter, deze ascosporen worden gevormd in het mycelium en worden niet zo gemakkelijk verspreid als conidia, de asexuele sporen. Conidia worden onder gunstige condities in grote aantallen geproduceerd in lange ketens en worden ondermeer verspreid door de lucht en via water. Doordat ze in overvloed aanwezig kunnen zijn in het milieu, kunnen ze bederf veroorzaken in milder bewerkt voedsel of door contaminatie na het bewerkingsproces. Bederf van margarine, roggebrood en andere producten die conserveermiddelen bevatten worden regelmatig in verband gebracht met contaminatie door *P. variotii* conidia. Op dezelfde manier zijn conidia van *Aspergillus niger* verantwoordelijk voor rot in groenten en fruit en conidia van *Penicillium roqueforti* voor bederf van zuivel- en bakkersproducten.

De mogelijkheid van deze schimmels om te groeien in dit soort producten wordt bepaald door het vermogen om de barrières die door de hordentechnologie in deze producten aanwezig zijn te overwinnen. Hitteresistentie van schimmelsporen wordt geassocieerd met de accumulatie van componenten met een beschermende werking in het cytosol, zoals hiteschok eiwitten, trehalose en mannitol, terwijl resistentie tegen osmotische stress in verband wordt gebracht met accumulatie van kleinere moleculen zoals glycerol en erythritol. Aan de nadere kant wordt resistentie tegen ultraviolette straling geassocieerd

met melanine in de celwand en resistentie tegen zwakke zuren door aanwezigheid van enzymen die deze stoffen kunnen omzetten.

Heterogeniteit binnen de soort is te vinden tussen en binnen stammen van filamenteuze schimmels. Genetische verschillen leiden tot fenotypische verschillen tussen stammen, terwijl stochasticiteit en epigenetische aanpassingen belangrijke mechanismen zijn om heterogeniteit aan te brengen in een populatie die genetisch identiek is (**Hoofdstuk 1**). Ook omgevingsfactoren en het rijpingsproces van sporen kunnen een belangrijke invloed hebben op de resistentie en ontkieming van schimmelsporen (**Hoofdstuk 1**). Om nauwkeurig de houdbaarheid van producten te voorspellen, moet men heterogeniteit van de stressresistentie in kaart brengen. Echter, voor filamenteuze schimmels is dit tot op heden nauwelijks bestudeerd.

In dit proefschrift is de variabiliteit tussen en binnen stammen van *P. variotii*, *A. niger*, en *P. roqueforti* bestudeerd, met een focus op de eerstgenoemde schimmel. Omdat conidia in grote getale voorkomen en makkelijk door de lucht verspreid worden, is het aannemelijk dat zij meer voedselbederf veroorzaken dan ascosporen. Om deze reden ligt de focus van dit proefschrift op de conidia. In totaal zijn 108 *P. variotii* stammen, 21 *A. niger* stammen en 20 *P. roqueforti* stammen gebruikt in deze studie. De identiteit van deze stammen werd bevestigd volgens de taxonomische standaarden, om te verzekeren dat de variabiliteit beschreven in dit proefschrift echt intraspecifiek is.

Alle 108 *P. variotii* stammen zijn getest op hitteresistentie in **Hoofdstuk 2**. Deze resultaten gaven een goede inschatting welke stammen hitteresistent of hittegevoelig zijn. In **Hoofdstuk 2-4** is de hitteresistentie van in totaal 25 stammen gekwantificeerd door het bepalen van *D*-waarden. Hieruit bleek dat stam DTO 195-F2 het meest hitteresistent is met een D_{60} -waarde van 27.6 ± 3.1 minuten (dit wil zeggen dat 27.6 minuten nodig was om 90% van de sporen te doden bij 60 °C), terwijl de meest gevoelige stam DTO 212-C5 een D_{60} -waarde had van 3.5 ± 0.3 minuten. Het verschil in *D*-waarden tussen deze twee stammen, geeft aan dat bij een hitte behandeling van ongeveer 28 minuten bij 60 °C er van de hittegevoelige stam 10 miljoen keer meer cellen worden geïnactiveerd. Deze variabiliteit kan dus grote invloed hebben op het bederf van voedsel en daarom is het van belang dat dit meegenomen wordt in microbiologische modellen. Tot op heden is DTO 195-F2 de stam met de meest hitteresistente conidia ooit gemeten. Daarbij komt dat zelfs de meest hittegevoelige *P. variotii* stam resistentier is dan de conidia van *A. niger* en *P. roqueforti*, waarvan de *D*-waarden zijn bepaald bij 54 en 56 °C, respectievelijk (**Hoofdstuk 4**).

Omgevingsfactoren kunnen een significant effect op hitteresistentie hebben. Conidia van *P. variotii* die opgegroeid waren bij 37 °C hadden een 2.3 tot 3.9 keer hogere D_{62} -waarde in vergelijking met conidia opgegroeid bij 25 °C (**Hoofdstuk 5**). De hitteresistentie van conidia die gekweekt waren bij 45 °C bleek niet verder toegenomen te zijn ten opzichte van de sporen die bij 37 °C waren gevormd. Deze resultaten suggereren sterk dat conidia die bijvoorbeeld in (sub)tropische zones worden gevormd mogelijk hitteresistentier zijn dan in gematigde klimaatszones. Het kan dus ook van groot belang zijn om geografische locaties mee te nemen in voorspellende modellen. Tenslotte kunnen

naast omgevingsfactoren ook de rijping van de sporen en de intrinsieke eigenschappen van het menstroom (het medium, de buffer of het voedsel waarin de sporen geïnactiveerd worden) invloed hebben op de hitteresistentie van schimmelsporen (**Hoofdstuk 6**).

Naast de bovengenoemde factoren die invloed hebben op hitteresistentie, zijn micro-organismen inherent variabel. Deze variabiliteit zorgt ervoor dat hitteresistentie tussen stammen en binnen stammen kan verschillen. Deze variabiliteit is gekwantificeerd op drie verschillende niveaus voor *A. niger*, *P. roqueforti* en *P. variotii* (**Hoofdstuk 4**). De experimentele variabiliteit is bepaald tussen replica's waar dezelfde sporensuspensie voor is gebruikt, de biologische variabiliteit met replica's van dezelfde stam die opgekweekt zijn op verschillende momenten en de stamvariabiliteit is bepaald door het gebruik van meerdere stammen van dezelfde soort. Voor elke soort was de experimentele variabiliteit het laagst en de stamvariabiliteit het hoogst. Echter, tussen de drie schimmelsoorten zijn er geen verschillen gevonden in de spreiding van hitteresistentie tussen de stammen. Deze resultaten waren vergelijkbaar en in dezelfde orde van grootte als de variabiliteit van verschillende bacteriesporen en -cellen. Mogelijk kan dus dezelfde aanpak uit het bacterieonderzoek gebruikt worden om de variabiliteit van schimmels in modellen te implementeren.

Omdat stressresistentie van schimmelsporen regelmatig in verband is gebracht met accumulatie van beschermende stoffen, is in **Hoofdstuk 2** en **5** de concentratie compatibele opgeloste stoffen (trehalose en polyolen) gemeten in conidia. Omdat in **Hoofdstuk 2** werd waargenomen dat sporengrootte en -distributie per stam significant kon verschillen, was het van belang dat de conidia nauwkeurig konden worden meten. Omdat de conidia van *P. variotii* ellipsoïde zijn, bracht dit extra uitdagingen met zich mee. In **Hoofdstuk 3** zijn er vier meetmethoden met elkaar vergeleken om de conidiagrootte te meten. De Coulter Counter was hierin nauwkeurig en het meest efficiënt. Doordat we de sporengrootte mee hebben genomen in de resultaten met de compatibele opgeloste stoffen, waren we in staat om voor het eerst concentraties te schatten binnen de spore, in plaats van een absolute gemiddelde hoeveelheid te bepalen per spore. Van de verschillende compatibele opgeloste stoffen bevatten *P. variotii* conidia overheersend trehalose, wat mogelijk de hoge hitteresistentie kan verklaren ten opzichte van andere soorten. De trehalose concentratie en sporengrootte correleerden beide significant met hitte resistentie (**Hoofdstuk 5**).

Naast hitte-inactivatie wordt er in de voedingsmiddelenindustrie algemeen gebruik gemaakt van zwakke organische zuren als conserveringsmiddel. Daarom zijn verschillende *P. variotii* stammen getest op resistentie tegen sorbine- en benzoëzuur in **Hoofdstuk 5**. Hoewel er geen significante correlatie was tussen resistentie tegen deze zuren en hitteresistentie, waren de twee meest resistente stammen tegen sorbinezuur, DTO 195-F2 en DTO 282-E5, ook hitteresistente stammen. Vergelijkbaar, de hitteresistente stammen DTO 195-F2 en DTO 282-F9 waren twee van de meest resistente stammen tegen benzoëzuur. Stammen DTO 195-F2, DTO 282-E5 en DTO 282-F9 kunnen derhalve beschouwd worden als meest problematisch in termen van voedselbederf.

De DNA volgorde van de genomen van alle *P. variotii* stammen die in **Hoofdstuk 3** en **4** zijn gekwantificeerd op hitteresistentie werd bepaald in **Hoofdstuk 5**, behalve van stam CBS 101075, waarvan het genoom al eerder gepubliceerd was. Een fylogenetische boom, gebaseerd op 6331 orthologe genen, liet twee clusters van stammen zien waarin de hitteresistente stammen waren gegroepeerd (**Hoofdstuk 5**). Dit laat zien dat de genetische verschillen die verantwoordelijk zijn voor het verschil in hitteresistentie mogelijk in twee afsplitsingen is ontstaan. Door fenotype aan genotype te koppelen, zijn 93 genen geïdentificeerd in **Hoofdstuk 5** die een mogelijke functie hebben met betrekking tot hitteresistentie. Daarnaast is er gekeken naar differentiële genexpressie in conidia die waren gekweekt bij verschillende temperaturen. Ook dit leverde kandidaatgenen op; de resultaten laten zien dat hydrophilines mogelijk een belangrijke rol spelen bij stressresistentie van conidia. Echter, de precieze rol van deze genen in hitteresistentie zal in de toekomst verder uitgezocht moeten worden.

Een DNA fragment van ongeveer 60 kilobasen, dat een aantal genen bevat, werd geïdentificeerd in 6 van de 8 hitteresistente stammen, maar was afwezig in alle gevoelige stammen (**Hoofdstuk 5**). Ondanks dat het cluster in de meeste hitteresistente stammen aanwezig was, zijn er geen aanwijzingen gevonden dat het cluster ook daadwerkelijk betrokken is bij hitteresistentie van conidia. Verwijdering van het gehele cluster in een hitteresistente leidde namelijk niet tot een gevoeliger fenotype. De oorsprong van het cluster wordt bediscussieerd in **Hoofdstuk 5**.

Vermindering van voedselverlies en -verspilling draagt bij aan de globale voedselzekerheid. Dit proefschrift draagt bij aan een beter begrip over de inter- en intraspecifieke heterogeniteit van *P. variotii* en algemener, de schimmels in de orde Eurotiales. Deze data kan gebruikt worden voor het verbeteren van voorspellende modellen in de voedingsindustrie die bederf door contaminatie met conidia beschrijven. Implementatie van variabiliteit in het modelleren van schimmelbederf kan leiden tot risico analyses met grotere precisie, wat leidt tot minder terugvorderingen, minder economische verliezen en het belangrijkste: minder voedselverlies.

CURRICULUM VITAE

Tom van den Brule was born the 28th of June 1987 in Breda, the Netherlands. In 2006, he graduated from his secondary education at the Onze Lieve Vrouweylyceum in Breda. After a one-year sabbatical in which he travelled through Ecuador, he started the Bsc Biology program at Utrecht University. During this period, he joined the student association (Utrechtse Biologen Vereniging) as a full-time board member and treasurer in the academic year 2009-2010. Because of his interest in marine biology, Tom joined the Wadden association (Waddenvereniging) as a voluntary tourist guide, for which he gave mudflat and fishing excursions to educate people about the most astonishing nature in the Netherlands: the Wadden sea. However, his passion for microbiology guided him to a short internship at the Molecular Microbiology group at Utrecht University, led by Prof. Han Wösten. After obtaining his BSc degree, he enrolled the master's program Environmental Biology at the same university. For his major research internship, he decided to continue at the same research group to study the ligninolytic activity in *Schizophyllum commune* under the supervision of Dr. Aurin Vos. He performed his minor research project in industry. He studied low oxygen adaptation of food spoilage moulds at Unilever R&D Vlaardingen under the supervision of Dr. Robèr Kemperman. After obtaining his MSc degree in 2015, he started a PhD project under the supervision of Prof. Han Wösten and Dr. Jan Dijksterhuis within the Food and Indoor Mycology research group at the Westerdijk Fungal Biodiversity Institute. This project was part of the TiFN project 'Heterogeneity in spores of food spoilage fungi' and was a collaboration between Utrecht University, Leiden University, Wageningen University, Westerdijk Fungal Biodiversity Institute, Unilever, PepsiCo, Heineken and DuPont. During this project, the heterogeneity in conidial resistance of food spoilage moulds was investigated. The results of this project are described in this thesis. Currently, Tom works as a microbiological modeller at Unilever R & D in Wageningen, the Netherlands.

LIST OF PUBLICATIONS

- van den Brule, T.**, Lee, C.L.S., Houbraken, J., Haas, P.-J., Wösten, H., and Dijksterhuis, J. (2020) Conidial heat resistance of various strains of the food spoilage fungus *Paecilomyces variotii* correlates with mean spore size, spore shape and size distribution. *Food Res Int* **137**: 109514.
- van den Brule, T.**, Punt, M., Teertstra, W., Houbraken, J., Wösten, H., and Dijksterhuis, J. (2020) The most heat-resistant conidia observed to date are formed by distinct strains of *Paecilomyces variotii*. *Environ Microbiol* **22**: 986–999.
- Punt, M., **van den Brule, T.**, Teertstra, W.R., Dijksterhuis, J., den Besten, H.M.W., Ohm, R.A., and Wösten, H.A.B. (2020) Impact of maturation and growth temperature on cell-size distribution, heat-resistance, compatible solute composition and transcription profiles of *Penicillium roqueforti* conidia. *Food Res Int* **136**: 109287.
- Seekles, Sjoerd J, Teunisse, P.P.P., Punt, M., **van den Brule, T.**, Dijksterhuis, J., Houbraken, J., Wösten, H.A.B, and Ram, A.F.J. (2021) Preservation stress resistance of melanin deficient conidia from *Paecilomyces variotii* and *Penicillium roqueforti* mutants generated via CRISPR/Cas9 genome editing. *Fungal Biol Biotechnol* **8**: 4.
- van den Brule, T.**, Punt, M., Seekles, S.J., Segers, F.J.J., Houbraken, J., Hazeleger, W.C., Ram, A.F.J., Wösten, H.A.B., Zwietering, M.H., Dijksterhuis, J., and den Besten, H.M.W. (2022). Intraspecific variability in heat resistance of fungal conidia. *Food Res Int* **156**: 111302.

ACKNOWLEDGEMENTS

This journey started six years ago. In this period, there were many moments of joy in which we could celebrate small and big breakthroughs. But like in every PhD project, there were tough moments when experiments failed or when experiencing a writer's block. I totally underestimated the time it would take to finalize this thesis while working on a full-time job and moving houses with two young children. It has not been the easiest route and I am proud that I pulled it off. Or better said: that WE pulled this off. I could not have done this without the help of many others. So here is a big THANK YOU to all of you.

Jan, I really enjoyed working with you. Your passion for the research you do motivated me a lot. I value your creative mind and knowledge. Sometimes it was a challenge to filter the best ideas from all the suggested experiments after a meeting. Luckily, this was beautifully complemented by Han's pragmatism. Han, I appreciate the time you take for all your students. This quality makes you a great professor. I am happy to have had you both as supervisors. I really enjoyed our meetings in which you first needed to catch up for 45 minutes and then discuss the progress in the project with me for the remaining 15 minutes.

Collaboration was key to success in the TiFN Spores project. I repeatedly heard people say that this was the best collaborating consortium they worked with. This is my only point of reference, so I cannot confirm, but the collaboration was a big motivational driver for me. Thanks to the great diversity in the project team, I learned many things about modelling, physiology, taxonomy, genomics, genomic editing, etc. Thanks Jan, Jos, Han, Robin, Wieke, Arthur, Mark, Marcel and Heidy for bringing your expertise into this project. Thanks Jan Willem, John, Trevor, Petra, Heike and the other experts from industry for your involvement and valuable discussions. Aafke, thanks for managing the project and for organising and joining our dinners, away days and business trips. Inge, Maarten and Sjoerd, working together with you was awesome! It was a pleasure to be part of this project.

Jos, formally you were my boss, but it never felt like you were my boss. I don't know if that is a good thing or a bad thing, but fact is that I always felt very comfortable in your team. Thanks for putting a bit more structure in our weekly meetings together with Jan. Martin, many thanks for your support and effort to create a tidy and organized working environment in the lab for everyone. Sorry for my chaotic ways of working in your super structured lab. And Bart, thanks for relativizing my ways of working to Martin. Thanks Frank, Eunice, Sherlin, Mattijs and Véronique for the excellent work you delivered and the contributions to my project. Manon, thanks for your help in editing the thesis. And a big thank you to the kitchen who poured all the plates of the experiments described throughout this thesis. Joanna, Ronnie, Martin and Bart, thanks for organizing a borrel almost every Friday. It was always good to blow off some steam with cold beer, pizza, a game of Jenga, goats, shitty flutes and great company of everyone who joined.

Freek, you take the cell wall questions, Jaap, you take the plant questions. You lunatics. Thanks for being such great friends and your input for the celebrations. If you do not like the party, blame them, not me.

Thank you friends, for all the moments of joy besides work. Thank you football team, adonises, Westerdijk buddies, quattro, PMFC, grimbros, WEXies, 96e, weekendje wildlands and micro trutjes.

Thank you, family, for always asking laymen's questions. This forces me to reflect on my work from time to time. Thanks mom and dad, for always supporting the choices that I make, the great advice that you give and the great conversations that we have. The thesis would not look as good without the beautiful cover design by the best mother in the world. Special thanks to tante Johanna and ome Leo, who kindly accommodated a quite environment to write.

During this journey two events happened that changed my life more than a COVID pandemic or obtaining a PhD grade. Pepijn and Bram, it is a big pleasure to witness you growing up. It is amazing to see you explore the space and world around you. I love to rediscover everything through your perspective. There is so much beauty and joy in simple things. You are the best things that happened to me.

Anoukie. There is nothing I like more than going on adventure with you. I am the luckiest man on earth to have you as my wife. Your contribution to this thesis is significant and I see it as a communal effort. Do not forget to congratulate Anouk if you congratulate me, she deserves it. Thank you for your unconditional support. I will never forget that. Love you.